# Process-based modelling of morphological response to submerged breakwaters

R.J. Vlijm

Delft University of Technology

Deltares
Enabling Delta Life

# Process-based modelling of morphological response to submerged breakwaters

By

Roland Justin Vlijm

1269844

A thesis submitted as partial fulfilment of the Master of Science degree in Coastal Engineering at the Delft University of Technology, The Netherlands

Delft, December 2011

Graduation committee:

| | |
|---|---|
| Prof. Dr. Ir. M.J.F. Stive | TU Delft |
| Assoc. Prof. Dr. R. Ranasinghe | TU Delft, UNESCO IHE, Deltares |
| Ir. A.P.Luijendijk | TU Delft, Deltares |
| Dr.Ir. G.J. de Boer | TU Delft, Deltares |

Deltares

**Keywords**
**Submerged breakwaters, artificial reefs, numerical modeling, Delft3D.**

## Abstract

Submerged breakwaters (SBWs) are becoming increasingly popular as alternative coastal defence system due to the lack of impact on beach amenity and aesthetics compared to common emerged beach protection measures. However, the recent significant amount of failing SBWs resulting in additional shoreline erosion reported in [Ranasinghe and Turner 2006], indicates the importance of understanding the driving processes of salient development before routinely adopting SBWs in practice. The main objective of this thesis is to gain more insight into single shore-parallel detached SBW induced hydrodynamic processes driving morphological changes.

In order to study SBW induced hydrodynamic conditions resulting in morphological response, a depth-averaged Delft3D model is used. By online coupling of Delft3D-FLOW and SWAN, the wave-current interaction is accounted. To exclude site-specific conditions, an idealized approach is used, including an alongshore uniform beach profile and shore normal short wave forcing. For this idealized situation, a sensitivity analysis of numerical parameters is performed, as well as a validation on individual SBW induced processes based on published literature.

By examining the cross- and alongshore momentum balance for a variety of results from numerical simulations only changing alongshore length and offshore distance of the SBW, dominant SBW induced alongshore differences in water level and resulting currents are explained in detail. In addition, SBW design parameters are studied using the same momentum balances. Besides offshore distance, alongshore length of the SBW and directionality of the incoming waves, these include the crest width, crest height, incoming wave height and breakwater roughness. To confirm the findings from the hydrodynamic analysis as the important driving processes of SBW induced morphological changes, additional morphological simulations are included and morphological SBW induced response is compared to initial hydrodynamic conditions.

As a result, a computationally efficient depth-averaged Delft3D model is obtained, which is capable of simulating SBW induced processes accurately compared to published literature. From the idealized simulations, more insight is given in two distinct SBW induced processes driving morphological response. These processes reducing nearshore water level set-up are the spatial distribution of wave forcing (commonly referred as wave sheltering effect) and the momentum balance between wave forcing and bottom stresses over the SBW. In addition to the parameters presented in [Ranasinghe et al. 2010], the breakwater roughness and directional spreading of waves are important parameters to take into account when constructing SBWs. Morphological simulations confirm the relation between the hydrodynamic processes described and the morphological response to SBWs. The ability of Delft3D to simulate morphological response to SBWs, enables a powerful numerical tool for future studies on SBW induced (morphological) processes.

| Version | Date | Author | Initials | Review | Initials | Approval | Initials |
|---|---|---|---|---|---|---|---|
| Final | December 2011 | R.J.Vlijm | RJV | | | | |

**State: Final**

**Summary**

Introduction

Submerged breakwaters (SBWs) are becoming increasingly popular as an alternative for common emerged coastal defence systems, due to the lack of impact on beach amenity and aesthetics. Particularly the growing recognition that a submerged beach protection measure can be combined with recreational purposes like surfing increases the interest in SBWs. However, the significant amount of SBWs recently reported resulting in additional shoreline erosion [Ranasinghe and Turner 2006], indicates the importance of understanding the SBW induced hydrodynamic changes, before routinely adopting SBWs in practise.

The main objective of this thesis is to gain more insight into the hydrodynamic processes, which contribute to the morphological changes behind a single shore-parallel detached SBW. In order to study these processes an idealized approach is used, excluding site-specific conditions, containing constant shore-normal short wave conditions and an alongshore uniform beach profile, locally changed to include a given design SBW.

Numerical modelling with Delft3D

To study the SBW induced morphological response, a depth-averaged model is set-up in Delft3D. By online coupling of the Delft3D Flow-module with the SWAN wave model, important governing SBW induced processes are accounted. The wave transmission/breaking is simulated by depth induced wave breaking using SWAN. In order to test this methodology and to obtain a computationally efficient model while not impairing on accuracy, a sensitivity analysis of numerical parameters and a validation of individual SBW induced processes published in literature is performed. Based on these results, a computationally efficient model is obtained. In addition, confidence is built in the capabilities of Delft3D in accurately representing SBW induced hydrodynamics compared to published literature.

Hydrodynamic analysis

To study the nearshore SBW induced hydrodynamics, the cross and alongshore momentum balance are examined. By integrating each term of the cross-shore momentum balance in cross-shore direction and normalise it using the integrated wave forcing on the undisturbed beach, relative contributions of each term are studied compared to the undisturbed coastline. In addition to the momentum balance, the wave spectra in the lee of the SBW reveal the importance of offshore wave conditions.

Results from the hydrodynamic analysis of the momentum balance indicate the importance of the spatial distribution of wave forcing, see Figure 1.1 The offshore wave conditions, length and offshore distance and wave transmission, result in a total increase of wave forcing over and in the lee of the SBW. For all simulations, just next to the breakwater head a reduction of wave forcing is computed. This is explained by the fact that oblique waves break offshore over the SBW, instead of nearshore next to the SBW.

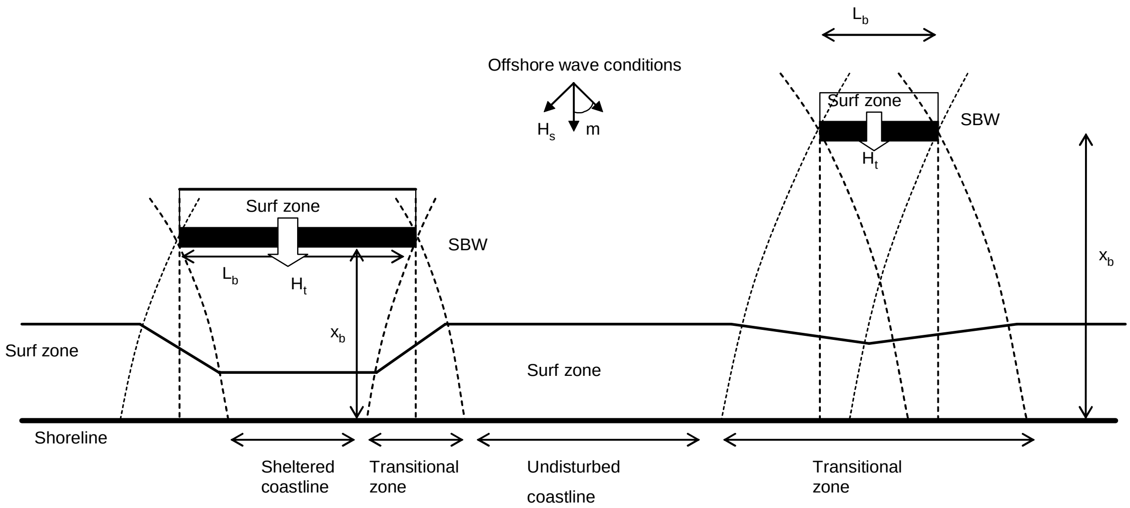


*Figure 1.1 Overview of the redistribution of wave forcing due to a submerged breakwater*

A second important contribution to SBW induced hydrodynamic conditions near the shoreline is the momentum balance of wave forcing by bottom stresses (Figure 1.2 and Figure 1.3). Because of alongshore limitations on water level set-up, a net onshore-directed flow over the SBW will result in offshore-directed bottom stresses. As a result, only part of the deceleration of the net depth averaged onshore flow resulting from the wave forcing, is compensated by a water level set-up.

Due to these two processes, the near shore water levels in the lee of the SBW are lower, compared to the undisturbed coastline. This reduction of nearshore water levels will result in an alongshore flow towards the centre of the SBW, which cause sediment to accrete behind the SBW.

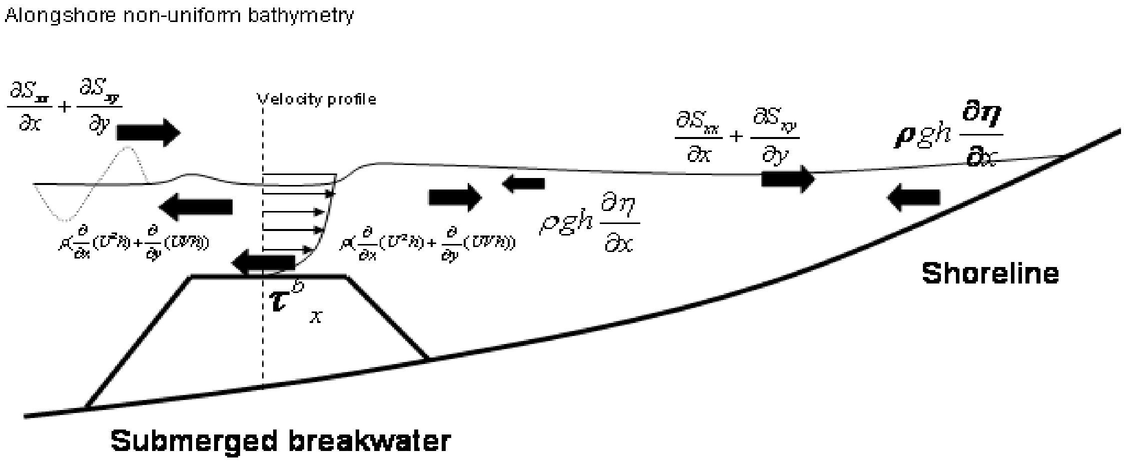


*Figure 1.2 Theoretical cross-shore momentum balance over the submerged breakwater*

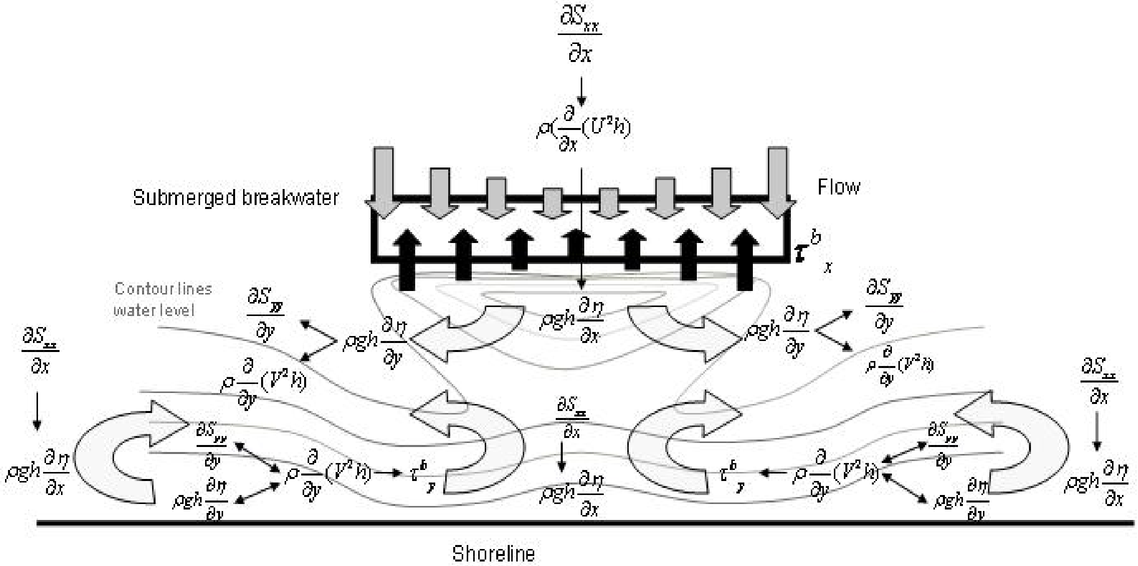


*Figure 1.3 Spatial distribution of cross- and alongshore momentum balance for 4 cell pattern*

Engineering design parameters

In order to asses the influence of several key SBW design or environmental parameters [Ranasinghe et al. 2010], the same cross-shore momentum balance is studied. By only changing a single parameter per simulation, the influence of that single parameter is illustrated. Besides the alongshore length, offshore distance of the structure and directional spreading of the waves; the crest height, crest width, breakwater roughness, incoming wave height and a more or less alongshore uniform case with a relative low value of xb/Lb are examined. In general, these parameters act according to published literature, but more insight is given in how these parameters affect alongshore currents. In a way, this also confirms the conclusions found in the hydrodynamic analysis. In addition to the important design parameters presented in [Ranasinghe et al. 2010], the breakwater roughness and directional spreading have a profound effect on the resulting SBW induced hydrodynamic conditions. Due to the choice of materials, breakwater roughness can be regarded as a design parameter. Concluding from results, a rougher SBW results in larger alongshore differences in water level set-up.

Morphological analysis

In order to confirm the relation obtained from the hydrodynamic analysis as the cause of morphological changes, morphological simulations are performed. Though morphological changes in Delft3D have not been validated in detail, a distinct qualitative trend is obtained compared to the initial conditions. The equilibrium profiles obtained from the idealized simulations indicate the importance of morphological response and the governing reduction of alongshore differences in water level set-up. This confirms the previously described hydrodynamic processes as the governing processes for morphological response to SBWs. In addition, due to the ability of Delft3D to simulate morphological response to SBWs, new studies on SBW induced morphological processes as well as practical applications of SBWs using the powerful depth-averaged process based Delft3D model are enabled.

Conclusions

Resulting from this thesis, a computationally efficient depth-averaged Delft3D model is set-up and applied, which is able to accurately simulate SBW induced processes known from literature. From the idealized simulations performed, two distinct processes contribute to the resulting morphological changes behind a SBW. First process is the distribution of wave forcing, commonly referred as wave sheltering effect. Second process is the momentum balance between wave forcing and bottom stresses over the SBW, induced by alongshore limitations on water level set-up behind the SBW. Although these described individual processes are familiar to previous findings, more insight is given in the origin of these processes as well as the relation with the initial mode of shoreline response.
In addition to the environmental and design parameters presented in [Ranasinghe et al. 2010], the bottom roughness of the SBW and the directional spreading of waves have a profound effect on SBW induced hydrodynamics. These are important design parameters to keep in mind for future research on morphological response to SBWs.
Although no absolute values of morphological response were considered, an important step in understanding the driving processes of SBW induced morphological changes is taken. Results from the idealized simulations are in good agreement with the expected morphological response to SBWs. In addition, the ability of Delft3D to simulate morphological response to SBWs, enables a variety of additional studies using the depth-averaged process-based numerical model Delft3D on SBW induced processes, as well as studies on practical applications of SBWs.
As a start, it is recommended that future research should focus on morphological data from field measurements, as well as the vertical flow structure and depth-averaged velocity over the SBW for alongshore non-uniform bathymetries. As a first step, it is recommended to focus on the flow over the SBW head, as it seems undependable of the breakwater length.

**Acknowledgements**

I hereby would like to acknowledge the following people for their important contributions to my study in Delft and in particular my Master thesis,

First, I would like to thank my graduation committee, Prof. Dr. Ir. M.J.F Stive, Assoc. Prof. Dr. R. Ranasinghe, Ir. A.P. Luijendijk and Dr. Ir. G.J. De Boer for sharing their knowledge, expertise and enthusiasm for submerged breakwaters and coastal engineering in general during my thesis. Particularly Arjen is thanked for all his help and expertise on Delft3D and being my daily supervisor at Deltares.

Deltares in general is greatly thanked for giving me the opportunity and support to graduate at one of the leading institutes on research and expert consultancy in coastal engineering. Special thanks goes out to the 'Deltarians' from HYE, for sharing their enthusiasm, numerous on and off-topic conversations during coffee breaks and Wednesday-night football matches. In addition, I would like to thank my fellow graduate students and especially my roommates at Deltares for their constructive and unconstructive comments.

Furthermore, thanks go out to my fellow students and friends from Delft, for the good times during my study and for encouraging me throughout my thesis.

Finally, I would like to thank my family and friends from my hometown for their interest and support during my study and master thesis. Special thanks to Annelies for her unconditional love and care, particularly during the end of my thesis.

Roland Vlijm

Delft, December 2011

# Contents

## Appendices

# List of Tables

# List of Figures

# List of Symbols

| Symbol | Unit | Description |
|---|---|---|
| A | $m^2$ | Cross sectional area of breakwater |
| B | m | Breakwater crest width |
| $B_0$ | [-] | Wave shape factor |
| C | $m^{1/2}s^{-1}$ | Chezy coefficient |
| c | $ms^{-1}$ | Wave celerity |
| $c_f$ | [-] | Bed friction coefficient |
| $C_f$ | [-] | Courant number |
| $c_g$ | $ms^{-1}$ | Wave group velocity |
| D | m | Grain size |
| d | m | Bottom depth |
| D | [-] | Wave energy distribution |
| E | $Jm^{-2}$ | Wave energy |
| $E_r$ | $Jm^{-2}$ | Wave roller energy |
| F | $Nm^{-2}$ | Wave forcing |
| f | $s^{-1}$ | Wave frequency |
| f | [-] | Mannings friction parameter |
| $f_p$ | $s^{-1}$ | Wave peak frequency |
| $f_r$ | [-] | Reduction factor wave reflection |
| g | $ms^{-2}$ | Gravitational acceleration |
| H | m | Wave height |
| h | m | Water depth |
| $H_0$ | m | Deep water wave height |
| $H_{1/3}$ | m | Significant wave height |
| $H_b$ | m | Breaking wave height |
| $h_b$ | m | Depth at sbw |
| $H_i$ | m | Incoming significant wave height |
| $H_{max}$ | m | Maximum wave height |
| $H_{rms}$ | m | Root mean square wave height |
| $H_s$ | m | Significant wave height |
| $H_t$ | m | Transmitted significant wave height |
| k | $m^{-1}$ | Wave number |
| $K_D$ | [-] | Diffraction coefficient |
| $K_{d,t}$ | [-] | Total wave transmission coefficient |
| $K_r$ | [-] | Wave reflection coefficient |
| $K_t$ | [-] | Wave transmission coefficient |
| L | m | Wave length |
| $L_0$ | m | Deep water wave length |
| $L_b$ | m | Alongshore length breakwater |
| m | [-] | Directional spreading |
| n | [-] | Ratio between wave group velocity and wave celerity |
| $q_{in}$ | $m^2s^{-1}$ | Mass transport over sbw |
| $R_c$ | m | Crest submergence level |

| | | |
|---|---|---|
| S | Nm$^{-1}$ | Radiation stress |
| $s_0$ | [-] | Deep water wave steepness |
| $s_b$ | m | Offshore distance sbw |
| $S_{max}$ | [-] | Frequency parameter |
| t | s | Time |
| $T_m$ | s | Mean wave period |
| $T_p$ | s | Wave peak period |
| U | ms$^{-1}$ | Flow velocity in x-direction |
| Ur | [-] | Ursel number |
| V | ms$^{-1}$ | Flow velocity in y-direction |
| x | [-] | Cross-shore direction |
| $x_b$ | m | Offshore distance sbw |
| y | [-] | Alongshore direction |

| **Greek Symbol** | **Unit** | **Description** |
|---|---|---|
| α | $^{0}$ | Bed level gradient |
| β | $^{0}$ | Wave angle |
| Γ | [-] | Gamma function |
| γ | [-] | Wave height to depth ratio |
| δ | m | Water level set-up |
| η | m | Water surface elevation |
| θ | $^{0}$ | Wave angle |
| ξ | [-] | Iribarren number |
| ρ | kgm$^{-3}$ | Water density |
| $\sigma_\theta$ | $^{0}$ | Directional spreading |
| $\tau^b$ | Nm$^{-2}$ | Bottom stress |

# 1 Introduction

## 1.1 Background

In the past, emergent coastal structures like groynes or detached offshore breakwaters, have been used commonly as coastal/beach protection measure. These conventional structures are studied extensively and applied successfully many times. Main purpose of a coastal structure near or in the surf zone is to counter shoreline erosion. A frequently adopted structure is an emerged rubble-mound breakwater. Primary function of such a breakwater is to reduce the wave energy in the lee of the breakwater and initiating shoreline accretion by changing the corresponding local currents [Ranasinghe and Turner 2006]. Amongst others, [Pope and Dean 1986] and [Hsu and Silvester 1990], already quantified the shoreline response to (single) emerged breakwaters as a function of the dominant breakwater design parameters.

Despite the successful applications, emergent structures are becoming increasingly less popular, due to their negative impact on beach amenity and aesthetics.[Ranasinghe et al. 2006] As a result, alternatives for these conventional protection measures are sought. A possible alternative is a detached offshore submerged breakwater (SBW). SBWs are capable of providing the necessary beach protection while not having the downside of adverse impact on beach amenity and aesthetics. In addition, the recognition that a beach protection measure can be combined with other functions, has a wide community appeal [Ranasinghe et al. 2006]. According to [Black and Andrews 2001a] artificial sub-tidal and sub-aerial offshore reefs, which are similar to SBWs, can have different functions, like beach protection, enhancement of marine habitat, surfing, diving and possible swimming safety. In [Ranasinghe et al. 2006], an example is given of such a multi functional design of a SBW which enhances local surfing conditions. Obviously, a multifunctional beach protection measure, which combines protection of the shoreline with other functions while not impairing aesthetics or beach amenity, will be the preferred choice to coastal management authorities when coastal problems arise.

## 1.2 Problem definition

Despite all the benefits of a proper-designed SBW, SBWs have rarely been adopted until now, which is the reason why their efficiency is still largely unknown. An overview of reported SBWs is given by [Ranasinghe and Turner 2006]. From this overview, it shows that in spite of all effort, in most cases enhanced shoreline erosion in the lee of the submerged breakwater occurred. Clearly, a better understanding of all the involving processes around SBWs is required before routinely adopting submerged breakwaters for coastal protection.

As stated above, before routinely adopting SBWs, more understanding is needed of the effect of a SBW on hydrodynamic and morphological processes close to the shoreline. In this highly complex zone, waves and currents interact with local conditions like bathymetry etc, enabling morphological changes around the breakwater. Previous studies have been focussing on individual hydrodynamic or morphological processes like wave breaking,[Van der Meer et al. 2005], wave set-up [Calabrese et al. 2008] and scour characteristics [Sumer et al. 2005]. Less is known about the morphological shoreline response to SBWs and which individual processes drive it.

One of the first attempts in quantifying the formation of a salient/tombolo in the lee of submerged breakwaters was done by [Black and Andrews 2001a]. This study focussed on the morphological effect of natural reefs in New Zealand and Australia, which are similar to submerged breakwaters. Another interesting study on the morphological effect of submerged breakwaters is done by [Ranasinghe et al. 2006]. In addition, [Ranasinghe et al. 2010] focussed on the initial mode of shoreline response, (accretive or erosive) to a single shore-parallel submerged breakwater. Previous studies as well as the other studies mentioned, show the complexity of the processes around SBWs. Though these studies show the relation between the morphological response and several SBW design parameters, a detailed explanation of governing processes is lacking.

## 1.3 Research objective

The main objective of this MSc thesis is establishing the relation between individual submerged breakwater induced hydrodynamic processes and shoreline response to a given design single shore-parallel detached submerged breakwater.

In order to study the driving hydrodynamic processes of submerged breakwater induced morphological response, this study will be specially focussing on:

- Literature on submerged breakwaters.
- Modelling of a submerged breakwater with a process based numerical model (Delft3D)
- Sensitivity analysis of Delft3D model results to various numerical model characteristics (Morfac, wave-current interaction, mass-flux etc).
- Delft3D validation of individual submerged breakwater induced hydrodynamic processes.
- The submerged breakwater hydrodynamic contributions to the total hydrodynamic conditions.
- Sensitivity analysis of submerged breakwater design parameters of the hydrodynamic conditions.
- The hydrodynamic processes driving submerged breakwater induced morphological changes.

## 1.4 Methodology

The proposed study can be divided into the following stages:

- *Literature review.* First, the hydrodynamic and morphological processes that may affect shoreline response to a SBW are studied from literature. This theoretical study indicates which are the important processes and corresponding parameters that are related to SBW induced morphological response. In addition, previous studies on SBWs will be summarised and conclusions are taken into account. This literature study will act as a starting point for this thesis.
- *Modelling of a submerged breakwater with a process based model (Delft3D).* Second the shoreline response to a SBW is modelled by a process-based model, Delft3D, developed by Deltares. A two-dimensional depth-averaged model is set-up to study the important driving processes behind SBW induced shoreline response, without having the large computational times of a full three-dimensional and phase resolving model. Using an initial alongshore uniform profile, a single shore-parallel SBW, shore normal short wave forcing and avoiding site-specific conditions ensures an idealized approach.

- *Sensitivity analysis numerical parameters.* Applying a numerical model introduces additional (numerical) parameters and assumptions that influence the shoreline response. In order to reduce the influence of these parameters/assumptions and total computational times, a sensitivity analysis of these parameters is performed. In this way, a computationally efficient model is obtained, while not impairing on model accuracy.
- *Validation of Delft3D on individual submerged breakwater induced hydrodynamic and morphologic processes.* From literature most important processes that govern SBW induced shoreline changes are known. Analysing model results of Delft3D will show whether this phase-averaged and depth-averaged model is capable of modelling the important hydrodynamic and morphologic processes from literature and results can be relied upon.
- *The submerged breakwater hydrodynamic contributions to the total hydrodynamic conditions*. Morphological response to SBWs is depending on the change in hydrodynamic conditions inflicted by the SBW. Studying the individual hydrodynamic processes, and focussing on each individual contribution to the cross- and alongshore momentum balance, will explain the obtained differences in hydrodynamics and especially water level differences close to the SBW.
- *Sensitivity analysis of submerged breakwater design parameters of the hydrodynamic conditions.* By understanding the SBW induced hydrodynamic changes, the sensitivity of these processes to SBW design parameters will be studied. This analysis result in practical preliminary guidelines to construct a single shore parallel detached SBW.
- *The hydrodynamic processes driving submerged breakwater induced morphological changes*. In addition to hydrodynamic conditions, morphological changes are studied. By comparing initial hydrodynamic conditions and morphological response, the relation between the initial driving hydrodynamic processes as cause of morphological changes and the actual resulting morphological changes is confirmed.

## 1.5 Reader

First, an overview is provided on published literature on SBWs (chapter 2). Important processes and governing parameters will indicate the key processes and design parameters to study. In chapter 3, the Delft3D model description and brief discussion on used settings is included. In addition, the sensitivity analysis of numerical parameters and validation of individual hydrodynamic processes are described. Based on the ability of Delft3D to simulate SBW induced hydrodynamic processes, chapter 4 will illustrate the origin of hydrodynamic conditions by studying differences in cross- and alongshore momentum balance for different simulations. Understanding the hydrodynamic processes and resulting alongshore currents, several important design parameters are studied in more detail in chapter 5. Chapter 6 will illustrate the relation between the governing hydrodynamic conditions causing shoreline erosion. Next, a discussion on used methodology and assumptions will be included in chapter 7. In addition, in chapter 8 the conclusions and recommendations for further research are provided.

# 2 Literature review

## 2.1 Introduction

Submerged breakwater induced shoreline changes are complex. Different hydrodynamic and morphologic processes eventually result in accretion or erosion of sediment behind the SBW. Figure 2.1 shows these two different modes of SBWs, of which accretive shoreline changes are obviously preferred. Literature on individual hydrodynamic processes is available, but sometimes limited to special cases, whereas literature on morphology is scarce. Although morphological processes are of most interest, the hydrodynamic processes are the driving mechanism of morphological changes.

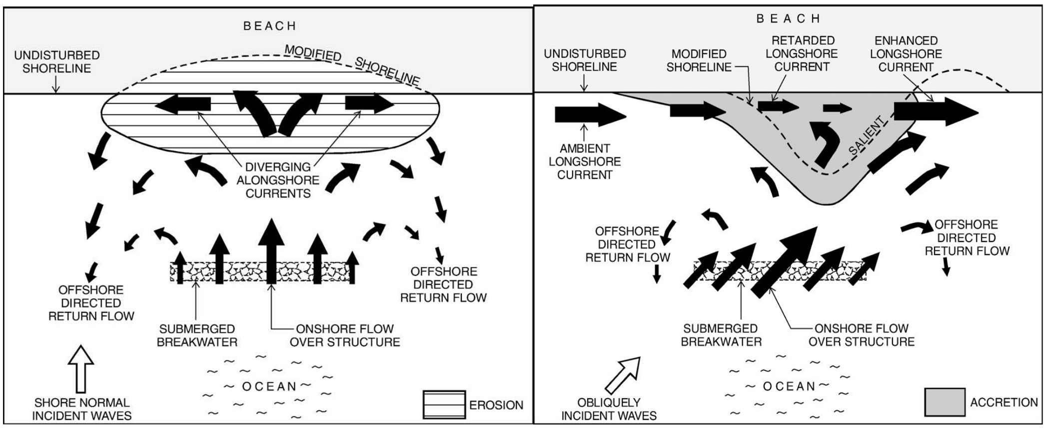


*Figure 2.1 Erosive and accretive shoreline changes. [Ranasinghe and Turner 2006]*

In this chapter, a summary is given of the important hydrodynamic and morphologic processes driving this submerged breakwater induced shoreline changes known from published literature. Starting from offshore conditions to, in the end, the morphologic changes and salient formation, a clear view can be given which are the dominant processes and corresponding parameters. This serves as starting point for further analysis. It is assumed that the reader is familiar with common theories in coastal engineering; however, the important processes for SBW induced shoreline changes are repeated here.

## 2.2 Offshore climate

As offshore conditions will often be mentioned and serve as boundary conditions for near shore processes, a short description of several processes will be given. To ensure a uniform approach, the offshore wave conditions are formulated using a JONSWAP (variance-density) wave spectrum [Hasselmann et al. 1973], see Figure 2.2. This originally Pierson-Moskowitz shaped spectrum for fully developed sea states is enhanced by a peak enhancement factor, describing a young wind induced sea state commonly obtained in wave field analyses worldwide, due to quadruplet wave-wave interactions and wave breaking which stabilizes this distribution [Holthuijsen 2007].

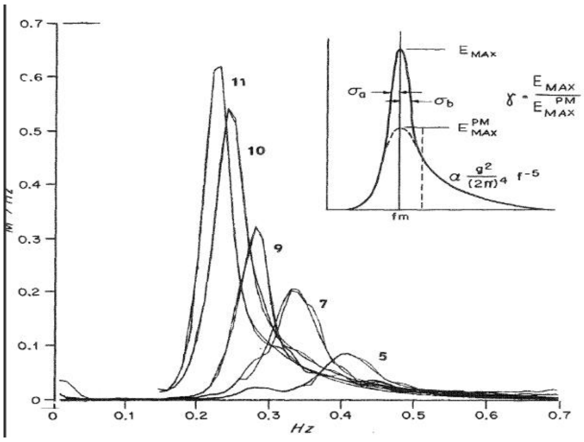


*Figure 2.2 Deep-water wave spectrum with fetch limitations and the peak enhancement factor for defining the JONSWAP spectrum from a Pierson-Moskowitz spectrum.[Hasselmann et al. 1973]*

Although the limitations in the research of [Hasselmann et al. 1973], the JONSWAP spectrum is a rather robust variance density spectrum for random deep water wave conditions. Due to this, the JONSWAP spectrum is an ideal spectrum for an idealized approach in describing sea states.

When accounting for the direction of waves, the one-dimensional spectrum can be transformed in a two dimensional frequency-direction spectrum. See Figure 2.3.

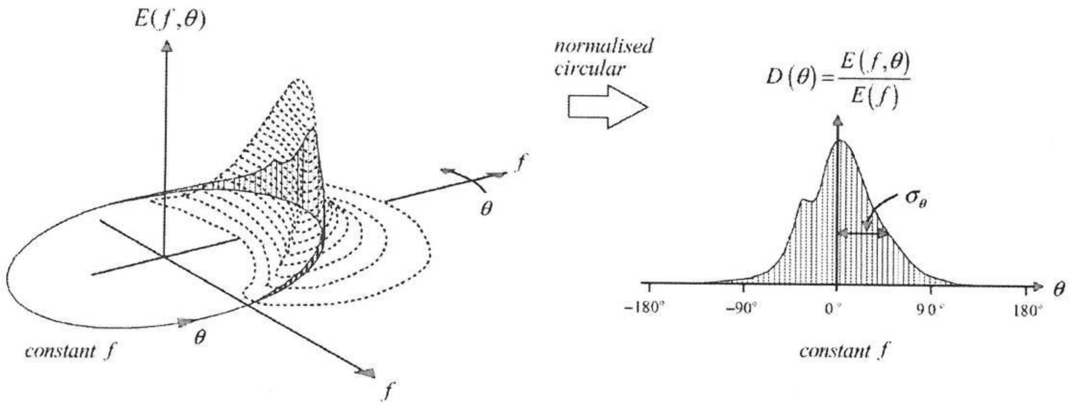


*Figure 2.3 Two dimensional frequency-direction spectrum and its directional width [Holthuijsen 2007]*

One of the important features is the directional spreading or directional width of the wave conditions σ. From common sense, it's clear that when the directional width is larger, the sheltering effect of a SBW is less. Studies that introduce the effect of directional spreading on wave deformation on the SBW slope are [Hur 2004] and the effect on diffraction for emerged breakwaters [Goda et al. 1978] [Yu et al. 2000]. This effect will be shown in next paragraphs. A relation for the directional spreading is given by [Young et al. 1996]:

$$\sigma_\theta = \begin{cases} 26.9(f / f_{peak})^{-1.05} \\ 26.9(f / f_{peak})^{-0.68} \end{cases} \; for \; \begin{matrix} |\theta| \leq 90^0 \\ |\theta| > 90^0 \end{matrix} \tag{2.1}$$

The shape of the distribution of energy over the direction is however difficult. An often used model to describe the shape of the variance/energy distribution over the wave angles is: [Pierson et al. 1952]

$$D(\theta) = \begin{cases} \frac{2}{\pi}\cos^2(\theta) & for \; |\theta| \leq 90^0 \\ 0 & \;\;\;\;\;\;\; |\theta| > 90^0 \end{cases} \tag{2.2}$$

or more generalised:

$$D(\theta) = \begin{cases} A_1 \cos^m(\theta) & for \; |\theta| \leq 90^0 \\ 0 & \;\;\;\;\;\;\; |\theta| > 90^0 \end{cases} \tag{2.3}$$

With:

$$A_1 = \frac{\Gamma(\frac{1}{2}m+1)}{\Gamma(\frac{1}{2}m+1)\sqrt{\pi}} \tag{2.4}$$

Of which $\Gamma(x)$ is a gamma function. In case of the original [Pierson et al. 1952] model the directional width would be around 30 degrees. With this spectrum the wave angles and peak-frequency (and inherent peak-period) are defined.

For defining the wave heights, the random phase-amplitude model or Fourier analysis is referred, see [Holthuijsen 2007]. As the random amplitude in a harmonic is only depending on one parameter varying over the frequencies (the expected value of the amplitude), the statistical approach is best described by a Rayleigh distribution for the probability density function , see Figure 2.4. Both, the variance-density spectrum and the Rayleigh distribution, are applicable for deep water. However also both the high end tails of the spectrum and distribution are still under discussion. [Holthuijsen 2007]

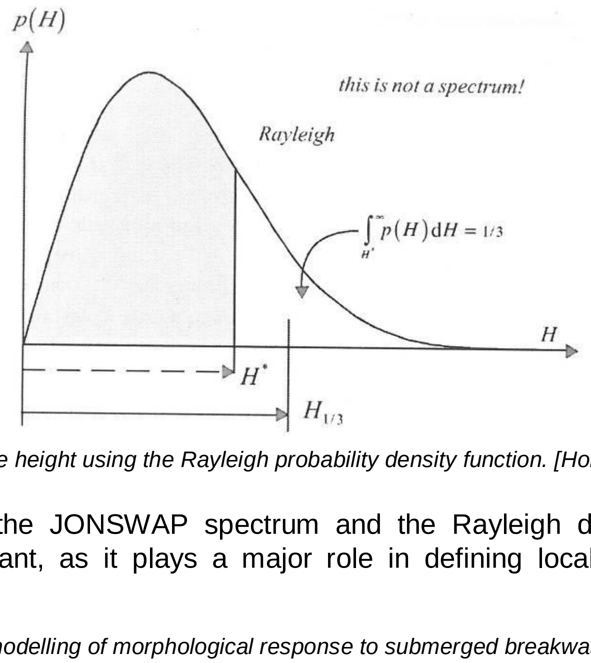


*Figure 2.4 Significant wave height using the Rayleigh probability density function. [Holthuijsen 2007]*

The importance of the JONSWAP spectrum and the Rayleigh distribution for the wave conditions is significant, as it plays a major role in defining local conditions near shore.

Phenomena like wave breaking, generation of higher harmonics and sheltering effect of a SBW are based on this spectrum and distribution. Next paragraphs will show the development of this wave spectrum and probability density function when moving closer to shore.

Swell conditions and tide will be neglected in this thesis. The subject submerged breakwaters has large similarities with rip current systems. In a way, by construction a SBW the current is converted to an accretive flow pattern or rip current [Ranasinghe et al. 2006]. Based on the review on rip currents of [Dalrymple et al. 2011], a SBW system can be classified as a bathymetry induced rip current, due to differences in short wave breaking. Although a wide variety of other driving mechanisms of rip currents are known the focus of this thesis is on the rip currents induced by differences in short wave motions. In addition, as mentioned by [Ranasinghe et al. 2010], the (vertical) tide seems to have no significant influence on the morphological shoreline response. Differences in hydrodynamics may however occur, due to the relative decrease/increase level of submergence [MacMahan et al. 2006]. Also storm conditions and inherent storm surges due to wind set-up and even barometric pressure differences are neglected, although mentioned by [Burcharth et al. 2007].

## 2.3 Wave propagation

As waves travel from deep to shallow water, waves get affected by the bathymetry. These processes determine local design conditions for the submerged breakwater. Using an idealized alongshore uniform coastline and assuming no energy sources or sinks, these processes where wave conditions are effected by the bathymetry can be described by simplified equations. [Burcharth et al. 2007].

### 2.3.1 Shoaling

Assuming an idealised case of a alongshore uniform beach, normal incident waves, no currents and gentle slopes, the frequency of a propagating wave remains constant, the dispersion relation is valid. When waves propagate into shallower water this results in a decrease in wave lengths, because of decreasing depth and inherent decrease of phase velocity [Holthuijsen 2007]. The group velocity initially increases slightly, but then decreases accordingly. By considering the depth induced changes and energy balance, the decrease in group velocity is compensated by an increase in wave height which is the ‘shoaling’ effect.

With the depth and phase/group velocity going to zero the wave height would theoretically go to infinity. However the wave height is limited by wave breaking (energy dissipation), which makes the above described approach invalid. This shoaling effect can be responsible for water level gradients in the vicinity of SBWs. As differences in water level set-up due to spatial differences in wave breaking are held responsible for rip currents this may become important.

### 2.3.2 Refraction

Using the same approach as for the shoaling effect, but now with oblique incident waves, the depth induced variation of the wave direction can be described. Differences in phase velocity due to the dispersion relation along a wave crest cause a wave to turn in the direction of lower phase velocities. Although this thesis is focussing mainly on normal incident waves, refraction may play an important role in the “sheltering effect” of submerged breakwaters combined with the directional spreading of the offshore wave conditions (Figure 2.5).

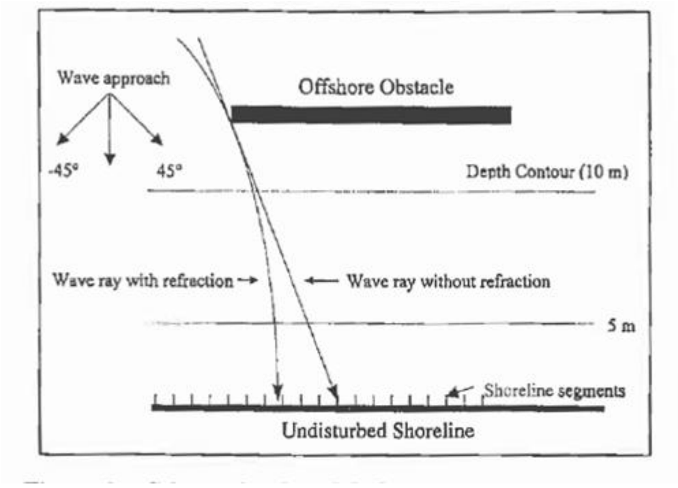


*Figure 2.5 Influence refraction and wave directionality [Black and Andrews 2001b]*

Besides the depth-induced refraction, also current induced refraction is possible. Based on similar theory, the wave refracts due to differences in (effective) dispersion.

### 2.3.3 Diffraction

When large differences in wave energy along a wave crest are present due to abrupt changes in for instance bathymetry, this leads to transfer of energy along the wave crest in perpendicular direction. This diffraction effect causes an increase in wave height in the 'shadow zone' and a decrease in wave height were the lateral transfer of energy is coming from. The effect of diffraction in irregular and short crested wave field is limited to one ore two wave lengths from an emerged breakwater head and is relatively small. For submerged breakwaters this effect would probably even less, because the energy differences (differences in wave height) along a wave crest are smaller, compared to a general emerged breakwater. However, for relative small breakwater lengths, the diffraction effect can be of influence. Although analytical solutions are almost impossible for random sea states and irregular bathymetry, and implicit relations need an iterative process often using a numerical model, still some quantitative results are known for using simplified conditions, for example [Penny and Price 1952].

In the study of [Vicinanza et al. 2009] the diffraction at low crested structures was studied in more detail. Previous remarks of, amongst others, [Seabrook and Hall 1998] on possible three dimensional effects of wave transmission, made [Vicinanza et al. 2009] to quantify this effect. By assuming an uncorrelated relation for the diffraction coefficient between the two breakwater heads, the total diffraction coefficient can be defined by:

$$K_D{}^2 = K^2{}_{D,A} + K^2{}_{D,B} \qquad (2.5)$$

For the individual diffraction coefficient of one of the two breakwater heads, different methods are available. Similar as mentioned by [Vicinanza et al. 2009] instead of using the [Goda et al. 1978] method which is applicable to random short crested waves, for the sake of simplicity the method of [Penny and Price 1952] can be used. Although based on linear wave theory, this can give a good approximation for linear long crested random waves when using the peak period [Boccotti 2000]. This gives however considerable scatter in the diffraction coefficients. [McCormick and Kraemer 2002] showed that instead of using the Fresnal integrals of [Penny and Price 1952] , simplified polynomial approximations can be used.

For a more illustrative based approach, as theory on diffraction has its limitations for submerged breakwater, the diagrams of [Goda et al. 1978] are presented for diffraction at a semi infinite emerged breakwater, but including normal incident irregular waves and including the effect of directional spreading:

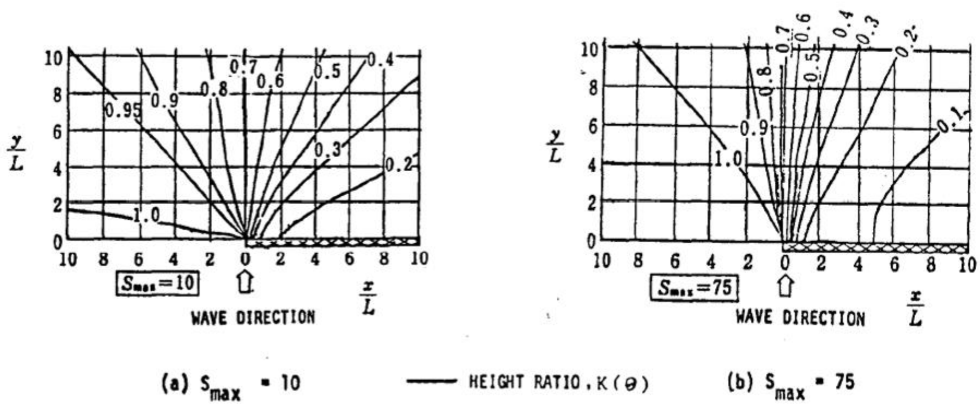


*Figure 2.6 Diffraction diagrams for normal incident random waves at a semi infinite emerged breakwater, including directional spreading.[Goda et al. 1978]*

As can be clear from Figure 2.6, the random wave field including directional spreading tends to smooth out the wave field behind a structure, in this case for a emerged breakwater. In addition, the effect of directional spreading on the wave field is evident by comparing a narrow spectrum (right) with a broad spectrum (left). The directional spreading is defined by using a dimensionless frequency parameter $S_{max}$, with inverse relation (high values correspond to narrow spectra and vice versa). For the calculation of the dimensionless frequency parameter, it will be referred to [Goda et al. 1978]. It is expected that this effect of diffraction is similar for a submerged breakwater.

Above methods are however based on the further simplifications of uniform depth and emergent or low crested breakwaters. Noted by [McCormick and Kraemer 2002] is also the effect of wave reflection of the leeward side of the breakwater on the diffraction coefficient. Considering the relative small wave heights of diffraction compared to the submergence level of SBWs, this may be an important difference with emerged breakwaters. Next paragraph will show that reflection is considerable less at SBWs compared to emerged breakwaters. Another interesting difference between submerged and emerged breakwaters might be the interaction of diffracted and transmitted waves. To the best of the author's knowledge this has not been studied. The effect of diffraction on submerged breakwaters is however based on similar grounds, but less significant compared to emerged breakwaters.

### 2.3.4 Wave reflection

As waves reach the shoreline or a structure, part of the wave is reflected, creating a (partial) standing wave. SBWs are in some way identical to a (emerged) structure and are capable of creating reflections. Although little is known about the reflection of waves at SBWs, common sense suggest that reflection at SBWs would be less, because of the partly transmitted wave and large dependency on the relative submergence. [Van der Meer et al. 2005] suggested using the standard formulas for reflection on slopes and using a reduction factor for the influence of crest submergence. Based on these results and assumptions mentioned, a simple relation between the reflection coefficient and the breaker parameter is given, that neglects the permeability effects:

$$K_r = 0.14\xi^{0.73} f_r \quad for \;\; \xi < 10 \tag{2.6}$$

With:

$$f_r = \frac{0.2R_c}{H_s} + 0.9 \quad for \;\; \frac{R_c}{H_s} < 0.5 \tag{2.7}$$

$$f_r = 1 \quad for \;\; \frac{R_c}{H_s} \geq 0.5 \tag{2.8}$$

However, as mentioned by [Van der Meer et al. 2005], the scatter in the data set shows the complexity of this phenomena and usage of the above equations should be done carefully. In other processes this phenomena is often ignored for the sake of simplicity.

## 2.4 Wave breaking and dissipation

When waves enter shallow water the shoaling effect describes the increase of wave height, but this process is physically limited by wave breaking. When the particle velocity exceeds the wave velocity, the wave crest becomes unstable and breaking of the wave starts. Wave breaking is often defined using the Irribarren number or surf similarity parameter, $\xi = \frac{\tan\alpha}{\sqrt{H_0 / L_0}}$ for which different 'modes' of breaking can be described. As wave breaking is the dominant mechanism in energy dissipation into turbulence at SBWs and differences in wave height also cause differences in radiation stresses, this paragraph will go in detail about the wave breaking and energy dissipation, starting by explaining a conceptual model for describing the wave transformation in the surf zone. The model described, is the original model proposed by [Battjes and Janssen 1978] as is it commonly used worldwide.

### 2.4.1 Conceptual model

The [Battjes and Janssen 1978] model is a parametric model describing the energy dissipation in random waves due to wave breaking. The dissipation rate of energy per wave is compared with a bore of similar characteristics, while the probability of wave breaking is described by a wave height distribution, which is cut-off at a certain maximum value mainly depending on the local water depth. [Battjes and Janssen 1978]. Although the comparison with a bore may be crude and is lacking physical processes like turbulence, the model shows good capabilities in describing the local sea state characteristics in general on a beach.

Starting point for the wave height distribution of broken waves is assuming the same Rayleigh distribution as for non-breaking waves (limited by a maximum wave height depending on the local water depth) and only depending on the root-mean squared wave height. The probability function of the presence of a broken wave can then be defined, which is proportional to the averaged local energy dissipation. The maximum wave height is defined by using Miche's criterion, but also including the tuneable parameter y, $H_m = 0.88k^{-1}\tanh(\frac{ykh}{0.88})$. In this way the maximum wave height in shallow water becomes only dependent on shallow water wave breaking $H_m = yh$ and neglecting steepness induced wave breaking, which is a common assumption for surfzone models. For the averaged energy dissipation, a comparison is made with a bore type model, based on the power dissipation per unit span, averaging per unit area. Now the mean energy dissipation in a random breaking wave field is defined by multiplying the energy dissipation times the probability of occurrence of a broken wave. This dissipation rate can be added to the energy balance to describe the decrease in wave energy in surf zones.

The reason for describing this model in such detail is that it is still subjected to discussion for the applicability to steep slopes, used at submerged breakwaters. Next paragraphs will go in more detail about these discussions.

### 2.4.2 Discussion on wave dissipation model

Since the introduction of the energy dissipation model due to wave breaking described in [Battjes and Janssen 1978] improvements have been made for the applicability of the model. Improvements to the underlying probability density functions as well as the wave-height-to-depth-ratio $\frac{H_m}{h} = y$, which was already defined by [Battjes and Janssen 1978] as a slightly adjustable coefficient, are made by others. This paragraph will give a short overview of several of these results.

First [Thornton and Guza 1983] propose a full Rayleigh distribution for the probability density function of the wave heights rather than a truncated Rayleigh distribution as used by [Battjes and Janssen 1978] and included a weighted function. As the focus of the study was on planar beaches the differences between the adjusted model and the original model were rather small, although a small over prediction in the high-end tail of the Rayleigh distribution is mentioned, which is probably due to the planar beach. [Battjes and Stive 1985] used an extensive data set for calibration and made a verification of the original wave dissipation model. Most important conclusion was the dependence of the adjustable breaking wave height coefficient y with the offshore wave steepness, which was quantified by best-fitting $y = 0.5 + 0.4\tanh(33s_0)$ with on average $y = 0.73$. They also made a comment on the systematically too far seaward predicted set-up gradient, later explained by a roller model. [Roelvink 1993] investigated, among other things, the probability density function of the wave height distribution. This study concluded that there is no significant difference in outcome using a Weibull distribution instead of a (clipped) Rayleigh distribution, but improved the model internally by adding more physical based parameters compared to the original [Battjes and Janssen 1978] model and made it more applicable for describing also the effect of short waves on wave groups. [Eldeberky and Battjes 1995] developed a spectral version of the bore model that conserved the spectral shape. Among others [Van Rijn and Wijnberg 1996] included the effect of bed slope divided by offshore steepness in the breaker-height parameters, while others studies defined y as function of bed slope only, or as a function of kh [Ruessink et al. 2003]. [Nelson 1997] argued that when having a horizontal bottom over a considerable distance, the breaker parameter is equal to $y = 0.55$. Similar to [Roelvink 1993] (part of) the wave height distribution in the surfzone is also discussed by other studies like [Battjes and Groenendijk 2000].

In the previous mentioned studies, only the energy dissipation on regular planar or barred beaches with mild slopes is discussed. [Baldock et al. 1998] examined the original [Battjes and Janssen 1978] model and the model by [Thornton and Guza 1983] for relatively steep beaches, especially focussing on the wave height distribution. In this study, it was found that a full Rayleigh distribution produces much better results compared to the truncated Rayleigh distribution, because on steep slopes the assumption that all waves higher than the assumed maximum wave height are broken is crude. In contrast, this study changed the underlying model for the proportion of wave breaking of the [Thornton and Guza 1983] model, and found that when the root-mean-squared wave height is close to the maximum wave height, the dissipation rate is even lower than for the original two models. This means that the new model of [Baldock et al. 1998] produces less energy dissipation compared to the [Thornton and Guza 1983] model when the defined maximum wave height is reached. As mentioned in its paper and also confirmed by [Raubenheimer et al. 1996] showing that y would increase and creating more 'shore breaks' when slopes are getting steeper. As for submerged breakwaters often very steep slopes are used, waves can travel far up the SBW before breaking starts, which assumingly comprises an even higher breaker parameter. A note is made by [Janssen and Battjes 2007], when consistently using [Baldock et al. 1998] this will lead to shoreline singularities and a small change is made to this model.

As may be evident from the previous, the wave breaking over a SBW is still under discussion. It can be concluded from [Baldock et al. 1998] that using a full Rayleigh distribution instead of a clipped Rayleigh distribution for steep slopes may be the most important feature for modelling of SBWs. Where others try to include the effect of bed level gradient in the height to depth breaker ratio, including the slightly different wave height distribution seems effective as well. In [Ruessink et al. 2003], which based the model on the work of [Baldock et al. 1998] no relation for the wave height to depth ratio to the bed level was found for steep barred beaches.

### 2.4.3 Roller model

The note made by [Battjes and Stive 1985] on the systematically to far seaward oriented water level gradient due to wave breaking (see next paragraph for this subject) was later explained by a roller model, described by amongst others, [Nairn et al. 1990]. Instead of instant energy dissipation, the energy is first converted to 'kinetic' energy in the surface roller on the wave front travelling with the phase velocity. Differences in velocity of the wave roller and the underlying water particles cause energy dissipation by means of shear stresses. This indirect way of energy dissipation is resulting in a spatial time lag between the point of incident wave breaking and energy dissipation into turbulence, causing a shoreward shift of the water level set-up. To imply this roller model , the original [Battjes and Janssen 1978] model is extended in the energy balance by adding an extra 'roller' term and inherent dissipation relations. The importance of a roller model is studied by amongst others [Reniers and Battjes 1997; Apotsos et al. 2007]

## 2.5 Water level set-up

When waves enter shallow water, first shoaling and later wave breaking starts, causing a significant increase in wave forces. Besides the energy balance, also the momentum balance or flux can be considered, defined by radiation stresses. Horizontal differences in these radiation stresses generate wave-induced forces on the water. These forces are setting of water level gradients or currents depending on local conditions. As these spatial differences in wave breaking and eventual set-up are responsible for rip currents [MacMahan et al. 2006], this process is important to study for SBWs.

In an idealised case of alongshore uniform beaches, the radiation stresses are defined by: [Longuet-Higgins and Stewart 1964]

$$S_{xx} = (n - \frac{1}{2} + n\cos^2\theta)E, S_{yy} = (n - \frac{1}{2} + n\sin^2\theta)E, S_{xy} = S_{yx} = n\cos\theta\sin\theta E \quad (2.9)$$

Gradients in radiation stresses in cross-shore direction are compensated by a water level gradient obeying the first order momentum balance (neglecting the vertical distribution of momentum). This generates set-up or set-down of the water level in the shoaling region and surf-zone. These gradients are quantified by:

$$F_x = -\frac{\partial S_{xx}}{\partial x} = \rho gh\frac{\partial \eta}{\partial x} = \rho g(h_0 + \eta)\frac{\partial \eta}{\partial x} \quad (2.10)$$

In addition to these results, several studies included the effect of the wave roller and the (bottom) stresses, for example [Apotsos et al. 2007]. However, for non-uniform beaches, the cross-shore momentum balance is not necessarily compensated by a water level gradient. Instead, a net acceleration of the water body balances part of the wave induced forces [Bosboom and Stive 2010]. To account for this process, as it is similar to rip current systems at barred beached, the momentum balances result in: (from [Haller et al. 2002]:

Cross-shore direction:

$$\rho(\frac{\partial}{\partial x}(U^2h) + \frac{\partial}{\partial y}(UVh)) + \rho gh\frac{\partial \eta}{\partial x} + (\frac{\partial S_{xx}}{\partial x} + \frac{\partial S_{xy}}{\partial y}) + \tau^b{}_x = 0 \quad (2.11)$$

Alongshore direction:

$$\rho(\frac{\partial}{\partial x}(UVh) + \frac{\partial}{\partial y}(V^2h)) + \rho gh\frac{\partial \eta}{\partial y} + (\frac{\partial S_{yy}}{\partial y} + \frac{\partial S_{xy}}{\partial y}) + \tau^b{}_y = 0 \quad (2.12)$$

Where the radiation stresses for shore normal waves are defined by:

$$S_{xx} = \frac{1}{8}\rho gH^2\left[n(\cos^2\theta + 1) - \frac{1}{2}\right] + \rho gH^2(\frac{0.9h}{L}) \quad (2.13)$$

$$S_{yy} = \frac{1}{8}\rho gH^2\left[n - \frac{1}{2}\right] \quad (2.14)$$

The bottom stress is defined by:

$$\tau_x{}^b = \rho c_f \left\langle |u| u \right\rangle \quad (2.15)$$

In this formulation, $c_f$ is an empirical coefficient and |u| and u are the total near bottom velocity vector and cross-shore component of the near bottom velocity vector.

## 2.6 Wave transmission

Important feature of SBWs is the reduction in wave conditions in the shoreward side of the breakwater. Due to, among others wave breaking, the characteristics that describe the local sea state are changing over a SBW. This paragraph will go into detail about the expected wave height and wave period in the lee of a SBW.

### 2.6.1 Wave height

Depth induced wave-breaking results in a wave height reduction in the lee of the SBW. This is recognised as an important parameter in defining the effectiveness of SBWs as coastal defence system. As these highly complex hydrodynamic processes are depending on multiple parameters, an empirical approach is chosen to define the wave transmission of a SBW to a given sea state.

Earlier studies describing the wave transmission of a SBW were amongst others [Ahrens 1987] and [Van der Meer and d'Angremond 1991]. Several SBW design characteristics are used to quantify the wave transmission, including the use of stone diameter and permeability. To get a more breakwater geometry based relation for wave transmission [D'Angremond et al. 1996] continued the work of [Van der Meer 1990] and reanalysed the previous datasets. Resulting relation for wave transmission excluded the influence of permeability effects and stone diameter. Previous relations are based on low crested structures. [Seabrook and Hall 1998] however, conducted a study on especially SBWs, but also included the effect of stone diameter. During the DELOS project, [Van der Meer et al. 2005] reanalysed the previous relations with the new extended data-set. Previous study of [D'Angremond et al. 1996] shows good predictive skills, but for values of $\frac{B}{H_i} > 10$ the formulation significantly overestimates the wave transmission coefficient ($K_t = \frac{H_t}{H_i}$). Refitting of the formulation for $\frac{B}{H_i} > 10$ led to a new formulation for relative large crest widths. The resulting two formulations for the wave transmission coefficient are:

From [D'Angremond et al. 1996]:

$$K_t = -0.4\frac{R_c}{H_i} + 0.64\left(\frac{B}{H_i}\right)^{-0.31}(1 - e^{-0.5\xi}) \quad for \quad \frac{B}{H_i} < 10 \qquad (2.16)$$

From [Van der Meer et al. 2005]:

$$K_t = -0.35\frac{R_c}{H_i} + 0.51\left(\frac{B}{H_i}\right)^{-0.65}(1 - e^{-0.41\xi}) \quad for \quad \frac{B}{H_i} > 10 \qquad (2.17)$$

Applying both formulas gives a discrepancy in the range of $\frac{B}{H_i} = 10$. Therefore [Van der Meer et al. 2005] suggested to interpolate the two relations for values between $8 < \frac{B}{H_i} < 12$.

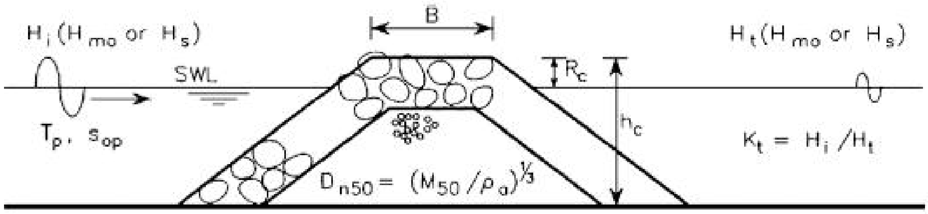


*Figure 2.7 Definitions of governing parameters involved in wave transmission. [Van der Meer et al. 2005]*

As both formulas are conducted using rough rubble mound permeable low crested structures, also smooth impermeable breakwaters are analysed by [Van der Meer et al. 2005]. Smooth impermeable structures are less effective in reducing wave heights. In addition, wave transmission is not depending on the crest width of the SBW. The final relation is [Van der Meer et al. 2005]:

$$K_t = -0.3\frac{R_c}{H_i} + 0.75(1 - e^{-0.5\xi}) \quad for \ \ \xi_{op} < 3 \tag{2.18}$$

The influence of wave angle on wave transmission is also studied by [Van der Meer et al. 2005], in summary:

*Table 2.1 Influence of incoming wave angle on transmitted wave angle and height.*

| | **Transmitted wave angle** | **Influence on transmission coefficient** |
|---|---|---|
| Rubble mound SBW | $\beta_t = 0.8\beta_i$ | No influence |
| Smooth impermeable SBW | $\beta_t = \beta_i$ for $\beta_i \leq 45^0$<br>$\beta_t = 45^0$ for $\beta_i > 45^0$ | $K_t = (-0.3\frac{R_c}{H_i} + 0.75(1 - e^{-0.5\xi}))\cos^{2/3}\beta$ |

When comparing the above formulas with the measured wave transmission coefficients during the DELOS project, the accuracy of the model is obtained. Figure 2.8 shows the differences and scatter of these formulas.

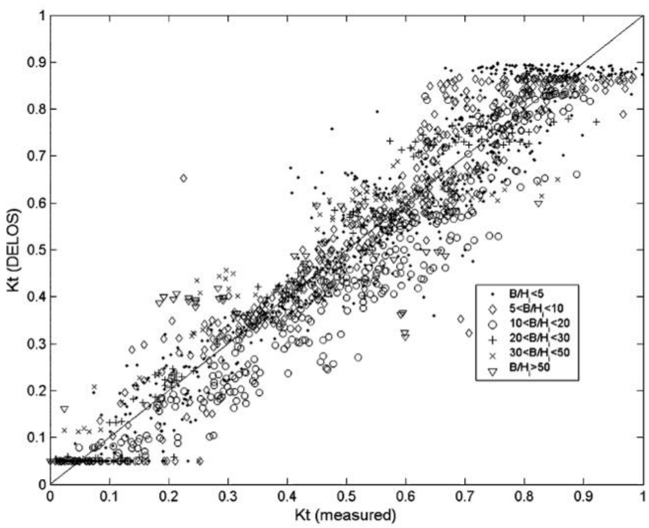


*Figure 2.8 Differences between measured and calculated wave transmission coefficients[Van der Meer et al. 2005]*

As the [Van der Meer et al. 2005] method is only valid for two dimensional wave breaking, three dimensional effects may occur, which were noted by [Seabrook and Hall 1998] . Ignoring the three dimensional character of wave transmission on relative short breakwaters (in alongshore length) may lead to under prediction of wave transmission. [Vicinanza et al. 2009] included the previous mentioned effect of wave diffraction to the wave transmission. Due to the uncorrelated relations between diffraction and wave transmission, the total wave transmission becomes:

$$K_{D,t} = \sqrt{K_D{}^2 + K_t{}^2} \tag{2.19}$$

However, as noted in the earlier paragraphs, the diffraction coefficient is valid only for emerged or low crested breakwaters. For the two-dimensional wave transmission parameter, previous mentioned relations are applicable. It should be noted that, following [Calabrese et al. 2002], the [D'Angremond et al. 1996] method shows the best capabilities in accurately predicting wave transmission, even in presence of broken waves.

### 2.6.2 Wave period

Besides the wave height, also the mean wave period changes over a SBW. Due to a sequence of processes, higher harmonic waves are generated. This generation of higher harmonic waves is responsible for a redistribution of wave energy to these higher harmonic waves. Other hydrodynamic processes, like wave dissipation and morphological changes depend on this wave spectrum information. Studying the offshore wave spectrum propagating onshore, a distinct pattern can be obtained in the shoreward side of a SBW. [Van der Meer et al. 2005], based on previous studies, came up with a crude model for defining the shoreward spectrum at a SBW.

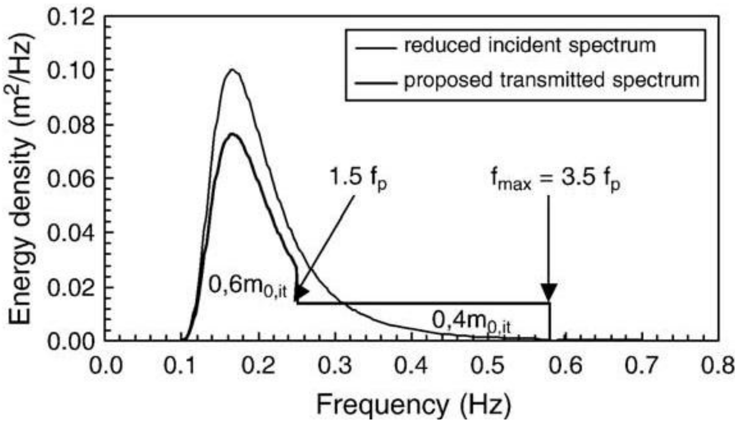


*Figure 2.9 Proposed wave spectrum in the lee side of a low crested structure[Van der Meer et al. 2005]*

As can be seen in Figure 2.9, in general the peak period remains more or less the same, but the mean period changes considerable. As mentioned by [Van der Meer et al. 2005] the above presented model is only applicable for low crested or submerged breakwaters. Cause of this redistribution of energy to higher harmonics was assigned to wave breaking. Wave breaking might generate two or more waves on the lee side of the breakwater.

In contrast, proposed model shows significant resemblances with the results of [Beji and Battjes 1993], although applicability of this study is limited to mild sloping bars. Main conclusion is that wave breaking is only a second order effect in the generation of higher harmonic waves, as there are hardly any differences in spectrum in the shoreward side of the SBW between a breaking wave field and a non-breaking wave field. More important are the processes of non-linearity and dispersion, which are dependent on the depth-to-wave-length ratio. When long waves propagate up-slope of a SBW, shoaling starts and the original linear waves deform asymmetrical. During this process, second order harmonics are generated by self-interactions. On the breakwater crest, triad wave-wave interactions redistribute the energy from lower harmonics to the generated higher harmonics. This energy distribution also sets of a so-called dispersive tail with nearly the same celerity, due to the limited influence of wave period on the celerity. This dispersive tail is also clearly visible in Figure 2.9. When further propagating down slope into deeper water behind the SBW, readjustments of energy distribution take place, due to the 'inverse' shoaling effect. Resulting in a similar normalised wave spectrum as proposed later by [Van der Meer et al. 2005].

Concluding, for defining especially the mean wave period in the shoreward side of the SBW for local processes like morphological changes, the spectral evolution is important. Following [Beji and Battjes 1993] the generation of higher harmonic waves is mainly depending on the initial wave periods/ wave lengths, rather than wave breaking. The peak period remains roughly the same, although it may be questionable not to account for the different energy distribution for other processes depending on the (peak) wave period.

## 2.7 Water level set-up and mass-transport over submerged breakwaters

Due to depth-induced wave-breaking, part of the difference in radiation stresses is compensated by a water level gradient. Important factor in this process is the wave induced net mass transport over a submerged breakwater. To obey the mass-balance this flow needs to return offshore by a return current. On a regular alongshore uniform beach, the depth averaged zero mass-transport results in an equilibrium between the Stokes drift and undertow. Submerged breakwaters are not bounded by a net zero mass-transport over the submerged breakwater crest. This paragraph will go more in detail about the processes described in previous paragraphs, but focussing on SBWs specifically. Due to these specific cases, new studies are presented.

### 2.7.1 Mass-transport over submerged breakwaters

One of the main differences between an emerged breakwater and a submerged breakwater is the net transport of water over the breakwater. This process is induced by, amongst others, the stokes drift and differences in radiation stresses.[Lesser et al. 2003]. In order to obey the mass balance the mass-transport can be compensated by a return current /undertow, porous flow trough the breakwater or an alongshore return current out of the shadow zone depending on the breakwater dimensions and permeability [Loveless et al. 1998; Calabrese et al. 2008].

[Calabrese et al. 2008] quantified the mass-transport over SBWs. The authors reasoned that, although this topic is still under discussion, the mass transport over the breakwater might be compared with the general theory for mass transport in the surf zone. [Svendsen 1984] quantified the total mass drift, due to the orbital motion and surface roller contributions. Following [Svendsen 1984] and the changes made by [Hansen 1990] the relation for mass transport over a SBW results in:

$$q_{in} = \sqrt{gh}H(B_0 \frac{H}{|R_c|} + 0.06) \tag{2.20}$$

Of which $H = H_i \frac{(1+K_t)}{2}$, to account for the wave breaking over the SBW. $B_0$ is the wave shape factor defined by using the cnoidal wave theory depending on the Ursell parameter: $B_0 = 0.125\tanh(\frac{11.4}{\sqrt{U_r}})$, applicable for narrow crested breakwaters. The Ursell parameter is defined as $U_R = \frac{2\pi}{s_0}(\frac{H_i}{|R_c|})^2(1+\frac{H_i}{|R_c|})$ when wave breaking occurs near the crest.

### 2.7.2 Water level set-up over submerged breakwater

As described, differences in wave radiation stresses are in cross-shore direction partly compensated by a water level gradient. To ensure the mass balance is obeyed, the mass transport has to return offshore due to a flow forced by a continuity set-up [Bosboom and Stive 2010]. This paragraph will describe both the momentum flux as well as the continuity contribution to the water level gradient over a submerged breakwater.

An interesting overview of the development and understanding of water level set-up is given by [Calabrese et al. 2008]. One of the first studies that quantified the water level differences analytically between two regions is [Longuet-Higgins 1967]. Based on this results the water level set-up for submerged breakwaters becomes (from [Calabrese et al. 2008]):

$$\delta' = \frac{H_i^2(1+K_R^2)k_1}{8\sinh(2k_1h_1)} - \frac{H_i^2K_t^2k_2}{8\sinh(2k_2h_2)} \tag{2.21}$$

In this expression, the importance of wave reflection is accounted. Several authors came up with new empirical formulas, as this relation is only valid for harmonic incident waves and significantly underestimates water level set-up when breakwaters are close to the shoreline. [Dalrymple and Dean 1971] used a new approach, by dividing the total set-up by contributions of the wave induced momentum flux and the return current to compensate the mass transport over the breakwater. For the momentum flux contribution a similar approach based on the results of [Longuet-Higgins 1967] was used, while for the continuity set-up a return current over the crest is assumed when the ‘pilling up’ of water is in equilibrium with the return current forced by an additional water level gradient. [Loveless et al. 1998] reasoned that part of the return current is due to porous flow trough the breakwater, creating a misbalance in the mass-balance and focussed on the water level set-up due to this mass transport.

Previous models encountered several simplifications, which was the reason for [Calabrese et al. 2008] to present an alternative method, based on the [Dalrymple and Dean 1971] model. The momentum flux contribution is accounted, but the generation of higher harmonics, wave shoaling, and initial water level set-up/down are neglected. In addition, by assuming a flat bottom, the momentum flux contribution to the set of equations for describing the water level set-up is:

$$\delta_{mf} = 0.5(-b + \sqrt{(b^2 - 4c)}) \tag{2.22}$$

$$b = (2h - A) \tag{2.23}$$

$$A = (1 + \frac{x_b + B}{L_s})h_c - (x_b \frac{h_b + R_c}{L_s}) \tag{2.24}$$

$$c = -\frac{1}{8} H_i^{\,2} (1 + \frac{4kh}{sinh(2kh)})(1 + K_r^{\,2} - K_t^{\,2}) \tag{2.25}$$

For the continuity water level set-up the process of a return current over the breakwater crest in seaward direction is leading. This current is forced by an additional continuity water level set-up and described by a Gauckler-Strickler formula for uniform turbulent flows, which results in the expression [Calabrese et al. 2008]:

$$\delta_c = \frac{q_{in}}{f^2 \left|R_c\right|^{10/3}} \frac{A_c}{h_c} \tag{2.26}$$

With f being Manning's friction parameter and A the cross sectional area of the breakwater. The mass-transport is already defined in previous paragraph according to [Svendsen 1984]. It is further noted that although included in [Calabrese et al. 2008], the wave reflection has little influence and may be neglected from the equations.

Disadvantage of the [Calabrese et al. 2008] model for applying it in practice, is the two dimensional approach. For describing shoreline changes the alongshore dimension, especially the breakwater length, is of influence for a variety of processes. Despite this simplification, the underlying theories are similar for three-dimensional applications. Nevertheless, the model is an upper limit for wave induced water level set-up over a breakwater and shows that due to the zero mass-transport relation water level set-up increases.

## 2.8 Flow patterns

Gradients in water level, or hydraulic head, generate a current. These currents are important for transporting sediment to or from the shoreward side of the submerged breakwater. The total current pattern around a SBW is a good indication of the initial shoreline response to SBWs [Ranasinghe et al. 2010]. Although the cause of these patterns is still under discussion, several qualitative results are published.

### 2.8.1 Horizontal flow structure

The idea that the resulting depth-averaged current around a SBW is responsible for shoreline changes, is not new. Among others, [Dean et al. 1997] already mentioned that the cause of the additional shoreline erosion was probably due to the alongshore current generated by the submerged breakwater. Several studies describe these currents qualitatively, of which [Ranasinghe et al. 2006] gives a clear view on possible currents, resulting two distinct initial 2/4cell patterns. Despite the somewhat different shape of the SBW to induce surfing capabilities, the described patterns showed good resemblances with previous scale tests and numerical models [Dean et al. 1997], [Torrini 1997], [Schaap 1997] and [Lesser et al. 2003].

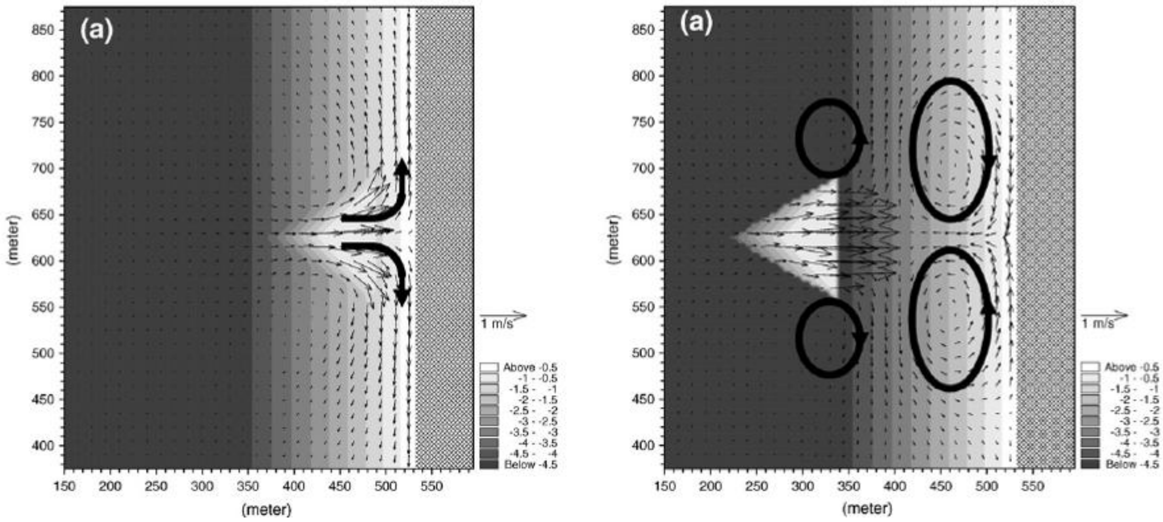


*Figure 2.10 Left: erosive 2 cell current pattern, right: 4cell accretive current pattern.[Ranasinghe et al. 2010]*

It is clear from Figure 2.10, when the current close to the shoreline is in the direction of the lee of the SBW, sediment is also transported to the lee of the SBW. The erosive horizontal flow structure results show good similarities with results obtained from rip current experiments, Described in for instance [Haller et al. 2002] [MacMahan et al. 2006] and [Dalrymple et al. 2011]. For SBWs [Ranasinghe et al. 2010] quantified this initial mode of accretive or erosive shoreline changes.

### 2.8.2 Vertical flow structure

Besides the depth-averaged horizontal flow structure, also the vertical flow structure is of interest, as this vertical flow structure determines the direction of bottom stresses. One of the recent studies on the effect of vertical flow structures on water level set-up is [Apotsos et al. 2007] for an uniform coastline. In this paper, the essence of bottom stresses is given; *“In the absence of breaking waves, an onshore directed streaming flow in the viscous boundary layer results in an offshore-directed bottom stress. However breaking waves in the surf zone drive an offshore-directed current (undertow) that dominates the onshore streaming, resulting in an onshore directed bottom stress that increases set-up in shallow water”*. Based on [Reniers et al. 2004] the principle of undertow is to a large extend depending on the alongshore uniformity of the beach. [Haller et al. 2002] discussed the direction and magnitude of bottom stresses for barred beaches, but concluded that the relative importance is low and direction questionable for the cross-shore momentum balance over a barred beach. In the overview on vertical flow structures on barred beaches [MacMahan et al. 2006] notes that for the RIPEX experiment the flow was mostly either shoreward or alongshore and no undertow occurred. For SBWs this is in agreement with previous numerical results of [Lesser et al. 2003], see Figure 2.11.

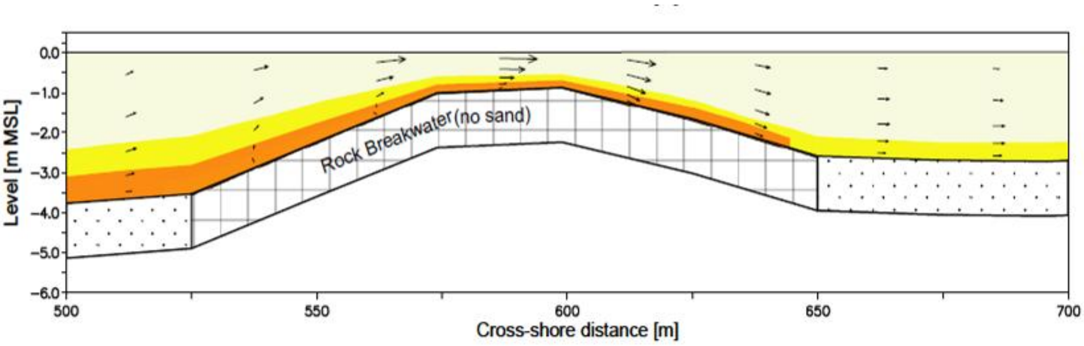


*Figure 2.11 Time averaged vertical flow profile over an submerged breakwater. [Lesser et al. 2003]*

## 2.9 Morphology

The flow and wave orbital motions near the bed described in previous paragraphs induce bed shear stresses, which when above the critical bed shear stress, starts to move the sediment. Gradients in this transport mechanism are cause of local erosion or accretion. From the initial current patterns and magnitudes from Figure 2.10 bed level changes are expected. Despite the fact that the concept of SBWs is not well understood, and morphological scale test are hard to compare with real life cases, still some predictions are made on the resulting bed level changes.

### 2.9.1 Scour around submerged breakwaters

When waves break over a SBW, many processes start. Turbulence, wave motions, mass-transport over the crest, induced averaged currents etc; all have influence on the morphological processes around a SBW. Problems with scour holes close to the breakwater, causing instabilities of the SBW, gave rise to several studies on this subject. Amongst others, [Sumer et al. 2005] and [Young and Testik 2009] studied these processes and quantified the possible scour statistics. The first of the two studies quantified the offshore scour around SBWs due to amongst others the partial standing wave field. In addition, the SBW roundhead scour was considered due to the alongshore flow forced by the mass-transport over the SBW. The later one studied the onshore scour patterns, which are defined as “attached” and “detached” scour. Main differences are in the dominant processes forcing the onshore side of the submerged (vertical) breakwaters. The two important driving forces are the turbulence generated by the wave jet ‘plunging’ into the water at instant wave breaking and the generation of a vortex, due to the shear stresses in the water column and mass balance due the two dimensional approach. To illustrate these patterns, Figure 2.12 shows this distinct scour, while Figure 2.13 illustrates the vortex generation over a vertical breakwater. However, for mildly sloping SBWs this vortex is not generated, see Figure 2.11.

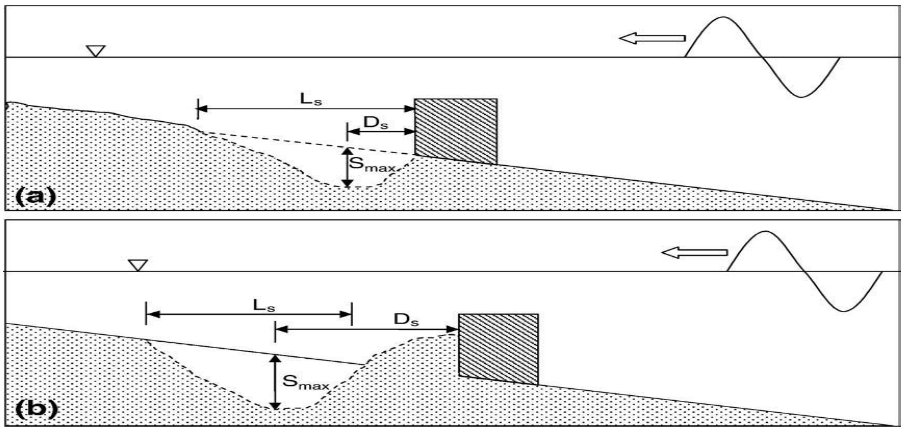


*Figure 2.12 Scour patterns, "attached" and "detached" scour. [Young and Testik 2009]*

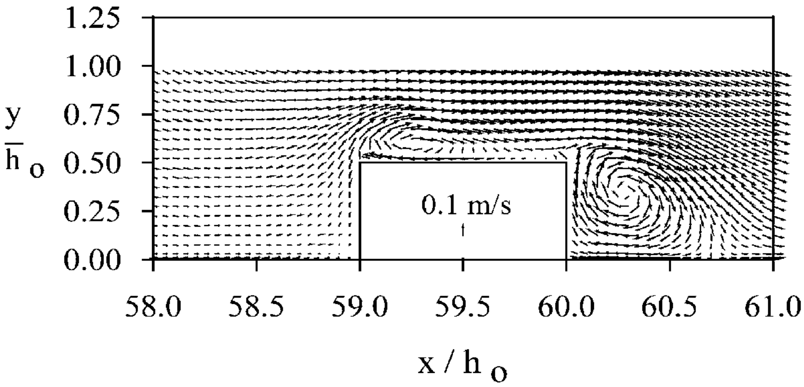


*Figure 2.13 Vortex generation on vertical breakwater.[Huang and Dong 2001]*

### 2.9.2 Submerged breakwater induced shore line changes

As described in previous paragraphs, the flow field generated by the SBW on an uniform coastline, may be of an erosive 2 cell- or accretive 4 cell pattern.[Ranasinghe et al. 2010]. A summation of constructed breakwaters in [Ranasinghe et al. 2006] shows that despite all the good intentions, in 70% the SBW cases only induced extra erosion instead of accretion. This shows that still a lot is yet to be discovered in the complex forcing mechanism for shoreline accretion.

Due to this complexity and difficulties of scale effects in morphological processes in physical model tests only a few relations for shoreline changes due to SBWs are published in literature. Often SBWs are simulated using numerical models, but, as for the reason of this thesis, a clear process based description why these morphological changes occur is lacking.

One of the first studies to describe the formation of a salient on the shoreward side of a submerged breakwater is [Black and Andrews 2001a]. In this study, the effect of a SBW is compared to natural reefs, using aerial photographs from the coast of Eastern Australia and New Zealand. The resulting relation indicates the importance of the offshore distance and breakwater length for the formation of a salient. As previous paragraphs have shown, multiple processes play part in shoreline changes, which are not solely based on breakwater length and distance. However, given the strong relation, the importance of these parameters is evident. In addition, due to the methodology used, erosion was not considered.

Likewise, [Ranasinghe et al. 2006] presented an indicative relation for the shoreline response to SBWs. Similar to the previous study, the dimensions of the salient are related to the offshore distance and alongshore breakwater length, but the possible erosive changes are included.

A more intensive study on the initial mode of shore line response with use of numerical modelling is done by [Ranasinghe et al. 2010]. This study resulted in physical based relation for the mode of shoreline response to SBWs and more breakwater design parameters were included. The final relation obtained during this study is:

$$\frac{h_B}{H_0} = 2\log_{10}[(\frac{s_B}{h_B})^{3/2}(\frac{L_B}{h_B})^2(\frac{A^3}{h_B})^{1/2}] + 0.65 \tag{2.27}$$

Although physical relations are presented in the non-dimensional parameter analysis, a clear description of driving processes is difficult, which implies the complexity of submerged breakwater induced shoreline response.

From above its evident, that clear insight in the effects of submerged breakwater is still lacking and further research is needed to tackle the physics behind shoreline response to SBWs.

## 2.10 Modelling of shoreline response to submerged breakwaters

In addition to the previous paragraphs, the complexity of SBWs is evident. A common approach to get insight in the hydrodynamic and morphological processes is by means of numerical modelling. By applying numerical modelling often other difficulties rise, however numerous successful attempts have been published. In [Burcharth et al. 2007] an overview is given of all the considerations for applying numerical models, of which the most important are the choice of a phase-averaged or phase-resolving wave model and a depth-averaged approach or full three dimensional computations. This choice depends amongst others on time scales of processes, accuracy, level of interest and computational time. Also an overview in [Burcharth et al. 2007] is given of different models applied to submerged breakwaters. Two of those models are presented here.

After earlier attempts of [Schaap 1997; Torrini 1997] in modelling SBWs with Delft3D, [Lesser et al. 2003] conducted a series of modelling test with the full three dimensional model of Delft3D to implicitly include the effects of undertow, wave forcing and different sediment transports. Previous problems of Delft3D with the correct wave height decay and shoreline morphology are addressed with new empirical improvements of Delft3D. Although a major step forward, some difficulties remained in modelling of SBWs. [Johnson 2006] describes the adaptations made to the wave dissipation model in a phase-averaged model (MIKE 21) to satisfactory obtaining wave transmission over a SBW. From both studies, it is evident that obtaining the right order of wave height decay is difficult, but important. Continuing the study of [Johnson 2006], the study of [Johnson et al. 2005] (published earlier) focused on modelling the wave and current field around a SBW with a phase resolving model, as well as a phase averaged model in a two dimensional depth averaged approach. Concluded from this study, both approaches are capable of representing good predictions for SBWs. Previous mentioned study of [Ranasinghe et al. 2010] used this phase averaged model MIKE 21 to predict SBW induced morphological changes.

# 3 Numerical modelling with Delft3D

## 3.1 Introduction

In order to study the hydrodynamic processes, numerical modelling can be a powerful tool. Numerical modelling is relative cheap compared to conducting extensive field- or scale model measurements and allows studying individual processes or individual design parameters relatively easy for idealized conditions.

Based on [Burcharth et al. 2007], several considerations contribute to the choice of which numerical model to use, for example the required accuracy of wave/flow conditions, the dominant physical processes to be reproduced, budget, time/computational efficiency etc. Because of these considerations, the software package Delft3D is used, developed by Deltares. Delft3D is capable of representing all the important hydrodynamic and morphologic processes accurately in a limited amount of computational time for longer (morphological) time scales [Deltares 2010a]. In addition, Delft3D has proven to be a robust model in a variety of coastal problems[Lesser et al. 2004]. To reduce the computational time, but still reproduce accurate results, a depth-averaged approached is used.[Johnson et al. 2005]

In this chapter, a brief description of Delft3D is given, as well as the model set-up used during this thesis. In addition, a sensitivity analysis of the numerical parameters and a validation of individual SBW induced processes in Delft3D are presented.

## 3.2 Delft3D

The Delft3D software package (v.3.28.10) is a modelling system that consists of a number of integrated modules in a shared user interface, which together allow to simulate a variety of physical processes. The main module is the Delft3D-Flow module. In this thesis, the Delft3D-flow module is online-coupled to the SWAN wave model to accurately simulate near-shore hydrodynamics. This paragraph will give a brief description of both modules, for more detail see [Deltares 2010a; Deltares 2010b]. A schematic overview of this coupled system is shown in Figure 3.1.

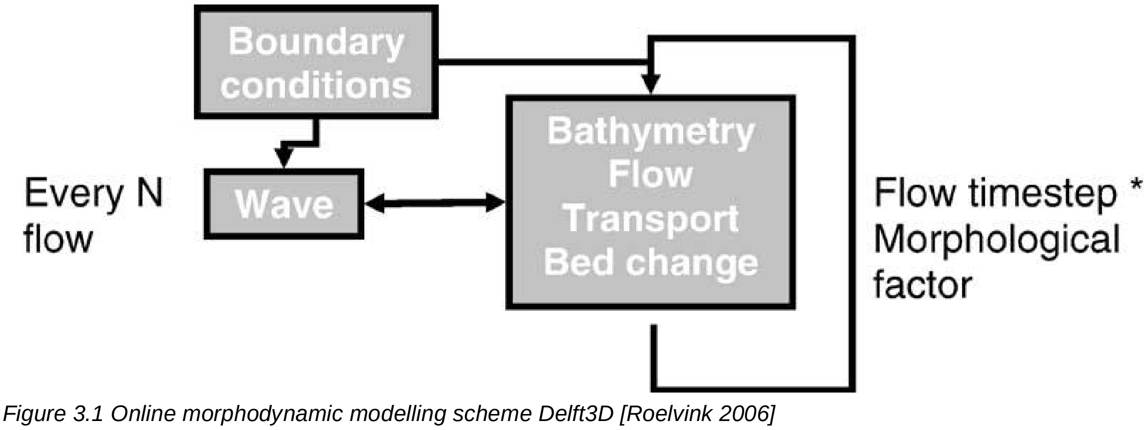


*Figure 3.1 Online morphodynamic modelling scheme Delft3D [Roelvink 2006]*

### 3.2.1 Delft3D-Flow

Delft3D-Flow is a non-stationary process based numerical model, which solves the Navier-Stokes equations for an incompressible fluid under the shallow water and bousinesq assumptions. In the vertical the Navier-Stokes equations reduce to the hydrostatic pressure assumption, so vertical accelerations are neglected. For the computation of the suspended sediment transport, an advection-diffusion equation is used. For the governing equations see [Lesser et al. 2004; Deltares 2010a].

### 3.2.2 SWAN

Delft3D-WAVE, or better known as SWAN [Booij et al. 1999; Deltares 2010b], is a third generation spectral wave model using an Eulerian approach. In SWAN, the evolution of wind-generated waves is based on a two-dimensional wave action-density spectrum and is calculated simultaneously for each point in space. SWAN is capable of simulating wave propagation, wave generation by wind, non-linear wave-wave interactions and wave energy dissipation for given conditions like bathymetry, wind, flow and water level. By online coupling of SWAN to Delft3D-flow, wave-induced processes like, wave induced (shear) stresses, and additional turbulence are accounted in the flow computations.

## 3.3 Model approach

In order to include the bed level changes for the wave calculations, an online coupling of the Delft3D-Flow module and SWAN is made. In contrast to [Lesser et al. 2003] , the effect of the SBW on the wave field is taken into account by depth induced wave breaking instead of empirically with the results of, for instance [Seabrook and Hall 1998; Van der Meer et al. 2005]. As noted by, amongst others, [Lesser et al. 2003] for obtaining the wave height decay, mild slope equations may not always provide accurate results for steep slopes and narrow crested SBWs, but results from [Booij 1983] may suggest that using mild slope equations can be accurate up to slopes of 1:3. In addition, this thesis focuses' on the individual spatial varying processes, so it may be more satisfactory to be able to study the spatial distribution of wave breaking/ transmission. To study the accuracy of this approach, a validation of Delft3D on individual processes is included. This paragraph will briefly explain the considerations of the Delft3D model set-up.

### 3.3.1 Delft3D-Flow set-up

#### *3.3.1.1 Grid*

The numerical model of Delft3D-FLOW is based on finite differences. In order to solve the mathematical formulations of Delft3D-FLOW, the shallow water equations are discretized in time and space. For the spatial discretization based on the finite differences approach, a staggered grid is used. For simulation of an idealized SBW, a two dimensional (depth-averaged) grid containing 200x175 (alongshore and cross-shore) grid cells is used, of which the apex of the structure in alongshore direction is situated in the centre (y=1500m), see Figure 3.2. The grid cell resolution of the flow grid is constant: 5x10m (cross- and alongshore direction). These dimensions confine the breakwater dimensions to certain extend, but differences in results are expected to be small compared to the gain in computational efficiency. The latitude and longitude in Delft3D are set to zero degrees, to exclude Coriolis forces.

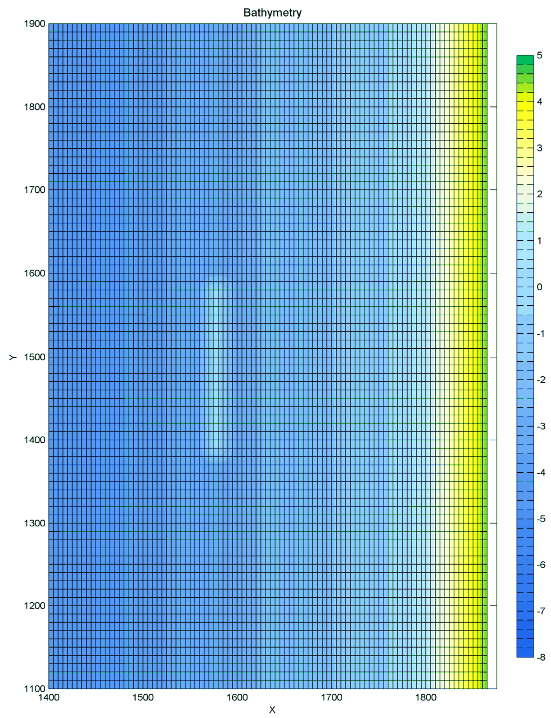


*Figure 3.2 Flow grid and bathymetry submerged breakwater.*

#### *3.3.1.2 Bathymetry*

To satisfactory obtain a universal idealized approach; an alongshore uniform bathymetry is used. In cross-shore direction, the bathymetry matches the Dean's equilibrium profile, with a depth of 8m at the offshore boundary, see Figure 3.3. To include the SBW, the bathymetry is locally changed based on the design parameters like slope, crest width and crest submergence level. To avoid errors due to, amongst others, using the mild slope equations for wave breaking and the lack of vertical accelerations (shallow water equations assumption) in the Delft3D-flow module, a relatively mild breakwater slope (tan $\alpha$=1:5) compared to constructed SBWs is used. Though local bathymetry of the initial alongshore uniform beach and breakwater slope are of influence on several processes [Van der Meer et al. 2005], in this thesis these parameters remain constant.

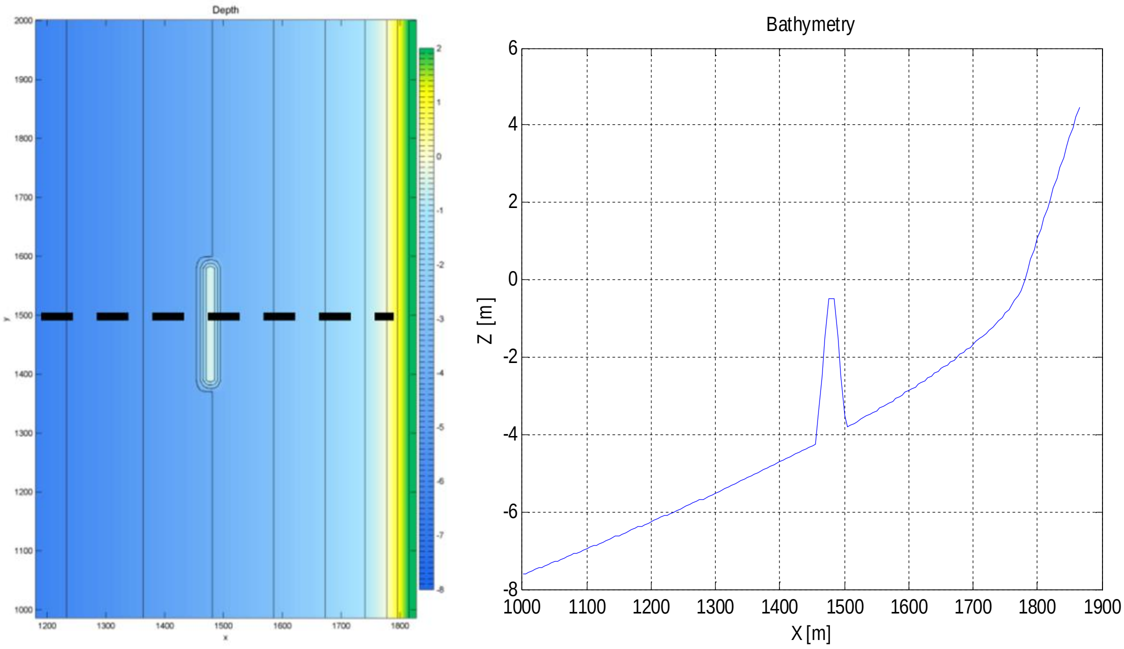


*Figure 3.3 Example cross-section bathymetry submerged breakwater*

### *3.3.1.3 Time Frame*

As discussed the numerical model of Delft3D-Flow is based on finite differences. To discretize the equations in time, different schemes can be used. Explicit schemes are preferred in numerical modelling when it comes to computational efficiency. In contrast to implicit schemes, explicit schemes are fast, but require a limited time step to maintain stable. To improve computational efficiency of implicit schemes, the Alternate Direction Implicit (ADI) method is used. The ADI method splits one time step into two stages. For both stages all the equations within Delft3D are solved in such a consistent way that the accuracy in space is at least second order. Despite the fact that the implicit scheme is unconditionally stable, for accuracy constrictions the Courant number should be less than:

$$C_f = 2\Delta t \sqrt{gH\left(\frac{1}{\Delta x^2} + \frac{1}{\Delta y^2}\right)} < 4\sqrt{2} \tag{3.1}$$

Based on this time step limitation, a time step of 0.05 minutes is used. The total simulated hydrodynamic time of each run is 12 hours (spin up interval) for hydrodynamic computations and 6.5 days (including spin up time) for morphologic computations (to reach an equilibrium profile), which is comparable to 90 days on morphological time scale with a morphological factor of 15, see paragraph 3.4.

### *3.3.1.4 Processes and initial conditions*

To obtain a universal idealized approach as much as possible, only sediments (constituents) and waves by online coupling with SWAN (physical) are taken into account, while wind is neglected. The initial conditions, water level and initial sediment concentration remain zero.

#### 3.3.1.5 Boundary conditions

The Northern and Southern boundary conditions for the flow grid consist of Neumann boundaries [Roelvink and Walstra 2004]; and the Western offshore boundary is an open water level boundary. This results in a well posed numerical model of a coastal system [Stelling 2009]. As mentioned previously, tide is not included. Paragraph 3.5 will show that, in agreement with the statements of [Ranasinghe et al. 2010] the (vertical) tide can be neglected for morphological processes. As discussed previously, the tide can have considerable effect on (time varying) hydrodynamics and shoreline changes[Baldock et al. 2010].

#### 3.3.1.6 Physical parameters

The physical parameters for Delft3D-Flow used are defined in Table 3.1. Comments on these parameters:

- Bottom roughness; to account for the differences in bottom roughness in Delft3D-Flow between a sandy bottom and the (rough) SBW, a spatial varying Chezy coefficient is used. [Lesser et al. 2003] used the bottom roughness as a calibration parameter for the depth-averaged transport of water over the SBW. In addition to literature on the momentum balance and especially the bottom stresses [Haller et al. 2002], paragraph 4.5.4 will show the importance of the spatial varying bottom roughness.
- Horizontal eddy viscosity; In the sensitivity analysis a HLES run is made, as the horizontal eddy viscosity parameter is a calibration parameter to account for turbulence and scale effects instead of representing the actual viscosity. However, horizontal differences in the horizontal eddy viscosity will only have a small effect, so a constant horizontal eddy viscosity will suffice for accurate results. [Apotsos et al. 2007]
- Median sediment diameter; as this thesis is focusing on establishing the relation between the initial and individual processes, which drives shoreline changes, the median sediment diameter is kept constant, despite of its influence it has on hydrodynamic and morphologic processes.
- Initial sediment layer thickness; to include the “non erosive” SBW, locally an initial sediment layer of zero is formulated. For the surrounding bathymetry, the bottom consist of a sediment layer of 5m, enabling no restrictions on morphological changes.
- Wave related suspended and bed load transport. The wave related- and suspended bed load transport factor are calibration parameters to account for the wave related transport. Despite the importance of these parameters at first glance, including these parameters, even for low values, sets of unrealistic net onshore sediment transports, including for the undisturbed coastline. Due to time constraints, these parameters are not further studied and set to zero to obtain satisfactory morphological changes.

*Table 3.1 Physical parameters Delft3D Flow*

| Subject | Parameter | Settings |
|---|---|---|
| Constants | Gravity | 9.81 $m/s^2$ |
| | Water density | 1025 $kg/m^3$ |
| | | |
| Roughness | Bottom roughness formula | Chezy |
| | Uniform/file | From file (see comment) |

| | | |
|---|---|---|
| | Stress formulation due to wave forcing | Fredsoe |
| | Slip condition (wall roughness) | Free |
| | | |
| Viscosity | Background horizontal viscosity / diffusivity | Uniform |
| | Horizontal eddy viscosity | 1 $m^2/s$ ,see paragraph 3.4 |
| | Horizontal eddy diffusivity | 0.5 $m^2/s$ |
| | | |
| Sediment | Sediment sand | |
| | Reference density for hindered settling | 1600 $kg/m^3$ |
| | Specific Density | 2650 $kg/m^3$ |
| | Dry bed density | 1600 $kg/m^3$ |
| | Median sediment diameter $d_{50}$ | 250 µm |
| | Initial sediment layer thickness at bed | From file, see comment |
| | | |
| Morphology | Update bathymetry during FLOW simulation | True |
| | Include effect of sediment on fluid density | False |
| | Equilibrium sand concentration profile at inflow boundaries | True |
| | Morphological scale factor | 15, see paragraph 3.4 |
| | Spin-up interval before morphological changes | 720 min |
| | Minimum depth for sediment calculation | 0.1 m |
| | Van Rijn's reference height factor | 1 |
| | Threshold sediment thickness | 0.05 m |
| | Estimated ripple height factor | 2 |
| | Factor for erosion of adjacent dry cells | 1 |
| | Current-related reference concentration factor | 1 |
| | Current-related transport vector magnitude factor | 1 |
| | Wave-related suspended transport factor | 0 |
| | Wave-related bed load transport factor | 0 |

#### *3.3.1.7 Numerical parameters*

The numerical parameters used in Delft3D-Flow, are presented in Table 3.2. Comments on these parameters:

- Advection scheme for momentum; for the numerical scheme of the advection terms of the momentum balance several options are available [Deltares 2010a]. Based on the description of these schemes, the Flood scheme may be the preferred choice for steep slopes. A sensitivity analysis (not shown here) of the schemes shows that there are no significant differences between these schemes. Therefore, the default option in Delft3D-Flow, a cyclic scheme is used.

*Table 3.2 Numerical parameters Delft3D Flow*

| Subject | Parameter | Settings |
|---|---|---|
| Numerical parameters | Drying and flooding check | Grid cell centres and faces |
| | Depth specified at: | Grid cell centres |
| | Depth at grid cell faces | Mor |
| | Threshold depth | 0.1 m |
| | Marginal depth | -999 m |
| | Smoothing time | 60 m |
| | Advection scheme for momentum | Cyclic |
| | Advection scheme for transport | Cyclic |
| | Forester filter horizontal | on |

#### *3.3.1.8 Additional parameters and output*

Especially for the output parameters, the Delft3D flow model settings are mainly depending on the level of interest, so only comments on part of the parameters are given.

- Additional parameter: Cstbnd #yes#; To avoid the creation of artificial boundary layers at the offshore boundaries (due to the advection terms), the advection terms containing normal components are switched off.[Deltares 2010a]
- Additional parameter; Msflux #false#. In order to obtain morphological satisfactory results, the mass flux term, which accounts for the (wave induced) onshore directed sediment transport, should be set off. This term is however not standard included in Delft3D, so a research version is used. (See paragraph 3.4.1.5)
- No transport formulation is defined, so the standard option (the transport formula of van Rijn [Van Rijn 1993; Deltares 2010a]) is used. It is reasoned that after each simulation the bathymetry behind the SBW will be in equilibrium with the (constant) offshore wave forcing. Therefore, no significant differences are expected using different transport formulations.
- Output: Store: communication file interval (coupling interval); The online coupling of Delft3D-Flow and SWAN is defined by a period after which these modules exchange information, see Figure 3.1. For a rapidly varying morphological system, this interval is set to 10 min, see paragraph 3.4

### 3.3.2 SWAN set-up

#### *3.3.2.1 Grid and bathymetry*

The wave grid used, consist of 89 cross-shore- and 289 alongshore grid cells. The grid-cell resolution smoothly varies from 40x10m offshore (cross and alongshore direction respectively), to 5x10m near shore, where the SBW is constructed, hereby overlaying the flow grid abundantly to avoid boundary problems, see Figure 3.4. The bathymetry used in the wave computations result from the flow grid (online) coupling and is extended with the boundary values.

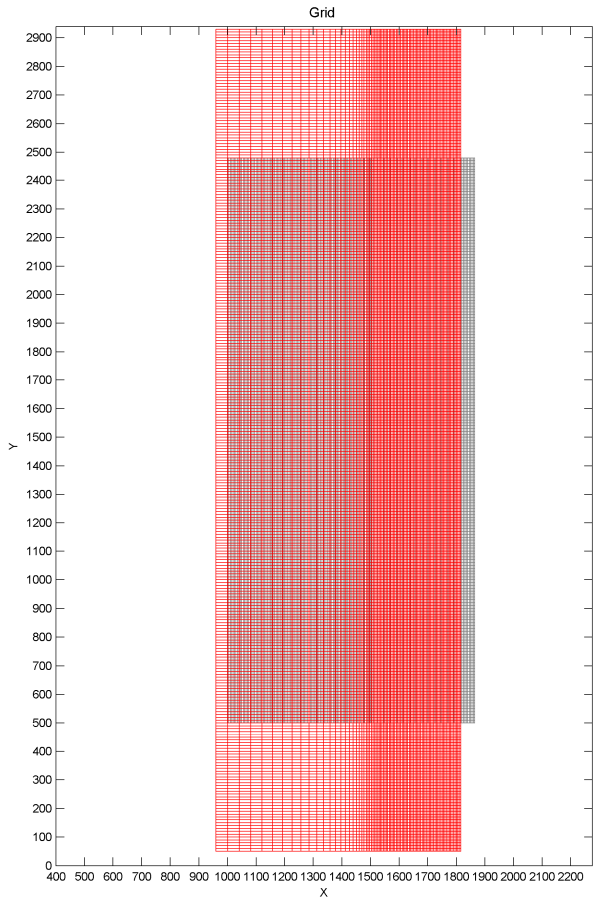


*Figure 3.4 Grids, red: SWAN grid, gray: Delft3D flow grid*

To simulate the spectral evolution of waves, SWAN distributes the wave energy in directional and frequency bins. For this thesis, 72 directional bins are used, to illustrate the effect of the directional spreading of waves, see paragraph 2.2. Focussing on the offshore short wave forcing as driving mechanism for near-shore changes, 24 wave frequency bins are used in the range of 0.05 Hz to 1 Hz.

To account for the flow-wave coupling, the water level, current and bathymetry from the Delft3D Flow results are used in SWAN, see paragraph 3.4.

#### *3.3.2.2 Boundaries*

For the offshore boundary, as well as for the Northern and Southern boundaries, the JONSWAP spectrum is used with a peak enhancement factor of 3.3. For the directional spreading, the cosine and gamma function are used, see paragraph 2.2. The uniform and stationary boundary conditions in time and space can be defined by Hs=1.5m, Tp=9s, shore normal wave direction ($\theta=270^0$) and a directional spreading of m=4, but may vary throughout this thesis, as these parameters are important for a diversity of hydrodynamic processes, see chapter 2.

#### 3.3.2.3 Physical parameters

Table 3.3 summarizes the physical parameters used for SWAN. Comments:

- Wave set-up and forces; to account for the effect of wave forcing in the Delft3D-Flow module, radiation stresses are exchanged from SWAN to Delft3d-Flow. To avoid accounting twice for these radiation stresses, the water level set-up is not taken into account in the SWAN computations.
- Depth induced wave breaking; The spectral version [Eldeberky and Battjes 1995] of the original model of [Battjes and Janssen 1978] including the averaged maximum wave height to depth ratio from [Battjes and Stive 1985] is used, despite of the discussion presented in paragraph 2.4. Paragraph 3.4 will go in more detail about this decision.
- Non-linear triad wave interactions; although the generation of higher harmonic waves has a profound effect on near shore hydrodynamics, see paragraph 3.5, due to stability reasons non-linear triad wave interactions are switched off.
- Bottom friction; where bottom friction is important for Delft3D-Flow computations, in the wave module a constant bottom friction coefficient is used, as depth-induced wave breaking is the dominant process of energy dissipation. [Van der Meer et al. 2005]
- Diffraction; Despite the course grid resolution and lacking theory of diffraction for submerged breakwaters, diffraction is taken into account for the SBW simulations using default settings, due to its influence on near shore processes, see paragraph 3.5.

*Table 3.3 Physical parameters SWAN*

| **Subject** | **parameter** | **Settings** |
|---|---|---|
| Constants | Gravity | 9.81 m/s$^2$ |
| | Water density | 1025 kg/m$^3$ |
| | North w.r.t. x-axis | 90 degrees |
| | Minimum depth | 0.05 m |
| | Convention | Nautical |
| | Wave set-up | none |
| | Forces | Radiation stresses |
| | | |
| Processes | Depth-induced wave breaking | [Battjes and Janssen 1978] model |
| | Alpha | 1 |
| | Gamma | 0.73 |
| | Non-linear triad interactions | Off |
| | Bottom friction | On |
| | Bottom friction type | JONSWAP |
| | Bottom friction coefficient | 0.067 m$^2$s$^{-3}$ |
| | Diffraction | On |
| | Smoothing coefficient | 0.02 |
| | Smoothing steps | 5 |
| | | |
| Various | White capping | Off |
| | Refraction | On |
| | Frequency shift | On |

#### 3.3.2.4 *Numerical parameters*

Table 3.4 summarizes the settings used for the numerical parameters in SWAN. Paragraph 3.4 will go in more detail on the used settings.

*Table 3.4 Numerical parameters SWAN*

| Subject | Parameter | Settings |
|---|---|---|
| Spectral space | Directional space | 0.5 |
| | Frequency space | 0.5 |
| | | |
| Accuracy criteria | Relative change Hs Tm01 | 0.005 |
| | Percentage of wet grid points | 99% |
| | Relative change wrt mean value Hs and Tm01 | 0.005 |
| | Maximum number of iterations | 15 |

## 3.4 Sensitivity analysis

In order to obtain a computationally efficient Delft3D model without impairing on the accuracy of the results, a sensitivity analysis is performed on several important numerical parameters. Though absolute values of morphological response to SBWs are questionable at this stage, the relative difference compared to the 'most accurate' setting in hydrodynamics and morphology by changing a single parameter, indicates the sensitivity of individual parameters. Appendix A illustrates the results obtained. This paragraph will give a brief overview on the discussion and conclusions from this sensitivity analysis.

### 3.4.1 Parameters

#### 3.4.1.1 *Morphological acceleration factor*

To enable numerical simulations for longer time scales efficiently, the morphological acceleration factor (morfac) approach can be used, as commonly introduced nowadays in numerical modelling [Lesser et al. 2004; Roelvink 2006; Ranasinghe et al. 2011]. Basic principle of the morfac is to multiply bed level changes each hydrodynamic time step with a certain factor, to effective increase the morphological time step, see Figure 3.1. This approach is however limited based on several considerations and still a matter of judgement and sensitivity analysis, although preliminary relations for the maximum morfac are published [Ranasinghe et al. 2011]. Focussing on numerical modelling of a SBW and especially on the Delft3D model set-up described in previous paragraphs, the initial bed level changes are relatively large. These relatively large initial bed level changes are due to the modelling approach used; forcing a SBW on an alongshore uniform beach profile results in a coastal system that is far from an morphologic equilibrium. By increasing the morfac, eventually the morphological response per time step multiplied by the morfac will overestimate morphological changes in time.

Based on the results of appendix A, and the fact that several morphologic simulations became unstable for higher values of the morfac, a morphological acceleration factor of 15 is used for the remaining of this thesis.

#### 3.4.1.2 *Coupling interval between Delft3D- Flow and SWAN*

In addition to the morphological acceleration factor, the principle of the online coupling between the Delf3D-flow and SWAN is used to increase computational efficiency. Instead of calculating the new wave conditions due to bed level changes after each individual time step in the Delft3D flow module, the wave induced flow conditions remain constant for a certain period, the coupling time (defined in Delft3D flow as the ‘store communication file: interval’). During this period, differences in velocity due to bed level changes are accounted by the continuity equation. After this period, the new equilibrium wave conditions are calculated, using the updated bathymetry. The same considerations as for the morfac apply to the coupling interval between Delft3D-Flow and SWAN, as both parameters are limited by the relative bed level changes.

Similar to the morfac, reducing the coupling interval, significantly improved the stability of the morphological simulations. Based on efficiency, a coupling time of 10 minutes is used for the remaining of this thesis.

#### 3.4.1.3 *Relative change and percentage of grid points (SWAN)*

The numerical modelling of SWAN is based on stationary conditions, to exclude time. These stationary conditions are computed by iterative processes for each grid cell simultaneously. In order to terminate this iterative process, accuracy criteria are used based on the relative change of wave height or period for a defined percentage of grid points in one iteration step.

From appendix A, its evident that for strict accuracy criteria, an additional iteration step is used. In contrast, no significant differences in computational time or accuracy are obtained by changing the accuracy criteria or percentage of grid points. This is partly due to the stationary boundary conditions in time an space.

#### 3.4.1.4 *Wave current interaction (SWAN)*

By online coupling of Delft3D-flow and SWAN, the wave-induced effects on hydrodynamics and morphology are taken into account. The main processes included are the enhancement of vertical mixing processes due to turbulence by wave breaking and energy dissipation in the bottom layer, radiation stresses and enhancement of the bed shear stress. To include a two way coupling, the effect of local currents on the wave propagating can also be taken into account by wave current interaction.

Although no direct conclusions can be made from the sensitivity analysis, including hydrodynamic processes as much as possible agrees with the modelling philosophy of a process-based model. In addition, by including the wave current interaction, current induced refraction is included in the model simulation.

#### 3.4.1.5 *Mass-flux*

To account for the wave induced mass fluxes, the components of the Stokes drift are integrated over the vertical. This mass-flux results in an onshore directed sediment transport. However, the mass-flux is generally compensated by an undertow. In contrast, in a depth-averaged approach undertow is not taken into account. To study the influence of this parameter a research version of Delft3D is used.

In addition to previous mentioned, the mass-flux has an effect on morphology. As it can not be compensated by an undertow and results in morphological differences. It is therefore argued to turn the mass-flux off for morphological computations.

##### 3.4.1.6 Breaker depth index and Roller model

Short wave breaking is the driving mechanism for SBW induced hydrodynamic and morphologic differences. Therefore obtaining the right order of wave energy dissipation is crucial. Paragraph 2.4 illustrated the discussion on the breaker depth index, as well as the roller model. For Delft3D modelling purposes, two options are available for computing the energy dissipation. First option is using SWAN, second option is using the roller model within Delft3D-Flow. For SWAN, a constant breaker height to depth ratio can be used, where as in Delft3D-Flow also the relations from [Battjes and Stive 1985] and [Ruessink et al. 2003] are optional.

Summarized from appendix A, the wave breaking is a delicate processes and results change significant when changes are made in the wave breaking dissipation model. From paragraph 2.4, including a roller model and using the relation of [Ruessink et al. 2003] for the breaker height to depth ratio would improve hydrodynamic results for steep slopes [Apotsos et al. 2007]. In contrast, inclusion of the roller model in the morphological simulations resulted in spurious results travelling trough the domain. The reason for this problem remained unclear. Therefore to obtain reliable and satisfactory morphologic results, the wave energy dissipation model of SWAN is used with a constant breaker height to depth ratio, based on the averaged results of [Battjes and Stive 1985].

##### 3.4.1.7 Breakwater roughness (Flow module)

[Lesser et al. 2003] reasoned that for SBWs the breakwater roughness can be used as a calibration parameter to control the flow of water over the SBW. Several other studies confirmed the importance of studying the bottom/breakwater roughness for other applications, like [Apotsos et al. 2007; Calabrese et al. 2008]. In this analysis focus is only on the bottom roughness in the Delft3D flow module, whereas for the SWAN module wave energy dissipation due to wave breaking is dominant compared to bottom friction.

Appendix A shows that the breakwater roughness is a sensitive parameter affecting the obtained hydrodynamic and morphologic results significantly. For the remaining of this thesis, a Chezy coefficient of C=20 $m^{1/2}/s$ (rough breakwater), whereas a Chezy coefficient of C=65 $m^{1/2}/s$ is used for the smooth sandy bottom, default in Delft3D flow[Deltares 2010a]. Paragraph 5.2 will show the importance of the breakwater roughness, as this parameter can also be seen as a design parameter based on the materials used for the submerged breakwater. Paragraph 3.5 will compare the mass transport over the SBW with published literature for these Chezy coefficient values.

##### 3.4.1.8 Horizontal eddy viscosity

Delft3D is based on the finite differences approach. Due to this spatial discretization Delft3D is unable to resolve small scale turbulent motions. To account for these turbulent motions, the horizontal eddy viscosity and diffusivity can be used. These values depend on the flow and grid sizes used, but generally, values between 1 and 10 $m^2/s$ for grid sizes in the order of tens

of metres will result in satisfactory results. Another option is to resolve the turbulent motion using a horizontal large eddy simulation (HLES). By using this HLES, horizontal eddy viscosities will be spatial varying. However as discussed by [Apotsos et al. 2007] the total effect of a spatial varying horizontal eddy viscosity is small, so no morphological calculations are included.
Based on the above description, a constant horizontal eddy viscosity is used. Appendix A shows that the HLES simulation results in a horizontal eddy viscosity of 1 $m^2$/s near the SBW. Therefore, this value is used for the constant horizontal eddy viscosity in this thesis.

### 3.4.2 Conclusions

From previous paragraph, the results can be summarized in Table 3.5. By studying the numerical parameters and the effect on the computational time and differences in results, a computationally efficient model is obtained from a numerical point of view. Not surprisingly, the model set-up and results from the sensitivity analysis are in good agreement with previous modelling of SBWs or barred beaches. [Smit et al. 2008; Van der Hout 2008]. Next paragraph will treat the validation of this model (settings) based on physical considerations.

*Table 3.5 Parameters sensitivity analysis*

| **Parameter** | **Default Value** | **Range** | **Sensitivity wave height (m)** | | **Sensitivity bed level (m)** | | **Morph. Time (days)** | **New Value** |
|---|---|---|---|---|---|---|---|---|
| | | | Bias | MAE max | Bias | MAE max | | |
| Morphological factor | 1 | 1-60 | 0 | 0 | $-7*10^{-3}$ / 0 | 0.02 | 30 | 15 |
| Coupling interval | 1 min | 1-60 | $-7*10^{-4}$ / 0 | $1.5*10^{-3}$ | -0.02 / 0 | 0.08 | 60 | 10 |
| Relative change (wave accuracy) | 0.005 | 0.005-0.05 | 0 / $7.5*10^{5}$ | $1.5*10^{-4}$ | $-1*10^{-5}$ / $3*10^{-5}$ | $1*10^{-4}$ | 15 | 0.005 |
| Percentage of grid points (wave accuracy) | 99% | 90 – 99% | $-2*10^{-5}$ / 0 | $2.5*10^{-5}$ | $-1.2*10^{-5}$ / $1.5*10^{-5}$ | $5*10^{-6}$ | 15 | 99 |
| Wave-current interaction | on | off | -0.01 | 0.02 | 0.07 | 0.1 | 30 | on |
| Mass-flux | on | off | $3.5*10^{-3}$ | $6*10^{-3}$ | -0.1 | 0.14 | 15 | |
| Breaker depth index (SWAN) | 0.73 | 0.6 – 0.9 | -0.2 / 0.2 | 0.2 | -0.06 / 0.05 | 0.14 | 30 | 0.73 |
| Breakwater roughness (FLOW) | 20 | Off (C=65) | $-9*10^{-4}$ | $6*10^{-3}$ | -0.2 | 0.3 | 30 | on |
| Breakwater roughness (FLOW) | 20 | 10 - 40 | $-1.2*10^{-3}$ / 0 | $5*10^{-3}$ | -0.2/ 0.1 | 0.25 | 30 | 20 |
| Roller model | off | On , y= 0.51/ 0.73 BJ | 0.006 / 0.012 | 0.01 / 0.015 | 0 / 0.3 | 0.2 / 0.4 | 30 | Off, due to instabilities |
| | | On, y ~ kh | 0.012 | 0.013 | 0.17 | 0.35 | 30 | |
| Horizontal eddy Viscosity | 1 $m^2$/s | Varying, HLES | | | | | | 1 $m^2$/s |

### 3.5 Validation of Delft3D

In order to study SBWs using the described approach in Delft3D, confidence has to be build in obtaining reliable results. As this thesis focuses on the effect of individual SBW induced processes and in addition, a comprehensive data set on SBWs is lacking, each process is studied separately based on literature available. This method may be 'quick and dirty' and caution should be made with applying theoretical relations based on simplifications and limitations, but it will give a good view on the capabilities of Delft3D to simulate individual hydrodynamic and morphologic processes.

In appendix B, an elaborate overview is given of the capabilities of Delft3D. Table 3.6 gives an overview of the processes considered and the literature used. Summarized, although certain hydrodynamic processes are neglected for the sake of the model stability, Delft3D is capable of providing accurate results for a wide range of hydrodynamic and morphologic processes. Nevertheless, as Delft3D uses a phase averaged wave model and using hydrostatic assumptions, shoreline accretion cannot be modelled. Similar to other numerical studies on this topic, contour lines just below the mean water level will be used. In addition, in literature the three-dimensional effect of submerged breakwaters is ignored most of the time. As understanding of the three-dimensional effect of submerged breakwater on individual processes increases, Delft3D should be calibrated/validated accordingly.

*Table 3.6 Overview of validated processes in Delft3D*

| Process | Literature | Delft3D | Remarks |
|---|---|---|---|
| Shoaling | [Deltares 2010b] | √ | Calibrated/validated extensively by Deltares |
| Refraction | [Deltares 2010b] | √ | Calibrated/validated extensively by Deltares |
| Diffraction | unknown | √ | No literature for submerged breakwaters, but common sense suggest a small influence |
| Reflection | [Van der Meer et al. 2005] | | Not included, influence however small |
| Wave transmission | [Van der Meer et al. 2005] | √ | Based on direct comparison to rubble mound sbw results |
| Water level over breakwater | [Calabrese et al. 2008] | √ | Influenced by mass-transport for higher values |
| Mass transport over breakwater | [Svendsen 1984] [Calabrese et al. 2008] | √ | In general good, except 1 result |
| Spectral change | [Beji and Battjes 1993; Van der Meer et al. 2005] | | Due to stability reasons of Delft3D neglected |
| Flow patterns | [Ranasinghe et al. 2006] | √ | |
| Morphology | [Sumer et al. 2005; Ranasinghe et al. 2006; Young and Testik 2009; Ranasinghe et al. 2010] | √ | Although relative large grid sizes, overall trend visible |
| Shoreline changes | [Ranasinghe et al. 2010] | | No changes accretive pattern, erosion included reasonable. Take -0.5m contour |

# 4 Hydrodynamic analysis

## 4.1 Introduction

From previous chapters, literature on SBWs and capabilities of Delft3D are studied. Confidence in reliable results from Delft3D is obtained by comparing individual processes with apparent theory. Based on the ability of Delft3D to accurately simulate SBW induced hydrodynamic processes, important hydrodynamic effects for SBW induced shoreline changes are studied. This chapter will clarify the importance of these initial hydrodynamic processes by illustrating several individual processes and the influence to the overall hydrodynamics. To describe the initial hydrodynamic processes accurately, results presented in this chapter are obtained at the end of the spin-up interval, to exclude any morphological changes.

## 4.2 Occurrence of a 2/4 cell pattern

The difference between an accretive 4 cell- or erosive 2cell- pattern, is assumed to relate to the water level differences alongshore.[Ranasinghe et al. 2010] In order to test that hypothesis, several simulations are made with a varying distance offshore, as it is one of the dominant parameters determining the initial mode of shoreline response. Although the formation of eddies is not only depending on differences in water levels it may be a good indicator of the expected mode of shoreline response. Results are presented in appendix C.

The results obtained in appendix C are the difference in water level between the centre line of the SBW and the undisturbed uniform coastline. The v-velocity profile is obtained near the breakwater head, see Figure 4.1. Due to the low flow velocities at the two cross-sections for the water level differences (see Figure B.11), the difference in water level can be seen as the total difference in hydraulic head alongshore.

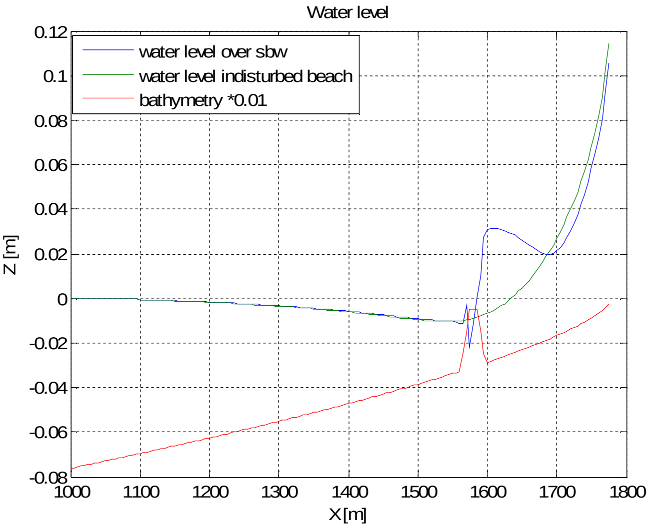


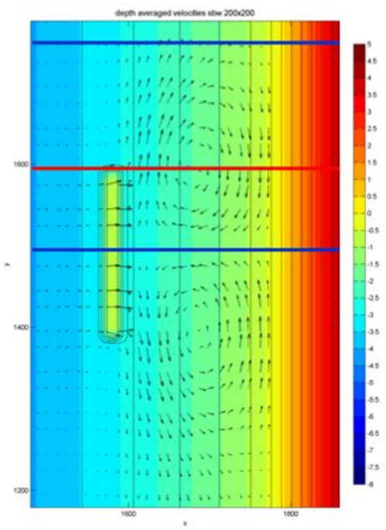

*Figure 4.1 Example of water levels and currents, xb=200, Lb=200, Hs=1.5, B=10,Rc=-0.5*

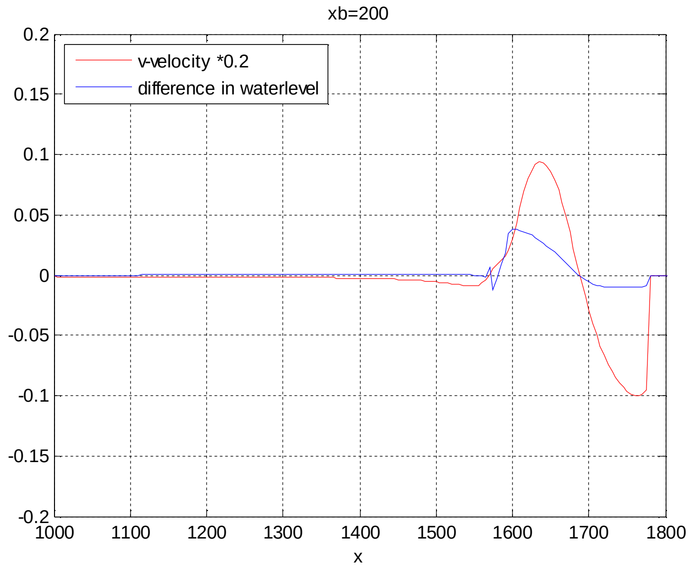


*Figure 4.2 Differences in water levels and v-velocities*

Concluding from appendix C, the water level difference corresponds surprisingly well to the direction of the v-velocity. For both erosive cases $x_b$=50 and $x_b$=100, the difference in water level and inherent flow velocities never become negative on the leeward side of the breakwater, this corresponds to the 2-cell pattern. For all other cases, the water level differences, as well as the v-velocity are both zero in the point of intersection.

Reason for these observations is the cross-sections used. Paragraph B.8 already introduced that for these two water level cross-sections, the alongshore flow velocities are more ore less zero. Due to this, the water level corresponds to the hydraulic head, or potential energy. As water will only flow from a high energy level to a low energy level, neglecting for the sake of simplicity energy sources and sinks, comparing the water levels of these two cross-sections will result in a rough estimate for the initial mode of shoreline response. However when only small differences are present, this relation is not that evident. In addition, the magnitude of the alongshore flow is depending on local gradients in water levels, wave forcing and bottom stresses. Next paragraphs will go in detail about this subject.

Another interesting notice is the magnitude of the difference in water level close to the shoreline (O($10^{-2}$)m). Close to the breakwater, differences in water level alongshore are larger, due to the spatial difference of depth induced wave breaking, but between the zero crossing and the shoreline difference of the water level and the shoreline the maximum difference is approximately O($10^{-2}$m).

## 4.3 Cross-shore momentum balance

### 4.3.1 Introduction

Previous paragraph introduced the influence of alongshore differences in water levels. This paragraph will study the origin of the water level gradients in more detail as well as the local water level gradients in cross-shore direction.

In order to study the water level gradients, the cross-shore momentum balance for barred beaches is applied for the SBW. To account for the bottom stresses and the flow induced terms (but still neglecting the mixing terms) the cross-shore momentum balance from [Haller et al. 2002] is used, see paragraph 2.5:

$$\rho(\frac{\partial}{\partial x}(U^2h)+\frac{\partial}{\partial y}(UVh))+\rho gh\frac{\partial\eta}{\partial x}+(\frac{\partial S_{xx}}{\partial x}+\frac{\partial S_{xy}}{\partial y})+\tau^b{}_x=0 \tag{4.1}$$

As reasoned by the authors, the flow terms and the bottom stresses are generally small for barred beaches. For this analysis however, all terms are taken into account and studied individually. Obtaining a fully closed balance is still difficult, due to among others, the staggered grid used, relative few grid cells over the breakwater and the (steep) breakwater (slope) compared to the shallow water assumptions. Still the influence of each individual term can clarify its relative importance.

Another discussion is on the direction of each term of the cross-shore momentum balance. Based on the conclusions of [Lesser et al. 2003; Reniers et al. 2004; MacMahan et al. 2006; Apotsos et al. 2007] about the vertical flow structure of (barred) beaches or SBWs, each term, and especially the bottom stress can be visualised including the direction. Due to the vertical structure (net flow over the SBW towards the shoreline), the bottom stress is directed offshore, see Figure 4.3 and Figure 4.4. Instead of increasing the water levels, the bottom stress balances the wave-forcing trough the induced flow and thereby effectively reducing the water level gradient (hydrostatic) induced stresses favouring lower water levels. Combining Figure 4.3 and Figure 4.4, it is expected that for an alongshore uniform bathymetry including a SBW, a similar time-averaged undertow will occur, see Figure 4.5. However, using a 2DH approach in Delft3D the depth-averaged velocity is zero for uniform bathymetries, thereby excluding undertow effects in flow calculations. However, assumptions in a 2DH approach for non-uniform bathymetries is in agreement with previous published literature on the vertical flow profile over non-uniform barred beaches and SBWs.

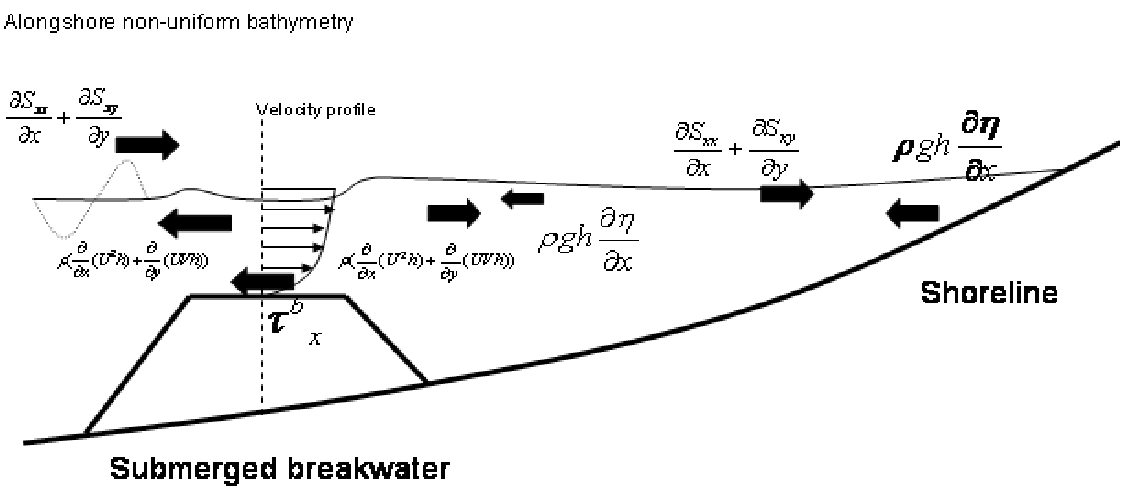


*Figure 4.3 Terms of the cross-shore momentum balance over a non-uniform bathymetry including submerged breakwater*

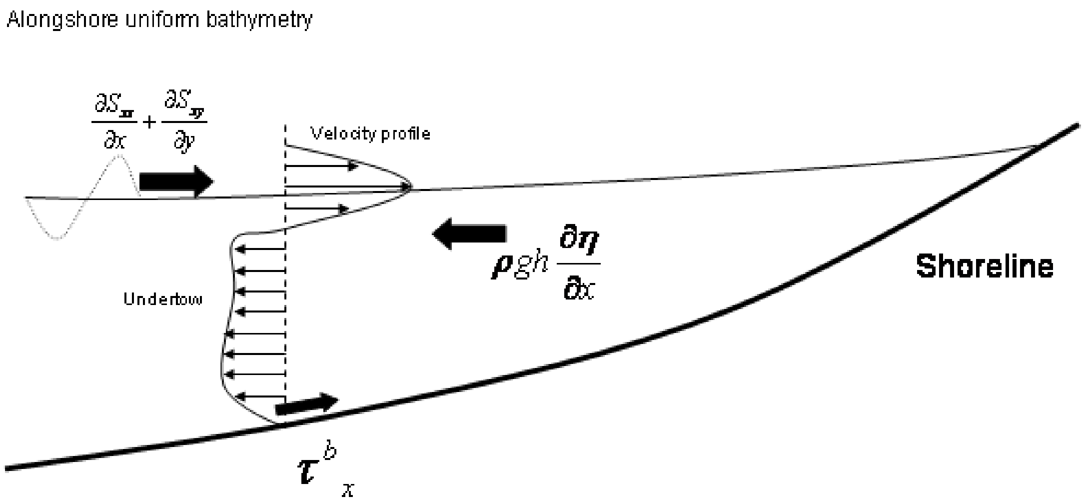


*Figure 4.4 Terms of the cross-shore momentum balance over a uniform bathymetry/mild sloping beach*

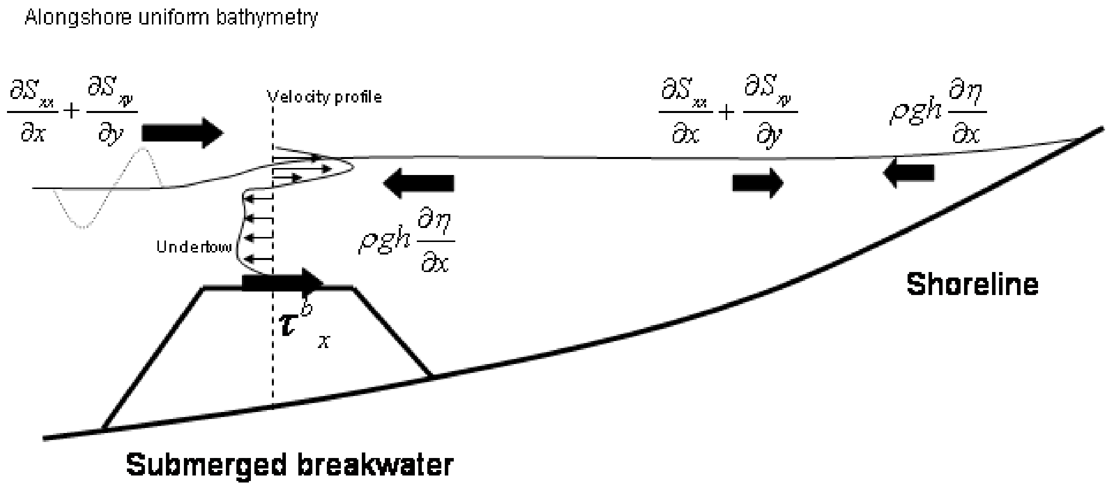


*Figure 4.5 Expected terms of the cross-shore momentum balance over a uniform bathymetry including submerged breakwater*

To study the cross-shore momentum balance for different cases, a dataset of multiple Delft3D simulations is used. As from the morphological studies presented in chapter 2, the length of the breakwater (Lb) and the distance from the shoreline (xb) to the apex of the structure are the most profound parameters effecting shoreline changes. Accordingly, combinations of these two parameters are used while other parameters remain constant, see Table 4.1. The (constant) offshore conditions; Hs=1.5m, m=4.0, Tp=9s and θ=270$^0$ (shore normal). In addition, the design parameters B=10, Rc=-0.5m, tanα=0.2 are kept constant, whereas the depth at the structure is related to the offshore distance using Dean's equilibrium profile. Influence of part of these parameters on near shore hydrodynamics is studied in chapter 5. An example of the obtained cross-shore momentum balance over the centre of the SBW is presented in Figure 4.6.

*Table 4.1 Varying design parameters for hydrodynamic analysis*

| | Constant value | Other values |
|---|---|---|
| Case 1 | Lb=100 m | Xb= 50 , 100, 150, 200, 300, 400 |
| Case 2 | Lb=200 m | Xb= 50 , 100, 150, 200, 300, 400 |
| Case 3 | Xb=150 m | Lb= 100, 200, 300, 400, 500 |
| Case 4 | Xb=200 m | Lb= 100, 200, 300, 400, 500 |

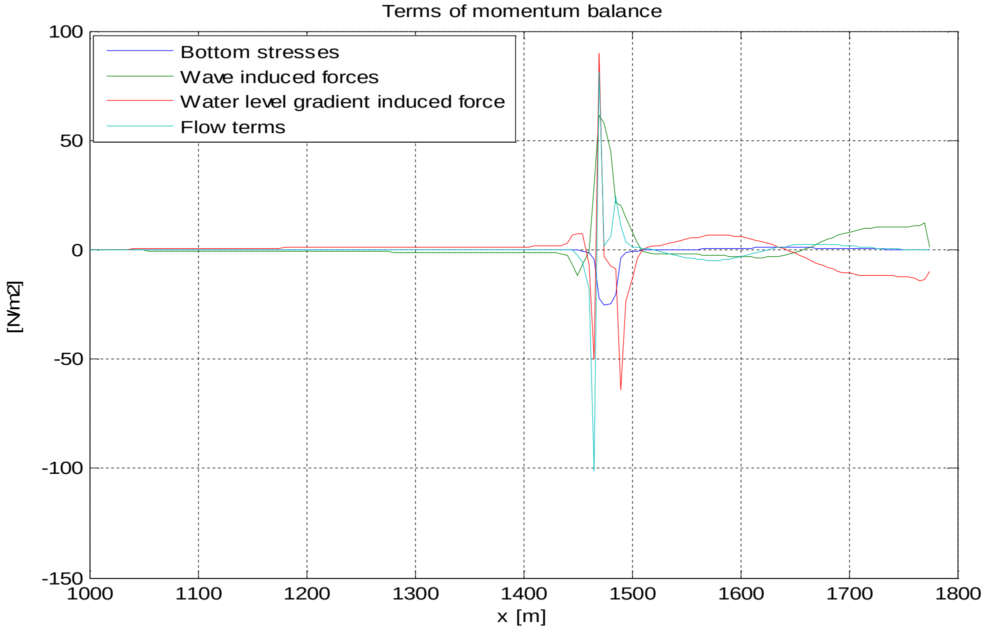


*Figure 4.6 Example of the cross-shore momentum balance, Lb=200m, xb=300m*

Note that due to the previous problems mentioned and neglecting others terms in the momentum balance, the cross-shore momentum balance is not fully in equilibrium. In contrast, the trend of each individual term compared to the (design) parameters used remains evident. Next paragraph will describe the individual terms and the relation with the length and distance offshore of the SBW in detail.

In order to compare each individual term on its relative importance, every term is integrated in cross-shore direction and normalised by the integrated (constant) wave induced forcing on the undisturbed coastline. In addition, the wave forcing is more or less equal to the hydrostatic balancing force. Alongshore differences in the cross-shore momentum balance are therefore easily compared. Appendix D shows the cross-shore integrated terms of the momentum balance for all four cases.

$$\frac{\int (term)\partial x}{\int (\frac{\partial S_{xx}}{\partial x} + \frac{\partial S_{xy}}{\partial y})\partial x \ \ (undisturbed\ beach)} \tag{4.2}$$

### 4.3.2 Wave induced stress

Figure 4.7 shows an example of the wave-induced stress. All stages like shoaling, depth induced wave breaking and reformation/shoaling behind the breakwater are visible. Also clear, the wave breaking is concentrated on the front slope and crest of the breakwater, whereas the transmitted waves break close to the shoreline.

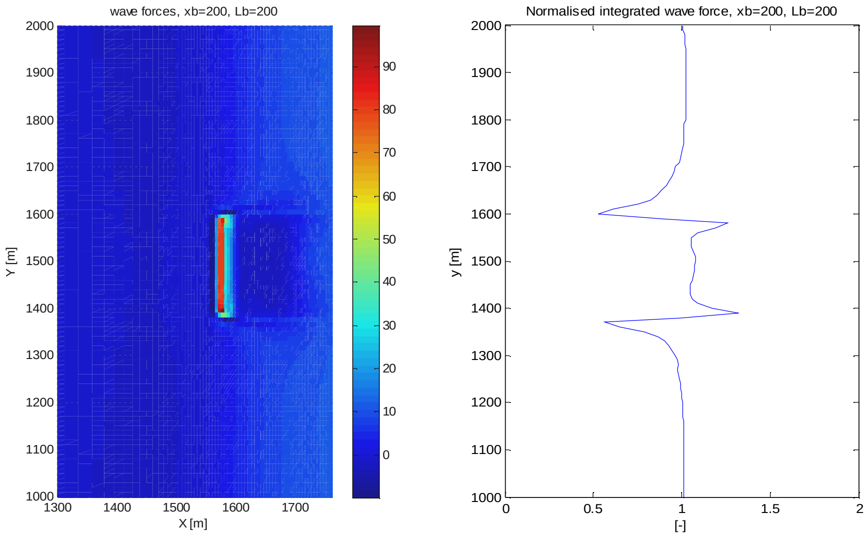


*Figure 4.7 Example of (normalised cross-shore integrated) wave induced stresses, Lb=200 m, xb=200m*

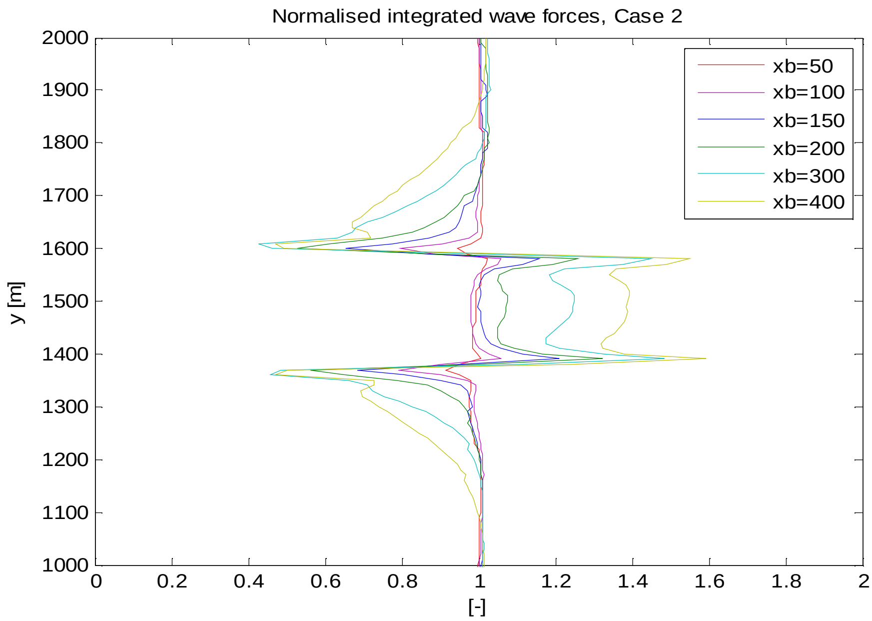


*Figure 4.8 Normalised cross-shore integrated wave induced stresses, case 2*

Figure 4.7 and Figure 4.8 show that a SBW redistributes the wave forcing in such a way that the total wave forcing over and behind the SBW increases. The area just next to the SBW compensates for this increase of wave forcing, as offshore wave conditions are constant. With increasing offshore distance, a larger stretch of coastline is affected by the SBW, though the maximum decrease in wave forcing near the breakwater head has its minimum value and increases again with larger offshore distances (see also Appendix D). In addition, the cross-shore integrated wave forcing over the centre of the SBW increases for offshore distances larger than 200m. As the incoming wave characteristics on the breakwater slope are more or less constant outside the surfzone, it is argued that this increase of wave forcing is due to the undisturbed waves entering the lee-side of the submerged breakwater under an angle (directional spreading) and break near the shoreline. Figure 4.9 confirms this statement, as an increase in wave breaking is visible only near the shoreline. As wave breaking on a uniform coastline is compensated by a water level gradient, this increase of wave forcing is expected to result in an increase of water levels near the shoreline. Next paragraph will illustrate this increase in water levels behind the SBW. Paragraph 4.4 will illustrate the effect of directional spreading of waves on SBWs by studying wave spectra.

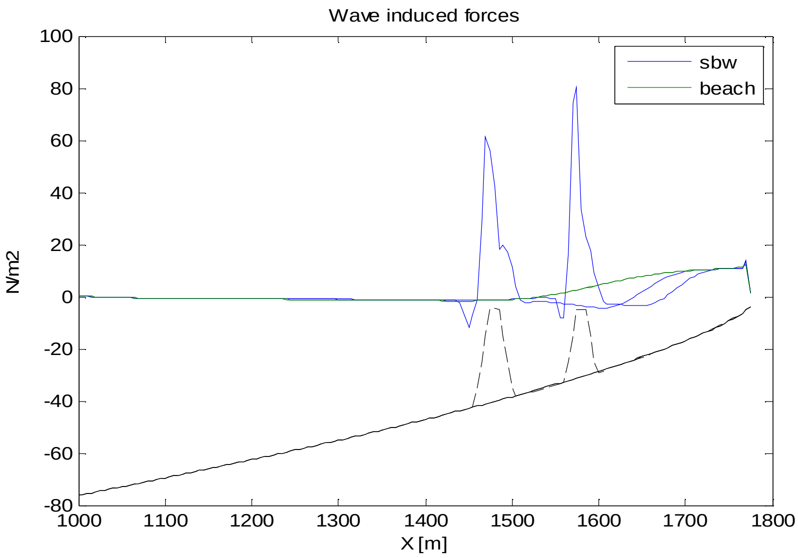


*Figure 4.9 Example of wave induced stresses for two different simulations: lb=200, xb=200/300*

In contrast, by increasing the length of the breakwater (see Appendix D), the integrated cross-shore wave induced forces over the centre of the SBW will converge to the same order as for the undisturbed coastline and only a spatial shift of the redistribution of wave forcing along the breakwater head is visible. Figure 4.10 shows the cross-shore distribution of wave-induced stresses of four distinct cross-sections.

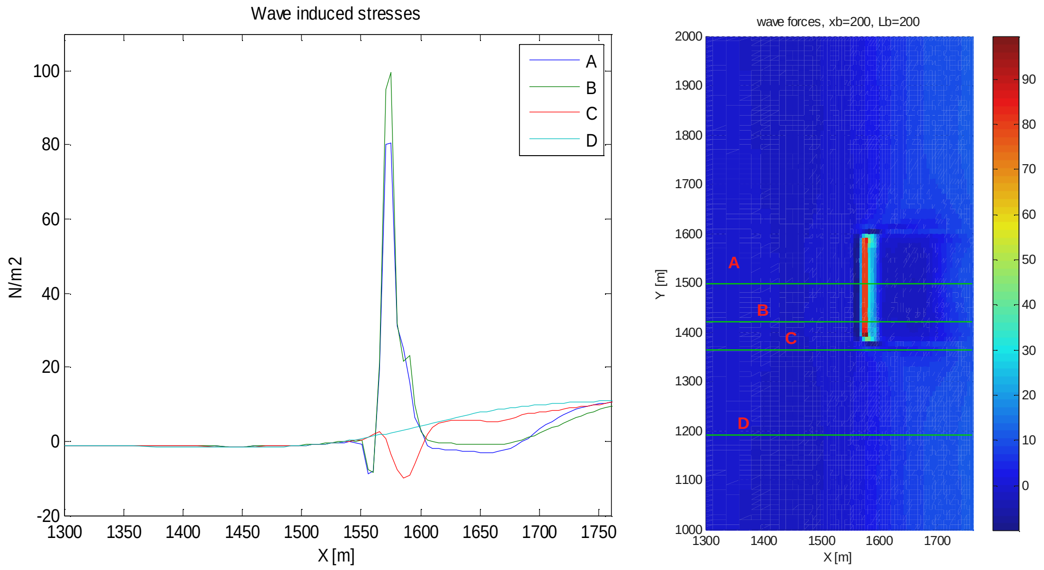


*Figure 4.10 Cross-shore variation of wave induced stresses*

### 4.3.3 Water level gradient induced stress

Net wave-induced stresses in cross-shore direction are (partly) compensated by a water level gradient. Due to this water level gradient, in the vertical a hydrostatic pressure difference will result in a net stress in the opposite direction of the positive water level gradient. In case of an alongshore uniform beach profile, the wave-induced stresses acting on the water are almost entirely compensated by a water level gradient induced stress, see paragraph 2.5 . Other terms like the flow terms or bottom stresses can be neglected, due to the relative deep water compared to the (second order) flow velocities, though this may lead to under prediction of the total water level set-up [Apotsos et al. 2007]. As for the non-uniform bathymetry induced by the SBW, the water level gradients are limited due to the alongshore water level gradients and other terms from the cross-shore momentum balance become important. Figure 4.11 shows an example of the obtained water level induced stresses in cross-shore direction and the normalised integrated water level gradient induced stresses. Figure 4.12 shows the normalised integrated water level induced hydrostatic stresses for case 2.

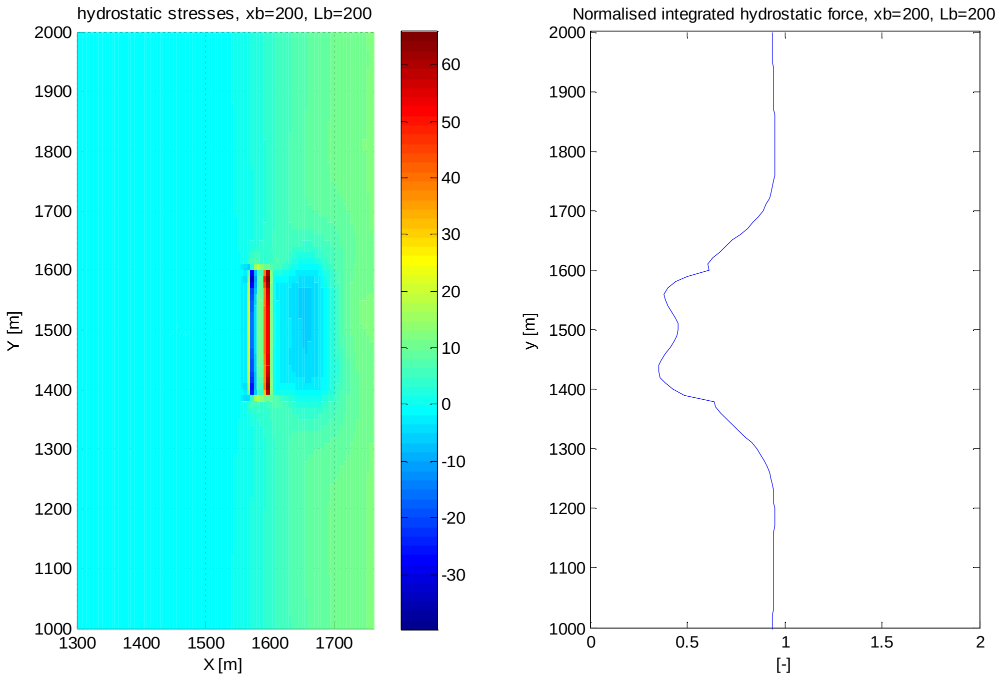


*Figure 4.11 Example of (normalised cross-shore integrated) water level gradient induced forces.*

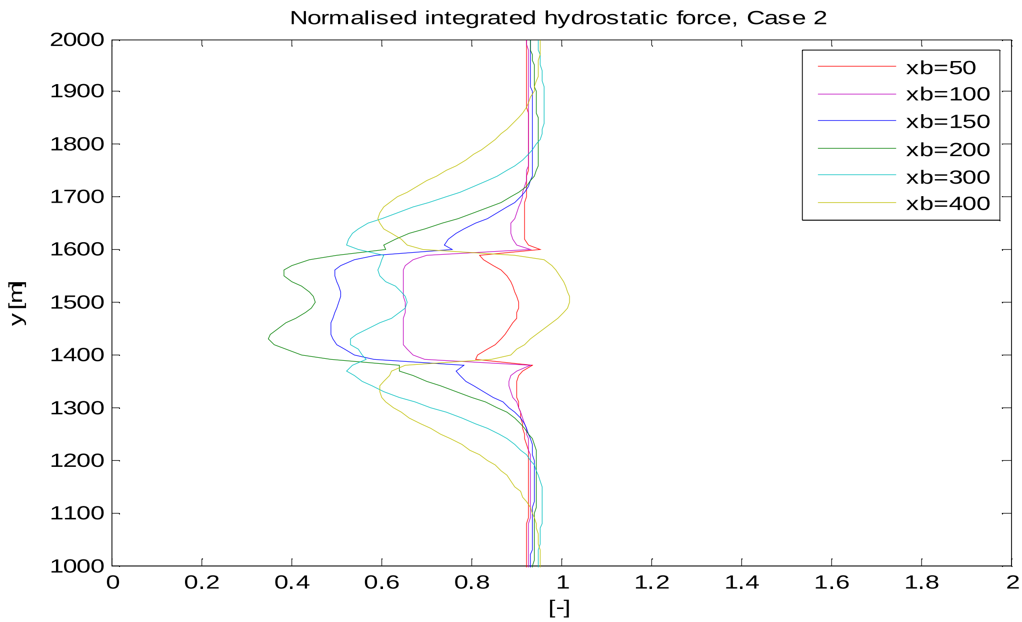


*Figure 4.12 Normalised cross-shore integrated hydrostatic stresses, Case 2*

Evident from Figure 4.12 is the relation between the distribution of wave forcing and the water level set-up next to the SBW, as expected from the relation of [Longuet-Higgins and Stewart 1964]. In addition, the increase of water level gradient induced momentum from xb=200 can be explained by the increase of undisturbed waves entering the lee of the SBW using the same relation from [Longuet-Higgins and Stewart 1964], as explained in previous paragraph. In contrast, a decrease of water level induced stresses over the SBW is visible for xb=50 till xb=200m. Paragraph 4.3.5 will show that this decrease in normalised integrated water level gradient induced force is due to the bottom stresses.

Opposite of an increase in offshore distance, an increase in SBW length results in more wave sheltering, resulting in a clear relation between the wave forcing and the water level gradient induced momentum (and bottom stress). Not that evident, but for case 3 the integrated normalised water level gradient induced momentum over the centre of the SBW increases again. Paragraph 4.5 and 5.1 will show that this is due to the water level set-up directly behind the submerged breakwater.

As paragraph 4.2 introduced the relation between water levels and mode of shoreline response, minimizing the water level gradient induced stresses is preferred, though direct conclusions on obtained water levels are difficult due to the dependency of the water level gradient induced stresses on local water depth. Figure 4.13 illustrates the cross-shore distribution of the water level gradient induced stresses.

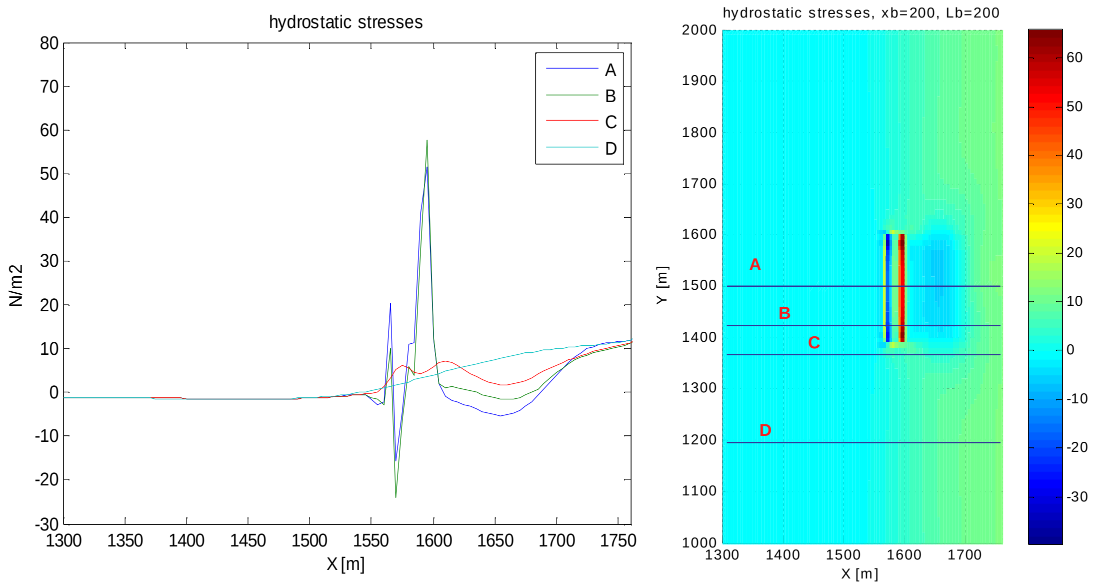


*Figure 4.13 Cross-shore variation of water level gradient induced hydrostatic stresses*

### 4.3.4 Flow induced stress

To account for the depth averaged acceleration and deceleration of the water body due to wave forcing; also the flow terms are accounted. For barred beaches or alongshore uniform coastlines, this term is generally more or less zero, but for SBWs, it may become important. Figure 4.14 gives an example of the flow-induced stresses.

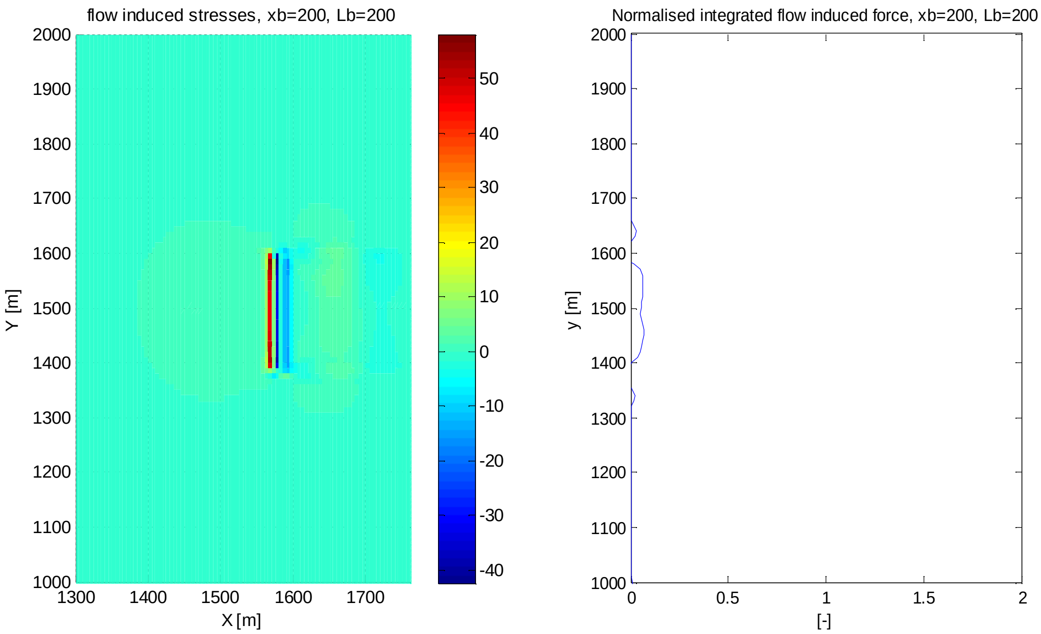


*Figure 4.14 Example of (normalised cross-shore integrated) flow induced forces, Lb=200 m, xb=200m*

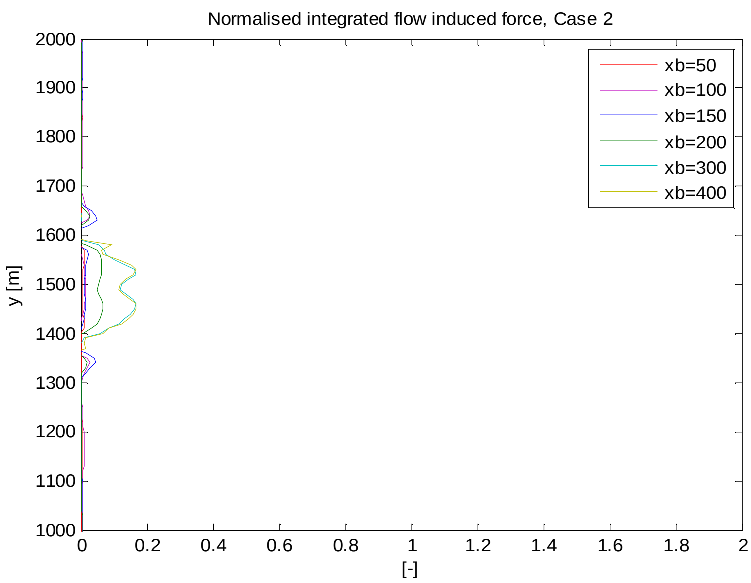


*Figure 4.15 Normalised cross-shore integrated flow induced stresses for case 2.*

At first glance, the results from Figure 4.14 and Figure 4.15 may be neglected, but there are some important details, see Figure 4.16. The flow-induced stresses are of interest in the area close to the SBW, and especially close to the breakwater crest. As expected, a net flow is present over the SBW induced by the difference in radiation stresses. This mechanism causes to shift the process of wave breaking induced water level gradients to the lee of the submerged breakwater. Concluding from Figure 4.15, the total contribution of the acceleration/deceleration of the water column to the cross-shore momentum balance is more or less zero. In contrast, local influence of this term is evident. From Figure 4.6 it is clear that the deceleration of the cross-shore flow in the lee of the SBW still results in a water level gradient. Therefore, the net onshore flow over the SBW can be seen as a transport mechanism of wave energy to potential energy (increase of water level).

However due to this acceleration and deceleration of the water body, a net flow over the SBW occurs. As a result, bottom stresses are becoming important.

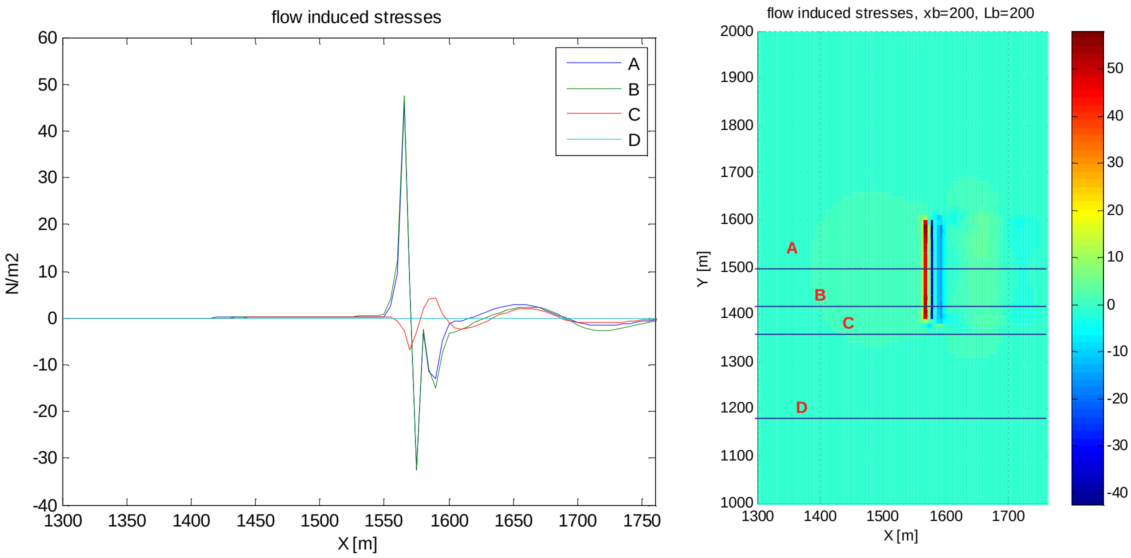


*Figure 4.16 Cross-shore variation flow induced stresses*

## 4.3.5 Bottom stress

In addition to previous paragraph, the flow induced by the wave forcing results in onshore directed flow in the viscous boundary layer enabling offshore directed bottom stresses. Studies on barred beaches generally conclude that the bottom stress is small compared to the other terms of the cross-shore momentum balance [Haller et al. 2002]. As for barred beaches, physical limitations are present by critical shear stresses of sediment. In contrast, for SBWs large stone diameters or concrete structures are unable to erode due to large flow velocities. Based on results of amongst others [Apotsos et al. 2007], an onshore directed flow near the viscous bottom boundary layer will result in offshore directed bottom stress, see Figure 4.3.

In order to influence the resulting water levels significantly, the bottom stresses has to be of significant order. Figure 4.17 illustrates the bottom stress over the SBW. The bottom stress is due to the large flow velocities in relative shallow water, significant on the crest of the SBW. (in a 2DH approach in Delft3D a quadratic bottom stress relation is used based on the depth averaged velocity, instead of the near bed velocity of an full three dimensional computation)

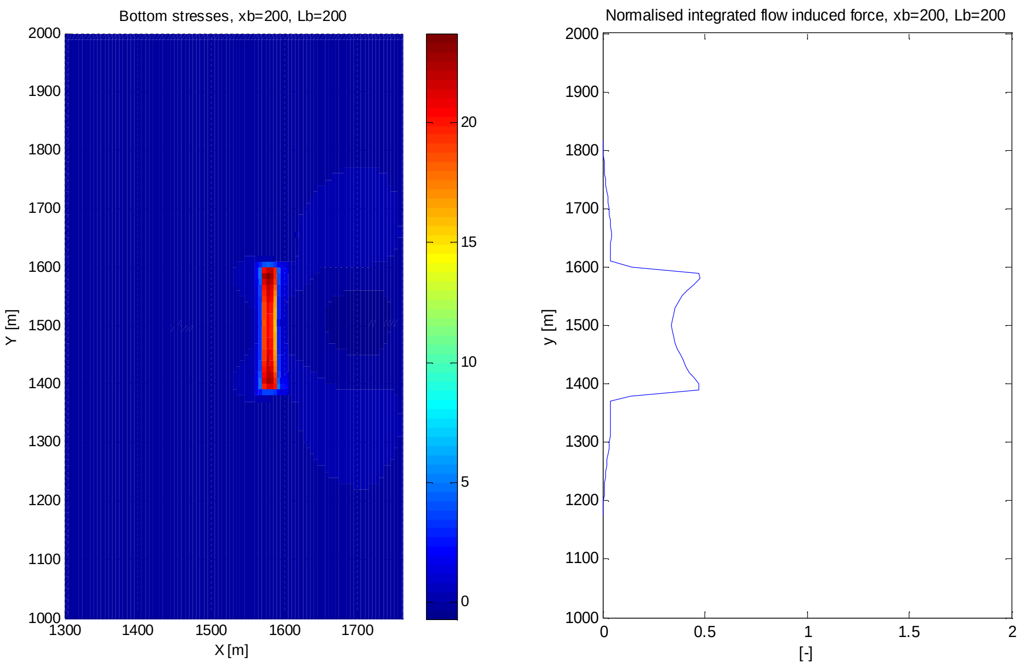


*Figure 4.17 Example of (normalised cross-shore integrated) bottom stress, Lb=200 m, xb=200m*

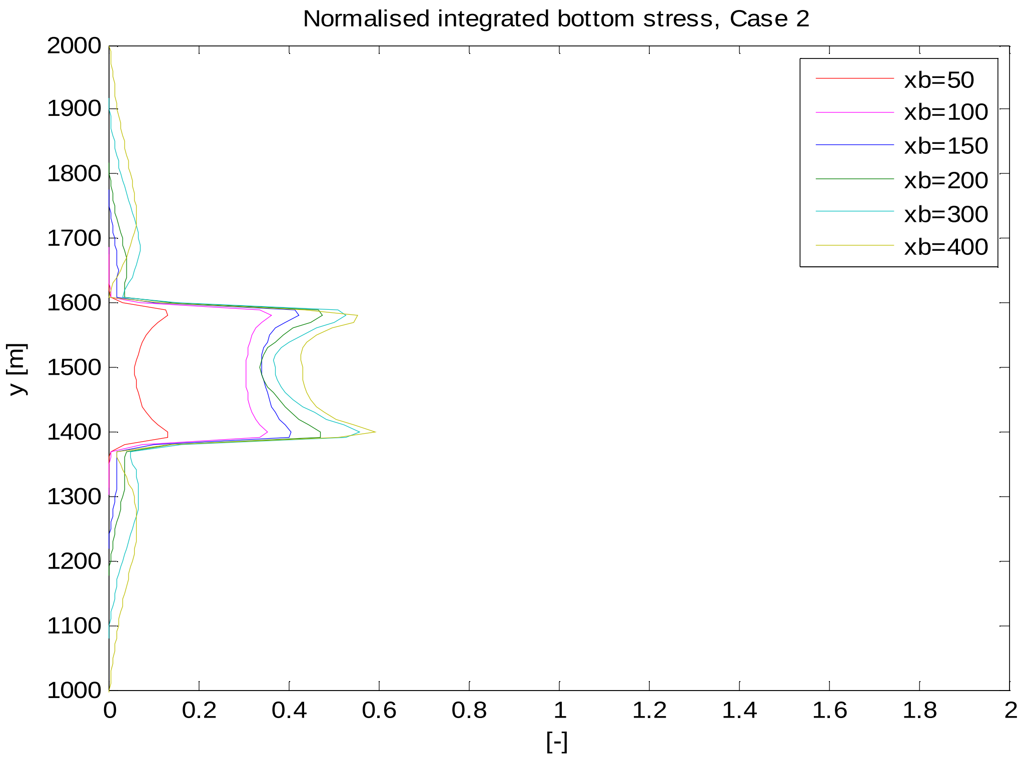


*Figure 4.18 Normalised cross-shore integrated bottom stress, case 2*

As can be concluded from Figure 4.18, the bottom stresses become more and more profound for SBWs with increasing offshore distance. As the flow over the SBW is depending on the total wave breaking, a higher incoming wave height (increasing offshore distance within the surfzone) will induce more wave-induced forces on the water body. This leads to higher (near bed) flow velocities over the SBW, followed by an increase in bottom stresses. In addition, the net flow over the SBW, as well as the near bed velocity is depending on the water level set-up and vice versa. Due to an increase of water depth and wider return channel or feeder channel (see appendix G), the water level gradients in alongshore direction decrease, resulting in limited water level set-up in cross-shore direction. This favours the balance of wave forcing and acceleration of the water body, resulting in an increase in bottom stresses (due to the increase of near bed velocities). Comparing the magnitude of integrated bottom stresses towards the centre of the SBW, a clear decrease of bottom stresses is visible, due to the water level increase in the direction of the centre of the SBW.

The opposite is true for an increase in breakwater length. Due to increase in length and increase of total flow over the SBW, more water has to be transported offshore, which results in an increase of water level gradients and water level set-up in alongshore direction. Similar to the decrease in offshore distance, this will result in a more profound effect of the water level set-up compensating the wave induced stresses and reducing the acceleration of flow, to eventually the net zero mass-balance is obeyed similar to a uniform beach and the Stokes drift is compensated by an undertow and porous flow [Loveless et al. 1998]. This is however not included in a 2DH approach. As a result, the wave forcing is compensated only by a water level gradient, see for example paragraph 5.1. Paragraph 4.5 will illustrate the relation between the increase of total flow and the increase of water level gradients in alongshore direction.

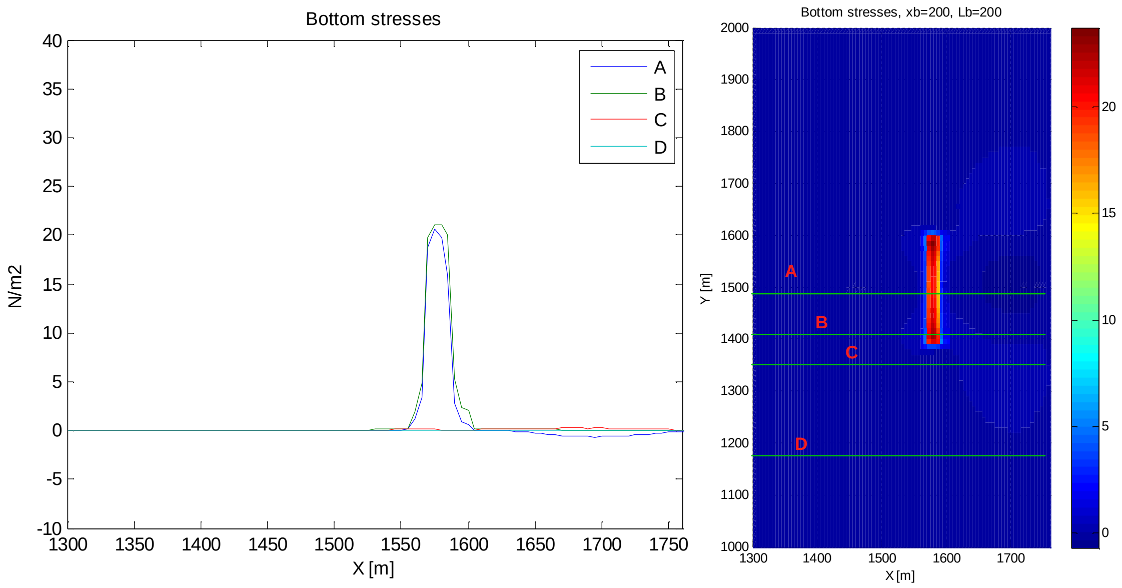


*Figure 4.19 Cross-shore variation bottom stresses*

## 4.4 Three dimensional effect of wave-field

Previous paragraph illustrated the influence of the directional spreading on the cross-shore momentum balance. To confirm this influence of the directional spreading on the redistribution of wave forcing, the wave conditions in the lee of the SBW are obtained using wave spectra. For comparison, also the wave spectra on the undisturbed beach is obtained for the same offshore distance. The same cases as in previous paragraph are used. The presented energy density spectrum results from using a wave frequency close to the defined offshore peak period $T_p$.

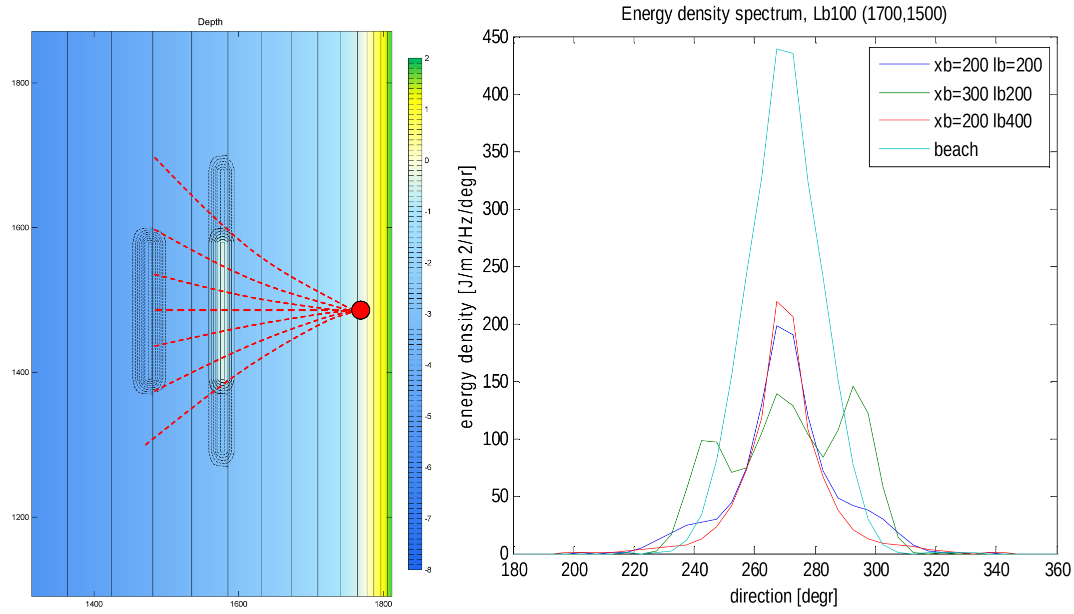


*Figure 4.20 Shadow effect of the submerged breakwater. In red individual wave rays, see paragraph 2.2*

From Figure 4.20 and Figure 4.21 it is evident that the length, offshore distance and the directional spreading of the waves has influence on which part of the incoming wave spectrum for an observation point is affected by the SBW, visible by the more energetic waves coming from the larger wave angles. In addition to the incoming undisturbed waves under an angle, the transmitted waves determine the magnitude of the energy distribution. By increasing the length of the SBW or reducing the distance from the shoreline the 'shadow' affect increases. Contrary, by increasing distance from the shoreline or decrease of breakwater length the effect of the SBW reduces. Concluded from theory, the directionality goes hand in hand with diffraction, see paragraph 2.3.3. Theory on diffraction is nevertheless lacking for SBWs.

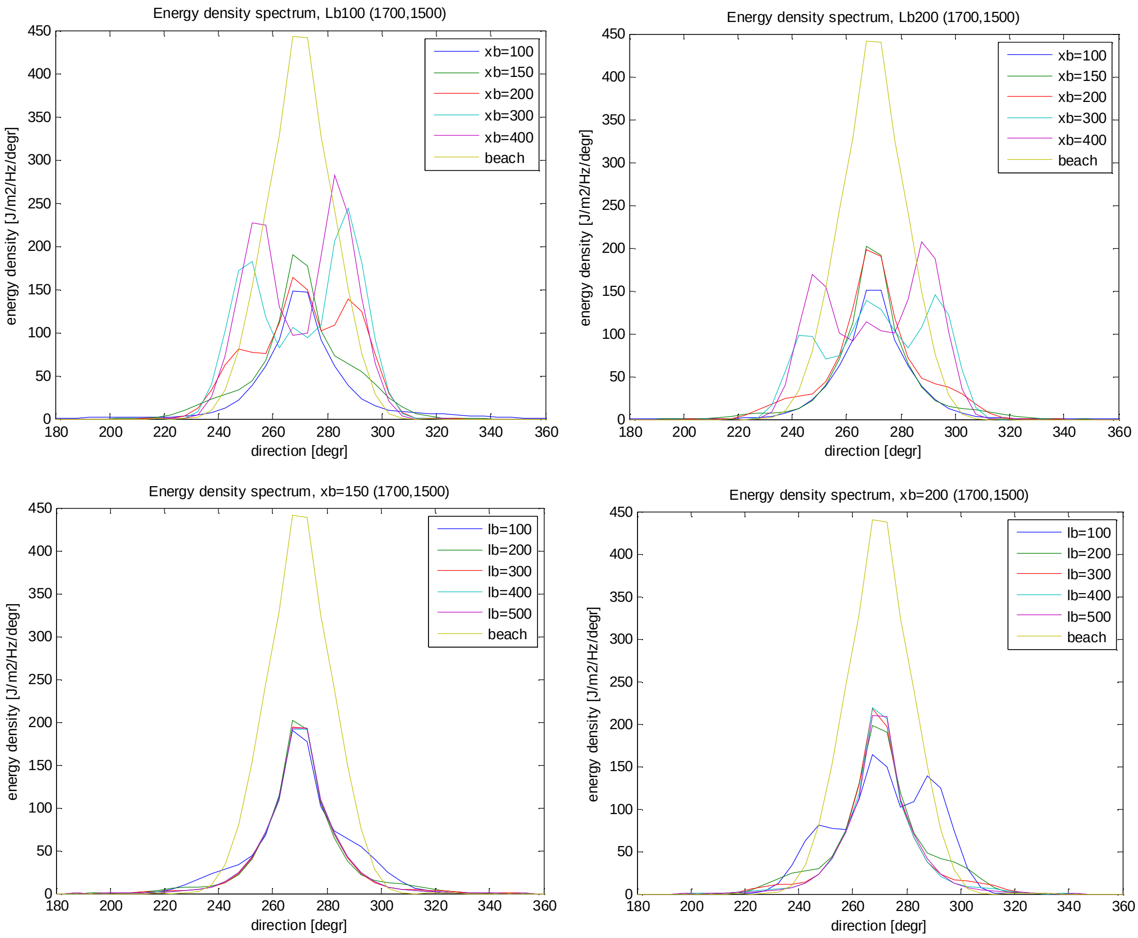


*Figure 4.21 Energy density spectra of all cases*

Concluding, a spectral approach illustrates the ‘shadow’ effect of a SBW. Offshore distance, length and wave transmission of the SBW are together responsible for the sheltering effect of a SBW.

## 4.5 Alongshore momentum balance

In order to explain the increase in water level alongshore in the lee of the SBW and the alongshore flow velocities near the shoreline in more detail, the alongshore momentum balance is studied. Similar to the cross-shore momentum balance, the alongshore momentum balance for barred beaches is used [Haller et al. 2002]:

$$\rho\left(\frac{\partial}{\partial x}(UVh)+\frac{\partial}{\partial y}(V^{2}h)\right)+\rho g h\frac{\partial \eta}{\partial y}+\left(\frac{\partial S_{yy}}{\partial y}+\frac{\partial S_{xy}}{\partial y}\right)+\tau^{b}{}_{y}=0 \qquad (4.3)$$

As no (integrated) reference term can be used to normalise results in alongshore direction, case 3 will be studied visually for three alongshore cross-sections, see Figure 4.22 and appendix E. An example of the alongshore momentum balance is given in Figure 4.23, whereas an example of the spatial variation of each term is given in appendix E.

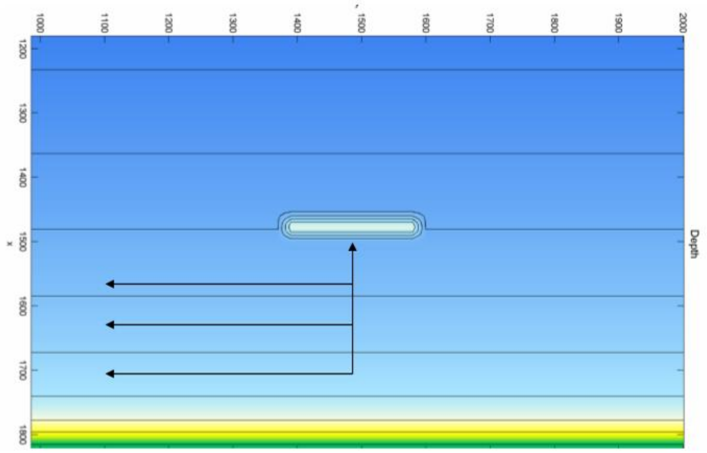

*Figure 4.22 Cross-sections used for the alongshore momentum balance*

Evident from Figure 4.23 is the relevancy of each individual term for each cross-section, despite the decrease of magnitude of each individual term towards the shoreline. This paragraph will comment on each individual term based on the results from appendix E.

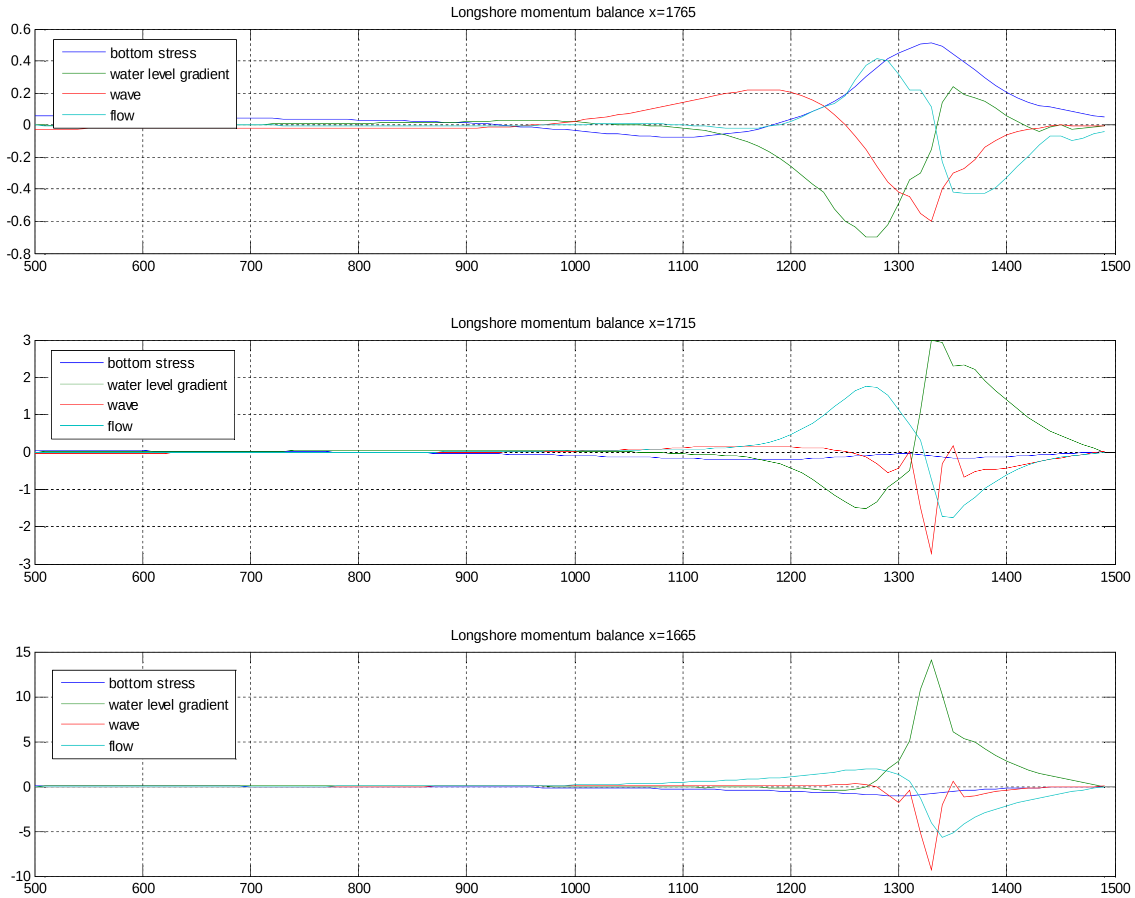


*Figure 4.23 Example of alongshore momentum balance, for xb=150,Lb=300.*

### 4.5.1 Wave induced stresses

Although a shore normal approach is used, the wave induced stresses in alongshore direction still play a significant role in the momentum balance. Figure 4.23 shows the influence of alongshore directed wave forcing, due to diffraction/directional spreading. As can be seen especially for the offshore cross-section, the wave induced forcing is in balance with the water level gradient in alongshore direction. Appendix E shows for the case considered; only changing the breakwater length, the alongshore directed wave forcing remains more or less constant in magnitude, as well as the spatial distribution around the breakwater head. This is because the transmitted wave height close to the breakwater head and the undisturbed wave height remain more or less constant only changing the breakwater length.

### 4.5.2 Water level gradient induced stresses

Figure 4.23 illustrates that spatial varying alongshore differences in water level are balanced by an acceleration or deceleration of the net flow. Appendix E shows for all cross-sections, an increase in (in positive direction) of spatial integrated water level gradients with increasing breakwater lengths, due to the increase of total flow over the SBW. As the depth is constant along this cross-section, the increase of spatial integrated water level gradient corresponds to higher water levels near the centre line of the SBW. Good comparisons on alongshore water levels behind a SBW can be made by studying river mechanics and especially, for example, the Chezy formulation for water level gradients. Limiting the alongshore gradient as much as possible, results eventually in more bottom stresses in cross-shore direction.

### 4.5.3 Flow induced stresses

As already mentioned in previous paragraphs, the depth averaged acceleration or deceleration of the water body in alongshore direction is a result of the water level gradient. The spatial integration of the flow induced terms is directly related to the total velocity, as depth is constant along the alongshore cross-section for all simulations. By increasing the total flow over the SBW due to an increase of breakwater length, the total integrated water level gradient, or total water level increases. As a result, the cross-shore bottom stresses towards the centre of the SBW decreases.

### 4.5.4 Bottom stresses

Figure 4.23 illustrates the increase in relative importance of the bottom stress in shallower water. In deep regions in the lee of the breakwater the alongshore differences in water levels are entirely compensated by an acceleration of flow, whereas for shallow water, the total velocity is reduced due to the bottom stresses. This explains the difference in obtained direction of the velocities near the shoreline when differences in water level between the lee of the SBW and the undisturbed coastline are small. Appendix E shows that bottom stresses increase in accordance with the increase of total velocity.

## 4.6 Water levels and flow velocities

In previous paragraphs, the relation between breaking waves, flow, bottom stresses and water level gradients is established using momentum balances. As previous mentioned, absolute magnitudes of alongshore currents dependent on local gradients in water level and total water level differences alongshore, wave forcing and bottom stresses. As the formation of a salient is to a large extend depending on the direction and (gradient in) magnitude of the alongshore currents near the shoreline [Ranasinghe et al. 2006; Ranasinghe et al. 2010], this paragraph will illustrate the relation between the obtained local water level differences and the direction and magnitude of the currents.

From paragraph 4.3, the relation between the individual terms of the cross-shore momentum balance is studied. By cross-shore integrating the water level gradient induced momentum, a qualitative trend for the total water level depending on the offshore distance and length of the breakwater is obtained. To illustrate the relation between the integrated normalised water level gradient induced forces and the resulting water levels, in appendix F the alongshore cross-sections of the near shore water levels for all four cases are given. From comparison of the water levels in the lee of the SBW and the undisturbed coastline of Figure 4.24 with the integrated water level gradient induced forcing of paragraph 4.3.3, it is concluded that the trend in water level gradient induced forces corresponds well with the obtained water level near the shoreline.

From paragraph B.7, it is evident that the direction of the flow is depending on the gradient of hydraulic head and shows a good correspondence by only comparing the overall water level difference between the water level behind the SBW and the undisturbed coastline. However when water level differences are small this is not entirely valid and other terms are important as well, see the alongshore momentum balance, see appendix F and E for more details.

The magnitude of the alongshore current, as can be concluded from Figure 4.24 and Figure 4.25, corresponds well to the obtained water level (gradients). Paragraph 4.3.2 explained the trend of these local differences in water levels, due to the spatial distribution of the wave breaking (mainly depending on xb, Lb, Ht and m for idealised conditions), as wave induced forcing reduces towards the breakwater head. In contrast, a transect over the SBW shows an increase in wave forcing. However, on this transect, water level gradients in cross-shore direction are limited due to the bottom stresses, therefore the resulting alongshore differences in water levels will be affected by the bottom stresses as well as the reduction of wave forcing near the breakwater head.

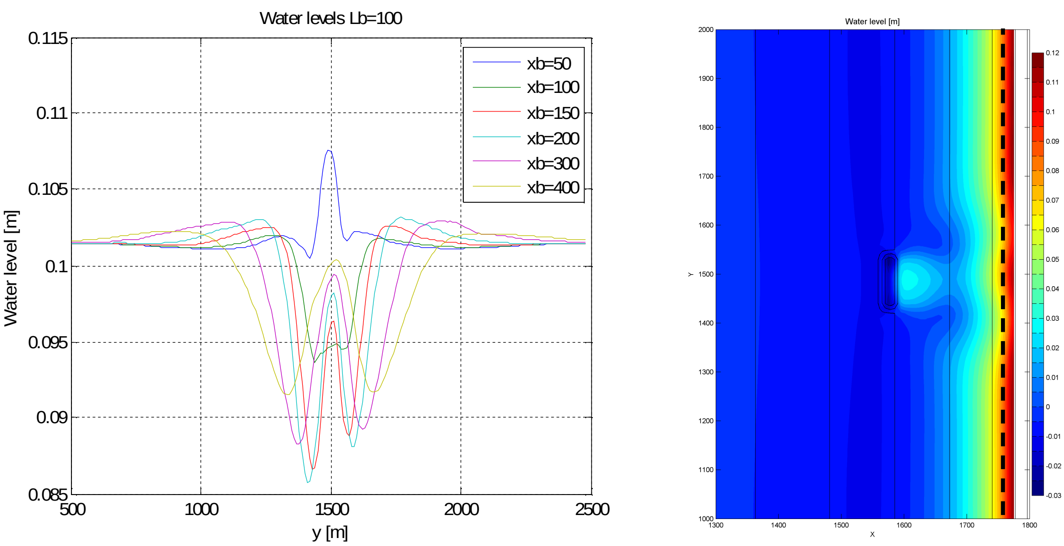


*Figure 4.24 Alongshore water levels near the shoreline case 1 and example of water levels Lb=100, xb=200*

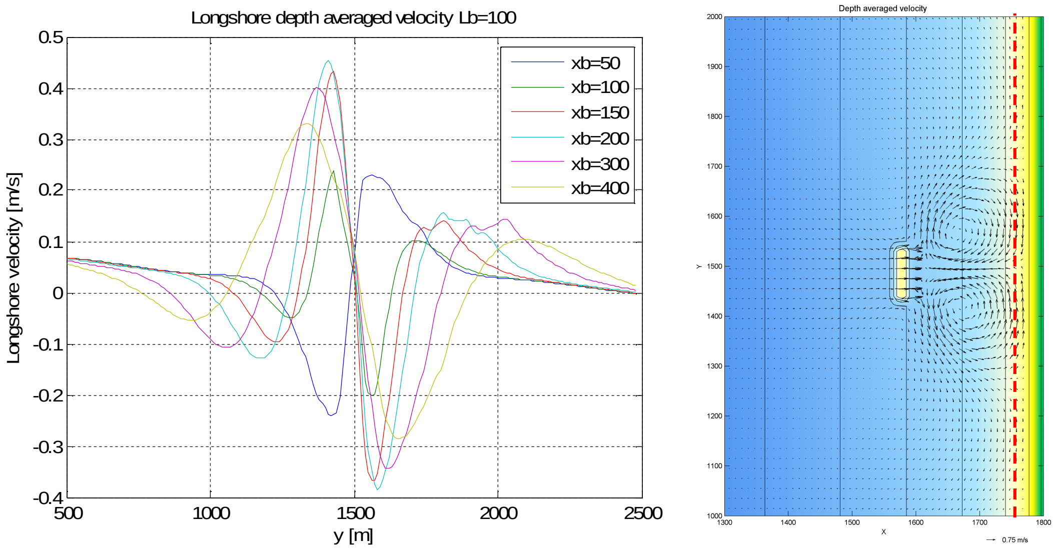


*Figure 4.25 Alongshore depth averaged velocities case1 and example of depth averaged velocity Lb=100, xb=200*

## 4.7 Conclusions

### 4.7.1 Conclusions

Previous paragraphs studied the hydrodynamic processes induced by the SBW. By using the cross- and alongshore momentum balance, a clear relation between individual processes and eventual resulting alongshore differences in water levels and current is obtained. Concluding from the momentum balances there are two distinct processes that determine the near shore hydrodynamics:

- **The spatial distribution of wave forcing** (See Figure 4.26, also often referred as wave sheltering effect; In contrast as this chapter illustrated, a SBW results in an increase of total wave forcing over and in the lee of the SBW, therefore this terminology is used )
  Due to the directional spreading of the offshore wave conditions, offshore distance, length of the breakwater and wave breaking over the SBW, a SBW will cause a redistribution of wave forcing. As a result, near the breakwater head, water levels decrease compared to the undisturbed coastline. In contrast, undisturbed waves will enter the lee of the SBW, reducing water level differences and increasing the total wave breaking over and in the lee of the SBW.

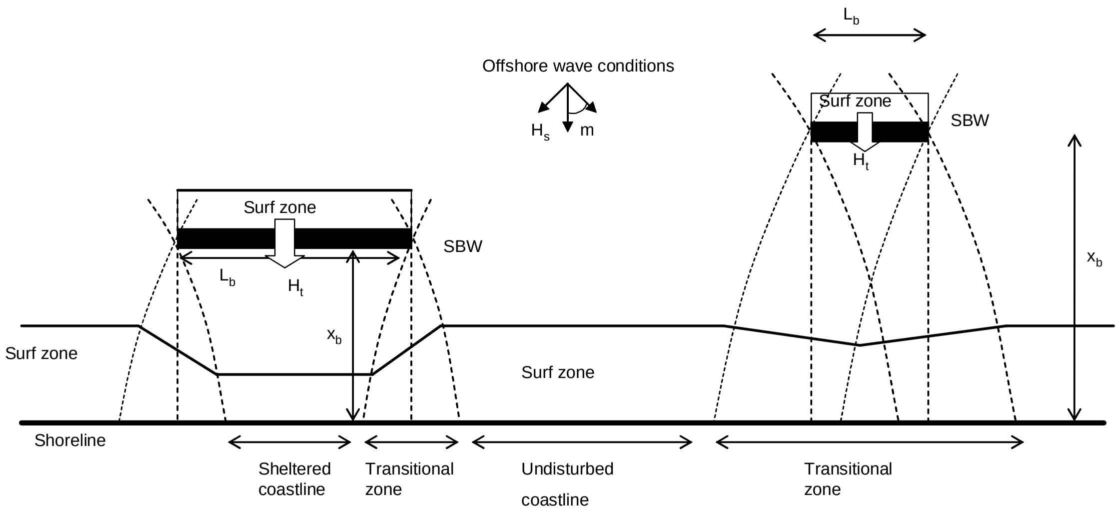


*Figure 4.26 Spatial distribution of waves, including influence of xb, Lb, $H_t$, m and refraction of waves.*

- **Bottom stresses.** (see Figure 4.27 and Figure 4.28) Due to water level gradient limitations in alongshore direction in the lee of the SBW, the wave breaking is partly compensated by a net depth averaged acceleration of water over the SBW. The resulting near bed velocities in the viscous boundary layer enables bottom stresses. Due to this momentum balance by bottom stresses, only part of the depth-averaged deceleration of water in the lee of the SBW is compensated by a hydrostatic pressure gradient (water level gradient). This results in a reduction water level set-up towards the shoreline. However, the flow over the SBW and inherent bottom stresses balance each other. Key essence is to maximize flow and resulting bottom stresses over the SBW, by minimizing the resulting alongshore water level gradient to return the water offshore, to reduce water level set-up near the shoreline effectively.

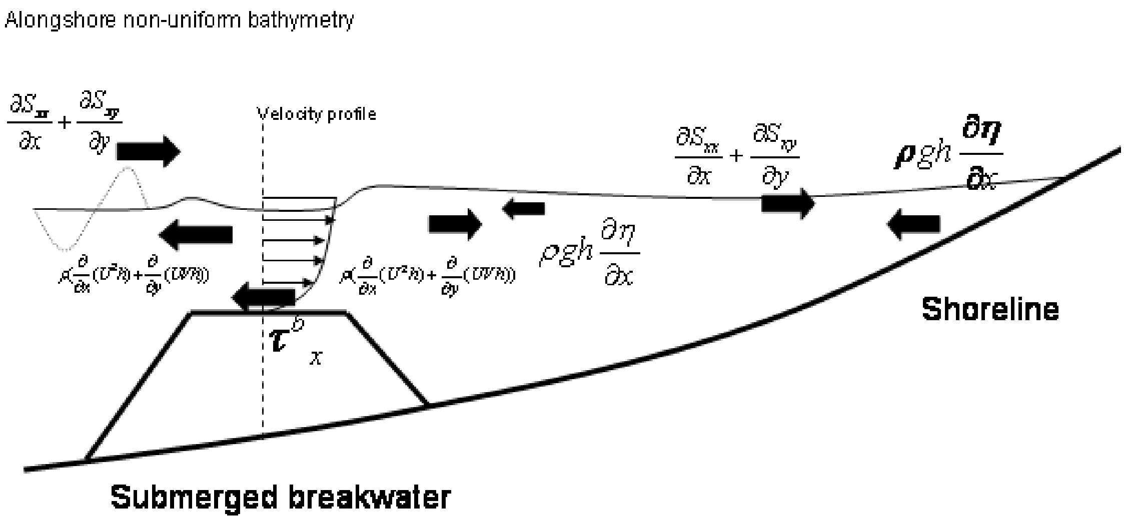


*Figure 4.27 Theoretical cross-shore momentum balance over the submerged breakwater*

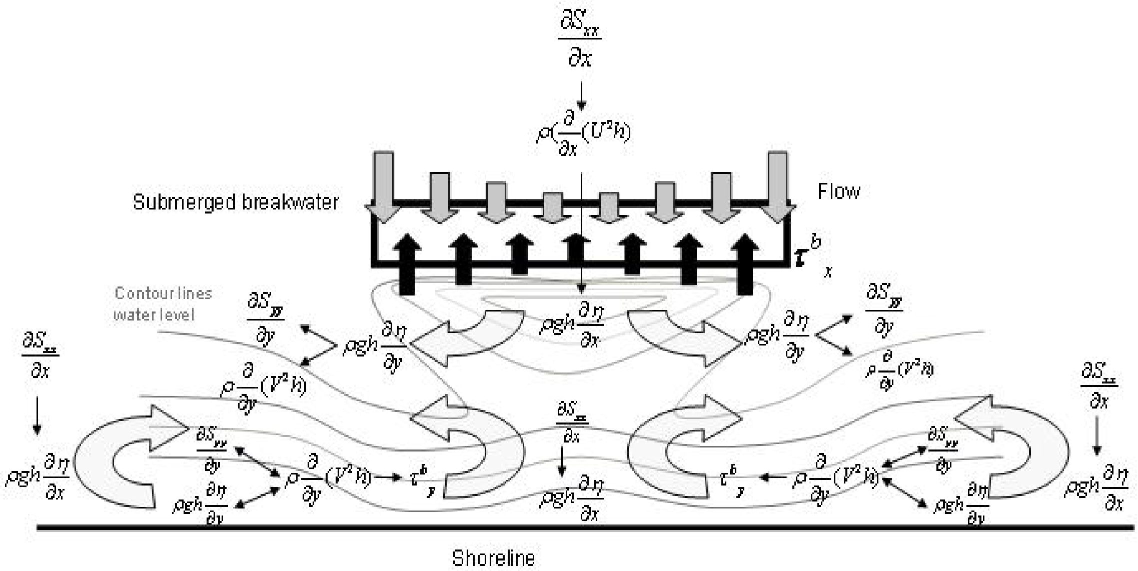


*Figure 4.28 Spatial distribution of cross- and alongshore momentum balance for 4 cell pattern*

Based on the distinct relation of hydrodynamic conditions near the shoreline and the two processes mentioned, the ‘ideal’ constructed SBW will be a balance by these two processes. To limit the undisturbed waves of entering the lee of the submerged breakwater and to increase alongshore water level gradient near the shoreline close to the breakwater head, an increase of breakwater length and decrease of offshore distance from the shoreline is preferred. In contrast, to maximize the bottom stresses by limiting the water level gradients in alongshore direction in the lee of the SBW, a decrease of breakwater length and an increase of offshore distance is preferred. Paragraph 4.7.2 will summarize the hydrodynamic processes in more detail. Next chapter will discuss the influence of other design parameters.

### 4.7.2 Summary on hydrodynamic processes

In general, single shore-parallel SBW induced hydrodynamic changes are governed by its own resulting alongshore non-uniform bathymetry in the vicinity of the SBW. Inducing restrictions on the water level set-up in alongshore direction, allows for a net current over the SBW in cross-shore direction. This current results from the depth induced wave breaking on the SBW. To balance these differences in radiation stresses, part of these forces are balanced by a water level gradient, while the remaining stresses are compensated by an acceleration of the water body. This net acceleration results in the current over the SBW. Due to the zero-velocity boundary at the shoreline, the net flow decelerates in the lee of the SBW balanced by a water level gradient. However, a net onshore flow near the viscous bottom layer results in bottom stresses. Due to these bottom stresses, only part of the net deceleration of the water body is balanced by a water level gradient. As a result, the bottom stress effectively reduce the total water level set-up obtained near the shoreline.

In contrast, minimizing the water level set-up capabilities in alongshore direction has its limitations. A second process that contributes to (additional) water level gradients, is the spatial distribution of wave forcing. Due to the directional spreading of waves and governing depth induced wave breaking, a spatial distribution of wave forcing occurs and thereby concentrating the total increase of wave forcing over- and in the lee of the SBW. This mainly depends on the geometry and directional spreading (Part of the undisturbed waves enter the lee of the SBW, whereas also part of the breaking waves over the SBW otherwise would break just next to the breakwater near the shoreline). Compensation of this local increase of wave forcing is just next to the head of the breakwater. Due to this reduction in wave forcing on a uniform beach just next to the breakwater, water levels locally reduce.

Due to the depth induced wave breaking and associated water level set-up, an initial increase of water level results in the lee of the SBW. In order to obey the mass-balance and balancing water level gradient, an acceleration of flow occurs from the centre of the breakwater in the direction of the breakwater head, resulting in a return current. This return current is also known as the 2cell pattern. Towards the shoreline on the undisturbed beach, difference in radiation stresses will entirely be compensated by a water level set-up. In the lee of the SBW, the transmitted wave over the SBW and deceleration of the water results likewise in a water level set-up. However, due to the bottom stresses, which decelerated the onshore net current, the water level set-up behind the SBW is less significant. As wave breaking in shallower water and steep slopes generally results in higher water level set-up, the water level set-up is depending on the relative importance of the bottom stresses to eventually result in lower water levels in the lee of the SBW compared to the undisturbed beach.

As in the centre of the lee of the SBW near the shoreline due to symmetry reasons velocities are more or less zero and all waves have been dissipated, the potential energy (head) corresponds entirely to the water level, likewise for the undisturbed beach. Due to the negative gradient in water level near shoreline from the undisturbed beach to the breakwater head, a net acceleration of water occurs near the shoreline from the undisturbed beach. Depending on the head difference between the undisturbed beach and the lee of the SBW and the alongshore bottom stresses, the current will enter the lee of the SBW or deflects offshore in advance (depending on the local gradient in head). If head differences are significant and bottom stresses near the shoreline remain relatively small, the flow enters the lee of the SBW and return offshore near the centre line, resulting in the 4-cell pattern. In a two cell pattern, the net near shore current from the undisturbed coastline towards the SBW head may however be overruled by strong shear stresses due to cross-shore differences in alongshore velocities.

# 5 Engineering design parameters

Previous chapter introduced the momentum balances in cross- and alongshore direction. Concluding from these momentum balances, the cross-shore momentum balance between the spatial varying wave forcing, bottom stresses and water level gradient is an important factor for water level differences near the shoreline. This paragraph will illustrate the effect of individual design parameters on the cross-shore momentum balance. As previous paragraphs focused on the length and offshore distance of the SBW, this paragraph will include several other structural and environmental parameters like breakwater roughness, crest height, crest width and incoming wave height (environmental parameter), with constant offshore distance and length of the breakwater (Lb=200m, xb=200m), but first a distinct alongshore uniform breakwater case is studied. Appendix H will illustrate the effect of individual design processes on multiple processes.

## 5.1 Alongshore uniform submerged breakwater

Previously mentioned in the introduction is the large percentage of failure of SBWs. Instead of salient development, additional shoreline erosion is reported for a variety of cases [Ranasinghe and Turner 2006]. Focussing on the hydrodynamics, especially the depth averaged and time averaged current pattern [Ranasinghe et al. 2010], already indicates if a SBW will induce erosion or accretion. As the overview of [Ranasinghe and Turner 2006] show a significant amount of cases where the length of the SBW is of an higher order than the offshore distance, this paragraph will study this design in more detail. Despite of the clear overview, it is noted that not every SBW from that overview is a single detached shore normal SBW without additional constructions, like groins etc.

In order to study this configuration, two simulations are compared. One from paragraph 4.3, with Lb=100 m and xb=50m, and a new simulation of Lb=500m and xb=50, while all other parameters remain constant, see Figure 5.2. However, Delft3D is used in a depth-averaged approach and therefore undertow is neglected and according bottom stresses will according to the depth-averaged flow will become zero instead of opposite values, see Figure 4.5, the difference between the two simulations will still be evident.

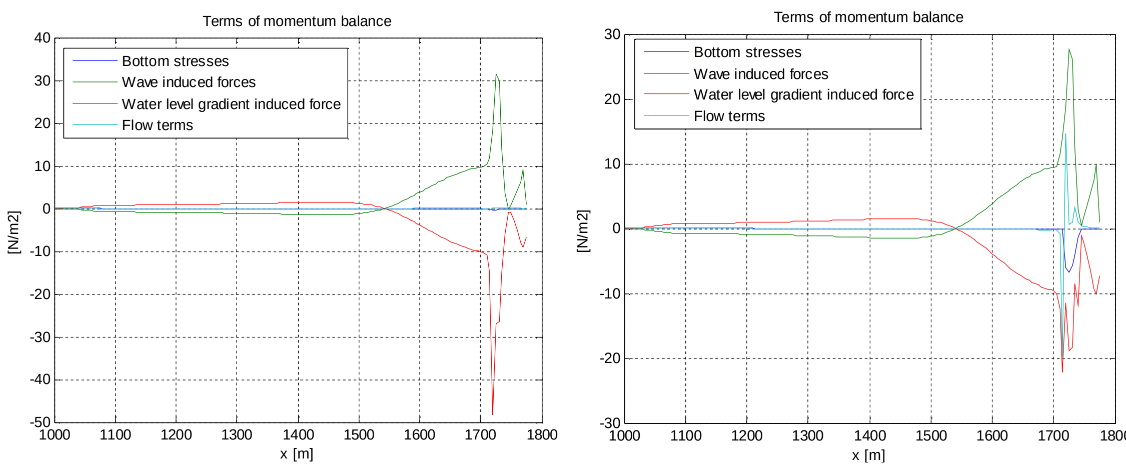


*Figure 5.1 Cross-shore momentum balance over the centre of the breakwater, Left: Lb=500m xb=50, Right: Lb=100 xb=50.*

Studying the difference in cross-shore momentum balance of the two simulations confirms previous results obtained for the momentum balance analysis for the four cases. For the simulation of Lb=500 the water level set-up balances the cross-shore wave forcing entirely, leading to higher water level set-up. Clearly, the influence of the bottom stress in cross-shore direction in effectively reducing the water level gradient is visible. In addition, the increase in current alongshore enabling higher water levels in alongshore direction is also visible, thereby significantly reducing the net flow over the SBW towards the centre, but maximizing the alongshore flow near the breakwater head. The obtained direction and magnitude of the alongshore flow suggests distinct erosive morphological changes. This result is in agreement with previous findings of [Dean et al. 1997].

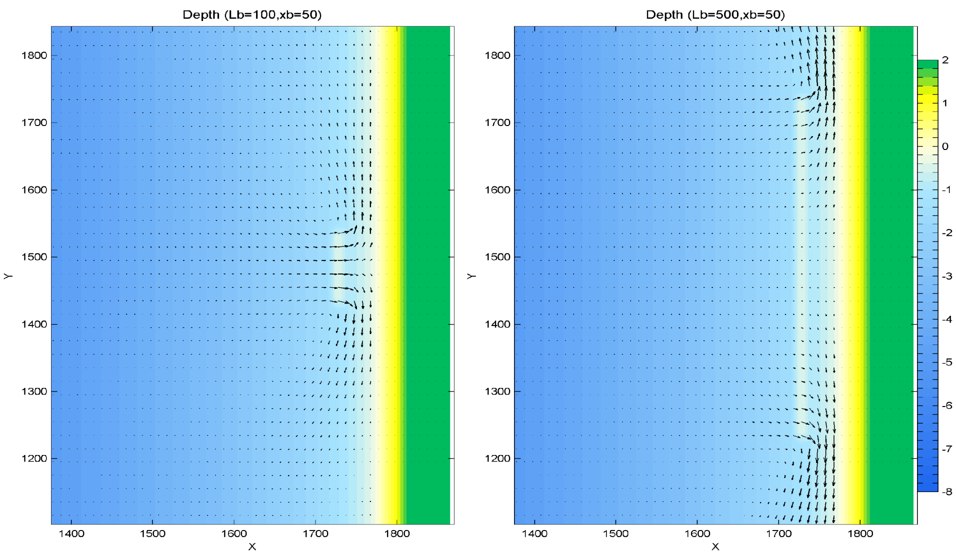


*Figure 5.2 Depth averaged velocity vectors of the two simulations*

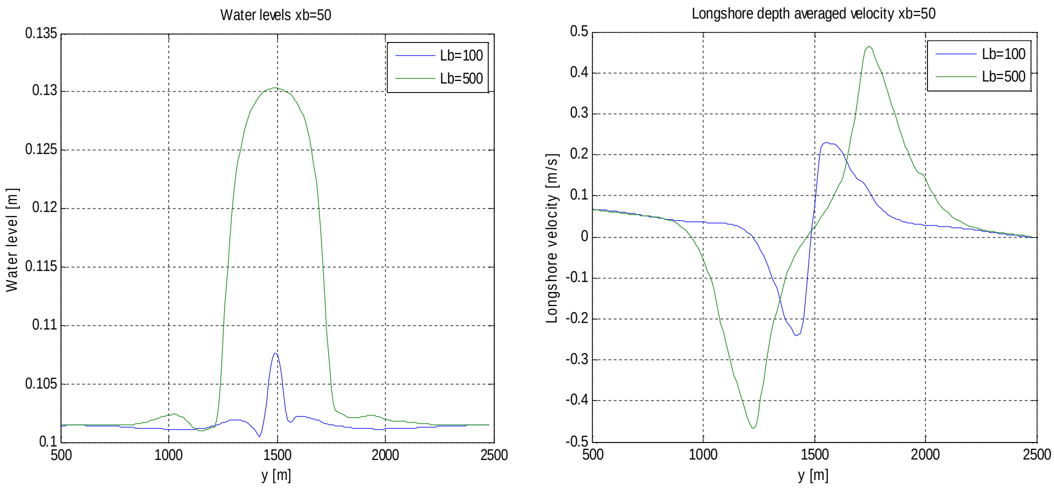


*Figure 5.3 Alongshore water level and depth averaged velocity near the shoreline (x=1765)*

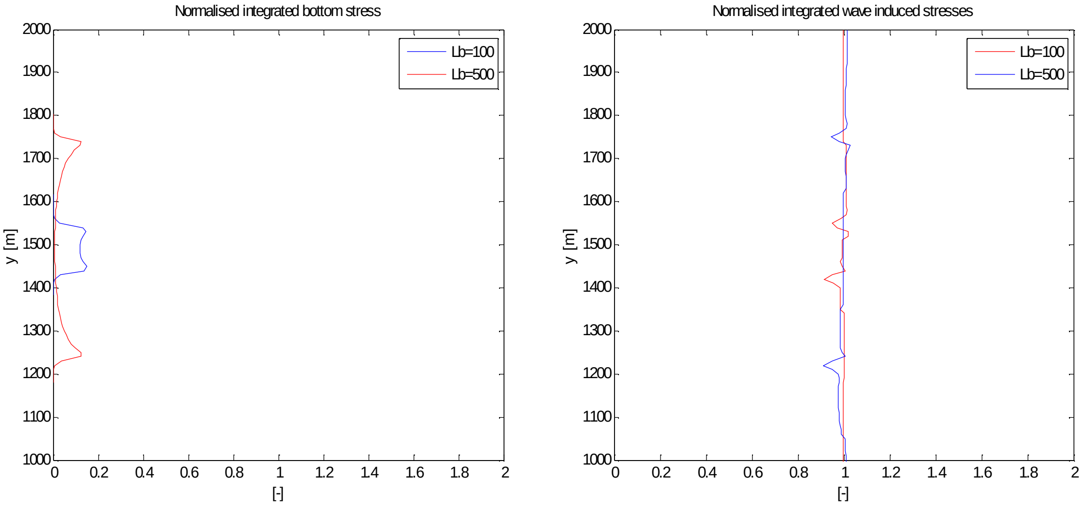


*Figure 5.4 Normalised cross-shore integrated bottom- and wave induced stresses*

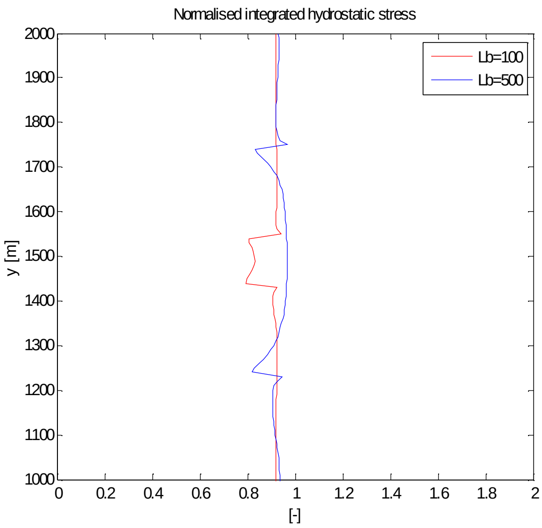


*Figure 5.5 Normalised cross-shore integrated water level gradient induced (hydrostatic) stresses*

## 5.2 Breakwater roughness

For the construction of a SBW, several different materials can be used, from (smooth) concrete elements to rough rubble mound submerged breakwaters. Choosing between different materials already includes a design parameter, from which its importance is evident from paragraph 4.3; the roughness parameter, defined in Delft3D by Chezy values. In contrast, [Lesser et al. 2003] argued to use the bottom roughness of the SBW as a parameter to calibrate the total net mass-transport of water, but as this paragraph will show, the bottom roughness of the SBW is important for multiple processes.

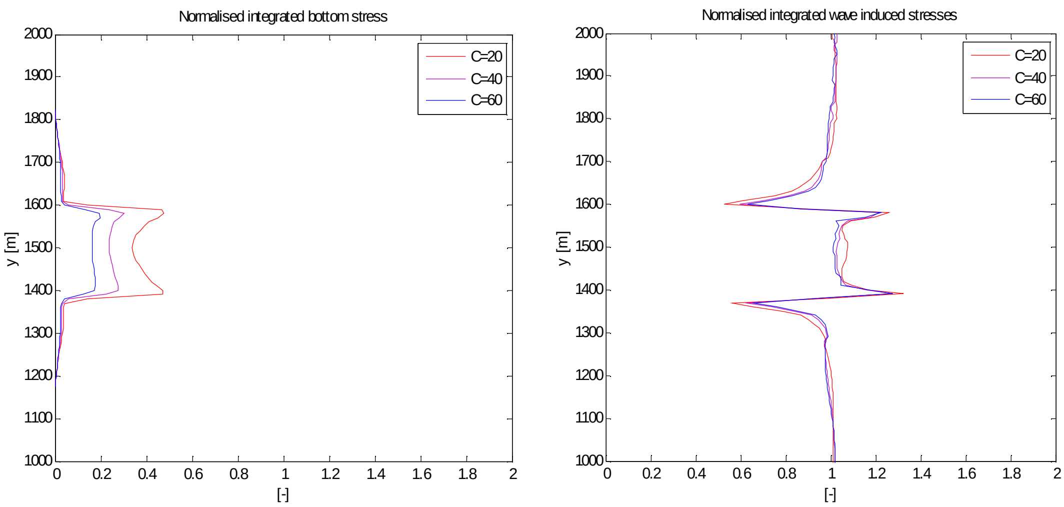


*Figure 5.6 Normalised cross-shore integrated bottom- and wave induced stresses*

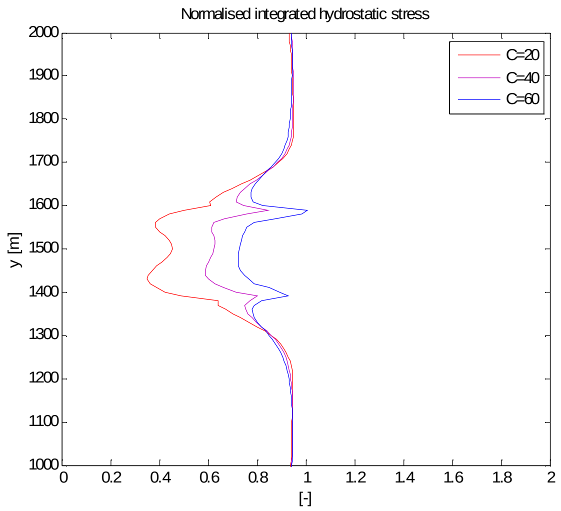


*Figure 5.7 Normalised cross-shore integrated water level gradient induced (hydrostatic) stresses*

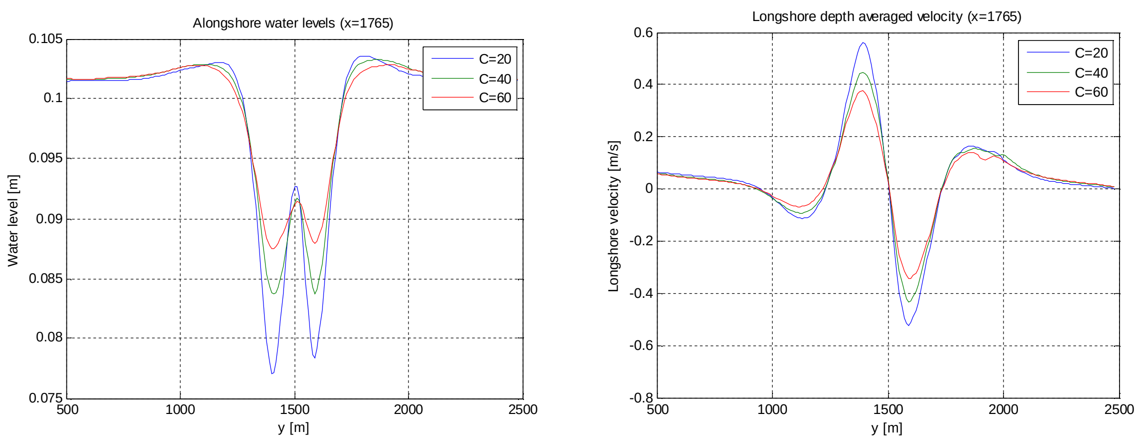


*Figure 5.8 Alongshore water level and depth averaged velocity near the shoreline (x=1765)*

Evident from Figure 5.6 and Figure 5.7 is the importance of the locally varying bottom roughness of the SBW. The local increase of bottom roughness has a negligible effect on the wave breaking (which is not included in SWAN, see chapter 3), but has a strong effect on the bottom stresses. Due to this increase of bottom stresses, the water level set-up behind the SBW decreases, resulting in large alongshore water level gradients. In return, this results in high flow velocities in the direction of the SBW. Concluding, a rough SBW is more effective compared to smooth SBW and are therefore preferred in practical applications.

## 5.3 Crest height

Chapter 2 illustrated the importance of the crest height of a SBW for several processes. Multiple studies have included the effect of the crest height on a variety of processes [Van der Meer et al. 2005; Calabrese et al. 2008; Ranasinghe et al. 2010], therefore the crest height is studied in this paragraph.

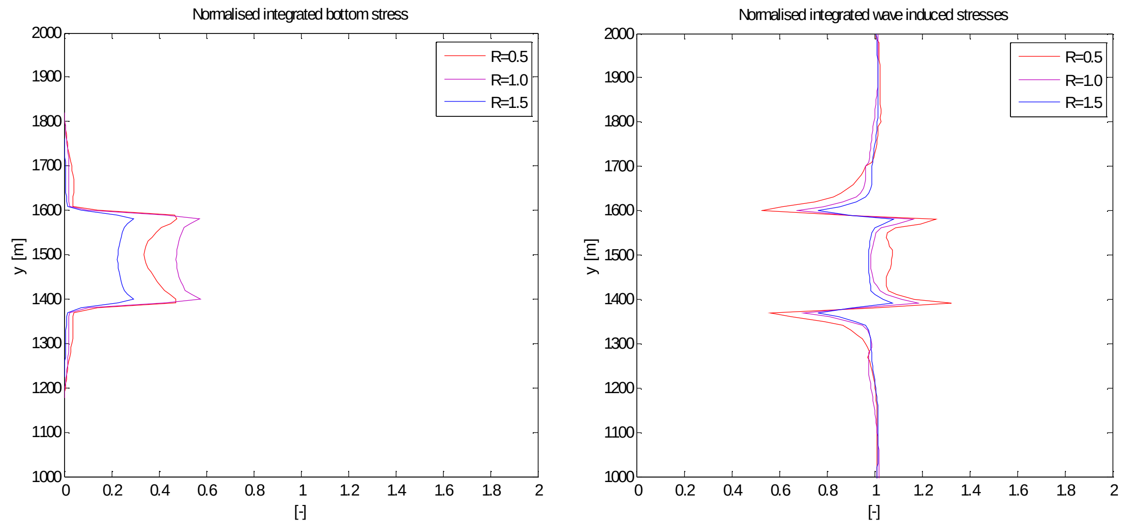


*Figure 5.9 Normalised cross-shore integrated bottom- and wave induced stresses*

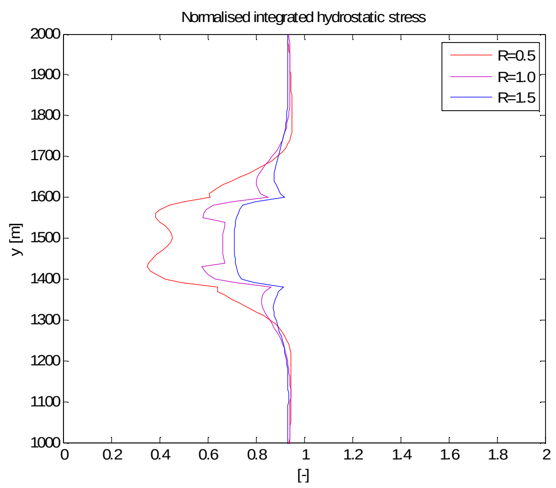


*Figure 5.10 Normalised cross-shore integrated water level gradient induced (hydrostatic) stresses*

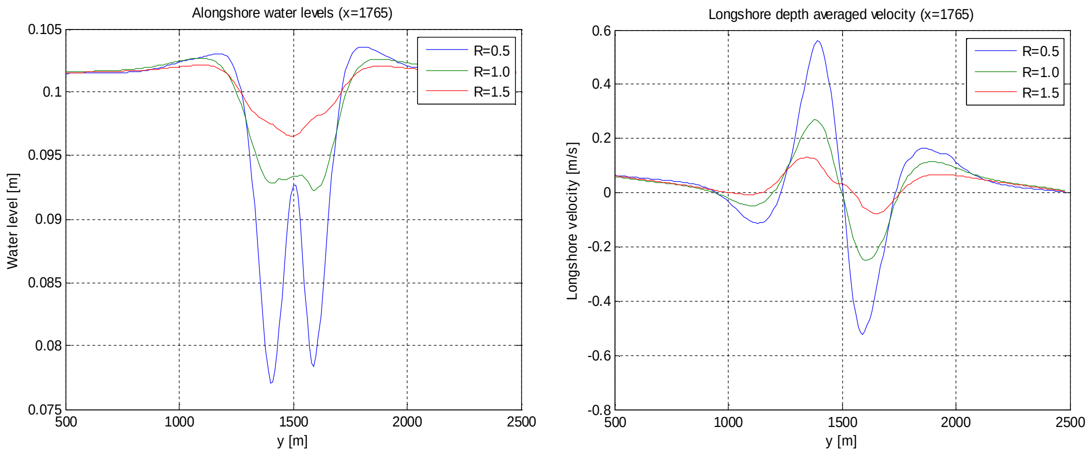


*Figure 5.11 Alongshore water level and depth averaged velocity near the shoreline (x=1765)*

From Figure 5.9, Figure 5.10 and Figure 5.11 it is evident that changing the crest height has a significant effect on the alongshore currents near the shoreline. Both processes, the spatial distribution of wave forcing and bottom stresses over the SBW are affected by the crest height. Despite the decrease of bottom stresses over the SBW for the case of R=-0.5m, decreasing the relative submergence level favours the near shore accretive flow velocities.

Concluding, a crest height/level close to the mean sea level is more effective in reducing near shore water levels. Keeping in mind the driving processes described in paragraph 4.7, the most effective breakwater is an emerged breakwater, as no transmitted wave height or flow enters the lee of the breakwater and no water level set-up will result due to this processes. In addition, an emerged breakwater results in maximum gradients in water level near the breakwater head as wave transmission is excluded. Optimal crest heights for SBWs could however not be studied in this thesis as non-hydrostatic processes are dominant when crest levels are near the mean sea level.

## 5.4 Crest width

Similar to the crest height, the crest width also plays a significant factor for a variety of SBW induced processes [Van der Meer et al. 2005; Calabrese et al. 2008; Ranasinghe et al. 2010].

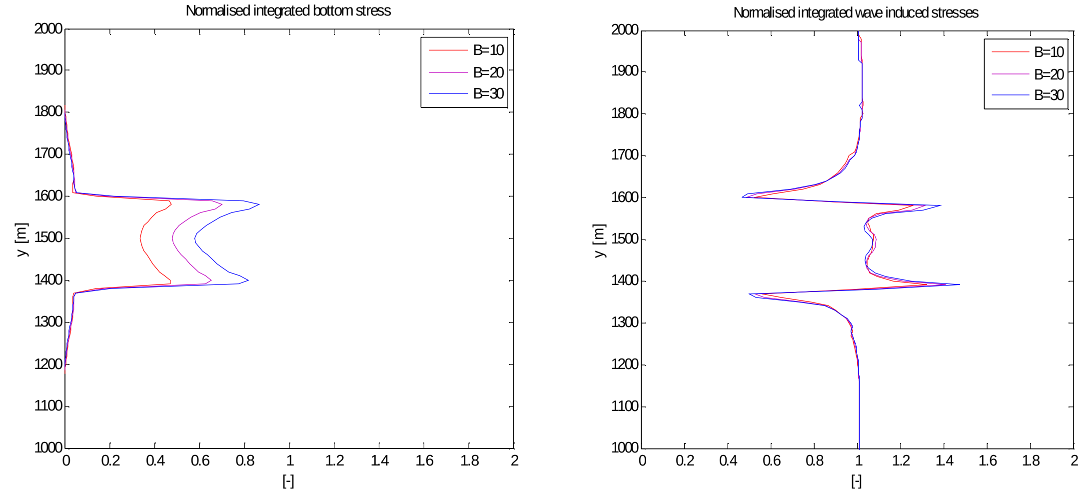


*Figure 5.12 Normalised cross-shore integrated bottom- and wave induced stresses*

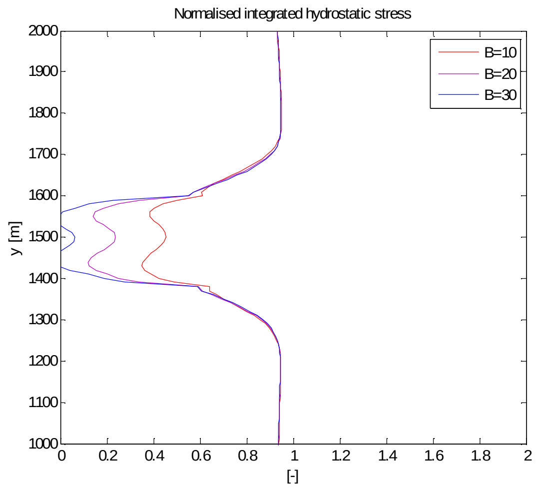


*Figure 5.13 Normalised cross-shore integrated water level gradient induced (hydrostatic) stresses*

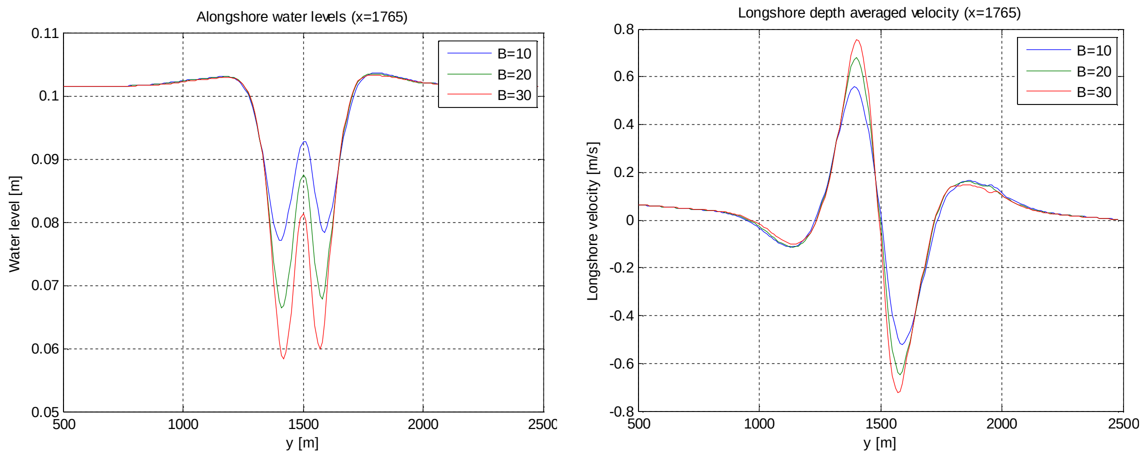


*Figure 5.14 Alongshore water level and depth averaged velocity near the shoreline (x=1765)*

Figure 5.12, Figure 5.13 and Figure 5.14 illustrate the effect of a varying crest width. It appears that depth-averaged velocities and net flow over the SBW are more or less constant and not depending on the crest width, but only on the breakwater slope. However, Figure 5.12 shows a clear increase of total bottom stress with increasing crest width, while only small differences in spatial distribution of wave forcing is visible. In accordance with the increase of total bottom stresses, the cross-shore integrated hydrostatic stresses decrease, though obtained results seems questionable. As a result the water level in the lee of the SBW decrease favouring the increase of alongshore velocities towards the SBW.

Concluding, wider crest of the SBW will increase the alongshore accretive velocities near the shoreline. However compared to other parameters the crest width has only a limited effect on near shore hydrodynamics.

## 5.5 Wave height

Short wave forcing is the driving mechanism for SBW induced differences in near shore wave- and flow conditions and eventually results in morphological changes. Several studies already describe the influence of the incoming wave heights on near shore processes. However, it is interesting to combine the findings of previous chapter in relation to different incoming wave conditions especially the wave height.

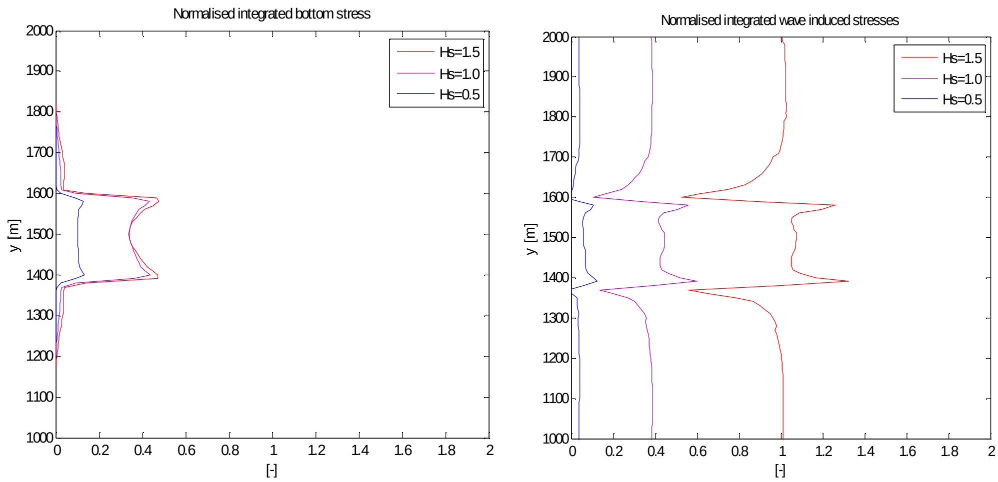


*Figure 5.15 Normalised cross-shore integrated bottom- and wave induced stresses*

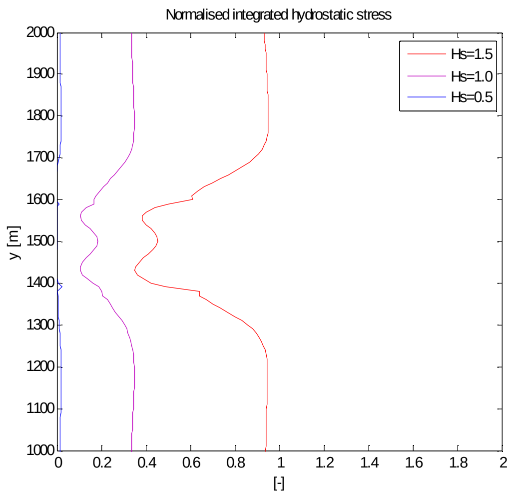


*Figure 5.16 Normalised cross-shore integrated water level gradient induced (hydrostatic) stresses*

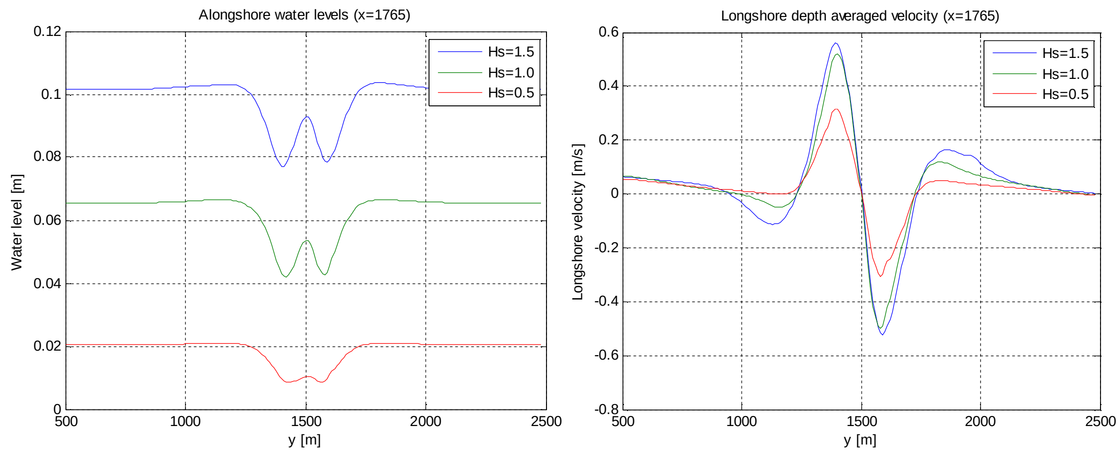


*Figure 5.17 Alongshore water level and depth averaged velocity near the shoreline (x=1765)*

Interesting feature of the results of Figure 5.15, and appendix H is the similarities in the simulations with Hs=1.5m and Hs=1.0 m on depth-averaged velocities, net flow, bottom stresses and differences in water levels. This can be explained by the fact that wave heights on the slope of the SBW are (depth) limited by the foreshore and breakwater slope. Due to these limitations, the bottom stresses remain constant over the SBW, contributing to a more or less constant difference in water levels between the SBW centre and the undisturbed beach. For lower wave heights however the flow and depth averaged velocities reduce, reducing the bottom stresses as well (and inherent water level differences as well).

Concluding from these results, more energetic (constant) wave conditions are in favour of the increase in bottom stresses over the SBW and thereby effectively increasing water level differences. In contrast, the effect of increasing wave heights is limited by the bathymetry, as incoming wave heights are depth-limited by the foreshore.

## 5.6 Conclusions

Combining the results of previous paragraphs and the hydrodynamic analysis, several conclusions can be drawn on individual design parameters of a SBW. In addition, a summary is included to describe the influence of each individual design parameters as well as preliminary design guidelines.

### 5.6.1 Conclusions

Several SBW design- or environmental parameters can effectively influence the near shore hydrodynamics. The most important parameters resulting from published literature are studied in this thesis. Most findings are in good agreement with published literature, but by studying, amongst others the cross-shore momentum balance more insight is given in how these parameters affect near shore hydrodynamics. In addition, new conclusions can be drawn:

- Alongshore length and offshore distance of the SBW are important for both the spatial distribution of wave forcing as well as bottom stresses, due to the associated flow velocities, alongshore currents and alongshore water level gradients.
- The directional spreading of the incoming waves is an important parameter for the redistribution of wave forcing near SBWs.
- The breakwater roughness can be seen as a design parameters as it is related to the materials used. To reduce water levels in the lee of the SBW and increase the alongshore flow near the shoreline towards the SBW, rough SBWs are preferred.
- Based on the hydrodynamic analysis and results from studying the crest height, an emerged breakwater is more effective compared to submerged breakwaters.

### 5.6.2 Summary on design and environmental parameters

SBW induced shoreline changes are governed by a variety of parameters [Ranasinghe et al. 2010]. For the hydrodynamic analysis already the influence of several parameters are studied. Besides the length, offshore distance and directional spreading of the waves, this thesis treats the breakwater roughness, crest height, crest width and incoming wave height. Based on these results, an overview can be given on how individual parameters influence alongshore flow velocities near the shoreline, moreover preliminary design guidelines can be given:

- *Offshore distance*. By increasing offshore distance within the surf zone the incoming wave height on the breakwater slope increases, eventually resulting in more bottom stresses over the SBW. In addition, by increasing the offshore distance of the SBW, the return channel width and averaged depth increase, favouring smaller alongshore water level gradients. As a result, the net flow over the SBW and inherent flow velocities increase. This results in more bottom stresses, which reduce the total water level set-up. In contrast, by increasing the offshore distance, the spatial distribution of wave breaking changes. This results in an increase of undisturbed waves entering the lee of the SBW and a more smoothly varying water level set-up along the shoreline is obtained. For practical applications the offshore distance will coincides with the breakwater length, because an equilibrium has to be found between the spatial distribution of wave forcing and the resulting bottom stresses over the submerged breakwater, see paragraph 4.7.

- *Alongshore length*. Opposite of the offshore distance, increasing alongshore length of the breakwater results in an increasing length of the return channel. Together with the increase of total flow over the SBW, this results in an increase of water levels gradients and thereby reducing the flow and bottom stresses over the SBW from the breakwater head towards the centre. Increasing alongshore length of the SBW results in an increase of total sheltered shoreline behind the SBW. Similar to the offshore distance, an equilibrium has to be sought between the two processes described.
- *Directional spreading*. The directional spreading is together with offshore distance and alongshore length of the breakwater, responsible for the spatial distribution of wave breaking and associated wave forces. For practical application the directional spreading is site specific, but narrow banded directional spectra are preferred, as SBWs can be moved more offshore to increase bottom stresses, while still sheltering the same coastline.
- *Breakwater roughness*. The breakwater roughness influences the bottom stresses over the breakwater. In practise, rough breakwaters will result in stronger accretive currents behind the SBW compared to smooth breakwaters.
- *Crest height.* By constructing a SBW with the crest close to the mean seal level, more wave breaking on the SBW occurs. However, with increasing crest height there are limitations on the flow over the SBW and bottom stresses. In contrast, the increase of wave breaking favours the decrease in water level near the breakwaters head, resulting in higher alongshore velocities. In addition more wave breaking result in lower transmitted wave heights and induced flow towards the shoreline, reducing the total water level set-up. Therefore for SBWs a crest level near the mean sea level is advised, but an emerged breakwater may even be better.
- *Crest width.* With increasing crest width more wave breaking occurs over the SBW, these local additional wave forces are balanced by an increase of bottom stresses. As a result, lower water levels are obtained. In addition, the crest width slightly increases differences in wave forces in the vicinity of the breakwater head, resulting in higher alongshore velocities. Concluding for practical application, a wider crest width is more effective than a small crest width.
- *Incoming wave height***.** Energetic waves cause more wave induced forces. In addition, this can result in an increase of bottom stresses. However the foreshore limits the incoming wave height. In addition to the directional spreading, the incoming wave height is site specific. However larger wave heights have the potential of creating larger alongshore differences in water levels in the vicinity of the submerged breakwaters, resulting in stronger alongshore velocities near the shoreline in the direction of the SBW.

# 6 Submerged breakwater induced morphological response

## 6.1 Introduction

Previous chapter introduced the hydrodynamic processes governing alongshore water level differences and according currents. To illustrate the relation between these initial processes and the eventual morphological results, the trend in water level differences and alongshore current obtained should be visual in the morphological changes, despite the time-depending morphodynamic character of SBW induced morphological response.

This chapter will study the equilibrium profiles and salient development obtained from Delft3D simulations, using the four cases from the hydrodynamic analysis, see paragraph 4.3.1. Although thorough calibration and validation of morphological results are lacking, studying the relative changes between individual simulations gives a clear view on the relation between SBW induced morphological response and initial hydrodynamic conditions. This confirms the importance of previous found relations between the SBW induced hydrodynamic processes and resulting initial near shore currents.

## 6.2 Equilibrium profile

SBW induced morphological changes are depending on local gradients in sediment transport and associated currents. This paragraph will introduce the equilibrium profiles obtained from Delft3D calculations.

In order to describe the morphological development, an accretive simulation will be studied in more detail (Lb=100m and xb=200m), appendix **Error! Reference source not found.** will show the resulting hydrodynamic and morphologic conditions for other simulations. From [Ranasinghe et al. 2006; Ranasinghe et al. 2010] the initial mode of shoreline response is related to the occurring 2/4 cell pattern.

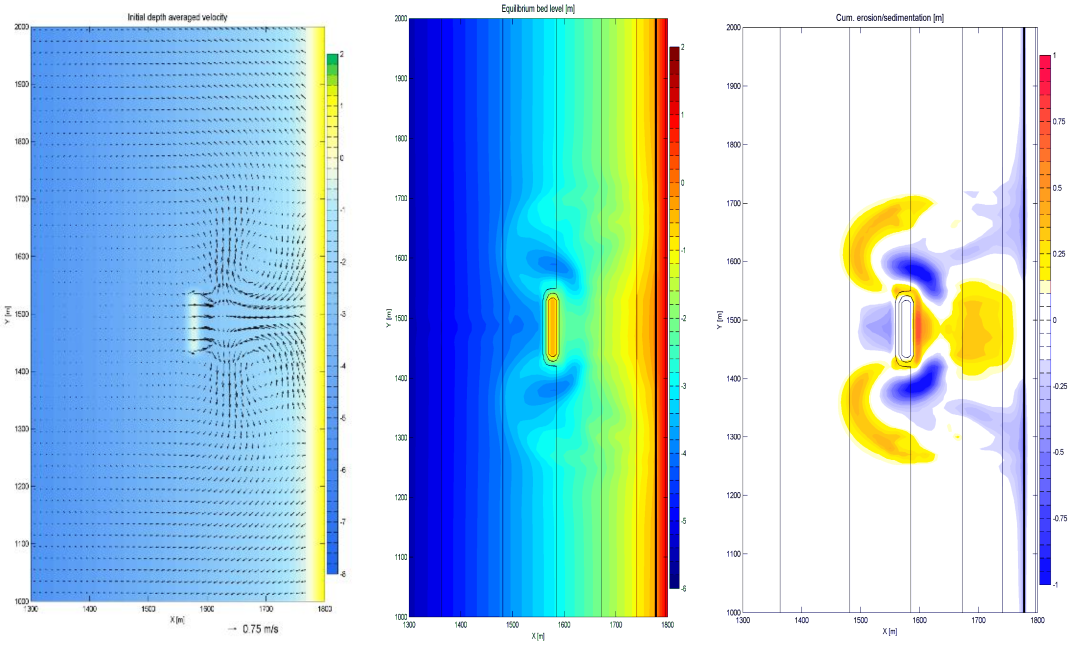


*Figure 6.1 Initial depth averaged velocity, equilibrium bed level and cumulative erosion and sedimentation*

From Figure 6.1, good correspondence is obtained between the initial four-cell pattern and the resulting equilibrium salient development. Though the morphodynamic character of morphological changes is neglected, a clear relation is visible on the spatial distribution of gradients in flow and resulting bed level changes. In the area just next to the SBW, an increase of depth-averaged flow velocities is visible whereas the obtained equilibrium bed level illustrates erosion. In contrast, where the alongshore current reduces near the shoreline, accretion is visible. From paragraph 4.6, it shows that this point of zero velocity gradients near the shoreline is roughly near the SBW head. This determines more or less the alongshore width of the salient developing. Reason for the clear correspondence between the initial conditions and corresponding morphological results is the relative small morphological changes and constant offshore wave conditions. Comparing obtained morphological results with other SBW induced morphological changes presented in paragraph 2.9, shows good correspondence despite the relative large grid sizes for some of these processes.

As a result, Figure 6.2 shows that the point of minimum water level near the SBW in alongshore direction remains more or less constant in space. As the hydrodynamic analysis has shown, this corresponds to the maximum flow velocity towards the breakwater. In addition, erosion is found near the breakwater head due to the offshore-directed return current. As a result, sediment is transported offshore to where depth averaged flow velocities gradually reduce.

In contrast, morphological changes do affect near shore hydrodynamics as an equilibrium profile is obtained. In order to reduce sediment transport to a minimum, according flow velocities and associated shear stresses reduce, until currents results in less than critical shear stresses. Previous findings illustrated the effect of alongshore differences in water level set-up as the most profound cause of alongshore currents. In order to compare the new equilibrium and driving alongshore differences in water level, the initial alongshore differences in water level are compared to the resulting equilibrium alongshore water levels for case 1. In addition, a cross-shore example is given of the xb=200m and Lb=100m case.

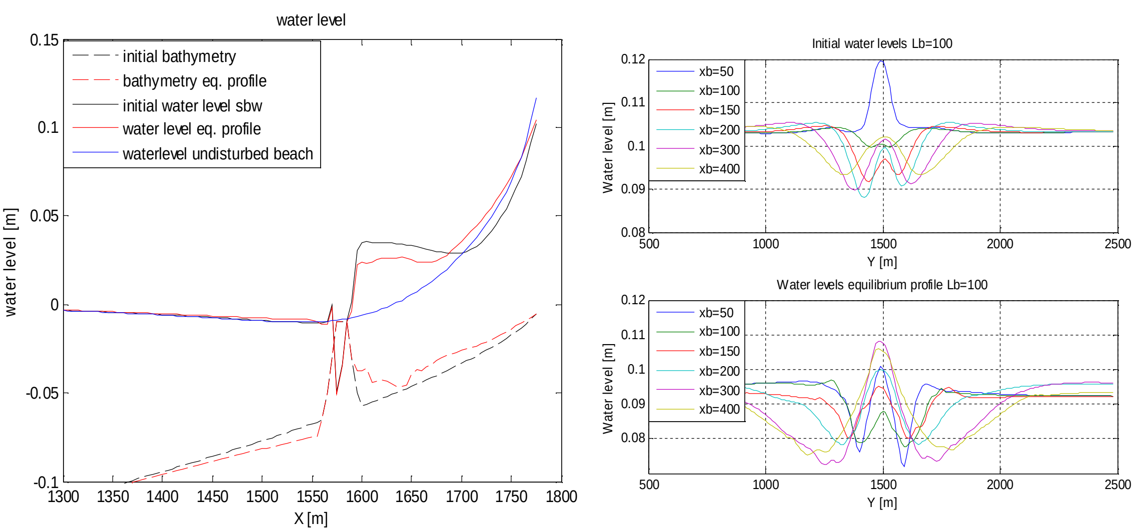


*Figure 6.2 Example of cross-shore water level over sbw (Lb=100m, xb=200m) and alongshore water levels near the shoreline for case 1*

Figure 6.2 shows an example of the changes in water level in cross-shore direction as well as the changing alongshore water levels (see also paragraph 4.6). Due to small-scale erosion and difference in alongshore flow velocities the absolute value of the water levels alongshore differs slightly for the undisturbed coastline. However, in general, water levels near the shoreline of the SBW reduce or increase to more or less the same order as for the undisturbed coastline. As a result, the magnitude of flow velocities near the shoreline reduce. From the example of Figure 6.2, a decrease of water level set-up is visible near the SBW. This result from the decrease of alongshore water level gradients, due to the erosion in the direction of the breakwater head, (see Figure 6.1)

To indicate the relation between the increase of water levels behind the SBW and the morphological response Figure 6.3 shows the cross-shore momentum balance including the bed level changes for an accretive case (Lb=100,xb=200).

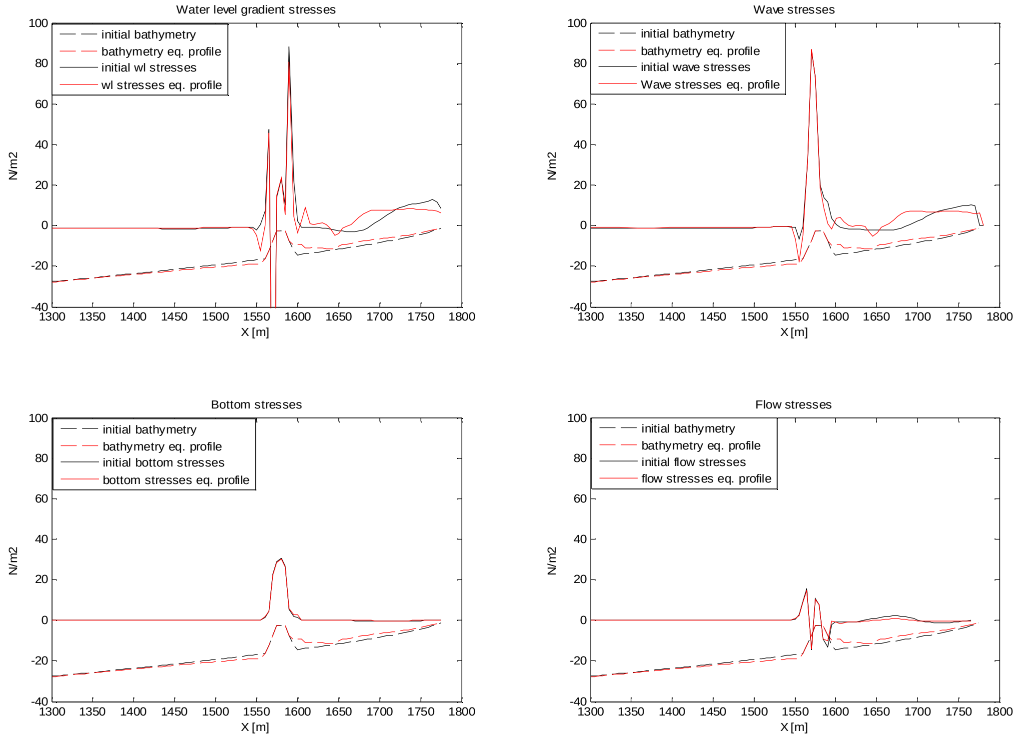


*Figure 6.3 Cross-shore momentum balance new equilibrium profile over centre sbw*

Figure 6.3 illustrates the effect of bed level changes on the spatial distribution of each term of the cross-shore momentum balance for one simulation. In general, bottom stresses and depth averaged acceleration and deceleration of the water in cross-shore direction remains more or less constant for the cross-section over the SBW. However, the bed level changes result in a (offshore) spatial shift of wave breaking in the lee of the SBW. As a result, the balancing water level gradients also shift offshore. By studying a cross-profile of the water level over the SBW and undisturbed coastline, see Figure 6.2, the reduction of alongshore differences for two cross-sections is visible.

Concluding, morphological changes result in a decrease of alongshore water level differences near the shoreline. As a result, the associated alongshore currents and resulting sediment transport decrease, obtaining an equilibrium profile or salient.

## 6.3 Relation initial conditions and morphology

Chapter 4 and 5 describe the hydrodynamic conditions and the influence of individual processes and design parameters. A clear relation between the different processes and eventually magnitude of the alongshore current near the shoreline is obtained. As sediment transport is depending on local flow velocities, gradients in the flow velocities may be a good indication for accretion or erosion. As the focus is on the development of an equilibrium profile/ salient, previous paragraph illustrated the effect of bed level changes and water level set-up in cross-shore direction due to the spatial shift of wave breaking. In appendix I, the morphological changes simulated by Delft3D are presented for all cases. This paragraph will compare the initial conditions to the morphologic changes. Reason is to test if the same trend is visible in obtained morphology, as visible in the hydrodynamic analysis. This will confirm the relation between the individual design parameters and the formation of a salient.

Overall, from Appendix I, the morphological changes are in good agreement with initial conditions. It is noted that some of the morphological developments are not symmetrical as should be. Using a shore-normal wave approach, the main (shore-normal) wave direction coincides with the boundary between two directional bins in the SWAN wave computations, resulting in small deviations of the main wave direction. This may explain the asymmetrical results. In addition, small disturbances are present, mainly for erosive cases. At the end of this paragraph, a discussion is included.

To study the relation between the initial conditions and the morphologic changes in more detail, the alongshore currents and water levels near the shoreline are compared to the morphological changes for accretive 4-cell patterns, visualised by the contour lines. As a phase-averaged model lacks accretive shoreline changes, the 0.5m depth contour is used as indicator of salient development. An example is given in Figure 6.4.

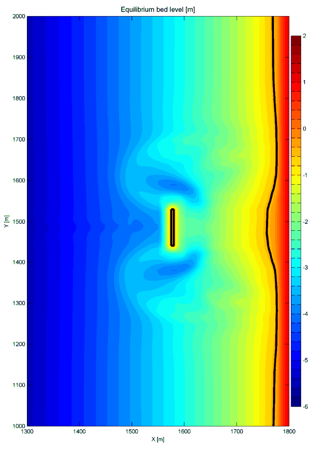


*Figure 6.4 Example of -0.5m contour lines for xb=200m , Lb=100m.*

From Figure 6.5 - Figure 6.8, the induced initial velocities and water level differences near the shoreline correspond well to the eventual accretive morphological changes, although a slightly offshore shifted ‘ideal’ geometry is obtained compared to what is expected from initial hydrodynamic conditions. Appendix I shows for all other simulations a good correspondence between the initial conditions and morphological changes. Although it is difficult to relate morphological changes to initial conditions, the same trend is visible. As for a single varying parameter (xb or Lb), an optimal value can be obtained.

Concluding, the processes governing the initial conditions near the shoreline are responsible for the SBW induced salient development. Despite the complexity and time depending morphodynamic character of SBW induced developments, this relation is evident.

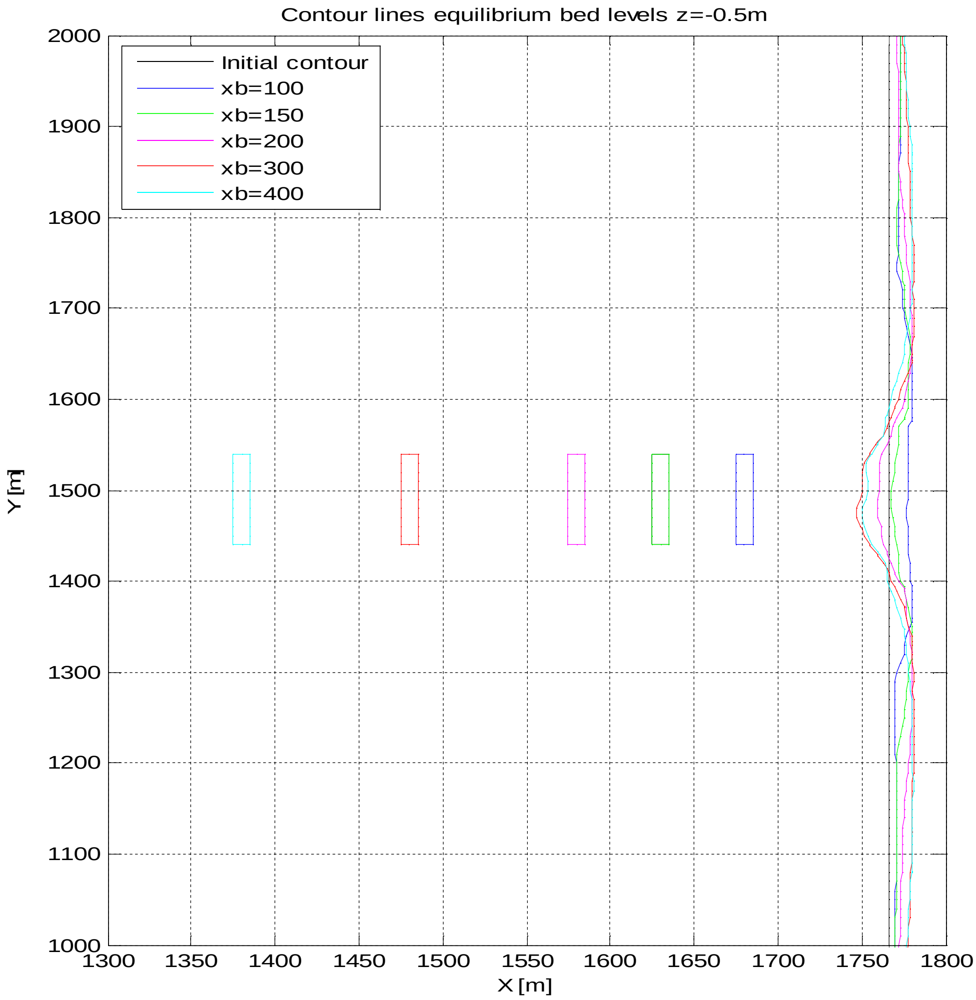


*Figure 6.5 -0.5 m depth contour, accretive simulations case 1*

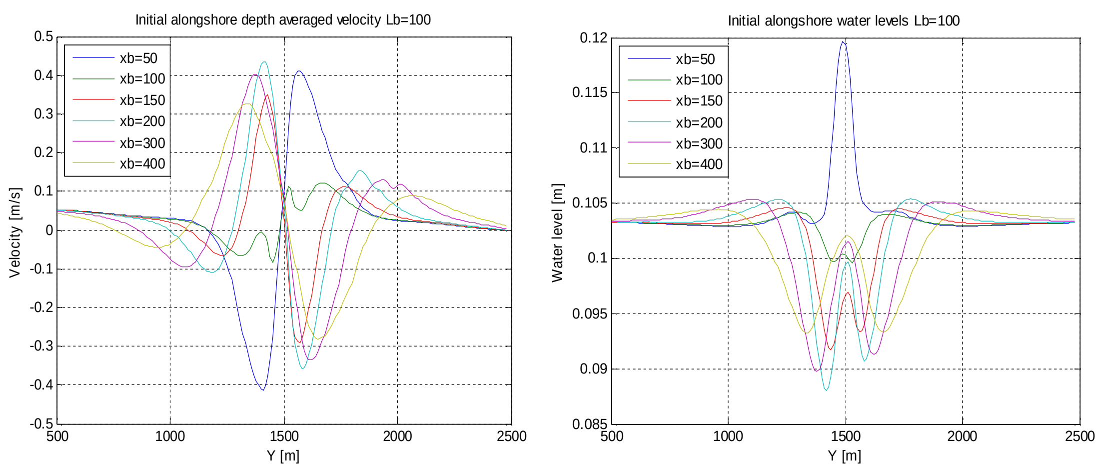


*Figure 6.6 Initial alongshore conditions near the shoreline (x=1765)*

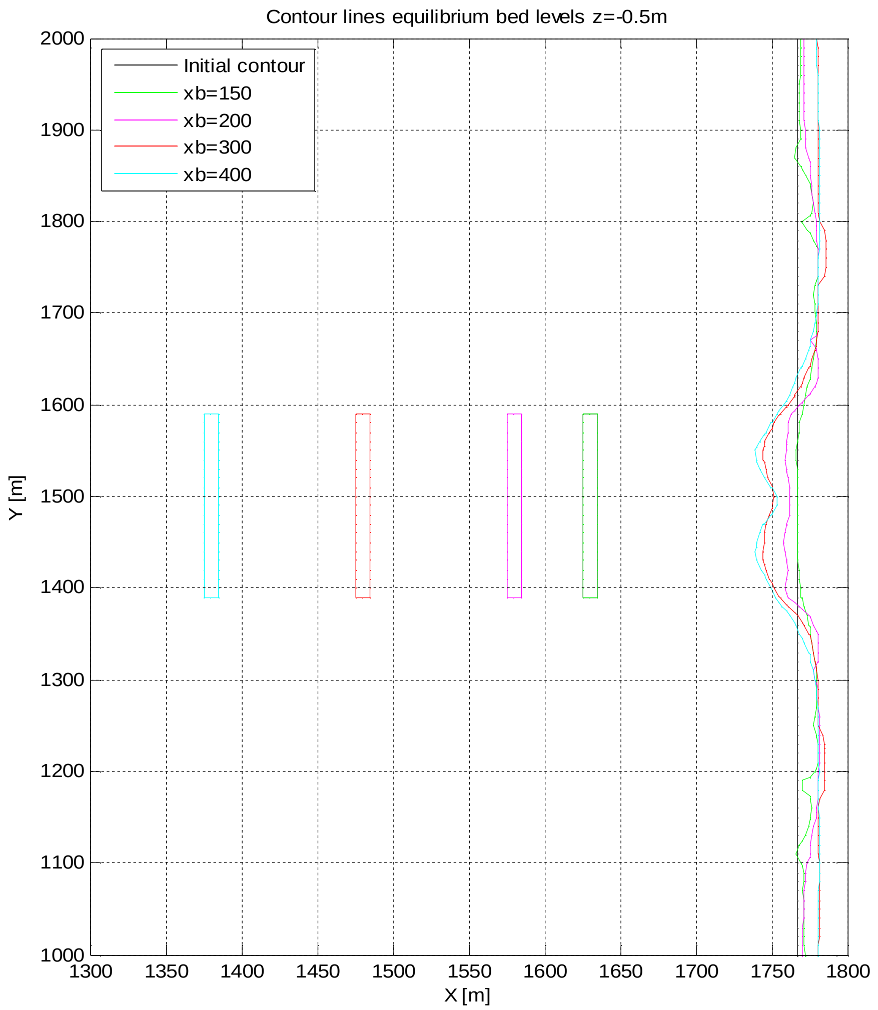


*Figure 6.7 -0.5m depth contour, accretive simulations case 2*

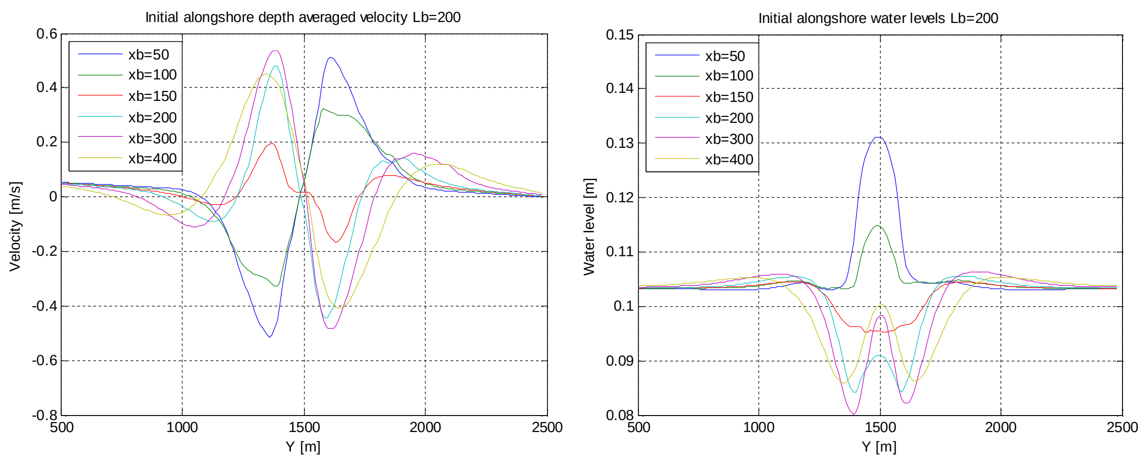


*Figure 6.8 Initial alongshore conditions near the shoreline (x=1765)*

Despite the clear smooth contour lines for accretive shoreline changes, for erosive cases, 0.5m contour lines were less accurate on the scale of O(10m), though overall results show a clear erosive trend. It seems there is a distinct relation between these small-scale fluctuations and the morphological changes. Due to the methodology used, the initial morphological changes are relatively large near the breakwater head. As a result, relative large differences in bathymetry occur for numerical wave modelling purposes, leading to small-scale fluctuations in morphological results. As for erosive SBW cases these morphological changes are in relative shallow waters, the -0.5m depth contour is affected by this process. In addition, for the same reason as morphological response near the breakwater head transfers offshore for accretive cases, no disturbances are obtained in the -0.5m depth contour. In order to counter these fluctuations several options are available, but due to time constraints not accessed. Future research should account for this process as well as the calibration and validation of morphological results in more detail.

## 6.4 Conclusions

In order to confirm the importance of the spatial distribution of wave forcing (or wave sheltering effect) and the momentum balance of wave forcing by bottom stresses over the SBW, additional idealized morphological simulations were performed. By examining the new morphological equilibrium profiles simulated by Delft3D, more insight is given in the hydrodynamic processes which contribute to morphological response to a given design SBW.

Results from the idealized simulations indicate the importance of the reduction of water level set-up in the lee of the submerged breakwater. Due to morphological changes, the new morphological equilibrium profile or salient development results in lower alongshore differences in water level se-up. This confirms the importance of the two distinct processes described in the hydrodynamic analysis as dominant processes for SBW induced morphological response.

In addition, the morphological response simulated by Delft3D is in good agreement with the expected shoreline response to SBWs. This illustrates the ability of Delft3D in a depth-averaged approach to simulate morphological response to a given single shore-parallel SBW.

# 7 Discussion

During this thesis, several simplifications or assumptions are made due to a variety of reasons. However, these simplifications may have an impact on obtained results. This chapter will give an overview on the main simplifications made as well as comments how these simplifications or assumptions will influence results.

## 7.1 Methodology

In the methodology used, important assumptions are already included. Specially to obtain a idealized approach, as used in this study leads to additions simplifications, main considerations to keep in mind are given here.

*Shore normal wave approach.*
In order to exclude site specific conditions, a shore normal wave approach is used, though wave angles are one of the important environmental design parameters for submerged SBWs [Ranasinghe et al. 2006] enabling alongshore currents. It is expected that for an averaged shore normal wave climate or only small wave angles the influence of wave angles is limited. For obliquely waves the alongshore currents will become one of the dominant factors for morphological response to SBWs, see Figure 7.1.

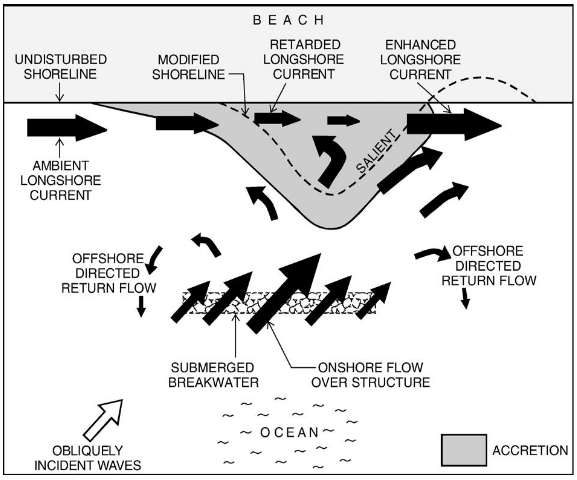


*Figure 7.1 Effect obliquely waves [Ranasinghe and Turner 2006]*

However, a review on shoreline changes of the Gold Coast surfing reef at Narrowneck Australia presented the weekly beach widths on a period of 10 years [Black 2009], see Figure 7.2. Although the morphological response is applicable to a longer stretch of coastline, a clear influence of the artificial surfing reef on beach width is visible, similar to the obtained results for the idealized cases in this thesis.

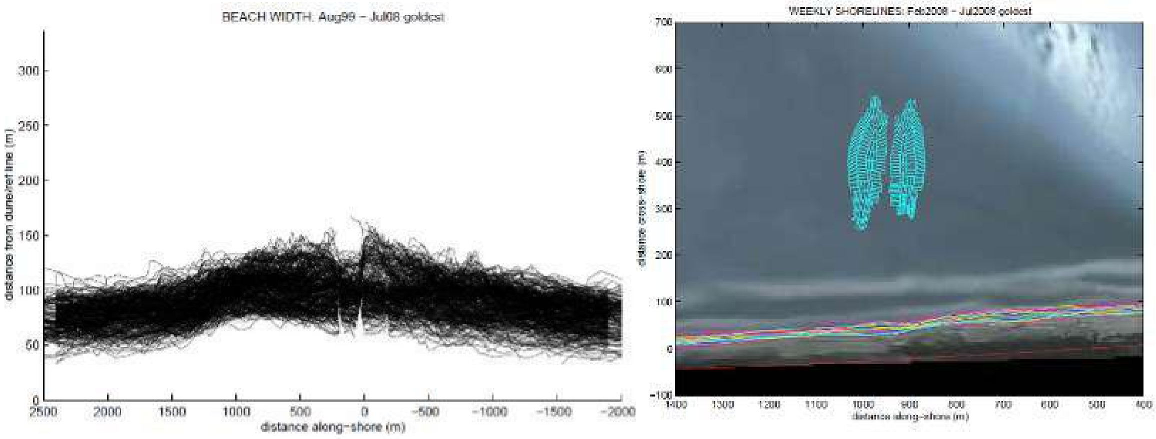


*Figure 7.2 Beach width Gold Coast surfing reef Narrowneck Australia*

*Short wave forcing*
Offshore wave boundary conditions are defined by a JONSWAP spectrum for short waves. Swell, wave groups and tide are neglected, but influence morphology in the surf zone [Baldock et al. 2011]. In addition, when modelling shoreline changes explicitly due to swash motions, long waves should be taken into account. Despite the importance, in general the influence of long waves is limited compared to the effect of short wave forcing and resulting horizontal current patterns.

*Site-specific conditions*
In addition to previous comments, application of a SBW in a site-specific environment may result in additional conditions to keep in mind. Examples of site-specific conditions are adjacent structures, non-uniform beach profiles, sediment budget, variable sediment characteristics, local flora and fauna etc. This is however impossible to take into account for a universal approach but may alter results for specific SBW applications.

## 7.2 Numerical modelling with Delft3D

Numerical modelling can be a powerful tool for studying SBW. However modelling of physical processes automatically results in assumptions and simplifications. Main simplifications governing numerical modelling are presented here.

*Depth-averaged approach Delft3D.*
In order to obtain a computational efficient model, a depth-averaged approach is used in Delft3D. Delft3D assumes for a depth-averaged approach a logarithmic vertical velocity distribution. Several processes like bottom stresses and sediment transport are depending on the near bed velocities and assumed vertical velocity profile. The logarithmic vertical velocity distribution is satisfactory for relatively mild sloping- and single shore normal detached SBWs with limited alongshore length compared to offshore distance. Therefore no significant changes are expected compared to a full three dimensional computation.

*Shore line changes.*
In order to include shoreline erosion in Delft3D, use can be made of the factor for erosion of adjacent dry cells. In this way, the erosion calculated by Delft3D is distributed over the neighbouring (dry) grid cells. In addition to the short wave forcing discussion, accreting shorelines are not accounted, as the swash zone is not incorporated due to the phase-

averaging wave approach. In contrast, using depth contour lines, a indication can be given on the resulting SBW induced shoreline changes.

*Wave breaking on steep slopes*
In this thesis, an online coupling between Delft3D-Flow and SWAN is made to account for the wave-current interaction. Wave breaking in SWAN is based on the spectral version of the original [Battjes and Janssen 1978] model. This model is however limited to mild sloping beaches and may result in over prediction of wave energy dissipation for steep slopes. In this thesis a slope of 1:5 is tested and in contrast to what is expected, an small over prediction of wave transmission was observed compared to the empirical results of [Van der Meer et al. 2005] for rubble mound SBWs, but overall results were still good. As porosity effects and additional friction were not explicitly included in the SWAN model, this also may be more profound compared to differences in wave breaking due to the underlying wave energy dissipation model. Still satisfactory results are obtained within the scatter presented by [Van der Meer et al. 2005].

*Roller model*
In addition to previous subject, the roller model was excluded to obtain satisfactory morphological results. However, the wave roller has an significant influence on set-up for steep slopes [Apotsos et al. 2007]. In contrast, wave breaking on the SBW results in a net depth-averaged flow over the SBW, therefore it remains unclear what the total influence of the roller model for SBWs will be.

*Porosity effects*
General rubble mound SBWs are porous structures. Several studies studied the effect of porosity on processes like, return flow trough the SBW, water level set-up, wave breaking etc. General conclusion is that the effect is relative small compared to other processes.

## 7.3 Hydrodynamic and morphologic analysis

*Design parameters*
Due to time constraints, several design parameters have not been assessed. Amongst others, breakwater slopes, beach profiles and wave periods are kept constant. Additional research is needed to study the influence of these individual parameters on described governing SBW induced processes.

*Initial conditions and morphological equilibrium*
In order to confirm the relation between individual hydrodynamic processes and the morphological response to SBWs, comparison is made between the initial alongshore currents and the resulting morphological response or salient development. Despite the morphodynamic character of SBW induced morphologic changes, the comparison agrees fairly well with expected shoreline results to SBWs.

*Directional spreading and diffraction*
An important factor for redistribution of the wave forcing is the directional spreading of the waves. Previous studies on emerged breakwater have illustrated the relation between the directional spreading of waves and diffraction [Goda et al. 1978]. As these two processes are closely related, difficulties arise to obtain a clear insight in the relative importance of each of the individual processes. In addition to the discussion on these processes in the literature

review, it is argued that the directional spreading is likely to have the most profound influence on near shore hydrodynamics for SBWs.

## 7.4 Conclusions

Concluding, several simplifications and assumptions will influence obtained results and should be studied in more detail to make decisive comments on the relative importance of these assumptions. In addition and because of the discussion presented her, the used methodology throughout this thesis is based on relative importance of individual parameters. By comparing a variety of simulations by only changing a single parameter, errors due to simplifications or assumptions are to a large extend excluded from the results.

# 8 Conclusions and recommendations

Despite the limitations described in previous chapter, conclusions can be made based on the results presented here in this thesis. In addition, recommendations are provided for further research and practical applications.

## 8.1 Conclusions

Recently, the significant amount of failing SBWs indicate the importance of understanding the governing hydrodynamic and morphologic processes before routinely adopting SBWs. Main objective of this thesis is to establish the relation between individual hydrodynamic processes and the governing morphological changes behind a single shore-parallel detached SBW. In order to study these processes, a universal approach is used, excluding site specific conditions, containing constant shore-normal offshore wave conditions and an alongshore uniform beach profile, locally changed to include a given design single shore-parallel detached SBW. In the process of answering the main objective, important conclusions can be made.

**Numerical modelling**

To study the SBW induced morphological response, a depth-averaged model is set-up in Delft3D. By online coupling of the Delft3D Flow-module with SWAN, important governing SBW induced processes are accounted. In contrast to previous studies, the wave transmission/breaking is simulated by depth induced wave breaking using SWAN. In order to test this methodology and to obtain a computational efficient model, sensitivity analyses of numerical parameters and a validation of individual SBW induced processes published in literature is executed.

- Overall, the process-based numerical model Delft3D used in a depth-averaged approach, is capable of accurately simulating SBW induced hydrodynamic and morphologic processes.
- For modelling of SBWs in Delft3D, wave breaking is important. From literature it is evident that using the original [Battjes and Janssen 1978] incorporated in SWAN on steep slopes may lead to undesired errors (see discussion). However, including a roller model and the wave dissipation model of Delft3D-flow to improve wave breaking led to unsatisfactory morphological results. In order to concede not too much on accuracy, while still representing a practical application of a SBW, relatively mild breakwater slopes (1:5) are used and wave breaking is simulated by SWAN. From the validation can be concluded that errors using this approach remained limited.
- Literature on the three dimensional effect of SBWs is to a large extend lacking. Nevertheless, Delft3D produces expected results. As insight in SBW induced processes increases, Delft3D should be calibrated and validated accordingly.

**Hydrodynamic analysis**

SBW induced response is believed to be depending on spatial differences in depth induced wave breaking, which results in differences in water level set-up. In this thesis the cross-shore and alongshore momentum balance are studied for a variety of cases to describe the hydrodynamic changes due to the presence of a SBW. This leads to the following conclusions:

- The difference in nearshore water levels between the lee of the SBW and the undisturbed beach is a good measure to roughly predict the occurrence of a two/four-cell current pattern. Absolute values of the alongshore flow near the shoreline depend on the local water level gradients, wave forcing and bottom stress.
- Resulting from the cross-shore momentum balance, bottom stresses effectively reduce water level set-up in the lee of the SBW due to the onshore-directed flow over the SBW. Important process enabling a net flow over the SBW, is the alongshore limitation on water level set-up, due to the non-uniform bathymetry induced by the SBW. See Figure 8.1.

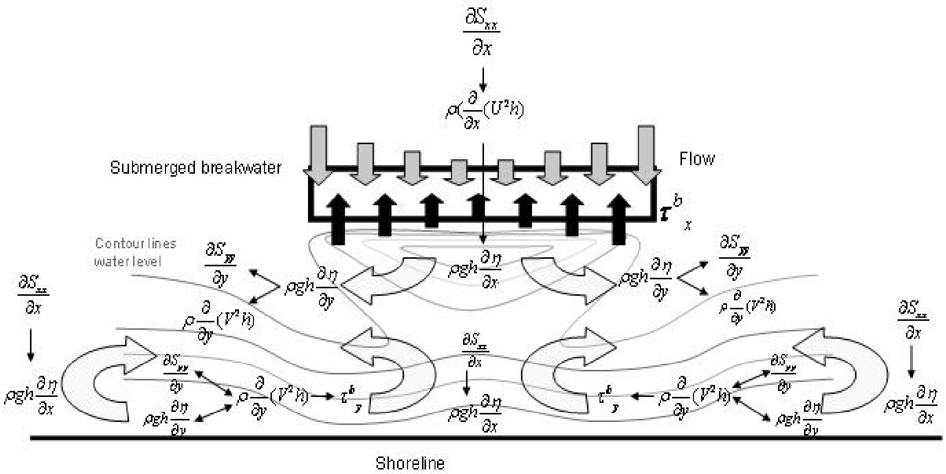


*Figure 8.1 Spatial distribution of cross- and alongshore momentum balance for 4 cell pattern*

- The spatial distributed wave forcing (commonly referred as wave sheltering effect), increases the total wave forcing in cross-shore direction in the vicinity (over and behind) the SBW. For all simulations a reduction of total wave forcing compared to the undisturbed coastline is found next to the SBW. This is explained by the oblique waves breaking offshore over the SBW. Together with the momentum balance by bottom stresses, this depends the reduction in water level set-up in the lee of the SBW, see Figure 8.2.

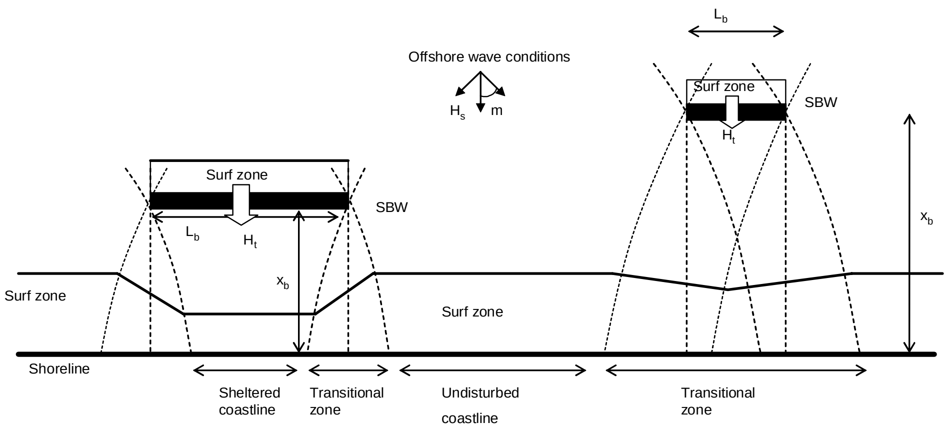


*Figure 8.2 Overview of the redistribution of wave forcing due to a submerged breakwater*

- Though not thoroughly accessed in this thesis, due to lacking literature (see previous chapter) on this subject, the vertical distribution of the velocities on the SBW will determine to a large extend the bottom stresses and eventual increase or decrease of water levels near shore.

**Submerged breakwater design parameters**
As the spatial distribution of wave forcing and the compensation of wave forcing by bottom stresses over the SBW are the main driving processes of eventually alongshore differences in nearshore water levels, several design parameters are studied to see the impact of the individual design parameters on these processes. Important conclusions from this analysis are:

- Breakwater length, offshore distance, crest height and crest width influence the nearshore hydrodynamics according to previously presented literature [Ranasinghe et al. 2010], though more insight is shown in how these parameters affect shoreline changes.
- Breakwater roughness can be seen as a design parameter. By using materials with large roughness coefficients, water level set-up in the lee of the SBW is further reduced.
- In addition to the breakwater roughness, the directional spreading of the incoming waves is an important parameter to take into account for SBW induced processes.

Based on the results presented for crest submergence level and the relation between the water level differences and the bottom stresses for SBWs, it can be argued that submerged breakwaters are less effective compared to emerged breakwaters. Reason for this is that the bottom stress induced water level reduction is usually an order lower compared to the total water level set-up on an undisturbed beach. In addition, the transmitted wave heights will still result in a water level set-up at the sheltered coastline for SBWs. In contrast, for an emerged breakwater only undisturbed waves under large angles and diffraction will enter the sheltered area, as similar to SBWs.

**Morphological analysis**
In addition to the hydrodynamic analysis, morphological simulations are made to confirm the relation between the different processes and the related governing parameters and the resulting morphological response to SBWs. Conclusions from these results are:

- Morphological changes or salient development result in a new morphological equilibrium profile, which reduces the alongshore water level differences and associated flow velocities.
- Morphological changes or salient development from numerical modelling with the depth-averaged Delft3D model is in good agreement with expected morphological changes from initial hydrodynamic conditions, especially obtained alongshore water level differences. In addition, the salient development is in good agreement with published literature on single shore-parallel SBW induced morphological response.
- Similar to [Ranasinghe et al. 2006], an ‘ideal’ offshore distance and alongshore length of the SBW are obtained for which morphological response is maximum. In order to optimise the morphological response to SBWs, the two processes

described in the hydrodynamic analysis should be considered, see recommendations.

- More research and extensive calibration/validation of Delft3D is needed to make decisive conclusions on morphological response to SBWs. However, the ability of Delft3D in a depth-averaged approach to accurately simulate hydrodynamic and morphological response to SBWs, enables a powerful tool for additional research on a variety of SBW processes. In addition, practical applications of SBWs can simulated in a computational efficient way.

**General**

Resulting from this thesis, a computational efficient depth-averaged Delft3D model is set-up and applied, which is able to accurately simulate SBW induced processes known from literature. From the idealized simulations performed, two distinct processes contribute to the resulting morphological changes behind a SBW. First process is the distribution of wave forcing, commonly referred as wave sheltering effect. Second process is the momentum balance between wave forcing and bottom stresses over the SBW, induced by alongshore limitations on water level set-up behind the SBW. Although these described individual processes are familiar to previous findings, more insight is given in the origin of these processes as well as the relation with the initial mode of shoreline response.
In addition to the environmental and design parameters presented in [Ranasinghe et al. 2010], the bottom roughness of the SBW and the directional spreading of waves have a profound effect on SBW induced hydrodynamics. These are important design parameters to keep in mind for future research on morphological response to SBWs.
Although no absolute values of morphological response were considered, an important step in understanding the driving processes of SBW induced morphological changes is taken. Results from the idealized simulations are in good agreement with the expected morphological response to SBWs. In addition, the ability of Delft3D to simulate morphological response to SBWs, enables a powerful numerical tool for additional studies on SBW induced morphological processes, as well as studies on practical applications of SBWs.

## 8.2 Recommendations

Although this thesis increases insight of governing SBW induced processes and can be beneficial to the engineering community to construct more efficient and successful SBWs, still a clear lack of knowledge on a variety of coastal processes is present. Therefore, this paragraph will sum up the main recommendations for further study.

**Future research**

- Diffraction

Current literature focuses on cross-shore directed processes and neglecting the alongshore dimension, because of amongst others, the cost reduction compared to full three-dimensional measurements. However, for relative short alongshore breakwaters the diffraction may become important for the processes described by the directional spreading of waves in this thesis. To the best of the author’s knowledge, diffraction for fully SBWs has not been studied yet, while comparison with emerged breakwater is difficult due to the dependency on the wave reflection.

- Flow velocities over the submerged breakwater.

Important factor in understanding the induced hydrodynamic processes are the vertical flow structure as well as the depth-averaged flow over the SBW. Current literature is limited by only accounting for the Stokes drift and roller contributions, but neglecting the contributions due to wave radiation stresses. A first step in accounting for the alongshore non-uniform affect of single shore-parallel SBWs is conducting a series of experiments on the flow over the head of the breakwater. Concluding from result of this thesis, the flow over the SBW head seems to be constant due to the zero water level set-up restriction. By excluding the length of the breakwater, small symmetrical scale test can be performed. In addition, the flow velocities and associated bottom stresses near the breakwater head can be assumed constant over the breakwater for small values of $L_b$/xb as a first approximation.

- Field measurements

In addition to previous recommendations, the amount of field measurements on morphological response to single shore-parallel detached SBWs before and after construction, excluding nourishments, but including extensive offshore wave data is limited. In addition, scale test on the morphological response are difficult due to scale effects of sediments. Nevertheless, field data is crucial for understanding morphological processes and serve as calibration data for numerical modelling. It is therefore recommended to always perform bathymetrical surveys prior and especially after a period of several months for each constructed SBW and gather all available data in an extensive data set. If nourishments are included, additional surveys should be made after completion of the nourishment. The resulting data set would be of significant value to the coastal engineering community in general.

**Numerical modelling**

- Calibration of Delft3D.

As discussed, data sets on morphological response due to a single shore-parallel SBW excluding nourishments are rare, however when data becomes available, Delft3D should be calibrated and validated accordingly. Currently an effort is made at Deltares to calibrate Delft3D based on a recently available dataset of a double SBW system.

- Roller model

To implement the effect of the wave roller, the wave dissipation model within Delft3D-flow should be used. Due to the unsatisfactory results obtained in morphological calculations this thesis neglects wave roller effects. Effort should be made to implement this model satisfactory for morphological simulations. In addition, using the wave dissipation model within Delft3D Flow, different maximum wave height to depth ratios based on the work of [Battjes and Stive 1985] and [Ruessink et al. 2003] can be studied.

- Mass-flux

One of the important additional parameters included to obtain satisfactory morphological results is the mass-flux term (switched off). This term accounts for the (wave-induced) onshore sediment transport and is (partly) balanced by an undertow in morphological computations. In a depth-averaged approach, undertow is disregarded, so therefore this term should be switched of for morphological computations. This is however not a standard option in Delft3D, but should be included (Keyword is xxx).

- Initial bathymetry

In this thesis, sand nourishments after construction to mitigate erosion near the submerged breakwater to balance the salient development are neglected. To include both in an integrated approach for practical and numerical improvements, an initial salient can be included in the bathymetry before starting morphological simulations. As initial morphological changes decrease significantly compared to an alongshore uniform profile, the morphological acceleration factor and the flow-wave coupling time can be increased significantly, reducing the computational time, while shoreline changes are accounted for. In addition to paragraph 6.3, this may even results in more smoothly varying results. A ‘smart’ dredging strategy would be to dredge near the head of the breakwater as morphological results indicate an offshore transport of sediment near the head of the breakwater for all cases. In this way, a satisfactory practical approach is used which allows for a numerical efficient study.

- Large initial morphological changes

In addition to previous recommendations, the effect of the large morphological changes near the breakwater head on small spatial scales for numerical modelling should be studied. This might be one of the important reasons for the morphological instabilities for the roller model.

- Shore normal wave approach

For a shore normal wave approach, the mean wave direction should not be on the boundary of two directional bins, as this may results in asymmetrical results. Otherwise, use can be made of multiple wave angles, which together results in a shore normal approach.

**Practical applications**

- Design formulations

  Ultimate objective of research on morphological changes to SBWs is to obtain a design formulation to quantify the equilibrium salient development in the lee of the SBW. As this thesis shows, two distinct processes contribute to the resulting morphological changes. First, the distribution of wave forcing near SBWs. This processes should accounted by a function containing at least $a = f(x_b, L_b, m, H_s, H_t, \theta, ...)$ (excluding refraction). The second processes is the bottom stress, which should be a formulation containing the parameters $b = f(x_b, L_b, R_c, B, \tan\alpha, C, H_s, T_p, \theta, h, ...)$ .In addition, sediment characteristics should be accounted. It is expected that the resulting ‘ideal’ design submerged breakwater will be an equilibrium of $\frac{\partial a}{\partial(parameter)} = -\frac{\partial b}{\partial(parameter)}$. Most parameters can however be determined using common sense and recommendations made in this thesis, however especially for the length of the breakwater and the offshore distance this equilibrium formulation will be of interest.
- Efficiency of submerged breakwater

  Based on the driving processes for SBWs, it can be argued that emerged breakwaters are more effective compared to submerged breakwaters. If beach aesthetics are unimportant, it is recommended to construct emerged breakwaters or low crest structures instead of SBWS. In contrast, when constructing for instance an artificial (surf) reef, the combined benefit of nature habitat, recreational purposes and additional coastline development will be an interesting combination.
- Swimmer safety

  The morphological response to SBWs is depending on accretive rip currents near the shoreline. However, the need for morphological development of coastlines is of often due neighbouring recreational purposes. These bathymetry induced accretive rip currents may however have a significant effect on swimmer safety.

# 9 References


Ahrens, J. P. (1987). "Characteristics of reef breakwaters." CERC Technical Report 87-17.

Apotsos, A., B. Raubenheimer, S. Elgar, et al. (2007). "Effects of wave rollers and bottom stress on wave setup." Journal of Geophysical research Vol. 112.

Baldock, T. E., J. A. Alsina, I. Caceres, et al. (2011). "Large-scale experiments on beach profile evolution and surf and swash zone sediment transport induced by long waves, wave groups and random waves." Coastal Engineering 58(2): 214-227.

Baldock, T. E., P. Holmes, S. Bunker, et al. (1998). "Cross-shore hydrodynamics within an unsaturated surf zone." Coastal Engineering 34(3-4): 173-196.

Baldock, T. E., P. Manoonvoravong and K. S. Pham (2010). "Sediment transport and beach morphodynamics induced by free long waves, bound long waves and wave groups." Coastal Engineering 57(10): 898-916.

Battjes, J. A. and H. W. Groenendijk (2000). "Wave height distributions on shallow foreshores." Coastal Engineering 40(3): 161-182.

Battjes, J. A. and J. P. F. M. Janssen (1978). Energy loss and set-up due to breaking of random waves. Proc. 16th Int. Conf. Coastal Engineering, ASCE. pp 1993-2004

Battjes, J. A. and M. J. F. Stive (1985). "Calibration and verification of a dissipation model for random breaking waves." Journal of Geophysical research vol. 90(NO. C5): 9159-9167.

Beji, S. and J. A. Battjes (1993). "Experimental investigation of wave propagation over a bar." Coastal Engineering 19(1-2): 151-162.

Black, K. P. (2009). "Gold Coast Reef, 10 year anniversary" http://www.surfingramps.com.au.

Black, K. P. and C. Andrews (2001a). "Sandy shoreline response to offshore obstacles part 1: salient and tombolo geometry and shape." Journal of Coastal Research(SI(29)): 82-93.

Black, K. P. and C. Andrews (2001b). "Sandy shoreline response to offshore obstacles part 2: discussion on formative mechanisms." Journal of Coastal Research (SI29): 94-101.

Boccotti, P. (2000). Wave mechanics for ocean engineering. Oxford, Elsevier.

Booij, N. (1983). "A note on the accuracy of the mild-slope equation." Coastal Engineering 7(3): 191-203.

Booij, N., N. C. Ris and L. H. Holthuijsen (1999). "A third-generation wave model for coastal regions, part 1, model description and validation." Journal of Geophysical research 104: 7649-7666.

Bosboom, J. and M. J. F. Stive (2010). Coastal Dynamics 1, lecture notes CT4305 Part 1.

Burcharth, H. F., S. J. Hawkins, B. Zanuttigh, et al. (2007). Environmental Design Guidelines for Low Crested Coastal Structures Elsevier Ltd.

Calabrese, M., D. Vicinanza and M. Buccino (2002). Large scale experiments on the behaviour of low crested and submerged breakwaters in presence of broken waves In proceedings of the International Conference on Coastal Engineering, ASCE Cardiff, UK.

Calabrese, M., D. Vicinanza and M. Buccino (2008). "2D Wave setup behind submerged breakwaters." Ocean Engineering 35(10): 1015-1028.

D'Angremond, K., J. W. Van der Meer and R. J. De Jong (1996). Wave transmission at low crested structures. Proc 25th Int. Conf. on Coastal Engineering, ASCE

Dalrymple, R. A. and R. G. Dean (1971). "Piling-up behind low and submerged permeable breakwaters." Journal of Waterways and harbors Division ww2 423-427.

Dalrymple, R. A., J. H. MacMahan, A. J. H. M. Reniers, et al. (2011). "Rip currents " Annual Review Fluid Mechanics

Dean, R. G., R. Chen and A. E. Browder (1997). "Full scale monitoring study of a submerged breakwater, Palm Beach, Florida, USA." Coastal Engineering 29(3-4): 291-315.

Deltares (2010a). Delft3D-FLOW, Simulation of multi-dimensional hydrodynamic flows and transport phenomena, including sediments, user manual

Deltares (2010b). Delft3D-Wave, Simulation of short-crested waves with SWAN, user manual

Eldeberky, Y. and J. A. Battjes (1995). Parameterization of triad interactions in wave energy models. Coastal Dynamics Conference '95 Gdansk, Poland.

Goda, Y., T. Takaiama and Y. Suzuki (1978). Diffraction diagrams for directional random waves. Proceedings of the International Conference - Coastal Engineering

Haller, M. C., R. A. Dalrymple and I. A. Svendsen (2002). "Experimental study of nearshore dynamics on a barred beach with rip channels " Journal of Geophysical research 107(C6).

Hansen, J. B. (1990). "Periodic waves in the surf zone: Analysis of experimental data." Coastal Engineering 14(1): 19-41.

Hasselmann, K., T. P. Barnett, E. Bouws, et al. (1973). "Measurements of wind wave growth and swell decay during the Joint North Sea Wave Project (JONSWAP)." Deutsche Hydrographische Zeitschrift vol. 8 (no12.).

Holthuijsen, L. H. (2007). Waves in oceanic and coastal waters.

Hsu, J. R. C. and R. Silvester (1990). "Accretion behind single offshore breakwater." Journal of Waterway, Port, Coastal and Ocean engineering Vol 116: p.362-380.

Huang, C.-J. and C.-M. Dong (2001). "On the interaction of a solitary wave and a submerged dike." Coastal Engineering 43(3-4): 265-286.

Hur, D.-S. (2004). "Deformation of multi-directional random waves passing over an impermeable submerged breakwater installed on a sloping bed." Ocean Engineering 31(10): 1295-1311.

Janssen, T. T. and J. A. Battjes (2007). "A note on wave energy dissipation over steep beaches." Coastal Engineering 54(9): 711-716.

Johnson, H. K. (2006). "Wave modelling in the vicinity of submerged breakwaters." Coastal Engineering 53(1): 39-48.

Johnson, H. K., T. V. Karambas, I. Avgeris, et al. (2005). "Modelling of waves and currents around submerged breakwaters." Coastal Engineering 52(10-11): 949-969.

Lesser, G. R., J. A. Roelvink, J. A. T. M. van Kester, et al. (2004). "Development and validation of a three-dimensional morphological model." Coastal Engineering 51(8-9): 883-915.

Lesser, G. R., J. H. Vroeg, J. A. Roelvink, et al. (2003). Modelling the morphological impact of submerged offshore breakwaters. Proc. Coastal sediments '03, World Scientific Publishing co. Florida, USA.

Longuet-Higgins, M. S. (1967). "On the wave induced difference in mean sea level between two sides of a submerged breakwater." Journal of Marine Research 25 148-153.

Longuet-Higgins, M. S. and R. W. Stewart (1964). "Radiation stress in water waves, a physical discussion with applications." Deep Sea Res. 11: 529-563.

Loveless, J. H., D. Debski and A. B. McLeod (1998). Sea level set-up behind detached breakwaters. Proceedings of the International Conference on Coastal Engineering, ASCE. .

MacMahan, J. H., E. B. Thornton and A. J. H. M. Reniers (2006). "Rip current review." Coastal Engineering 53(2-3): 191-208.

McCormick, M. E. and D. R. B. Kraemer (2002). "Polynomial approximations for Fresnel integrals in diffraction analysis." Coastal Engineering 44(3): 261-266.

Nairn, R. B., J. A. Roelvink and H. N. Southgate (1990). Transition zone width and implications for modelling surfzone hydrodynamics. Coastal Engineering Conference 1990, Delft.

Nelson, R. (1997). "Height limits in top down and bottom up wave environments." Coastal Engineering 32(2-3): 247-254.

Penny, W. G. and A. T. Price (1952). "The diffraction theory of sea waves and the shelter afforded by breakwaters." Philosophical Transactions of the Royal Society of London A 244: 236-253.

Pierson, W. J. J., J. J. Tuttel and Wooley (1952). The theory of the refraction of a short crested Gaussian sea surface with application to the northern New Jersey coast. Proc. 3rd Conf. Coastal Engineering (Cambridge, MA). New York, ASCE.

Pope, J. and J. L. Dean (1986). Development of design criteria for segmented breakwaters. 20th ICCE. Taipei, Taiwan.

Ranasinghe, R., M. Larson and J. Savioli (2010). "Shoreline response to a single shore-parallel submerged breakwater." Coastal Engineering 57(11-12): 1006-1017.

Ranasinghe, R., C. Swinkels, A. Luijendijk, et al. (2011). "Morphodynamic upscaling with the MORFAC approach: Dependencies and sensitivities." Coastal Engineering 58(8): 806-811.

Ranasinghe, R. and I. L. Turner (2006). "Shoreline response to submerged structures: A review." Coastal Engineering 53(1): 65-79.

Ranasinghe, R., I. L. Turner and G. Symonds (2006). "Shoreline response to multi-functional artificial surfing reefs: A numerical and physical modelling study." Coastal Engineering 53(7): 589-611.

Raubenheimer, B., R. T. Guza and S. Elgar (1996). "Wave transformation across the inner surf zone." Journal of Geophysical research Vol 101.

Reniers, A. J. H. M. and J. A. Battjes (1997). "A laboratory study of longshore currents over barred and non-barred beaches." Coastal Engineering 30(1-2): 1-21.

Reniers, A. J. H. M., E. B. Thornton, T. P. Stanton, et al. (2004). "Vertical flow structure during Sandy Duck: observations and modeling." Coastal Engineering 51(3): 237-260.

Roelvink, J. A. (1993). "Dissipation in random wave groups incident on a beach." Coastal Engineering 19(1-2): 127-150.

Roelvink, J. A. (2006). "Coastal morphodynamic evolution techniques." Coastal Engineering 53(2-3): 277-287.

Roelvink, J. A. and D. J. R. Walstra (2004). Keeping it simple by using complex models. Advances in hydro-science and -engineering, volume VI : proceedings of the 6th International conference on hydro-science and -engineering. , Brisbane, Australia.

Ruessink, B. G., D. J. R. Walstra and H. N. Southgate (2003). "Calibration and verification of a parametric wave model on barred beaches." Coastal Engineering 48(3): 139-149.

Schaap, J. (1997). Modelling the effects of submerged breakwaters in a wave basin Faculty of Civil Engineering Delft, TU Delft. MSc.

Seabrook, S. R. and K. R. Hall (1998). "Wave transmission at Submerged Rubblemound breakwaters." Coastal Engineering.

Smit, M. W. J., A. J. H. M. Reniers, B. G. Ruessink, et al. (2008). "The morphological response of a nearshore double sandbar system to constant wave forcing." Coastal Engineering 55(10): 761-770.

Sommerfeld, A. (1896). "Mathematische theorie der diffraktion." Mathematische Annalen 47: 317-374.

Stelling, G. S. (2009). "Computational modelling of flow and transport, CT4340 lecture notes, TU Delft ".

Sumer, B. M., J. Fredsøe, A. Lamberti, et al. (2005). "Local scour at roundhead and along the trunk of low crested structures." Coastal Engineering 52(10-11): 995-1025.

Svendsen, I. A. (1984). "Mass flux and undertow in a surf zone." Coastal Engineering 8(4): 347-365.

Thornton, E. B. and R. T. Guza (1983). "Transformation of Wave Height Distribution." Journal of Geophysical research Vol.88(Noc10): p.5925-5938.

Torrini, L. (1997). Nearshore effects of submerged breakwaters. Faculty of Civil Engineering Delft, TU Delft MSc.

Van der Hout, C. M. (2008). Morphological impact of a deep water reef. Faculty of Civil Engineering, TU Delft. MSc Thesis.

Van der Meer, J. W. (1990). "Low-crested and reef breakwaters." Delft Hydraulics report no. H986 2.

Van der Meer, J. W., R. Briganti, B. Zanuttigh, et al. (2005). "Wave transmission and reflection at low-crested structures: Design formulae, oblique wave attack and spectral change." Coastal Engineering 52(10-11): 915-929.
Van der Meer, J. W. and K. d'Angremond (1991). wave transmission at low crested structures Coastal structures and breakwaters, ICE. London.
Van Rijn, L. C. (1993). "Principles of sediment transport in rivers, estuaries and coastal seas." Aqua publications, The Netherlands
Van Rijn, L. C. and K. M. Wijnberg (1996). "One-dimensional modelling of individual waves and wave-induced longshore currents in the surf zone." Coastal Engineering 28(1-4): 121-145.
Vicinanza, D., I. Cáceres, M. Buccino, et al. (2009). "Wave disturbance behind low-crested structures: Diffraction and overtopping effects." Coastal Engineering 56(11-12): 1173-1185.
Young, D. M. and F. Y. Testik (2009). "Onshore scour characteristics around submerged vertical and semicircular breakwaters." Coastal Engineering 56(8): 868-875.
Young, I. R., L. A. Verhagen and S. K. Khatri (1996). "The growth of fetch limited waves in water of finite depth. Part 3. Directional spectra." Coastal Engineering 29(1-2): 101-121.
Yu, Y.-X., S.-X. Liu, Y. S. Li, et al. (2000). "Refraction and diffraction of random waves trough breakwater." Ocean Engineering 27: 489-509.

Deltares

# Appendices

# A Sensitivity analyses model characteristics

## A.1 Introduction

In order to test the influence of several numerical parameters, a sensitivity analysis is performed, see paragraph 3.4. Main objective of this sensitivity analysis is to obtain a computationally efficient model, while not impairing on accuracy of Delft3D results.

As this thesis focuses on morphological response to SBWs, this appendix will relate the influence of several numerical parameters on the computed morphological response to SBWs by Delft3D. For all simulations, the design SBW and offshore boundary conditions are kept constant (xb=200m, Lb=200m, B=10m, Rc=-0.5m, tanα=0.2, Hs=2m, Tp=9s, m=4, θ=270$^0$/shore normal). Main point of interest is the salient development in the lee of the SBW. Therefore a domain behind the SBW is chosen for which the in accuracy in morphological response is calculated, see Figure A.1.

*Figure A.1 Domain sensitivity analysis*

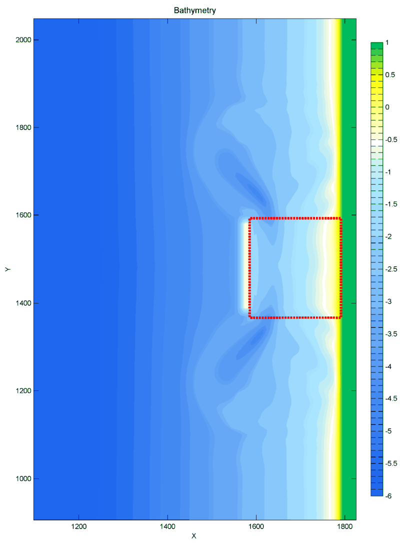


In order to quantify the accuracy of obtained morphological response to SBW, the bias and mean averaged error are calculated for morphological simulations:

$$BIAS = \frac{1}{M*N}\sum_{i=1,1}^{M,N}(Y_{m,n} - X_{m,n})$$

$$MAE = \frac{1}{M*N}\sum_{i=1,1}^{M,N}\left|Y_{m,n} - X_{m,n}\right|$$

In which Y is the considered simulation, and X the most accurate or reference value. To reduce the absolute computational time, most simulations are performed over a period of 30 morphological days, as large morphological changes are at the start of each simulation.

## A.2 Overview

| Parameter | Default Value | Range | Sensitivity wave height (m) | | Sensitivity bed level (m) | | Morph. Time (days) | New Value |
|---|---|---|---|---|---|---|---|---|
| | | | Bias | MAE max | Bias | MAE max | | |
| Morphological factor | 1 | 1-60 | 0 | 0 | $-7*10^{-3}$ / 0 | 0.02 | 30 | 15 |
| Coupling interval | 1 min | 1-60 | $-7*10^{-4}$ / 0 | $1.5*10^{-3}$ | -0.02 / 0 | 0.08 | 60 | 10 |
| Relative change (wave accuracy) | 0.005 | 0.005-0.05 | 0 / $7.5*10^{5}$ | $1.5*10^{-4}$ | $-1*10^{-5}$ / $3*10^{-5}$ | $1*10^{-4}$ | 15 | 0.005 |
| Percentage of grid points (wave accuracy) | 99% | 90 – 99% | $-2*10^{-5}$ / 0 | $2.5*10^{-5}$ | $-1.2*10^{-5}$ / $1.5*10^{-5}$ | $5*10^{-6}$ | 15 | 99 |
| Wave-current interaction | on | off | -0.01 | 0.02 | 0.07 | 0.1 | 30 | on |
| Mass-flux | on | off | $3.5*10^{-3}$ | $6*10^{-3}$ | -0.1 | 0.14 | 15 | |
| Breaker depth index (SWAN) | 0.73 | 0.6 – 0.9 | -0.2 / 0.2 | 0.2 | -0.06 / 0.05 | 0.14 | 30 | 0.73 |
| Breakwater roughness (FLOW) | 20 | Off (C=65) | $-9*10^{-4}$ | $6*10^{-3}$ | -0.2 | 0.3 | 30 | on |
| Breakwater roughness (FLOW) | 20 | 10 - 40 | $-1.2*10^{-3}$ / 0 | $5*10^{-3}$ | -0.2/ 0.1 | 0.25 | 30 | 20 |
| Roller model | off | On , y= 0.51/ 0.73 BJ | 0.006 / 0.012 | 0.01 / 0.015 | 0 / 0.3 | 0.2 / 0.4 | 30 | Off, due to instabilities |
| | | On, y ~ kh | 0.012 | 0.013 | 0.17 | 0.35 | 30 | |
| Horizontal eddy Viscosity | 1 $m^2/s$ | Varying, HLES | | | | | | 1 $m^2/s$ |

### A.3 Morphological factor and coupling interval

#### A.3.1 Coupling interval

| **Parameter** | **Comment** |
|---|---|
| Parameter | Delft3D Flow and SWAN coupling interval |
| Range | 1, 5, 10, 15, 30, 60 [min] |
| Reference value | 1 min |
| New value | 10 min |
| Morphological time | 60 days |
| | |
| Bias bed level | 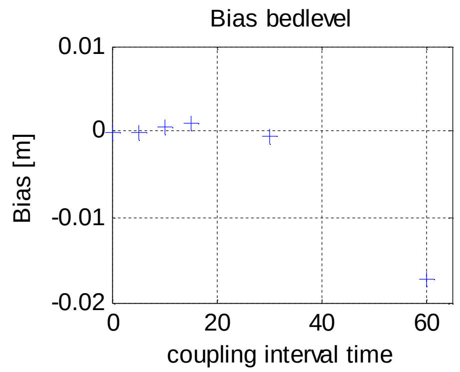 |
| MAE bed level | 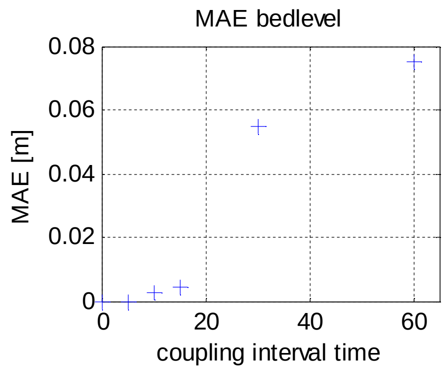 |
| Simulation time | 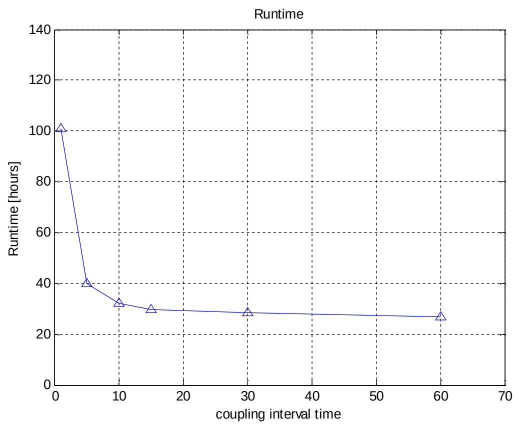 |
| Comments | Morphological acceleration factor is kept constant (m=15) for all simulations |

### A.3.2 Morphological acceleration factor

| **Parameter** | **Comment** |
|---|---|
| Parameter | Morphological acceleration factor |
| Range | 1, 5, 10, 15, 20, 30, 40, 60 |
| Reference value | 1 |
| New value | 15 |
| Morphological time | 30 days |
| | |
| Bias bed level | 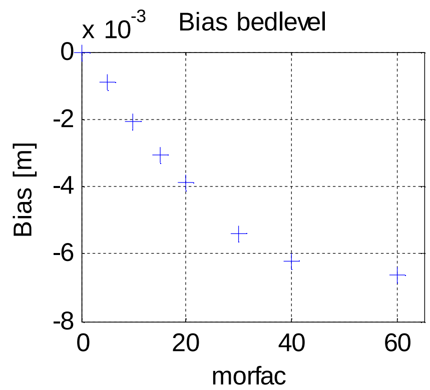  |
| MAE bed level | 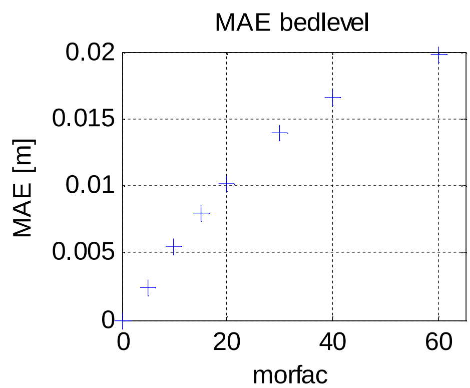  |
| Simulation time | 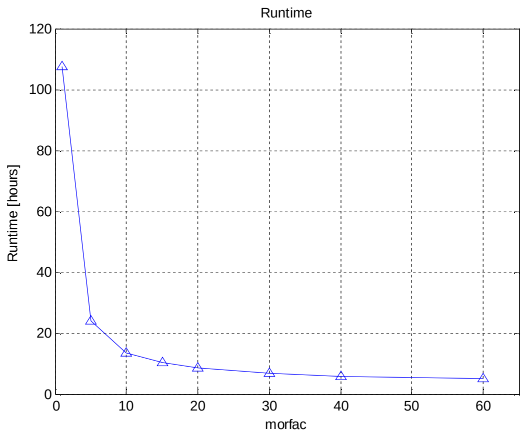  |
| Comments | Coupling time is kept constant for each simulation. |

### A.3.3 Morphological acceleration and coupling time

Number of computations equal in morphological time

<table>
<tr><th>Parameter</th><th>Comment</th></tr>
<tr><td>Parameter</td><td>Morphological acceleration factor and coupling time</td></tr>
<tr><td>Range</td><td>
<table>
<tr><td colspan="4">Keeping the morphological time steps equal:</td></tr>
<tr><td></td><td></td><td></td><td></td></tr>
<tr><td></td><td>Morfac</td><td>Coupling interval (min)*</td><td>Hydrological time (dd:hh:mm)**</td></tr>
<tr><td></td><td>1</td><td>60</td><td>62:12:00</td></tr>
<tr><td></td><td>5</td><td>12</td><td>12:12:00</td></tr>
<tr><td></td><td>10</td><td>6</td><td>6:06:00</td></tr>
<tr><td></td><td>15</td><td>4</td><td>4:04:00</td></tr>
<tr><td></td><td>20</td><td>3</td><td>3:03:00</td></tr>
<tr><td></td><td>30</td><td>2</td><td>2:02:00</td></tr>
<tr><td></td><td></td><td></td><td></td></tr>
<tr><td></td><td>*</td><td>60/Morfac</td><td></td></tr>
<tr><td></td><td>**</td><td>62:12:00/ Morfac</td><td></td></tr>
<tr><td></td><td></td><td></td><td></td></tr>
</table>
</td></tr>
<tr><td>Reference value</td><td>M= 1, coupling interval 60 min</td></tr>
<tr><td>New value</td><td>M=15, coupling time 10 min, see previous paragraphs</td></tr>
<tr><td>Morphological time</td><td>60 days</td></tr>
<tr><td></td><td></td></tr>
<tr><td>Bias bed level</td><td>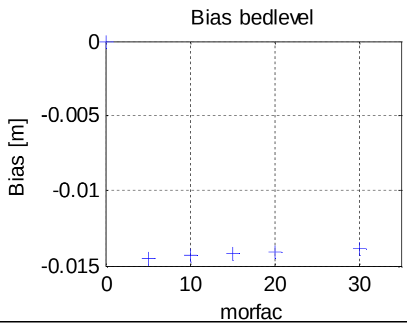
</td></tr>
<tr><td>MAE bed level</td><td>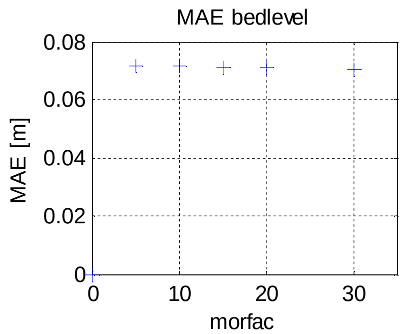
</td></tr>
<tr><td>Simulation time</td><td>Constant</td></tr>
<tr><td>Comments</td><td>The error in the base case induced by the “large” coupling time is of more influence than the error made by the increasing morfac, which results in the figure below.</td></tr>
</table>

## A.4 Wave solution accuracy level

### A.4.1 Relative change

| Parameter | Comment |
|---|---|
| Parameter | Relative change (accuracy criteria SWAN) |
| Range | 0.005, 0.01 0.02, 0.03, 0.05 |
| Reference value | 0.005 |
| New value | 0.005 |
| Morphological time | 15 days |
| | |
| Bias bed level | 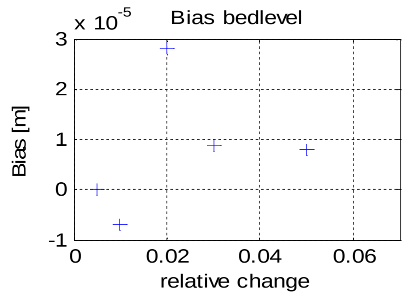 |
| MAE bed level | 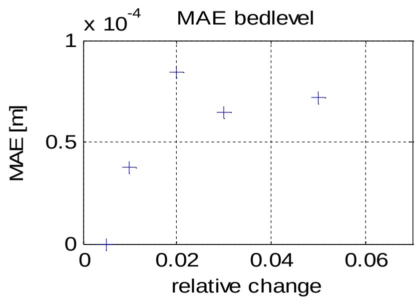 |
| Simulation time | 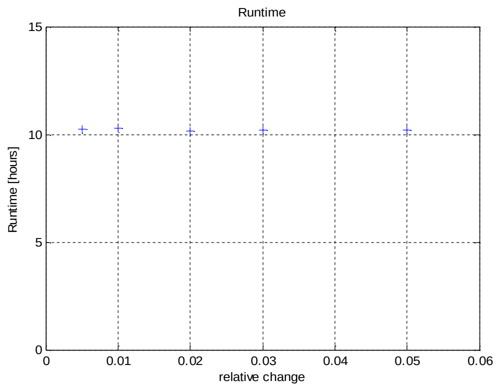 |
| Comments | Using a relative change <0.02 gives more accurate results compared to the base case, although the errors are still small. The relative change has hardly any influence on the runtime, due to amongst other the constant offshore wave conditions. |

A.4.2 Percentage of grid points

| Parameter | Comment |
|---|---|
| Parameter | Percentage of grid points (SWAN) |
| Range | 90, 95, 97, 98, 99 [%] |
| Reference value | 99 % |
| New value | 99 % |
| Morphological time | 15 days |
| | |
| Bias bed level | 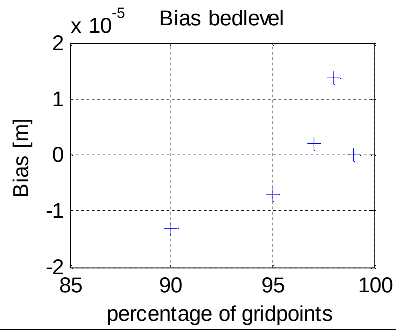 |
| MAE bed level | 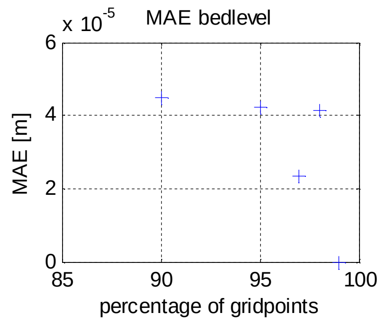 |
| Simulation time | Constant |
| Comments | Similar to the accuracy criteria of SWAN, the influence of percentage of grid points is relatively small, due to amongst others the constant wave conditions offshore |

## A.5 Wave-current interaction

| Parameter | Comment |
|---|---|
| Parameter | Wave current interaction |
| Range | On (=1)/off(=0) |
| Reference value | Off |
| New value | On |
| Morphological time | 30 days |
| | |
| Bias bed level | 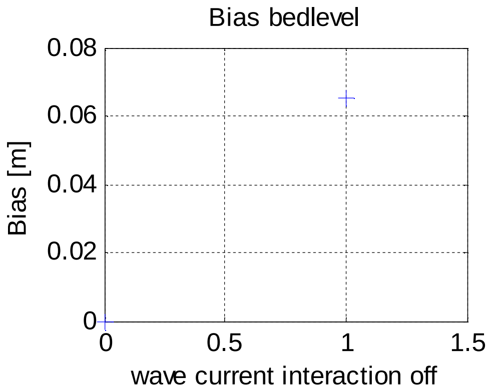 |
| MAE bed level | 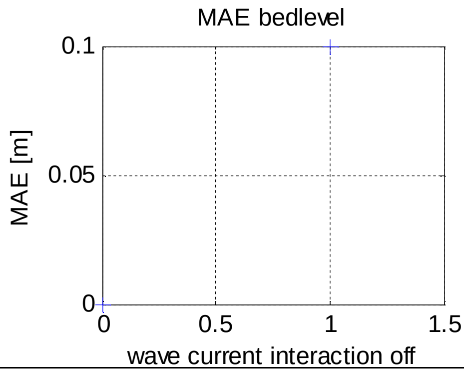 |
| Simulation time | Constant |
| Comments | Though no absolute conclusions can be made, including the wave current interaction is in good agreement with the modelling philosophy of a process based model and therefore included. |

## A.6 Mass flux

| Parameter | Comment |
|---|---|
| Parameter | Mass-flux |
| Range | On (=1)/off(=0) |
| Reference value | Off |
| New value | Off |
| Morphological time | 30 days |
| | |
| Bias bed level | 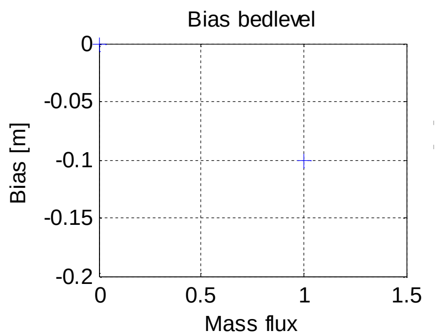 |
| MAE bed level | 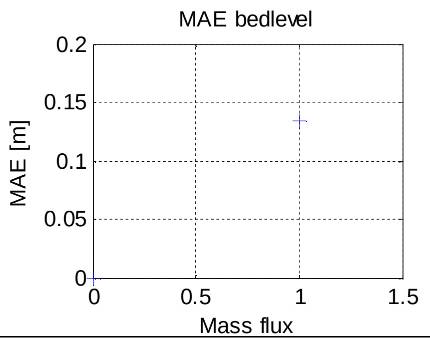 |
| Simulation time | Constant |
| Comments | Including the mass-flux term for morphological simulations in a 2DH model results in questionable sediment transport as for all conditions undertow is neglected |

## A.7 Breaker depth index

| Parameter | Comment |
|---|---|
| Parameter | Breaker depth index y (SWAN) |
| Range | 0.6, 0.73, 0.78, 0.83, 0.9. |
| Reference value | 0.73 |
| New value | 0.73 |
| Morphological time | 30 days |
| | |
| Bias bed level | 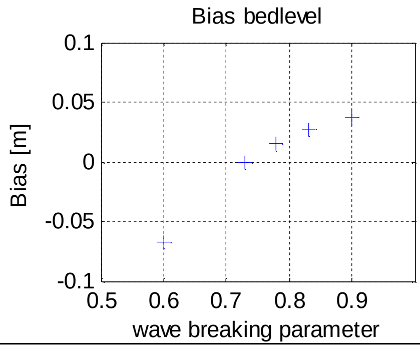  |
| MAE bed level | 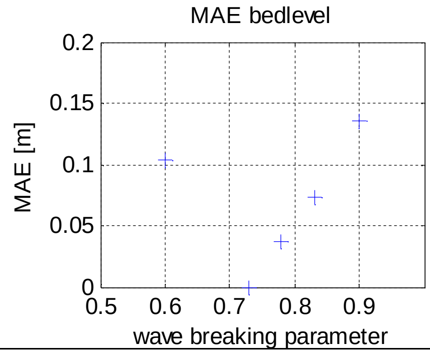  |
| Simulation time | Constant |
| Comments | |

## A.8 Breakwater roughness

| Parameter | Comment |
|---|---|
| Parameter | Breakwater roughness in Delft3D-Flow |
| Range | 10, 15, 20, 25, 30, 35, 40, 65 [$m^{1/2}s^{-1}$ ] (Chezy values) |
| Reference value | 20 |
| New value | 20 |
| Morphological time | 30 days |
| | |
| Bias bed level | 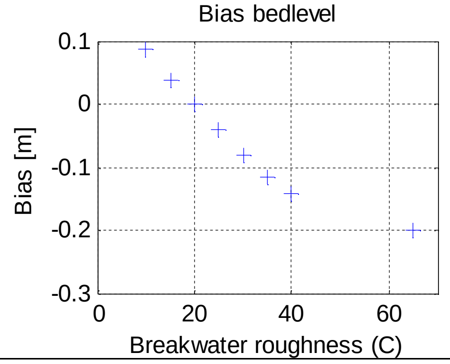  |
| MAE bed level | 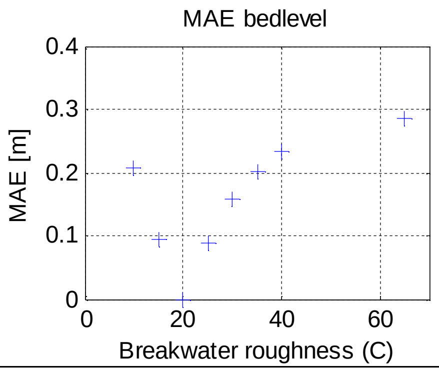  |
| Simulation time | Constant |
| Comments | In the hydrodynamic analysis, the influence of the breakwater roughness is further discussed, but the importance is evident. |

## A.9 Roller Model

| Parameter | Comment |
|---|---|
| Parameter | Roller model including breaker depth index |
| Range | Off (using SWAN), on y=0.73, on y=0.51, on y=0.56, on y~kh |
| Reference value | Off |
| New value | Off |
| Morphological time | 30 days |
| | |
| Bias bed level | Wave breaker parameter y=1 = Ruessink 2003 y~kh 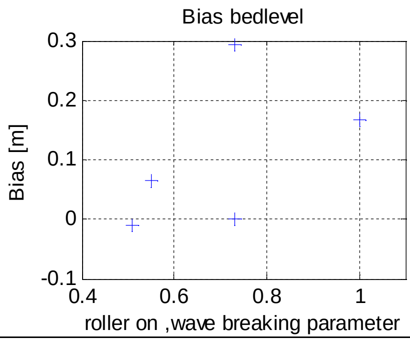  |
| MAE bed level | 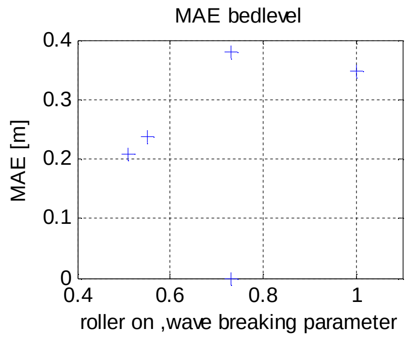  |
| Simulation time | Constant |
| Comments | Including the roller model leads to spurious morphological results, therefore the wave dissipation model of SWAN will be used |

## A.10 HLES

| **Parameter** | **Comment** |
|---|---|
| Parameter | HLES (horizontal eddy viscosity) |
| Range | - |
| Reference value | - |
| New value | 1 |
| Morphological time | 30 days |
| | |
| HLES | 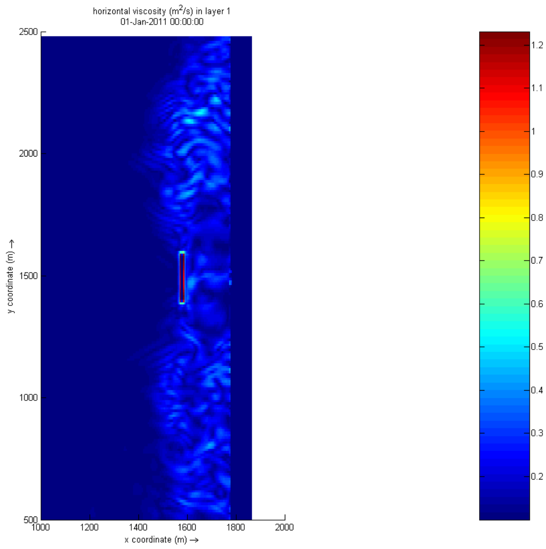 |
| Simulation time | Constant |
| Comments | |

# B Delft3D validation of hydrodynamic processes

## B.1 Introduction

Chapter 2 and 3 described the theory on SBW induced hydrodynamic and morphologic processes and the implementation of a SBW in Delft3D. As this model set-up is different compared to [Schaap 1997; Torrini 1997; Lesser et al. 2003; Van der Hout 2008], this chapter will go in more detail of the capabilities of Delft3D as a phase-averaging model and using a depth-averaged approach to describe all the important processes of a SBW. By comparing present theory on SBW with results of Delft3D, the capabilities of Delft3D are studied. Though no site specific case is used, comparing Delft3D results with literature will give a good indication of the capabilities of Delft3D to simulate SBW induced hydrodynamic and morphological processes.

This chapter will have the same order as chapter two. From offshore processes to the eventual morphological response to SBWs, the important individual processes are studied. To exclude effects of bottom changes, all hydrodynamic processes are described after the spin-up interval when equilibrium in hydrodynamics is reached. Used settings are included for each described process.

## B.2 Wave propagation

Wave propagation characteristics are one of the most important features of Delft3D and have been extensively calibrated. To illustrate the importance for the SBW case, several simulations are performed for a variety of conditions

### B.2.1 Shoaling

Shoaling influences the wave height near shore as describe in chapter two. Clearly Delft3D is capable of providing a good prediction on beach profiles, see [Deltares 2010b]. However, in a complex zone including refraction, diffraction, non-uniform beach profile and directional spreading of the incoming wave field, the shoaling effect may not be evident, as the wave field is composed of multiple processes. Previous studies on SBWs were adverse on this process, as several studies neglect the effect of shoaling while in [Lesser et al. 2003] the shoaling effect is explicitly mentioned to account for water level differences.

In order to quantify the wave height differences nearshore due to shoaling exclusively, a run is made in Delft3D were the diffraction is neglected and a narrow energy density spectrum in direction is forced at the offshore boundaries, by setting m=200 (see chapter 2), the directional width becomes $\sigma_\theta \approx 4^0$. As Delft3D is regularly applied for beaches, the wave conditions over a SBW is most interesting. The dimensions of the breakwater are chosen in a way that shoaling is also visible in the lee side of the breakwater. See Figure B.1 for the results.

*Figure B.1 Wave heights. No diffraction and small directional spreading (m=200), Rc=-0.5m, B=5m, xb=200m , L b=200m, tana=1/5, Tp=9s, Hs=1m.*

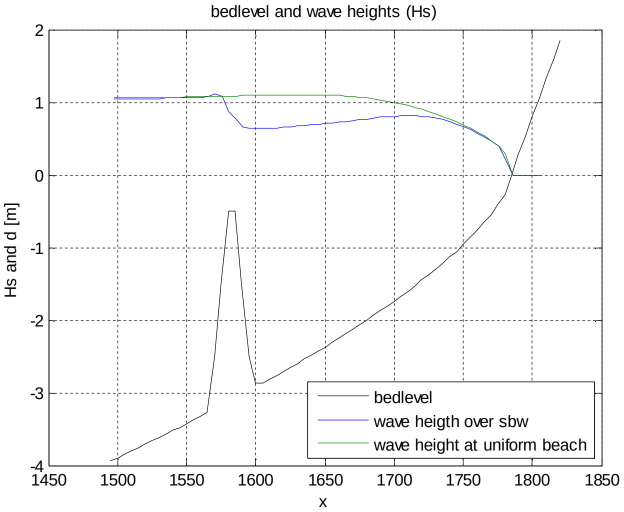


Evident from Figure B.1, shoaling is clearly visible in the leeside of the breakwater. This results in an increase of wave height from 0.63 m to 0.83m. From theory, it is known that wave height, wave length (and water depth) are the main characteristics in the shoaling process.

### B.2.2 Refraction

Refraction is often explained as oblique waves 'turn' to the shoreline due to differences in phase velocity. In a irregular, but shore normal wave field, this effect narrows the energy spectrum in direction, or reducing the directional spreading. To illustrate this effect, a similar run as previous paragraph is made, but including diffraction and defining the offshore directional width with $m = 4$ gives $\sigma_\theta \approx 25^0$. Figure B.2 shows the results by illustrating the directional spreading of the waves.

*Figure B.2 Directional spreading. Rc=-0.5m, B=5m, xb=200m, L b=200m, tana=1/5, Tp=9s, Hs=1m.*

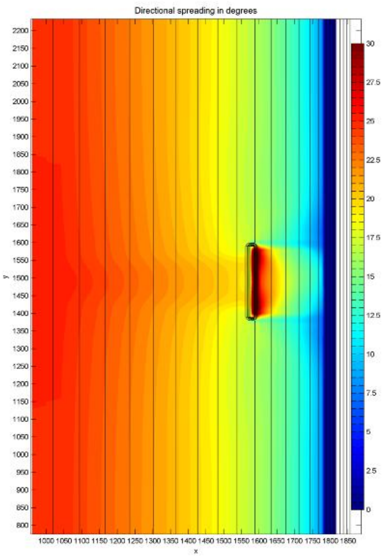

Apparently, from Figure B.2 and, as expected, the directional width reduces in shoreward direction. Important for the SBW location is the non-linear relation between distance to the shoreline and the directional width, due to the bathymetry. The “sheltering” effect is therefore also non-linear. Just after the breakwater the directional spreading increases due to diffraction.

### B.2.3 Diffraction

Diffraction plays a distinct role near the SBW head, as it increases the wave height in the leeside of the breakwater. Although theory is lacking on this subject for SBWs, the theory of ‘normal’ diffraction may serve as an upper limit. To account for the diffraction effect two runs are made, with and without diffraction.

*Figure B.3 Difference in wave height, diffraction, Rc=-0.5m, B=5m, xb=200m, L b=200m, tana=1/5, Tp=9s, Hs=1m.*

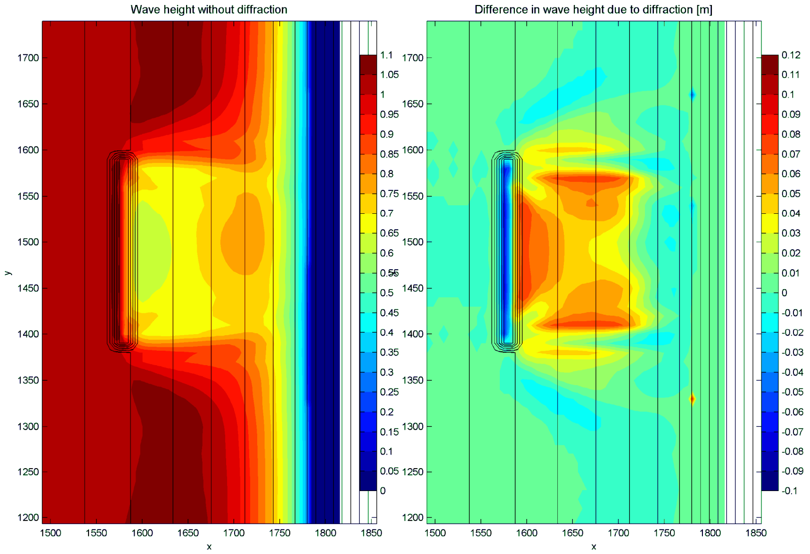


Figure B.3 shows the result of two runs with a offshore wave height of one meter were diffraction is turned on and off. The pattern obtained from the differences in wave height appears to combine the directional spreading and diffraction, having similar features as the [Sommerfeld 1896] and [Goda et al. 1978] illustrative patterns.
Theory on diffraction to SBWs is however lacking and solving diffraction with these grid sizes may be crude, so no conclusions can be directly drawn from this results. It is evident that diffraction will play a role in the shadow zone of a SBW. By using an offshore wave height of one meter also an indication of relative effect on the wave field is illustrated, which is accordingly to theory lower compared to emerged breakwaters.

### B.2.4 Wave reflection

Wave reflection is neglected in Delft3D, in accordance with several other studies on SBWs, as it is hard to implement in this model set-up. However when theory is considered, expressions including wave reflection will be taken account for.

## B.3 Wave breaking and transmission

Wave breaking (and transmission) is one of the most important driving processes for shoreline response to SBWs. From literature, it is known that wave breaking drives the water level set-up and the ‘ponding’ mechanism, the averaged flow over the breakwater. As it is one of the dominant processes driving shoreline response, errors made in the wave dissipation will also result in errors in wave set-up and mass-flux over the breakwater.

In order to quantify the performance of a phase-averaged model with wave dissipation based on mild slope equations, the results of Delft3D are compared with empirical formulas for wave transmission. Although the assumptions made in the mild-slope equation based wave dissipation are crude when applied to steep slopes, it is assumed that if the results of the calculated wave transmission coefficients by Delft3D are of similar order to the empirical wave transmission formulas, the total energy dissipation will also be in the right order.

In accordance with theory, due to the implementation of the SBW with a lack of sediment available (no stone diameters or permeability simulated) the [D'Angremond et al. 1996] and [Van der Meer et al. 2005] relations are used. In addition, within the paper of [Van der Meer et al. 2005] difference is made between regular rubble mound SBWs and smooth impermeable breakwaters. As numerous papers indicate that breakwater roughness can be disregarded as it plays no significant role in wave dissipation compared to depth-induced wave breaking, and Delft3D doesn’t represent permeability effects, the formula for smooth impermeable breakwaters should be used. Using the formula of smooth impermeable breakwaters may be a crude approximation, but may be satisfactory when keeping the physics and model set-up of Delft3D in mind. However, the purpose of this thesis is modelling of SBWs in general and in SWAN still a constant bed roughness is used, so therefore also the formula for rubble mound breakwaters is included in the analysis.

For quantifying the results of Delft3D, a constant given design SBW and offshore conditions are used, defined by $R_c$=-0.5 m, B=5 m, xb=200 m, $L_b$=200m, tana=1/5, Tp= 9s and a varying wave height, as it appears from literature to be dominant, which explains the multiple appearances in the wave transmission formulas. Figure B.4 shows the wave transmission from Delft3D for the mentioned case at the centre of the breakwater.

*Figure B.4 Wave transmission at centre of breakwater. Rc=-0.5, B=5, xb=200 , L b=200m, tana=1/5, Tp=9. varying wave height*

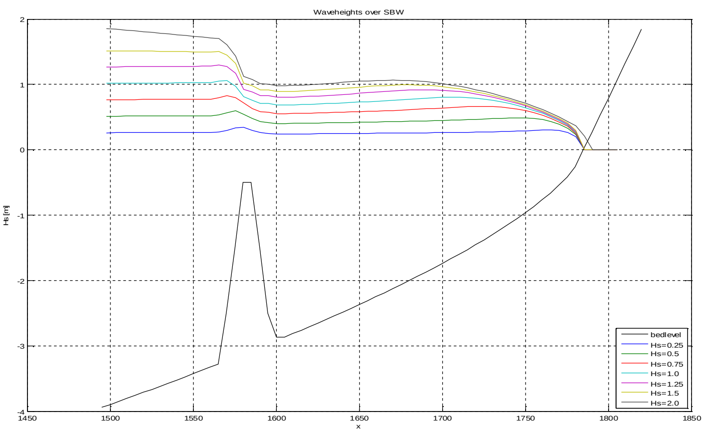

Figure B.4 shows the wave transmission at the centre of the breakwater. The results show some important characteristics. Beginning from offshore to onshore, the first thing noticed is that wave dissipation already occurs for the $H_s = 2m$ case in front of the breakwater. This is the result of using an irregular wave field at the boundaries described by a Rayleigh distribution and resulting higher wave heights. Second, although mentioned by several authors that the shoaling effect is negligible on steep slopes, some increase in wave height is shown on the offshore slope of the SBW. It is mentioned that using a slope of $\tan\alpha = 1/5$ is considered mild for a SBW slope, but is steep compared to the mild slope equations where the wave dissipation model is based on. Third point of interest is the result coming from the Hs=0.25 m case. As expected from physics, the incoming wave is fully transmitted to the onshore area behind the SBW. Fourth point of interest worthwhile mentioning is the re-shoaling effect on the onshore side of the breakwater, as discussed in previous paragraphs.

In order to quantify the results, a comparison is made with the empirical two dimensional formulas of [D'Angremond et al. 1996] and [Van der Meer et al. 2005] for smooth impermeable breakwaters and rough rubble mound breakwaters. TableApx B.1 shows the results of the Delft3D runs and the calculated Van der Meer transmission coefficients.

| Hs (m) | Delft3D Ht (m) | Delft3D Kt | VDM Kt smooth | VDM Kt rubble |
|---|---|---|---|---|
| 0.25 | 0.24 | 0.96 | 1* | 0.76 |
| 0.5 | 0.40 | 0.8 | 0.81* | 0.54 |
| 0.75 | 0.55 | 0.73 | 0.74 | 0.52 |
| 1.0 | 0.68 | 0.68 | 0.66 | 0.46 |
| 1.25 | 0.80 | 0.64 | 0.60 | 0.42 |
| 1.5 | 0.89 | 0.59 | 0.55 | 0.40 |
| 2* | 0.97 | 0.48 | 0.49 | 0.36 |

*TableApx B.1 Results on wave transmission of Delft3D and Van der Meer formula. Rc=-0.5m, B=5m, xb=200m, Lb=200m, tana=1/5, Tp=9 s and Hs varying. * Outside limits formulations*

TableApx B.1 indicates that there is an underestimation of wave dissipation or an overestimation of wave transmission in Delft3D for rubble mound SBWs. However this direct comparison is crude due to several reasons.

*Wave breaking parameter*

Reminding the original model of [Battjes and Janssen 1978] used as wave dissipation model, the model should indeed have problems with wave dissipation on steep slopes, as noted for example by [Johnson 2006]. Especially as the wave dissipation in this base case is largely dependent on what is happening on the breakwater slopes, due to the relative small breakwater crest width. Considering the empirical relations on maximum wave height to depth ratio in relation to bed slope for steep slopes ($y_{max}$>0.73), flat bottom ($y_{max}$<0.73) [Van Rijn and Wijnberg 1996] and even negative slopes, it is expected that with certain geometries differences will occur using the constant $y_{max}$=0.73. In the sensitivity analysis the influence was quantified for changing the wave height to depth ratio overall, however it is impossible to study the influence of a local varying wave height to depth ratio using the wave dissipation model SWAN.

*Bottom roughness and permeability effects*

Another note should be made on using the [Van der Meer et al. 2005] for wave transmission over smooth impermeable breakwaters. An important trend is the lack of crest width in the formula, indication that the crest width has no influence on the transmitted wave height.

However, Delft3D does take friction into account. With increasing crest width this will become important.

To quantify the above statements a new set of calculations is made in Delft3D with four times the crest width of the previous runs. Figure B.5 shows the results of the wave heights over the SBW and near shore area.

*Figure B.5 Wave transmission at centre of breakwater, Rc=-0.5, B=20, xb=200 , L b=200m, tana=1/5, Tp=9 s, varying wave height.*

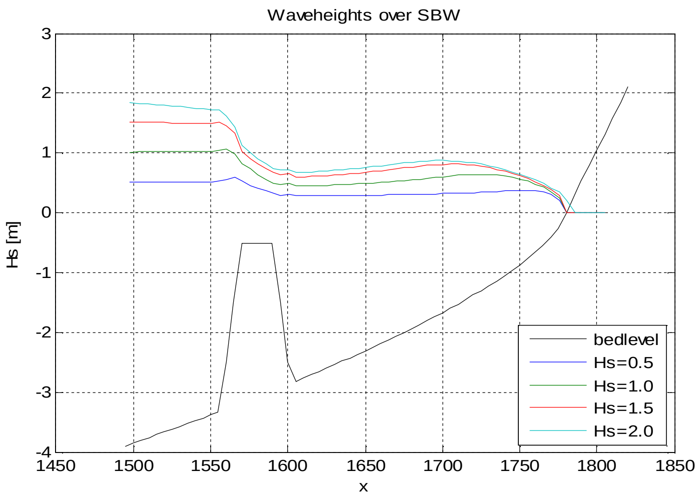


Figure B.5 shows similar features as the previous, B=5m case. To quantify the results of the new runs TableApx B.2 shows the results for this particular case, including the calculated transmission coefficients according to [Van der Meer et al. 2005] formulas for smooth impermeable and general (permeable) rubble mound breakwaters.

| Hs (m) | Delft3D Ht (m) | Delft3D Kt | VDM Kt smooth | VDM Kt rubble |
|---|---|---|---|---|
| 0.5 | 0.28 | 0.56 | 0.81* | 0.38 |
| 1.0 | 0.45 | 0.45 | 0.66 | 0.22 |
| 1.5 | 0.6 | 0.4 | 0.55 | 0.17 |
| 2.0(1.8) | 0.68 | 0.34 | 0.51 | 0.25 |

*TableApx B.2 Results on wave transmission of Delft3D and Van der Meer formulas. Rc=-0.5m, B=20m, xb=200m, Lb=200m, tana=1/5, Tp=9 s and Hs varying.*

There are a few important features. First of all, the difference between these results and the previous runs with a crest width of five meters shows that the transmission coefficients calculated by Delft3D are not the same. This indicates that the friction may not be negligible for the calculation of wave heights onshore of the breakwater and choice of formula. Using the [Van der Meer et al. 2005] formula for rubble mound breakwaters shows that wave dissipation is still underestimated instead of overestimated when using the smooth impermeable breakwater formula. Which partly can be explained by the extra energy dissipation due to permeability effects that is lacking in Delft3D.

*Diffraction*

In addition, the [Van der Meer et al. 2005] formulation is based on two dimensional wave breaking and excludes diffraction effects (see previous paragraph for the influence of diffraction). As theory on diffraction and the effect on wave transmission is lacking for SBWs, it is chosen to exclude the effect of diffraction in Delft3D and study the new results. The two dimensional formulas for wave transmission should be more justified to use. The same settings are used as Figure B.4, but diffraction is now excluded from the runs.

*Figure B.6 Wave transmission at centre of breakwater. Rc=-0.5, B=5, xb=200 , L b=200m, tana=1/5, Tp=9. varying wave height. No Diffraction*

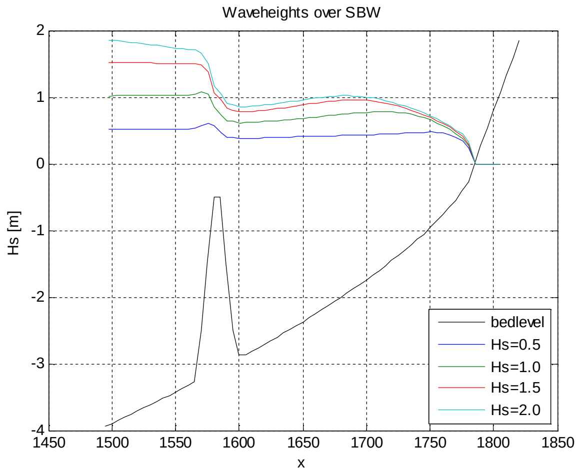


Comparing Figure B.6 with Figure B.4 differences in wave height are visible. TableApx B.3 quantifies the differences between these results.

| Hs (m) | D3D Kt With diff | VDM Kt smooth | VDM Kt rubble | D3D Kt No diff |
|---|---|---|---|---|
| 0.5 | 0.8 | 0.81* | 0.54 | 0.76 |
| 1.0 | 0.68 | 0.66 | 0.46 | 0.61 |
| 1.5 | 0.59 | 0.55 | 0.40 | 0.52 |
| 2* | 0.48 | 0.49 | 0.36 | 0.43 |

*TableApx B.3 Wave transmission, excluding diffraction effects. Rc=-0.5, B=5, xb=200 , L b=200m, tana=1/5, Tp=9. varying wave height. No Diffraction*

With the differences between the second and last column of TableApx B.3, it is evident that the three dimensional effect has its influence on wave transmission. Still the Delft3D results give an over prediction of wave transmission compared to the theory on rubble mound breakwaters, though differences have reduced significant.

<u>*Conclusions*</u>

Concluding, the wave transmission computed by Delft3D is complex. Previous mentioned limitations on friction, permeability, diffraction, wave dissipation model and generation of higher harmonic waves (see next paragraphs), all effect the computed wave transmission coefficient. It is however clear when comparing the results from the last runs to Figure 2.8, the results of [Van der Meer et al. 2005] for rubble mound breakwaters, that overall wave transmission is in good agreement with measurements.

*Figure B.7 Calculated wave transmission coefficients Delft3D compared to original results on rouble mound breakwaters [Van der Meer et al. 2005].*

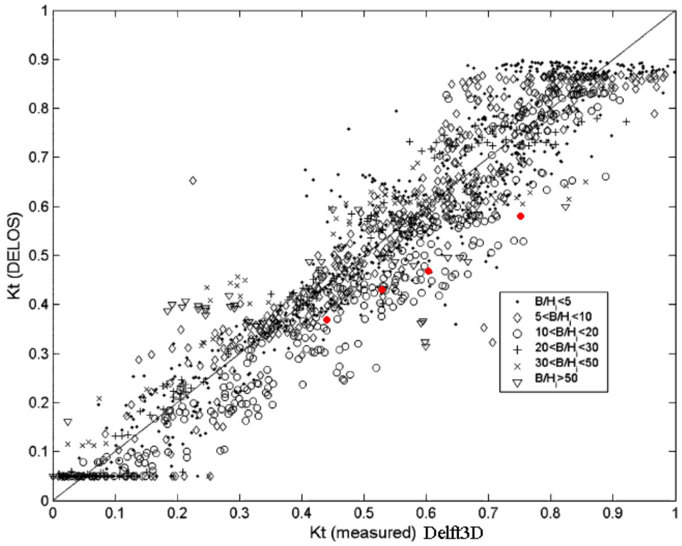


By increasing the friction or implementing permeability effects and different wave dissipation model including a spatial varying wave height to depth ratio [Baldock et al. 1998], results will become more accurate, however based on consistency (permeability effects) and simplicity (as well as a lack of data on wave height distribution over a SBW) this is not considered. However, care should be taken by directly comparing wave conditions in the shoreward side of the breakwater with offshore conditions. In contrast to above, improvements on obtaining the right wave height decay is evident, however due to time constraints this is not further concerned.

## B.4 Water level over submerged breakwater.

In response to the energy dissipation by wave breaking and a change in wave-induced momentum flux over the SBW, a water level set-up is generated. This water level set-up is one of the leading factors for the near shore current patterns which is responsible for the mode of shoreline response [Ranasinghe et al. 2010]. Although Delft3D is calibrated extensively for wave set-up due to differences in radiation stresses and applied in many different cases successfully, the importance of a correct water level set-up cannot be ignored. This paragraph describes the comparison of Delft3D with existing formulas for the water level set-up for this specific case.

The general difference between the formulas of water level gradient is the physics included. [Calabrese et al. 2008] take a two dimensional empirical approach and divide the water level set-up by a part of release of momentum flux and an other part by a water level gradient needed for the return current in the second half of a wave period, where others only account for the differences in radiation stresses. This piling-up of water behind the breakwater can be of influence for the order of water level set-up. As mentioned in this paper, the centre of a breakwater may be treated like a 2D case. During the DELOS project there were indeed SBWs with large breakwater lengths or SBWs with groins to the sides closing of the shadow zone so that this statement is satisfied and the breakwater can be treated in a two dimensional way similar to the reported SBW by [Dean et al. 1997]. However using short breakwater lengths and relative large distances from the shoreline, the incoming flow over the breakwater returns offshore trough the shadow zone of the SBW instead of over the breakwater in the second half of the wave period. Important factor in this process is the water level gradient needed to transport the water from the shadow zone back offshore. As this thesis handles the 3 dimensional effects of a SBW, the relation of [Calabrese et al. 2008] derived from [Longuet-Higgins 1967] is most satisfactory, despite the limitations on regular waves, see paragraph 2.7.2.

In order to quantify the performance of Delft3D, first the same dataset is used as previous paragraphs using the breakwater width of B=20 m, four different wave heights and including diffraction, see Figure B.5. For defining two cross sections, the offshore and onshore toes of the breakwater are used. Figure B.8 shows the wave induced water level set-up over the centre of the SBW. Wave reflection is neglected in the model.

*Figure B.8 Wave induced water level set-up over the centre of the breakwater, Rc=-0.5m, B=20m, xb=200m, Lb=200m, tana=1/5, Tp=9 s, varying wave height.*

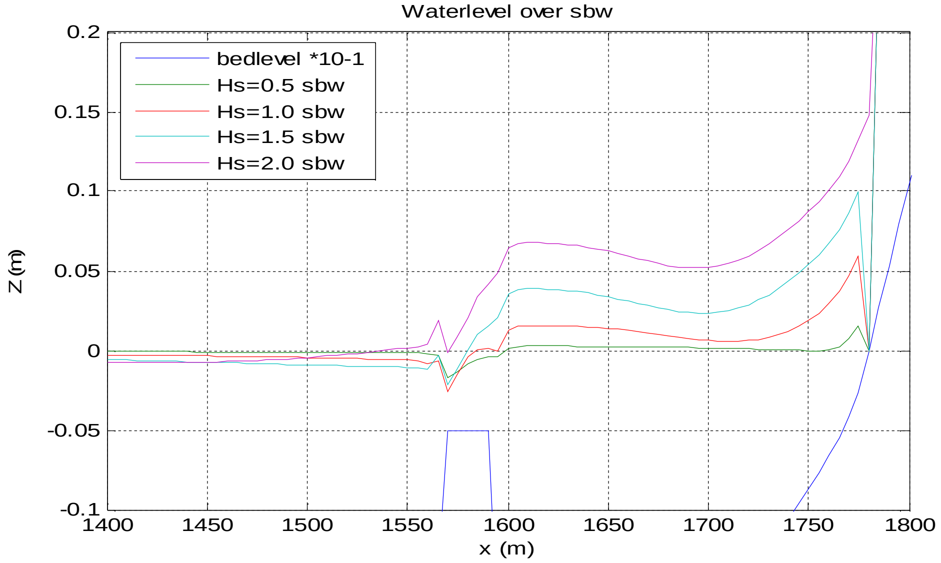


As can been seen from Figure B.8 several processes are represented well. First of all the small water level set-down due to the shoaling effect of waves. As mentioned by [Calabrese et al. 2008], the water level set-down is of different order than the set-up over the SBW. Second, the water level on the crest of the breakwater is showing ‘disturbances’. Delft3D assumes that the vertical pressure distribution is hydrostatic as assumed for the shallow water equations. In reality in this highly turbulent zone, the non-hydrostatic contributions can be important. It is clear that on such small scales Delft3D has difficulties, but the general tendency is more important. In the lee of the breakwater, a clear increase in water level is shown as expected. When waves travel further to shore, the re-shoaling effect is visible, as mentioned in the previous paragraph. This effect influences the water level as a clear decrease in water level in the shadow zone is seen for the higher wave heights.

For quantifying the performance of Delft3D, a comparison is made with the model derived from [Longuet-Higgins 1967] despite its limitations. When taking all the individual parameters from Delft3D (especially the wave transmission coefficient) a rough comparison can be made. TableApx B.4 shows these results.

| Offshore $H_s$ D3d | $K_t$ | k1 (1/m) | k2 (1/m) | h1 (m) | h2 (m) | δ' D3d (m) | δ' LH (m) |
|---|---|---|---|---|---|---|---|
| 0.5 | 0.56 | 0.154 | 0.162 | 3.33 | 2.8 | 0.0027 | 0.0024 |
| 1.0 | 0.45 | 0.150 | 0.161 | 3.33 | 2.8 | 0.015 | 0.012 |
| 1.5 | 0.4 | 0.150 | 0.159 | 3.33 | 2.8 | 0.038 | 0.0289 |
| 2.0 | 0.34 | 0.144 | 0.155 | 3.33 | 2.8 | 0.0677 | 0.055 |

*TableApx B.4 Comparison wave induced water level set-up.*

There is a good comparison between Delft3D and the derived model of [Longuet-Higgins 1967] despite its limitations for the lower wave heights. As the wave height increases also the predictions of the derived formulation of [Longuet-Higgins 1967] model tends to differ from the Delft3D results. It is noted that as the averaged wave height over the breakwater increases the influx or ‘pilling-up’ of water also increases which makes the [Longuet-Higgins 1967] model less convenient. This ‘underestimation’ is also reported several times by the [Calabrese et al. 2008] paper and has let to several new empirical models to account for these other factors in a two dimensional approach. Delft3D however produces the same order of results for the water level set-up over a SBW compared to literature.

## B.5 Mass-flux over submerged breakwater

As mentioned in previous paragraphs, the flow over the SBW and the possible return current play an important role in the hydrodynamics around a SBW. Although little is known about this phenomenon, a comparison can be made with regular wave theories. This approach is crude and limited, but it gives insight in the capabilities of Delft3D as a tool to describe the effect of SBWs.

A similar approach as [Calabrese et al. 2008] is chosen. In this research quantifying the return current as part of the wave set-up is done by the theory of [Svendsen 1984] based on mass transport in the surf zone on regular beaches. As reasoned by other authors like [Loveless et al. 1998] and [Dalrymple and Dean 1971] the flow over the SBW can be similar to a flow over a weir. However as a lack of knowledge on specific SBW cases, the [Svendsen 1984] is the most appropriate, despite the limitation to regular waves. Disadvantage of this approach is that it is only valid for narrow crested SBWs. Another problem is that in a 2DH approach of Delft3D the model only calculates the depth averaged velocities and flow averaged over the wave period. So to compare Delft3D and the [Svendsen 1984] model, processes like return current over the breakwater and inherent water level gradients over the breakwater should be kept to a minimum in the Delft3d calculations. With this in mind, the same configurations as in Figure B.4 are used.

*Figure B.9 Mass transport over submerged breakwater. Rc=-0.5m, B=5m, xb=200m, L $_b$=200m, tana=1/5, Tp=9 s and Hs varying.*

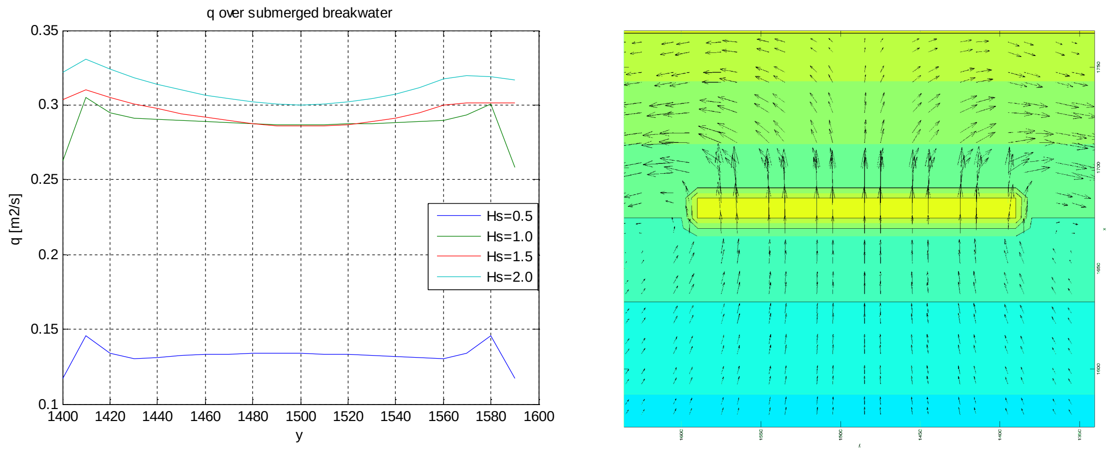


Figure B.9 shows the results of Delft3D. Between y=1400 and y=1600 the breakwater is situated. A small decrease in transport rates can be seen near the breakwater centre. This can be explained by the water level gradient being higher at the centre of the breakwater, due to differences in wave height and 'ponding' mechanism, forcing a return current. TableApx B.5 gives an overview of the comparison of Delft3D with the [Svendsen 1984] model.

| Hs Delft3D (m) | $q_{in}$ Delft3D (m2/s) | $q_i$ Svendsen (m2/s) |
|---|---|---|
| 0.5 | 0.13 | 0.11 |
| 1.0 | 0.28 | 0.20 |
| 1.5 | 0.29 | 0.27 |
| 2.0 | 0.32 | 0.33 |

*TableApx B.5 Mass transport over the breakwater, Delft3D calculations and [Svendsen 1984] model.*

From TableApx B.5 it is clear that Delft3D simulations are in good agreement with the analytical mass-transport rates, as for three out of the four cases mentioned, despite the limitations. It is not clear why with a wave height of 1.0m the results are almost identical to the significant wave height of 1.5 m case. As stated above, care should be made drawing conclusions from these results. In further analyses no direct link can be made between the offshore conditions and flow over the SBW using the [Svendsen 1984] model, due to the limited applicability to narrow crested SBWs. Delft3D however produces results in the same order as expected from literature. Further calibration and validation on extensive data sets is needed to include site specific conditions.

## B.6 Spectral change due to wave transmission

Theory suggested that a SBW also influences the wave period besides the wave height, by generation of higher harmonic waves and a redistribution of energy to these higher harmonic waves. This generation of higher harmonics, or frequency shift can be included in the Delft3D runs. Even, the dataset used by [Beji and Battjes 1993] for defining the spectral change, is used to calibrate the Delft3D-Wave/SWAN model [Deltares 2010b]. Important processes in the spectral change are the generation of higher harmonic waves due to shoaling and the energy transfer, due to triad wave-wave interactions.

To illustrate the effect of the generation of higher harmonic waves, similar runs as Figure B.4 are made with a wave height of 1.5 m. At the shoreward toe at the centre of the breakwater a spectral analysis is made. By neglecting triad wave-wave interactions in the Delft3D simulations the effect of spectral change can be quantified.

*Figure B.10 Spectral analysis at shoreward toe of the SBW.*

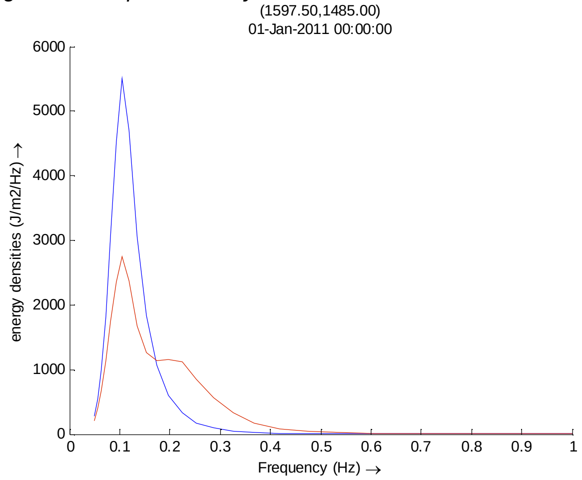


Clearly from Figure B.10 the generation of higher harmonic waves are visible. Energy is transferred to these higher harmonics accordingly. Results from this two runs are in accordance with the results of [Beji and Battjes 1993]. The importance of the generation of higher harmonics for SBW induced shoreline changes may however be questionable. However, Delft3D has often problems with converging to an unique solution when triad-wave-wave interactions are considered. Therefore it is chosen to neglect triad-wave-wave interactions.

## B.7 Water level set-up

To keep in mind the driving processes for shoreline response and the explanation by [Vicinanza et al. 2009; Ranasinghe et al. 2010] for water level differences and the mode of shoreline response, the water level set-up (and corresponding hydraulic head) may directly linked to the flow patterns in an equilibrium state. From the cross-shore differences in water levels alongshore it may be visible if a 4-cell or 2-cell pattern occurs. It can be reasoned that the ultimate goal of a SBW is reducing the water level set-up behind the breakwater as much as possible and forcing an (accretive) 4 cell pattern. This 4-cell pattern in this particular case with xb=200m also can be explained by taking cross-sections of the water level alongshore between the SBW and the coastline. Delft3D is extensively calibrated for processes like wave heights on planar beaches, radiation stresses, water levels etc. So for Delft3D results on this matter, see for instance [Deltares 2010a]. However, it is still interesting to see the water level obtained from a Delft3D calculation.

*Figure B.11 Alongshore cross-sections xb=200m case. Water levels and hydraulic head (breakwater between 1400m and 1600m)*

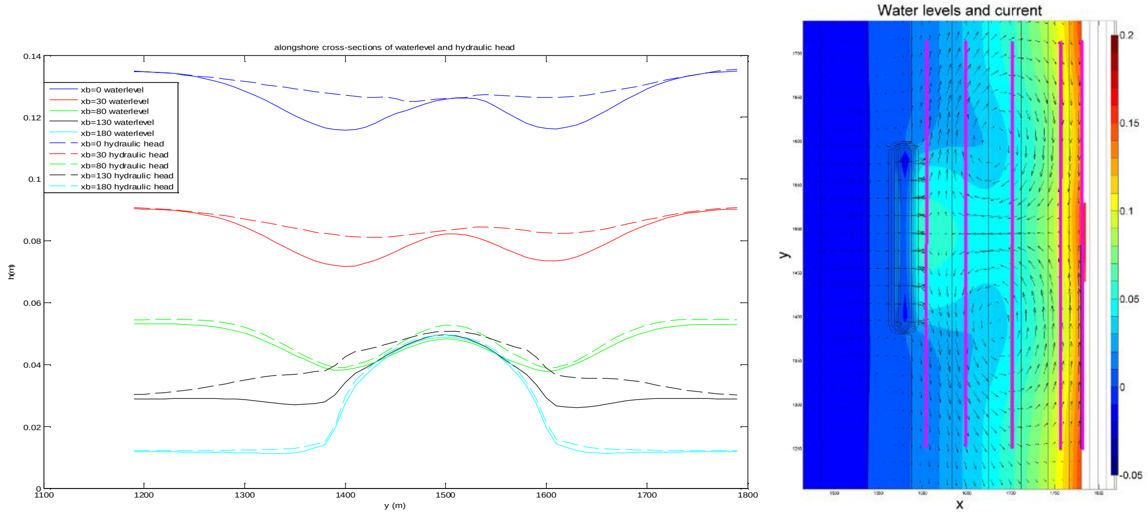


Figure B.11 shows the cross-sections of the water level alongshore. Close to the shoreline, the eddy type of flow is visible, where the gradient in hydraulic head alongshore forces a flow to the shadow zone of the breakwater. Along a offshore distance of x=80m, clearly the centre of the eddy is visible. Further offshore up to x=130m still the effect of the eddy, including the large velocity head is visible. Interesting feature in Figure B.11 is the water level set-up further offshore (black and light blue lines), as this trend also appears for the xb=100 and xb=50m case. Chapter 4 will go in more detail about the water level set-up around a SBW and which processes to account for.

## B.8 Flow patterns

As differences in hydraulic head force a net flow pattern, a clear difference in accretive and erosive patterns, as described by [Ranasinghe et al. 2010] can be seen. As this feature is leading for shoreline changes, but theory is lacking on the magnitude of the flow, a qualitative comparison can be made. The same settings are used as Figure B.4, but keeping the significant wave height constant at 2 meters, and changing the offshore distance of the breakwater, as is it one of the dominant parameters from literature.

*Figure B.12 Bed level and flow patterns around the submerged breakwater*

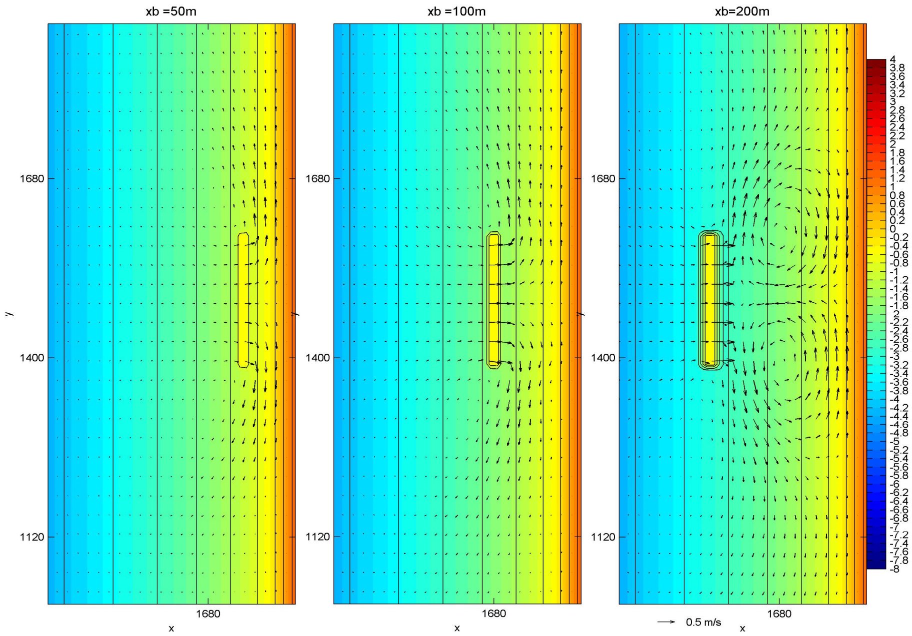


Comparing Figure B.12 with result from [Ranasinghe et al. 2006], the induced flow patterns show great similarities. With $x_b = 50m$ a clear erosive pattern is obtained, whereas the $x_b = 200m$ gives a clear accretive pattern. Even the magnitude of the flow is of the same order compared to for instance [Ranasinghe et al. 2010]. Next paragraph will go in more detail about the formation of a 2/4 cell pattern.

Another interesting point is the flow quantities. Obeying the mass-balance, the mass-transport over the breakwater should be compensated by an outgoing flow from the shadow zone to offshore. In all cases, the net mass-transport over the submerged breakwater is equal to two times the net outgoing flow on one side (North or South). In case of 2 cell pattern net flow is equal to the gross flow, whereas with a 4 cell pattern, net and gross flow rates diver, due to the formation of an eddy.

*Figure B.13 Flow out of shadow zone. Blue, xb=200, green, xb=100m, red xb=50m*

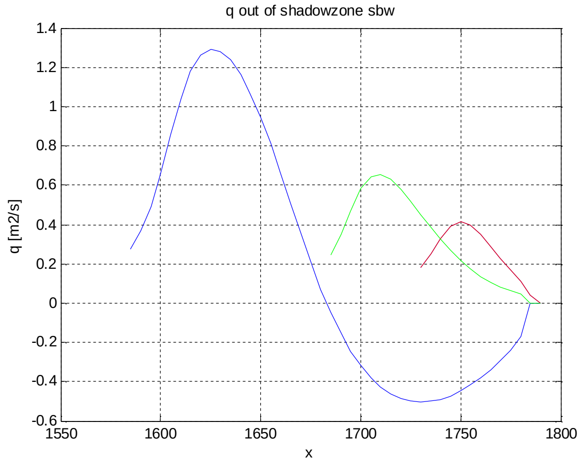


TableApx B.6 quantifies the total flow. Clearly, despite some interpolation errors, Delft3D obeys the mass-balance behind the breakwater. Another important notion is the significant gross flow in a 4 cell pattern.

| xb | $Q_{over\ sbw}$ m$^3$/s | $Q_{gross\ in}$ m$^3$/s | $Q_{gross\ out}$ m$^3$/s | $Q_{net}$ m$^3$/s |
|---|---|---|---|---|
| 50 | 30.4 | 0 | 15.7 | 15.7 |
| 100 | 63 | 0 | 34 | 34 |
| 200 | 81.1 | 36.4 | 78.7 | 42.3 |

*TableApx B.6Total depth averaged flow quantities*

Concluding, several processes play an import role in the near shore current patterns. Delft3D reproduces the important hydrodynamics in the right order of magnitude.

## B.9 Morphology

Previous described hydrodynamics will result in the time-averaged flow patterns. Together with the wave forcing, shear stresses will act on the sediment. When above a certain critical shear value, sediment starts to move. Gradients in the transport of sediment will cause erosion or accretion. From theory different distinct patterns in bathymetry can be seen. This paragraph will show that a depth-averaged model of Delft3D is capable of reproducing the same morphological changes.

From theory it's clear that different erosion or accretion patterns can occur around a submerged breakwater. Although this thesis is focussing on the formation of a salient, when all the scour patterns are accounted for in the model, more confidence is created in the capabilities of Delft3D and the depth averaged approach chosen. As Delft3D, in depth averaged mode, assumes certain vertical distributions of the flow, it is interesting to see whether the model can predict qualitatively the same morphological changes. In order to do so, a morphological run is made of 2 months.

*Figure B.14 Cumulative erosion and sedimentation, and bed level after 2 months $L_b$=200m, $x_b$=200m, $R_c$=-0.5m, B=10m, $H_s$=1.5m.*

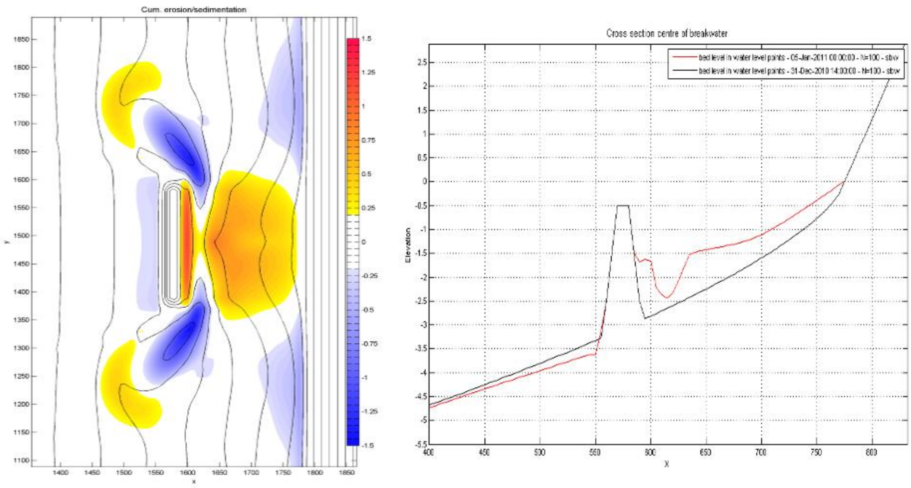


From Figure B.14 it is evident that three-dimensional effects are dominant. However, still some comparisons with literature can be made. First of all the erosion at the seaward side of the breakwater shows resemblances with [Sumer et al. 2005]. Second the onshore accretion along the breakwater is in agreement with [Young and Testik 2009], despite the “trench” created by the alongshore flow. Even some scour close to the SBW head is visible. However due to scale effects and grid sizes used in this model this process is hard to obtain correctly.

In addition, close to the shoreline which is not ‘protected’ by the SBW erosion is visible. As sediment is transported to the leeward side of the SBW this obeys the mass-balance. In contrast, there has not been any shoreline changes. Delft3D has difficulties in accretion in very low water levels. Due to the phase averaged approach the swash zone is not modelled. In order to try to improve the accretion behind the breakwater a second run is made, but including a semi diurnal tide with an amplitude of 0.25m, see Figure B.15.

*Figure B.15 Cross section centre breakwater morphological run, $L_b$=200m, $x_b$=200m, $R_c$=-0.5m, B=10m, $H_s$=1.5m, tana=0.2. black initial bed level, red equilibrium bed level with tide, blue equilibrium bed level no tide effects*

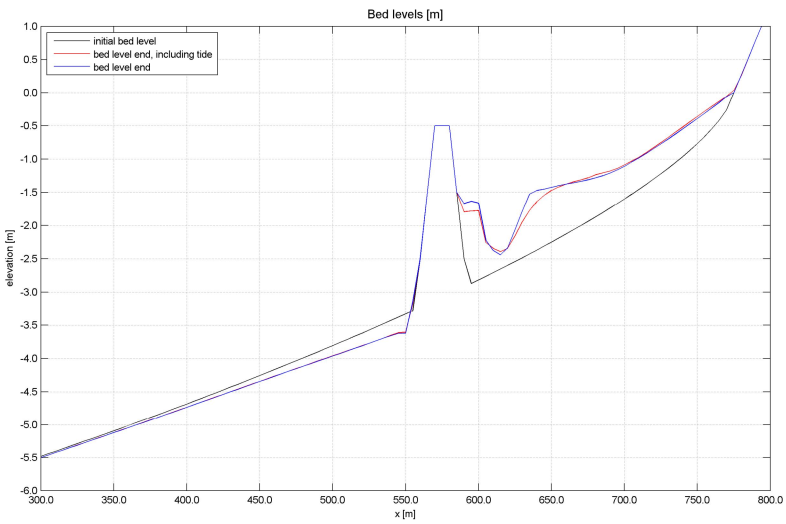

Concluding from Figure B.15, the tide does not improve the shoreline accretion. Due to the small differences in bed level, the previous assumption to neglect the tide is confirmed for small (vertical) tide amplitudes.

To also account for erosion, an erosive case is analysed, see Figure B.16. Tide effects are contrary to previous run neglected again.

*Figure B.16 Erosive submerged breakwater. , $L_b$=200m, $x_b$=50m, $R_c$=-0.5m, B=10m, $H_s$=1.5m, tana=0.2.*

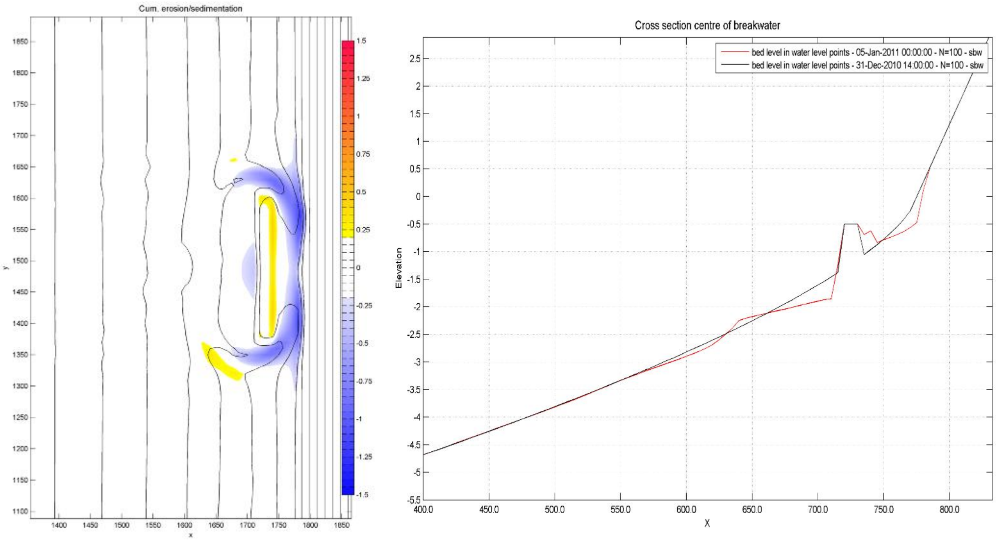


From Figure B.16 it is evident that erosion is accounted properly behind the SBW. The obtained erosive pattern shows resemblances with the obtained flow pattern. More interesting the shoreline erosion is properly accounted for behind the SBW. In general the obtained erosive and accretive bed level changes show great resemblances with previous work of, for instance, [Ranasinghe and Turner 2006].

Overall, the obtained morphological response to SBWs from Delft3D is in good agreement with expected salient development in qualitative sense. Due to a lack of quantitative results, no comparison can be made, but results are in good agreement with expected morphological changes.

## B.10 Conclusions

Although Delft3D has its limitations, results from the numerical simulations agree well with the theoretical formulations of individual processes. In addition, the obtained bed level changes agree qualitatively with previous work. Obtained results can be considered accurate enough to draw useful conclusions from.

However, Delft3D results are not completely in accordance with theory. First, the wave dissipation is a point of interest. Fortunately, the wave transmission is one of the most studied processes of submerged breakwaters. Several extensive studies give good insight in this individual process and the dominant parameters. Considering theory and the use of a numerical model, this can combine the best of both. Secondly, the shoreline accretion is not included. The formation of a salient-shaped bathymetry is nevertheless visible. TableApx B.7

gives an overview of considered literature and whether Delft3D is capable of reproducing results in the same order.

| **Process** | **Literature** | **Delft3D** | **Remarks** |
|---|---|---|---|
| Shoaling | [Deltares 2010b] | √ | Calibrated/validated extensively by Deltares |
| Refraction | [Deltares 2010b] | √ | Calibrated/validated extensively by Deltares |
| Diffraction | unknown | √ | No literature for submerged breakwaters, but common sense suggest a small influence |
| Reflection | [Van der Meer et al. 2005] | | Not included, influence however small |
| Wave transmission | [Van der Meer et al. 2005] | √ | Based on direct comparison to rubble mound sbw results |
| Water level over breakwater | [Calabrese et al. 2008] | √ | Influenced by mass-transport for higher values |
| Mass transport over breakwater | [Svendsen 1984] [Calabrese et al. 2008] | √ | In general good, except 1 result |
| Spectral change | [Beji and Battjes 1993; Van der Meer et al. 2005] | | Due to stability reasons of Delft3D neglected |
| Flow patterns | [Ranasinghe et al. 2006] | √ | |
| Morphology | [Sumer et al. 2005; Ranasinghe et al. 2006; Young and Testik 2009; Ranasinghe et al. 2010] | √ | Although relative large grid sizes, overall trend visible |
| Shoreline changes | [Ranasinghe et al. 2010] | | No changes accretive pattern, erosion included reasonable. Take -0.5m contour |

*TableApx B.7 overview of compared literature and Delft3D results*

# C Cross-profiles water level

*Figure C.1 Cross-sections difference in water level and v-velocity* $x_b$*=50m,* $L_b$*=200m,* $R_c$*=-0.5m, B=10m,* $H_s$*=1.5m,* $T_p$*=9s, tana=0.2.*

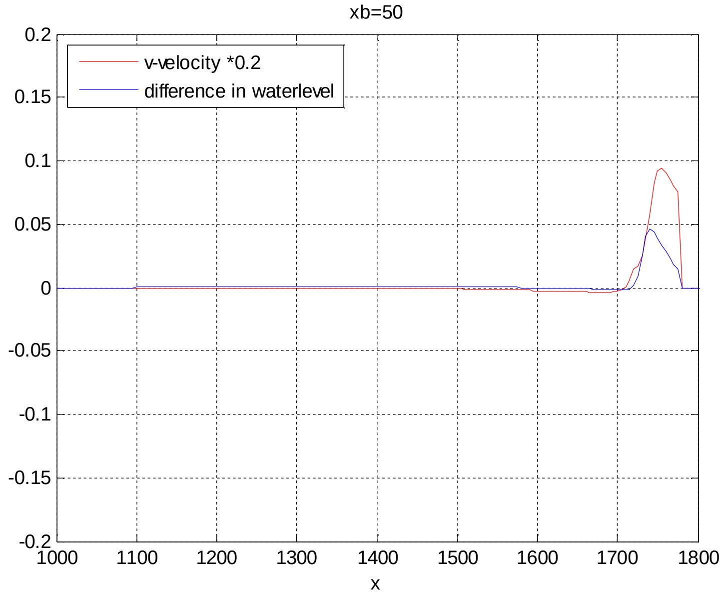


*Figure C.2 Cross-sections difference in water level and v-velocity* $x_b$*=100m,* $L_b$*=200m,* $R_c$*=-0.5m, B=10m,* $H_s$*=1.5m,* $T_p$*=9s, tana=0.2.*

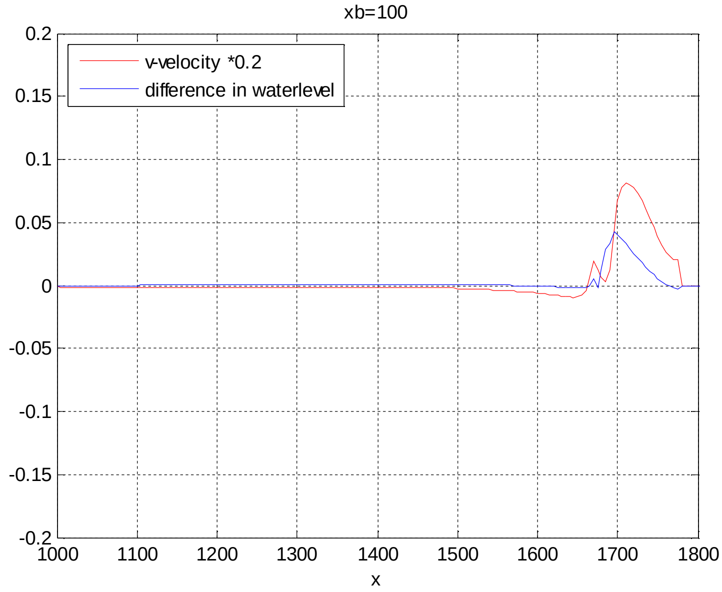

*Figure C.3 Cross-sections difference in water level and v-velocity $x_b$=200m, $L_b$=200m, $R_c$=-0.5m, B=10m, $H_s$=1.5m, $T_p$=9s, tana=0.2.*

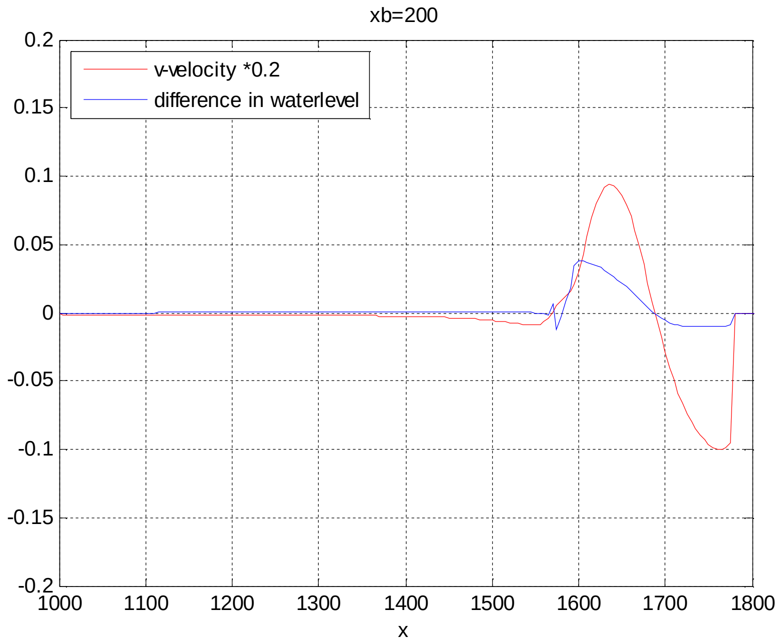


*Figure C.4 Cross-sections difference in water level and v-velocity $x_b$=300m, $L_b$=200m, $R_c$=-0.5m, B=10m, $H_s$=1.5m, $T_p$=9s, tana=0.2.*

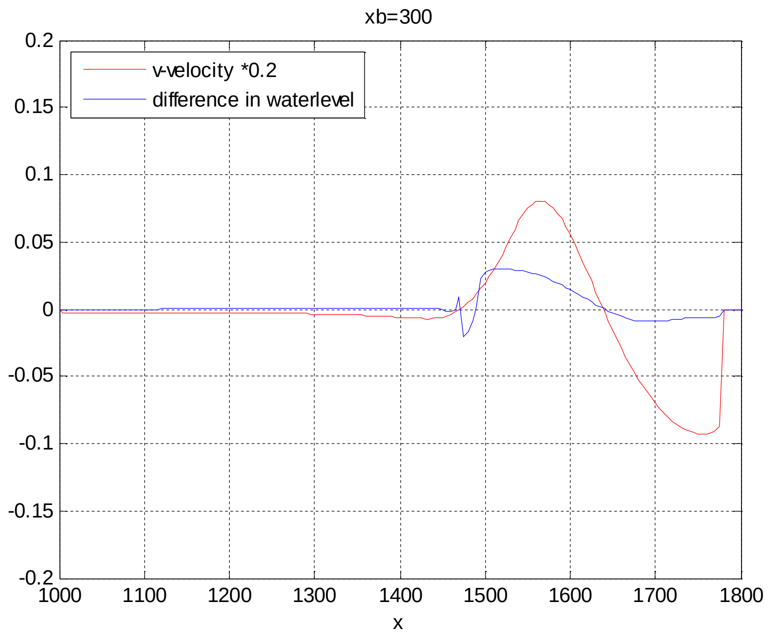

*Figure C.5 Cross-sections difference in water level and v-velocity $x_b$=400m, $L_b$=200m, $R_c$=-0.5m, B=10m, $H_s$=1.5m, $T_p$=9s, tana=0.2.*

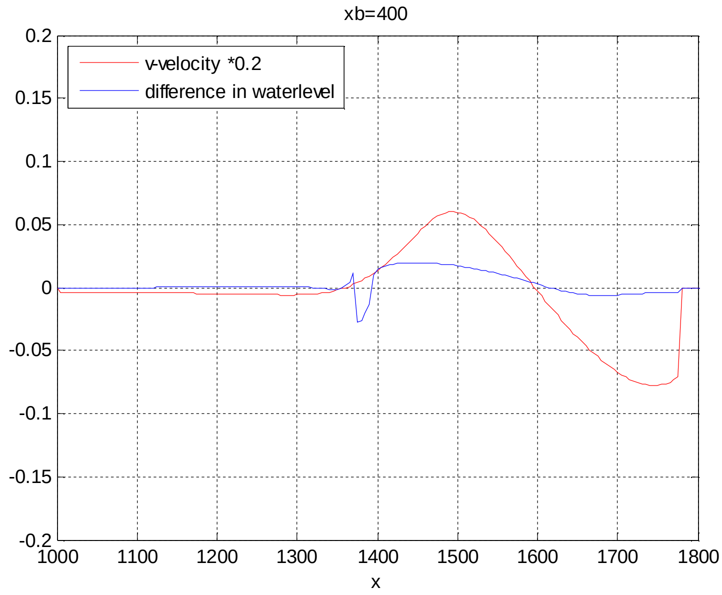


*Figure C.6 Difference in water level alongshore for Lb=200 m and different xb.*

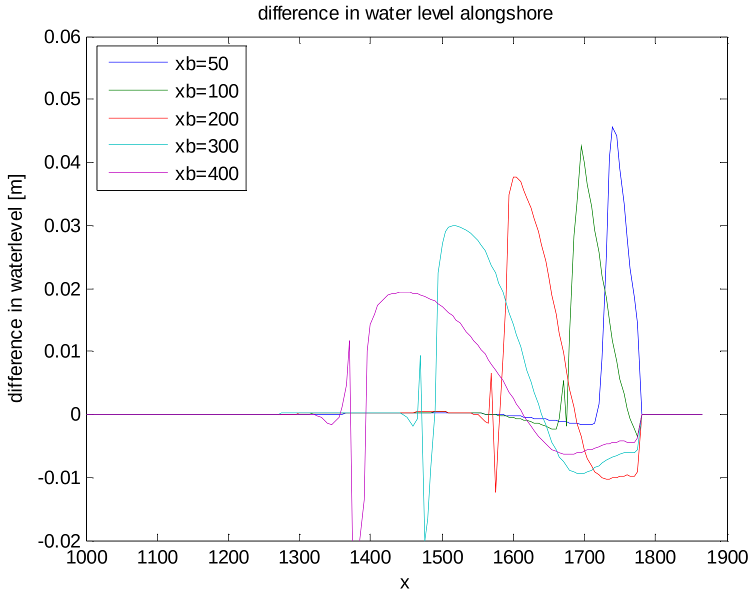

*Figure C.7    cross profiles v-velocities for Lb=200m and different xb.*

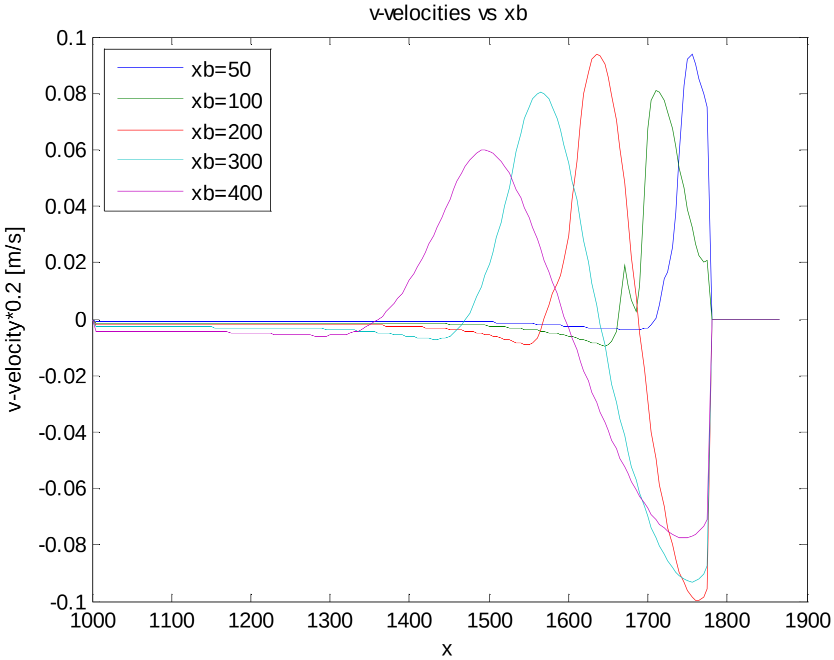

# D Cross-shore momentum balance

## D.1 Wave induced forces

*Figure D.1 Normalised cross-shore integrated wave induced stresses case 1*

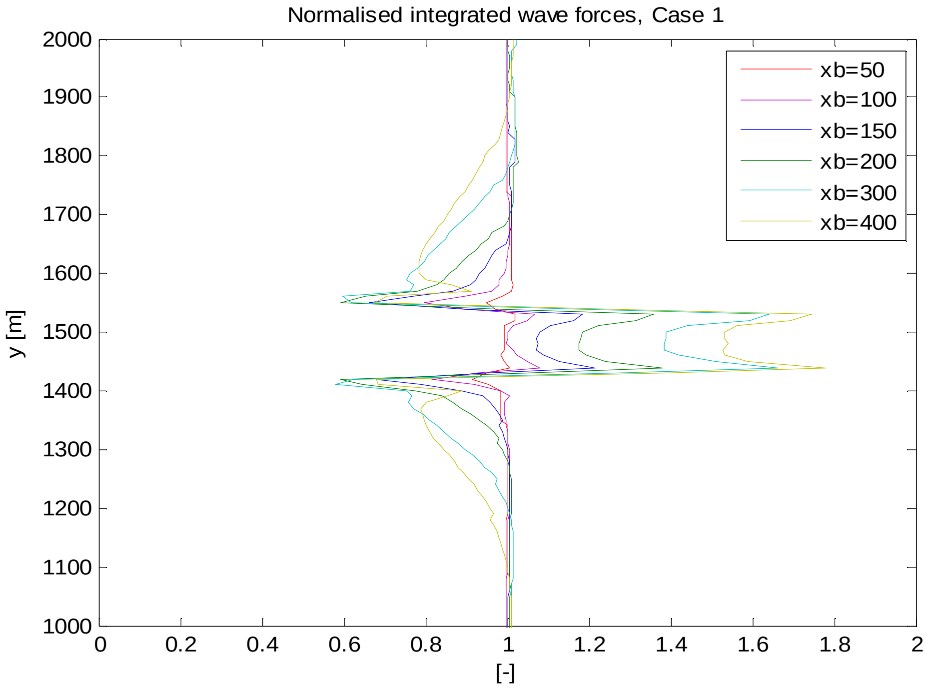


*Figure D.2 Normalised cross-shore integrated wave induced stresses case 2*

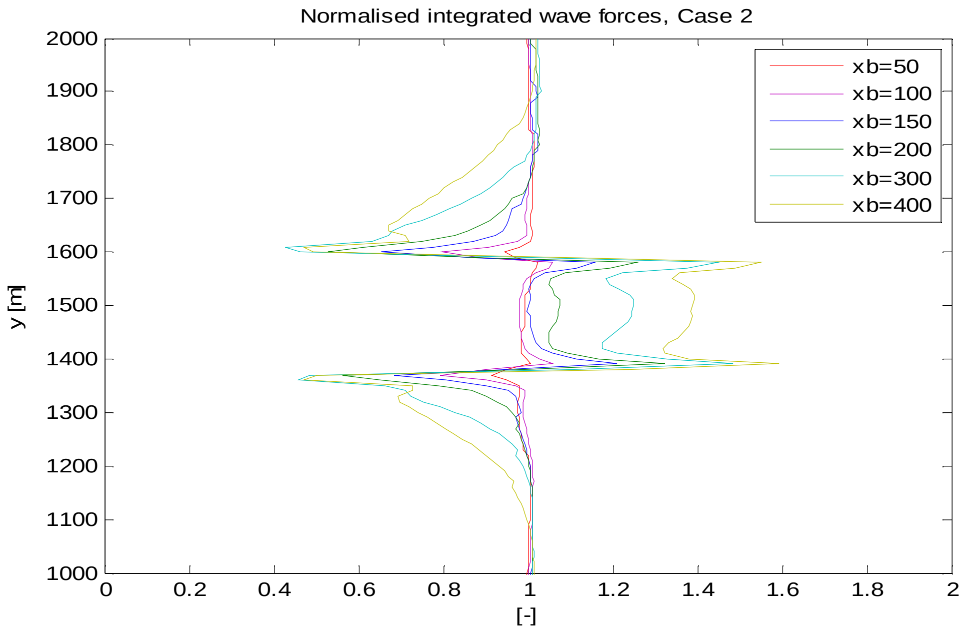

*Figure D.3 Normalised cross-shore integrated wave induced stresses case 3*

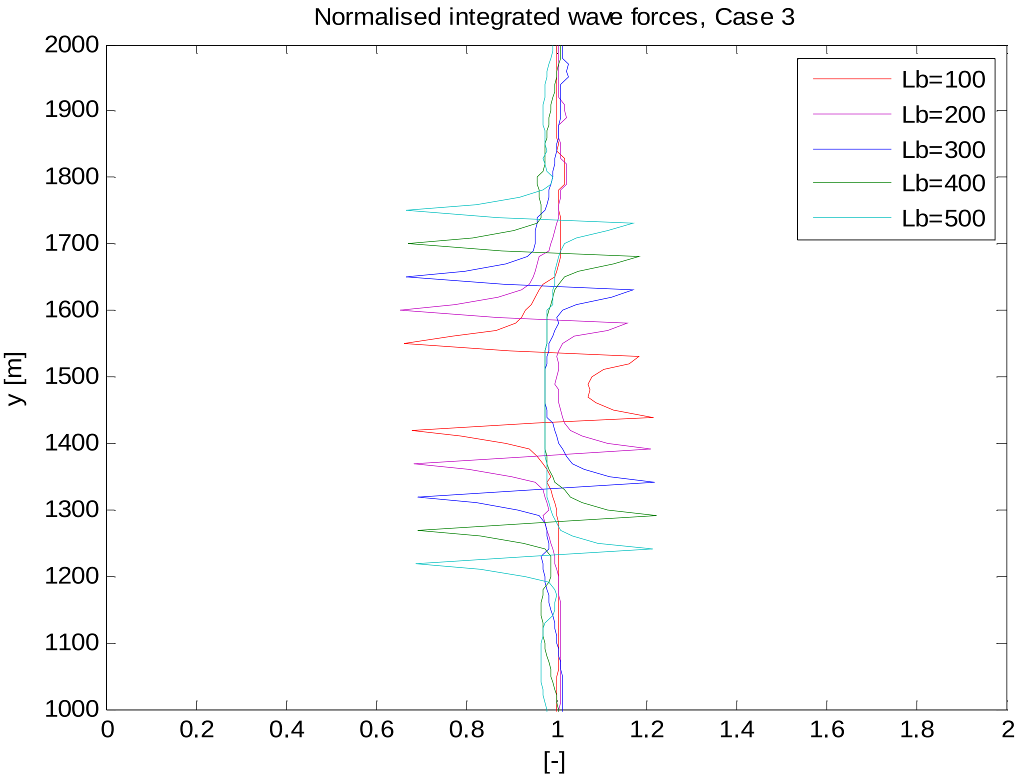


*Figure D.4 Normalised cross-shore integrated wave induced stresses case 4*

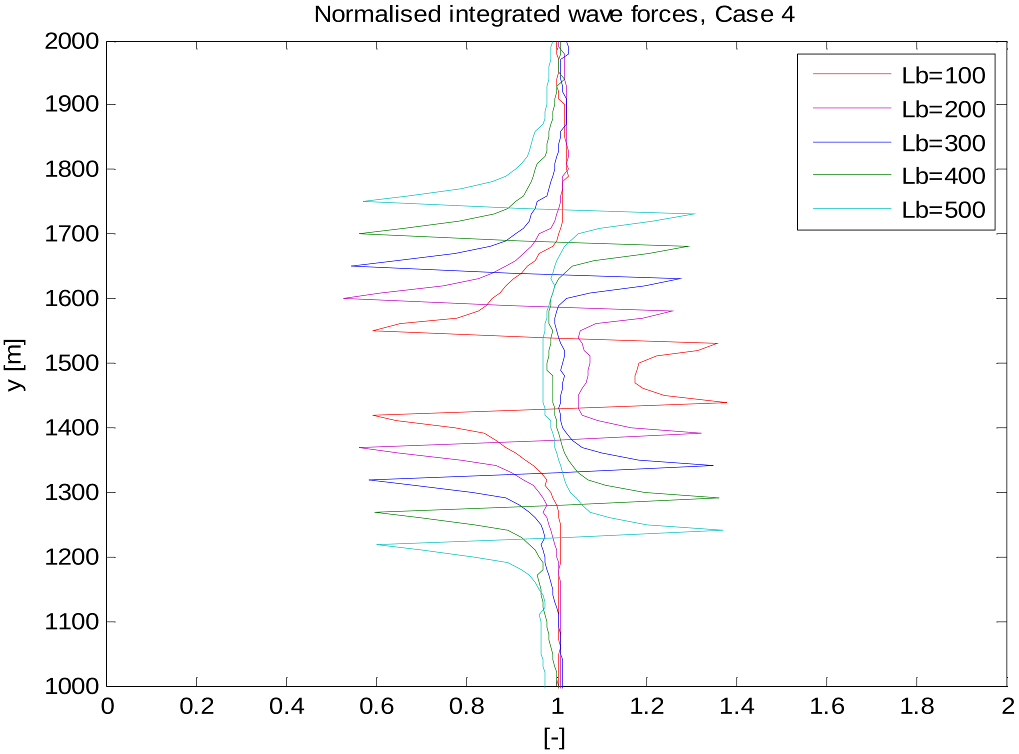

## D.2 Hydrostatic force due to water level gradients

*Figure D.5 Normalised cross-shore integrated hydrostatic stresses case 1*

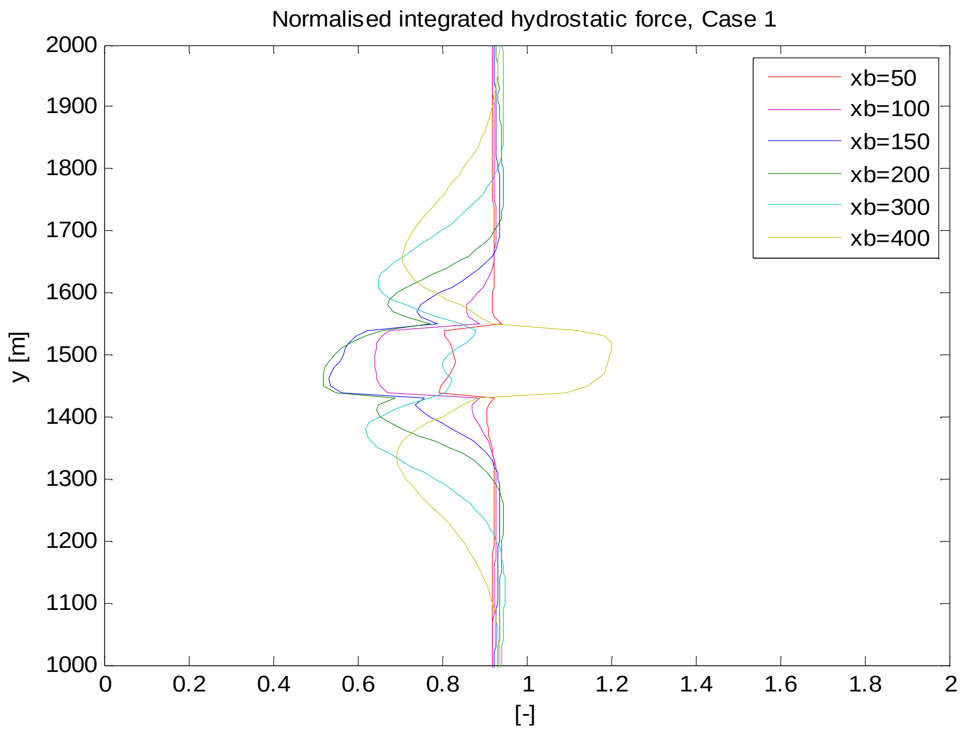


*Figure D.6 Normalised cross-shore integrated hydrostatic stresses case 2*

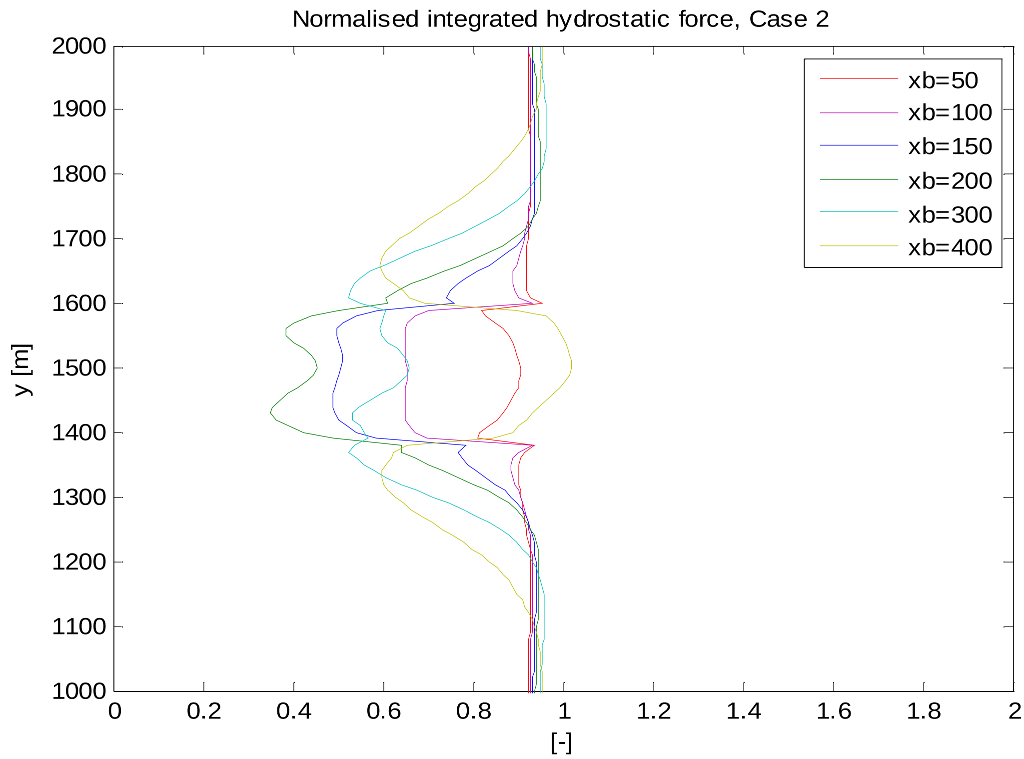

*Figure D.7 Normalised cross-shore integrated hydrostatic stresses case 3*

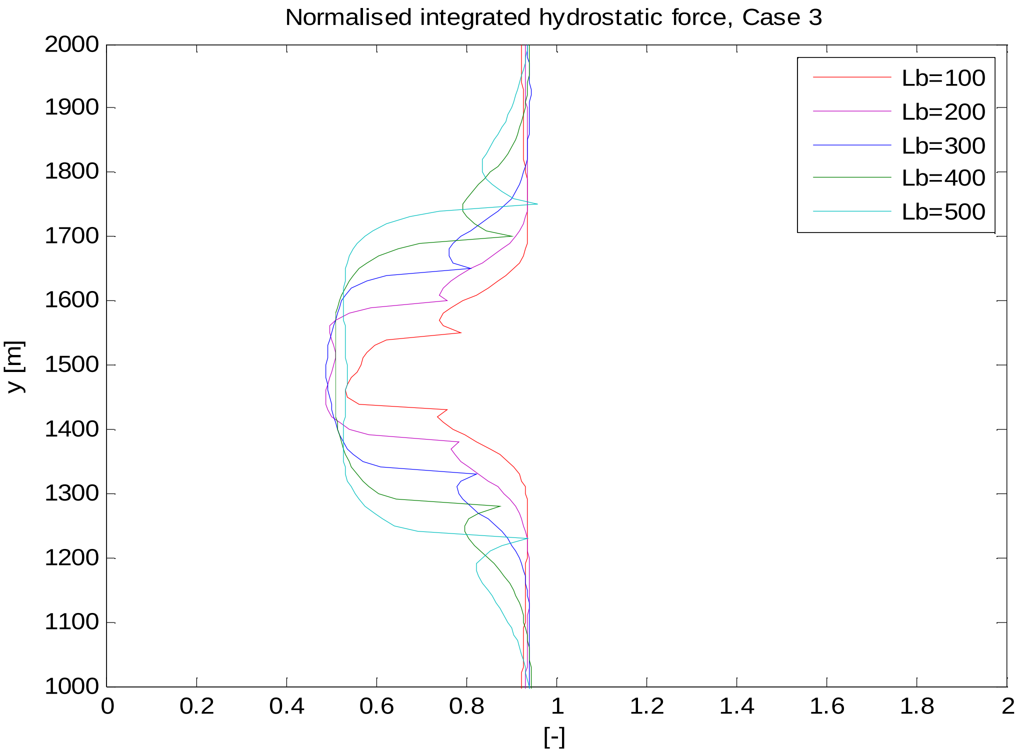


*Figure D.8 Normalised cross-shore integrated hydrostatic stresses case 4*

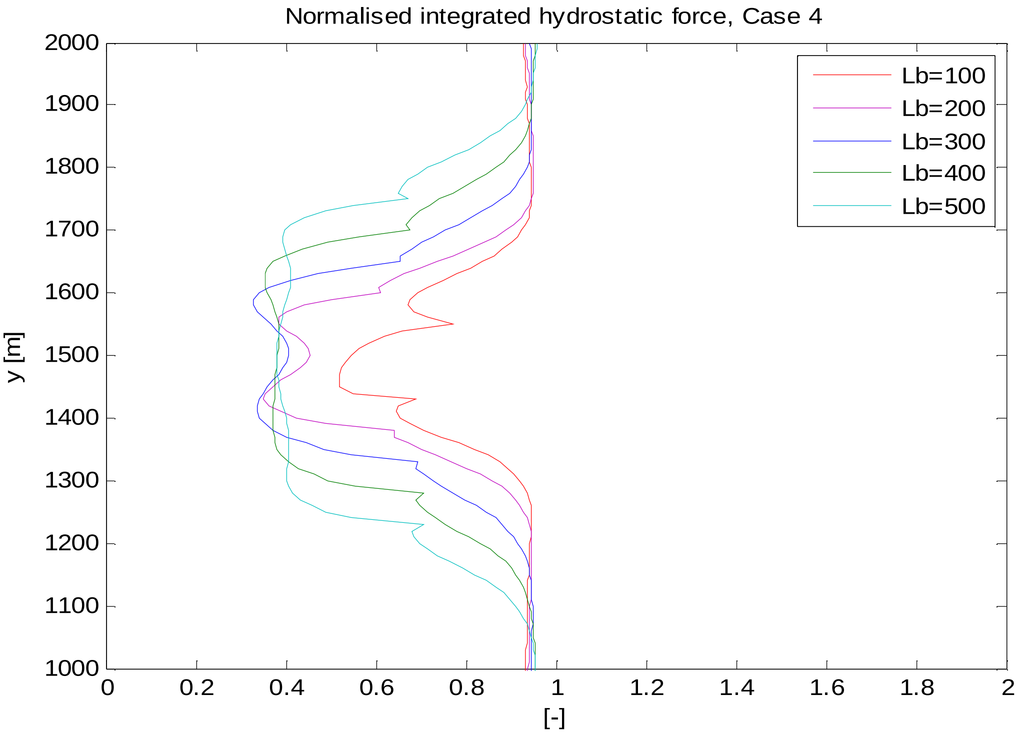

## D.3 Flow induced force

*Figure D.9 Normalised cross-shore integrated flow induced stresses case 1*

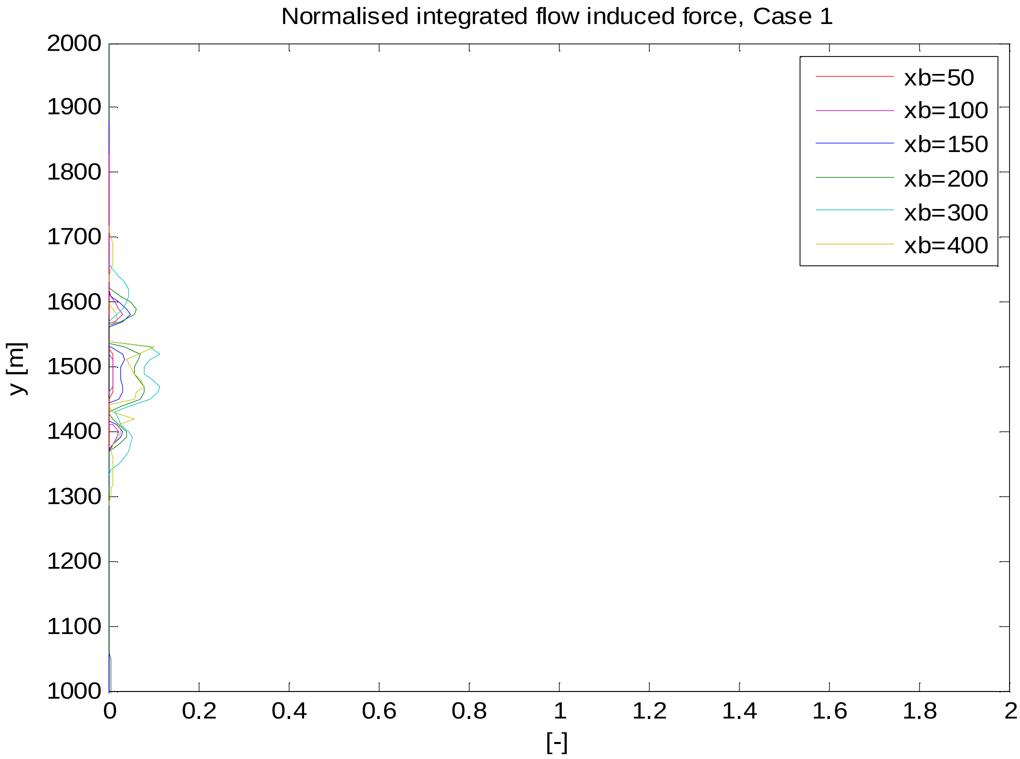


*Figure D.10 Normalised cross-shore integrated flow induced stresses case 2*

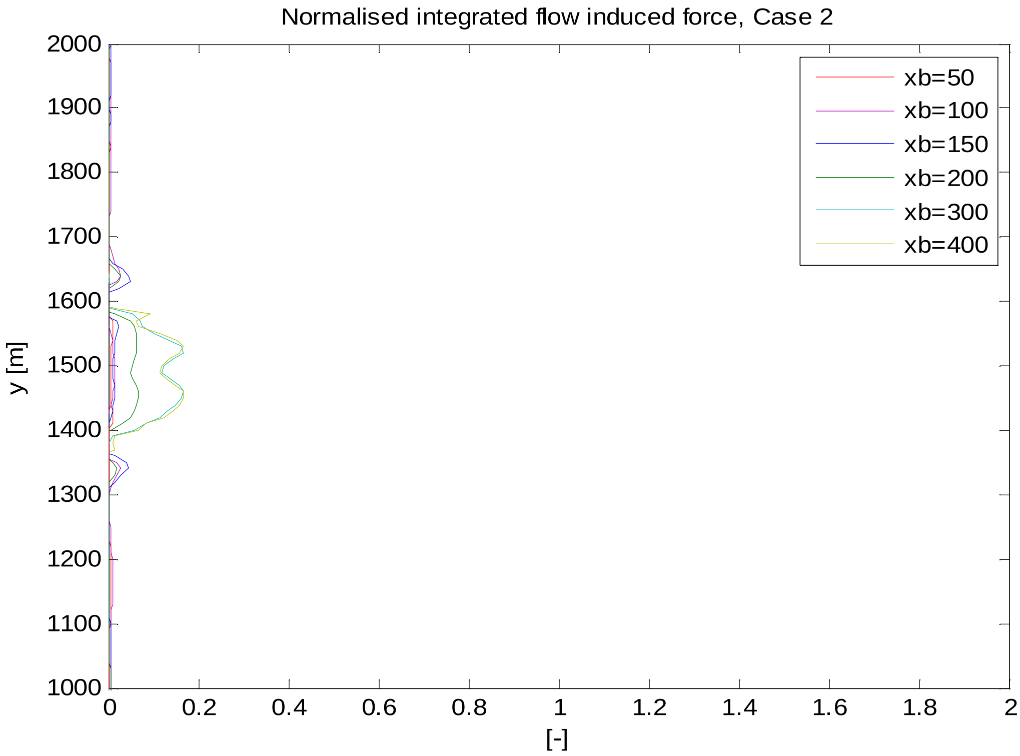

Figure D.11 Normalised cross-shore integrated flow induced stresses case 3

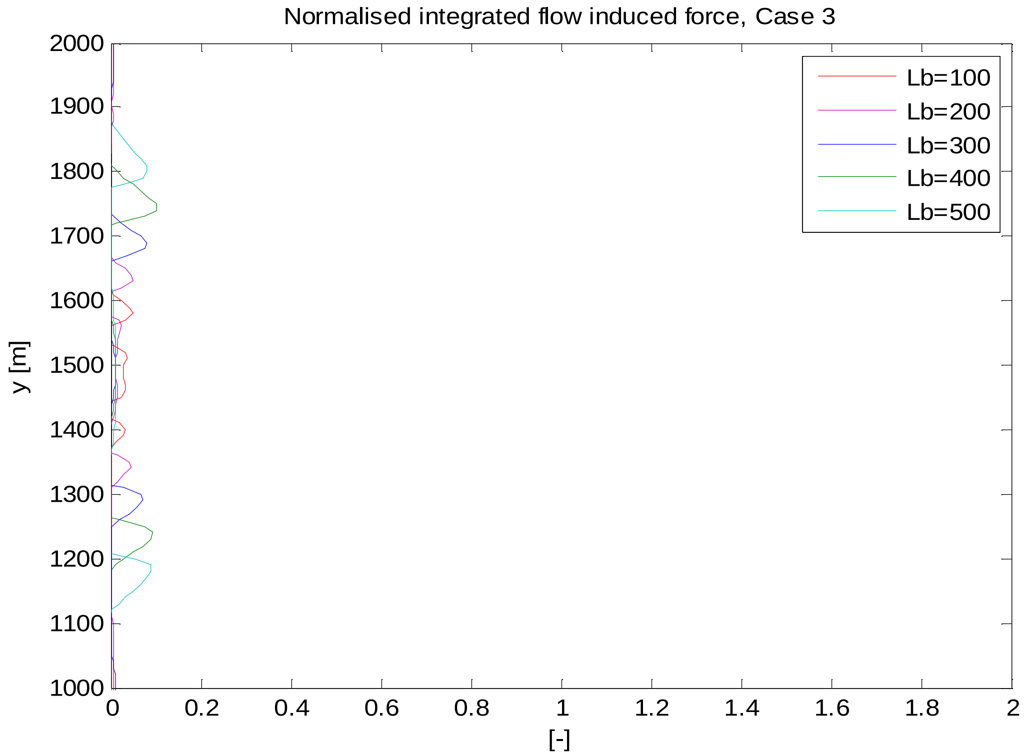


Figure D.12 Normalised cross-shore integrated flow induced stresses case 4

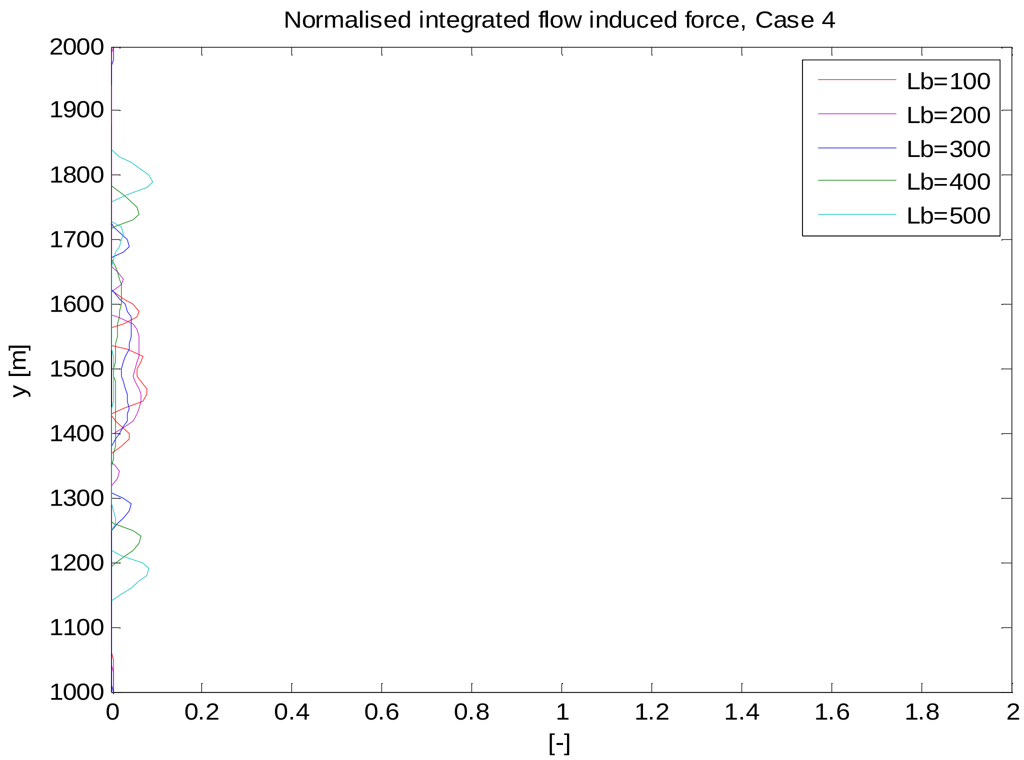

## D.4 Bottom stress

*Figure D.13 Normalised cross-shore integrated bottom stresses case 1*

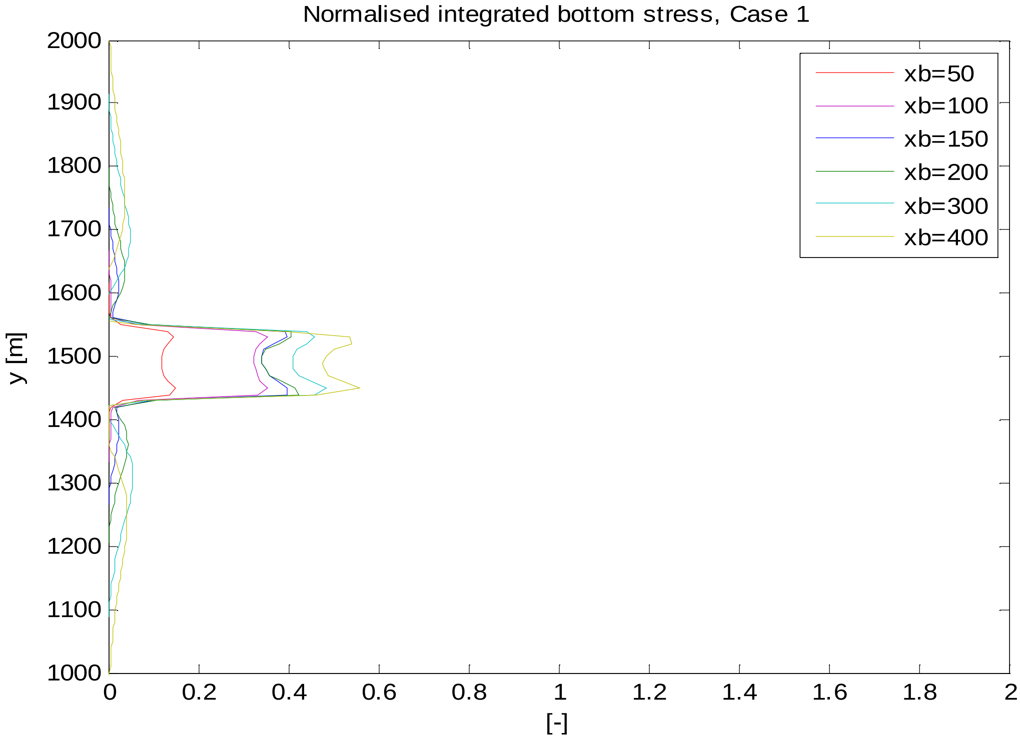


*Figure D.14 Normalised cross-shore integrated bottom stresses case 2*

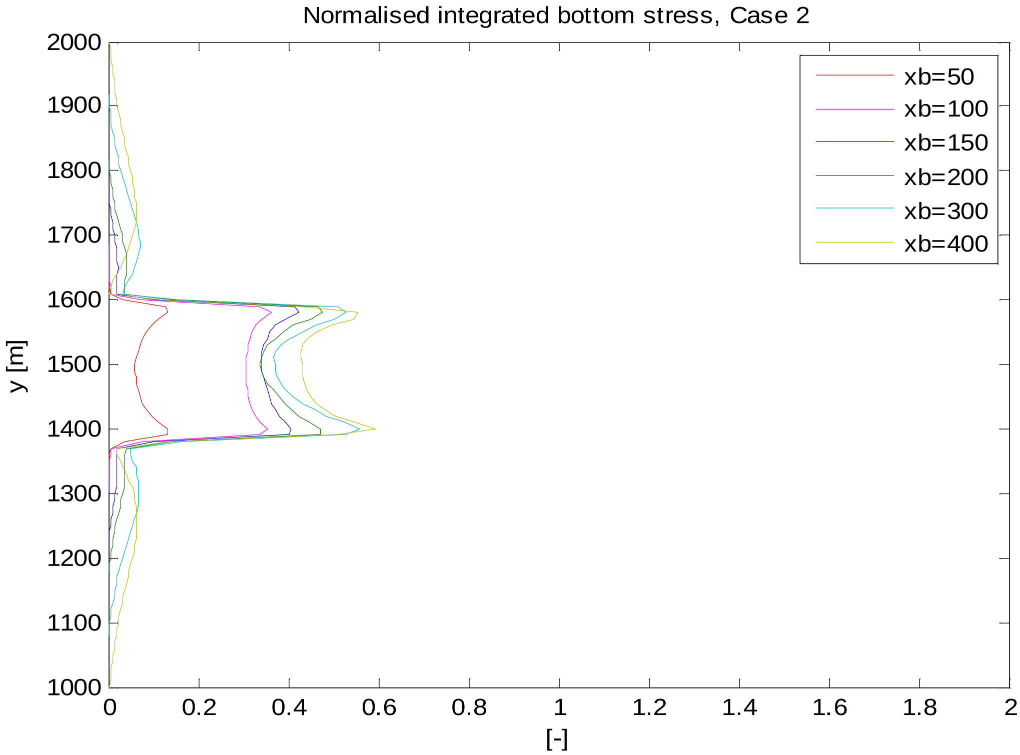

*Figure D.15 Normalised cross-shore integrated bottom stresses case 3*

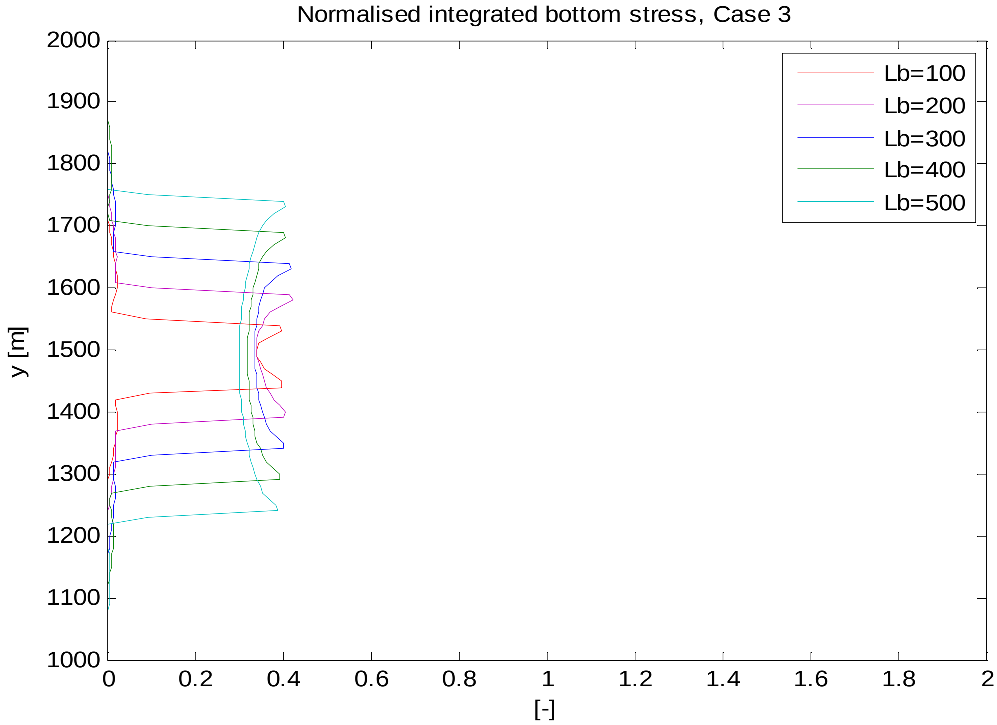


*Figure D.16 Normalised cross-shore integrated bottom stresses case 4*

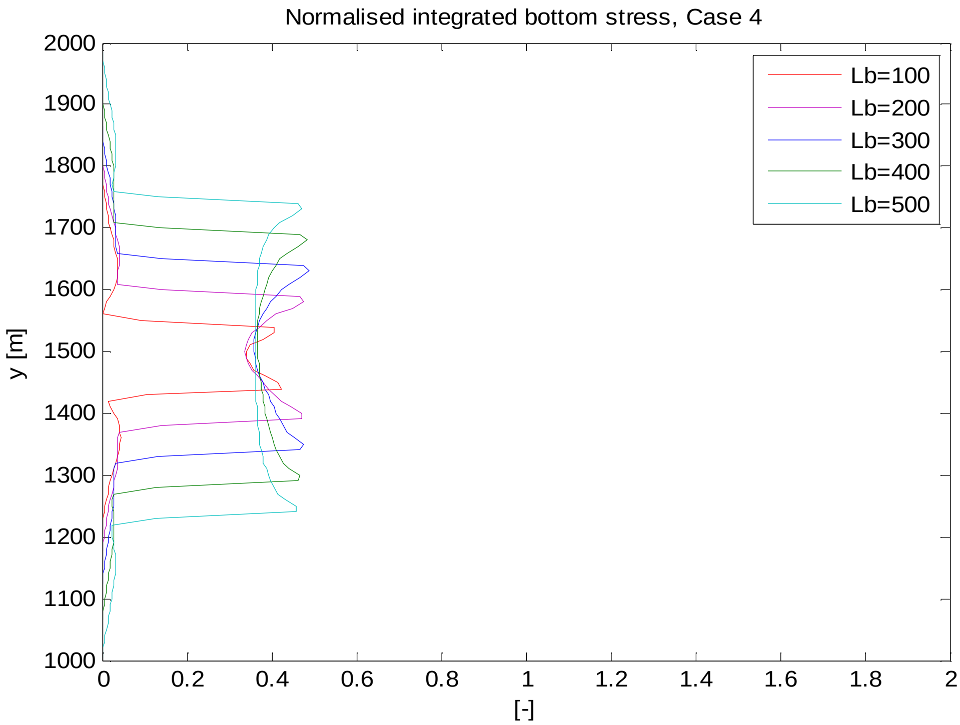

# E Alongshore momentum balance

*Figure E.1 Example of spatial distribution of long shore momentum balance, N/m2.*

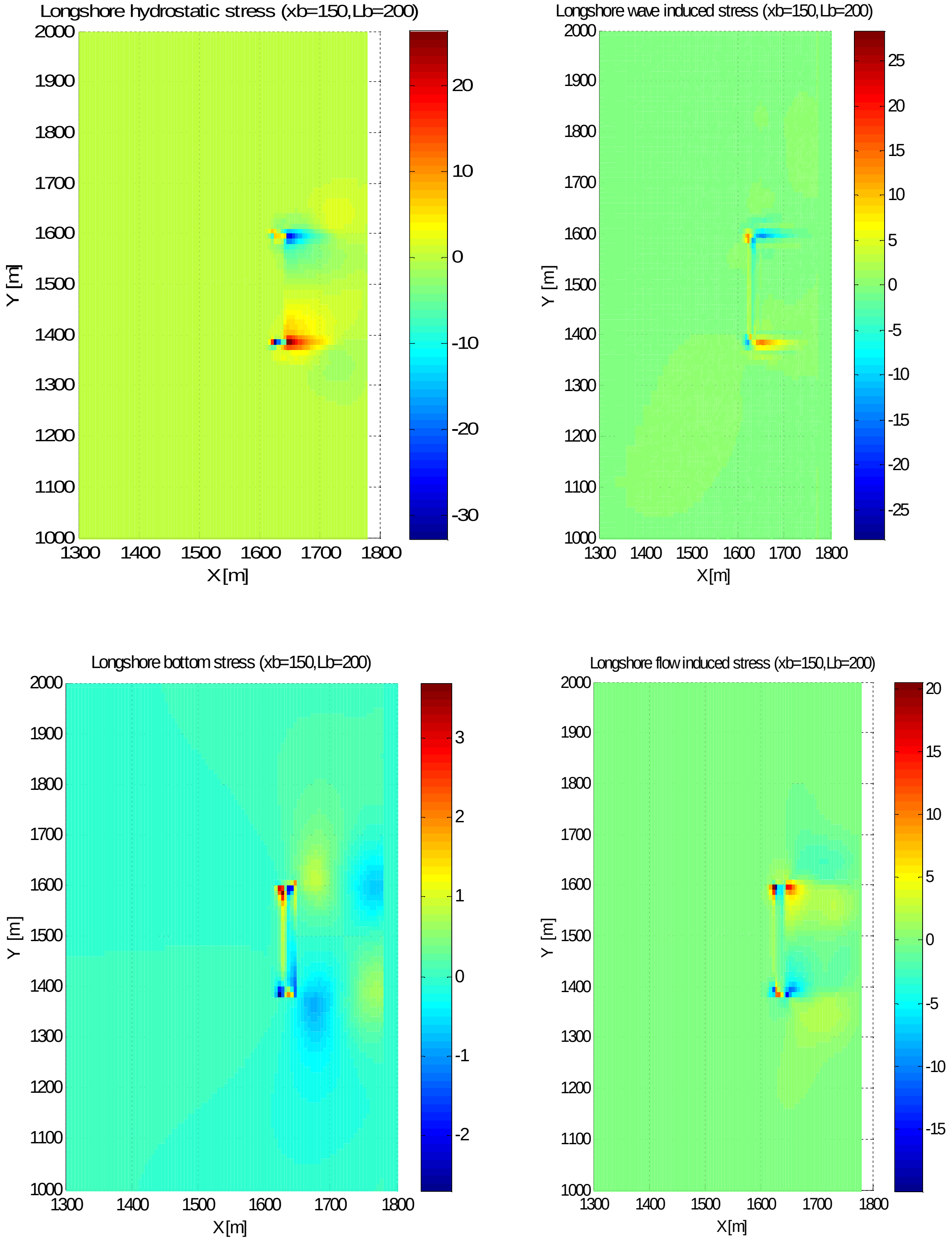

Deltares

*Figure E.2 Alongshore wave induced stresses*

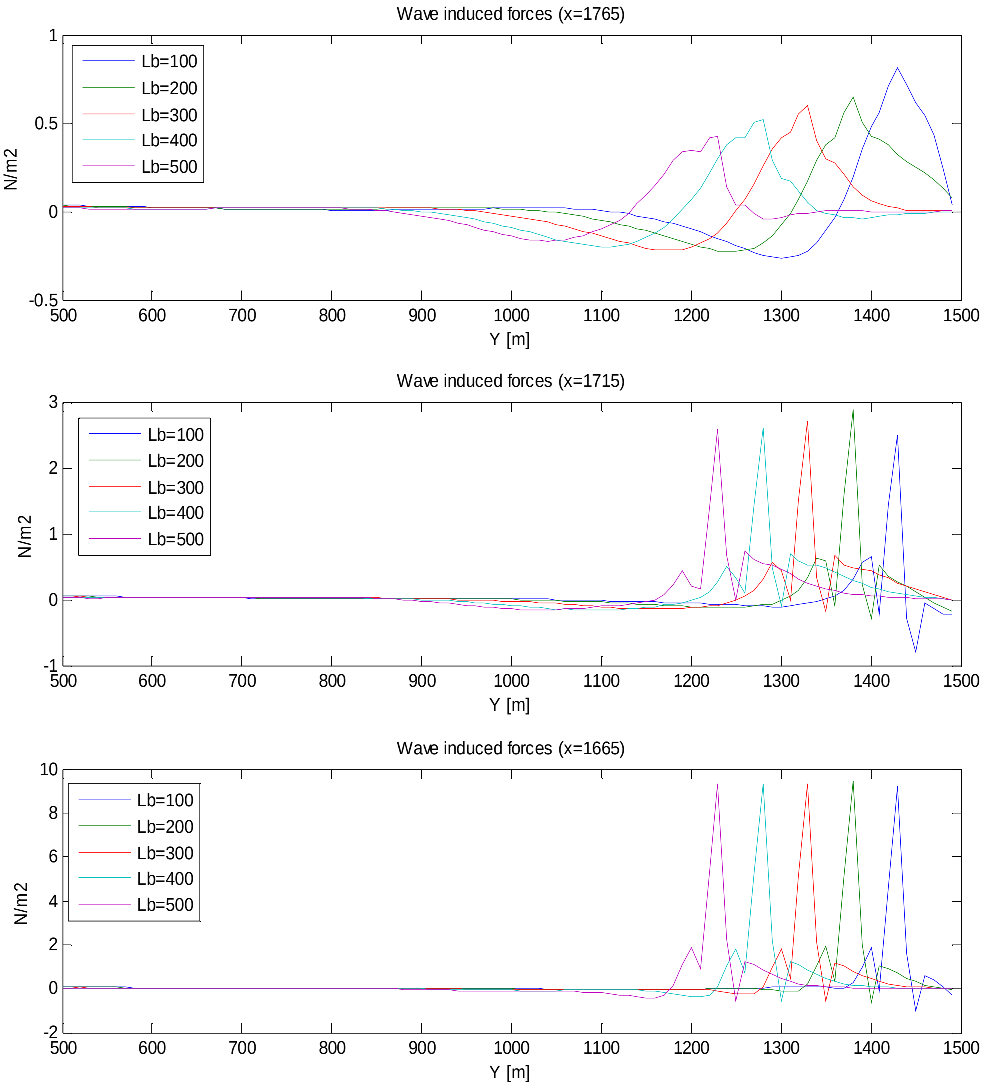

*Figure E.3 Alongshore water level gradient induced hydrostatic stresses*

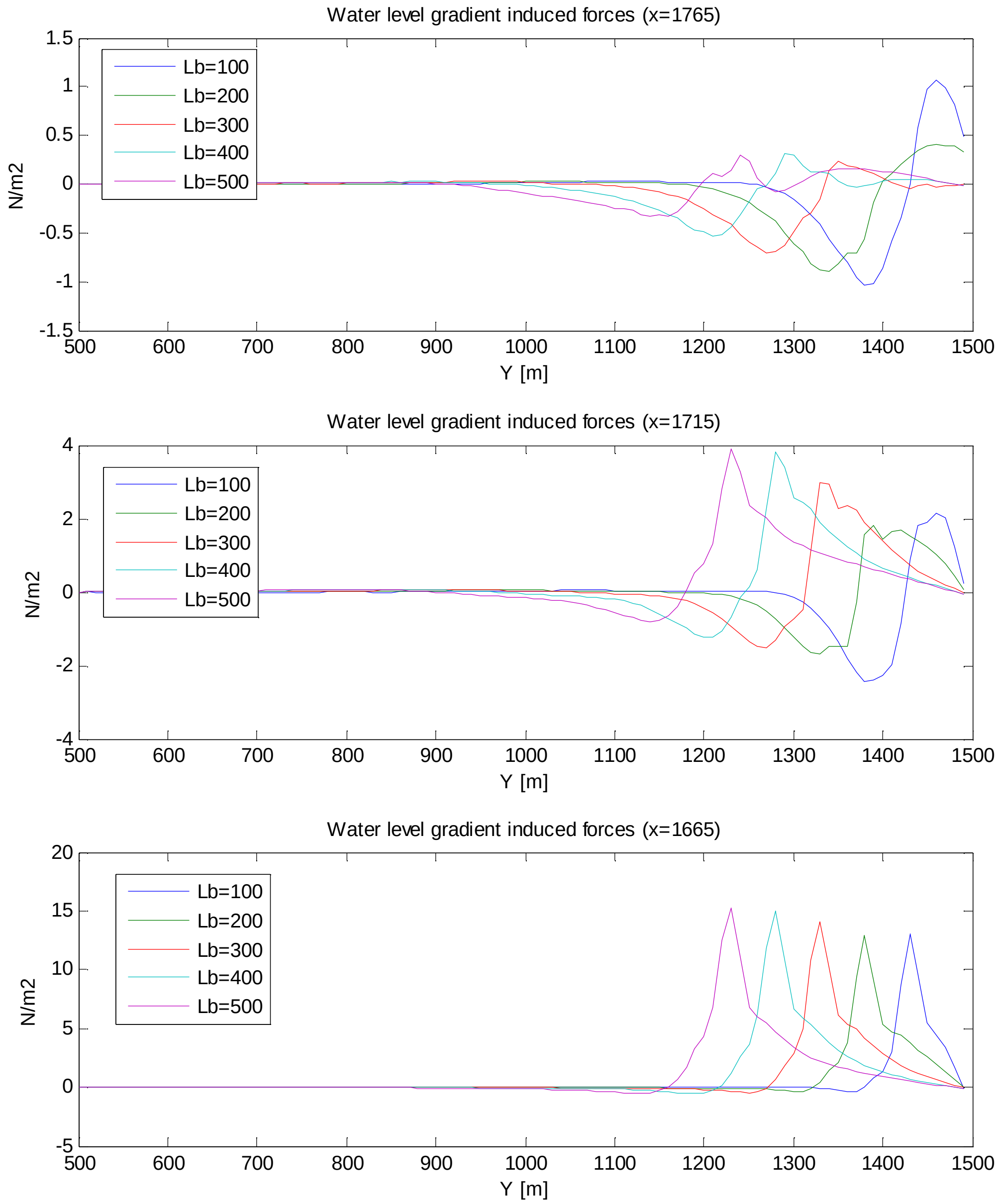

*Figure E.4   Alongshore flow induced stresses*

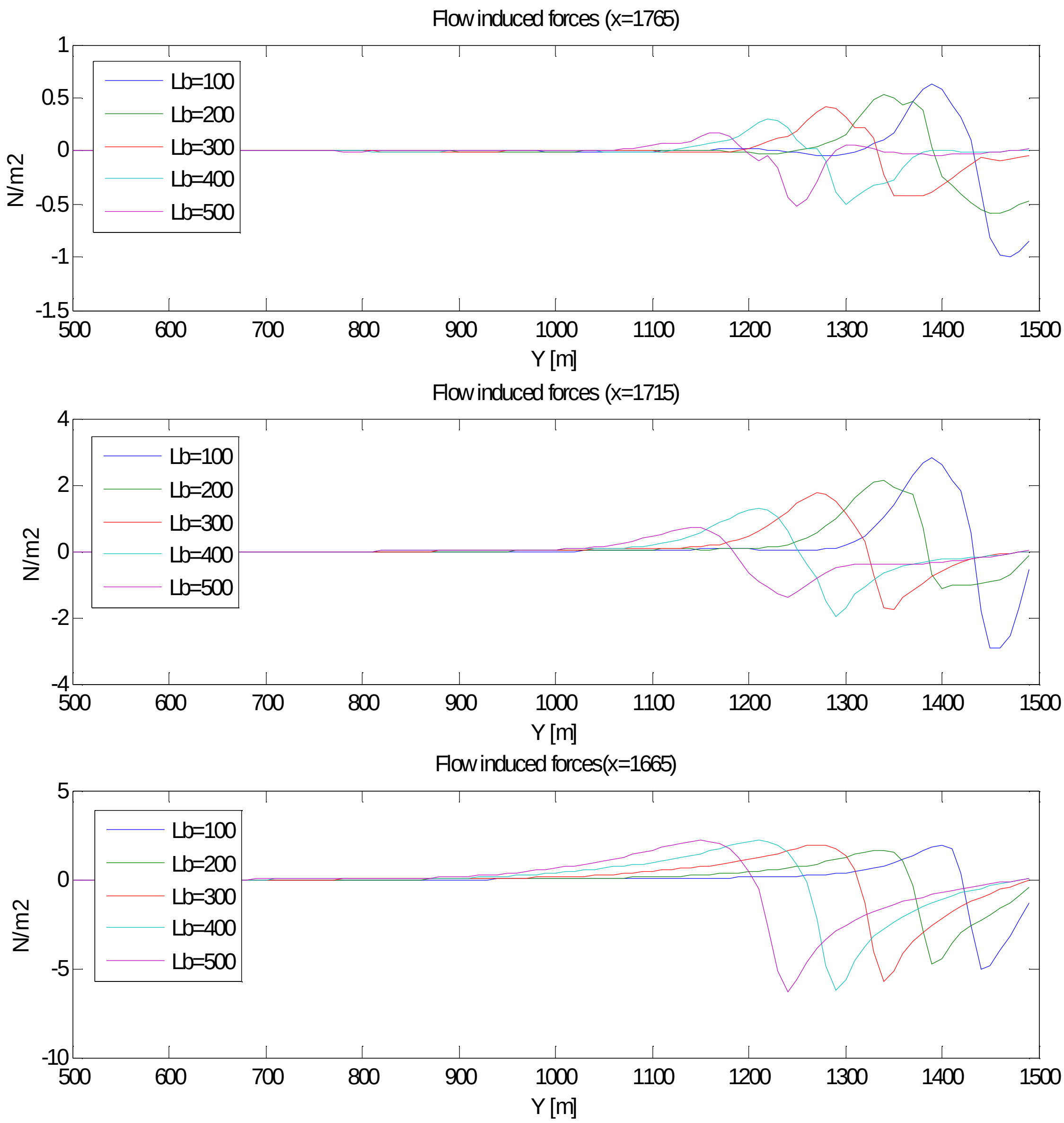

*Figure E.5 Alongshore bottom stresses*

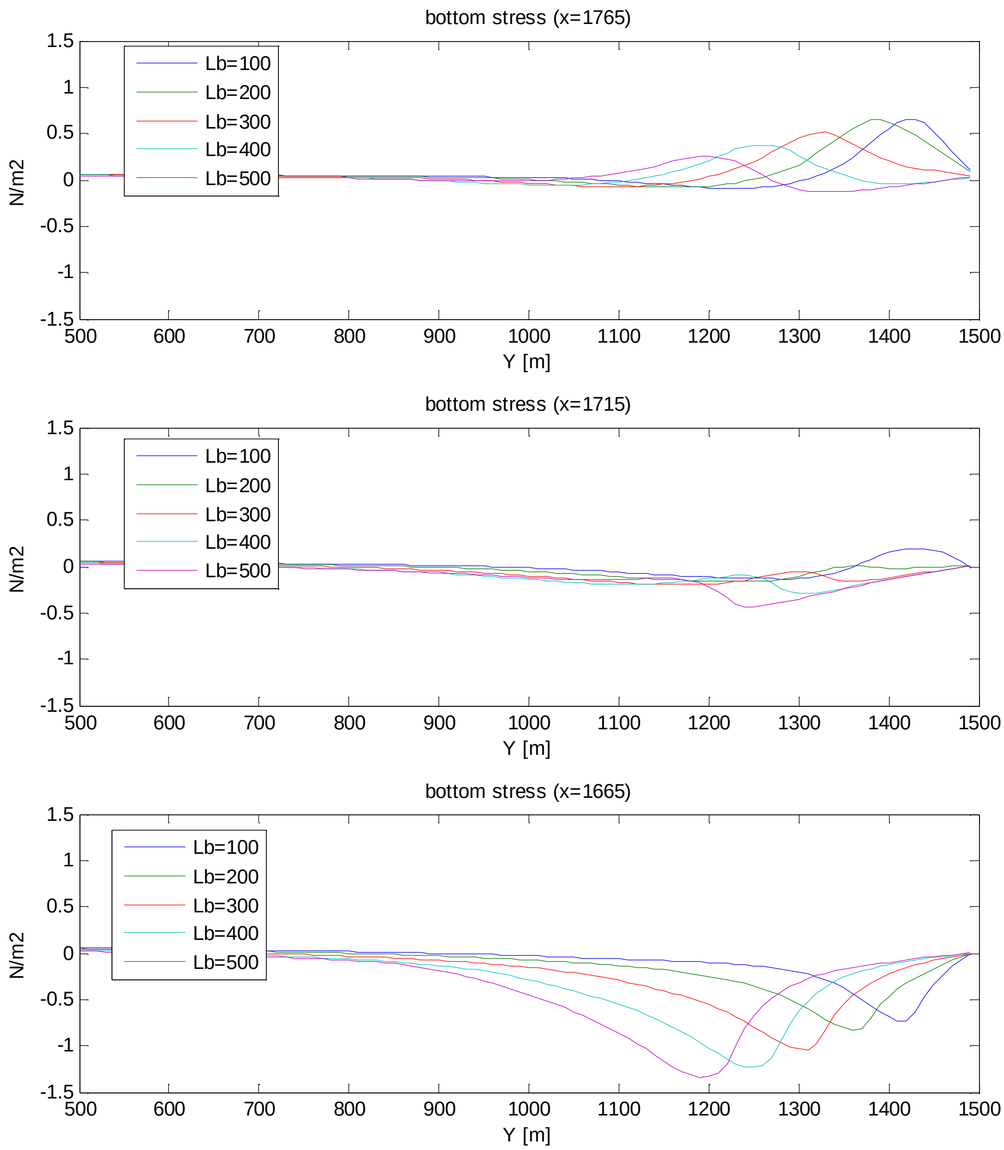

# F Alongshore depth averaged velocities and water level

*Figure F.1 Definition alongshore cross-section*

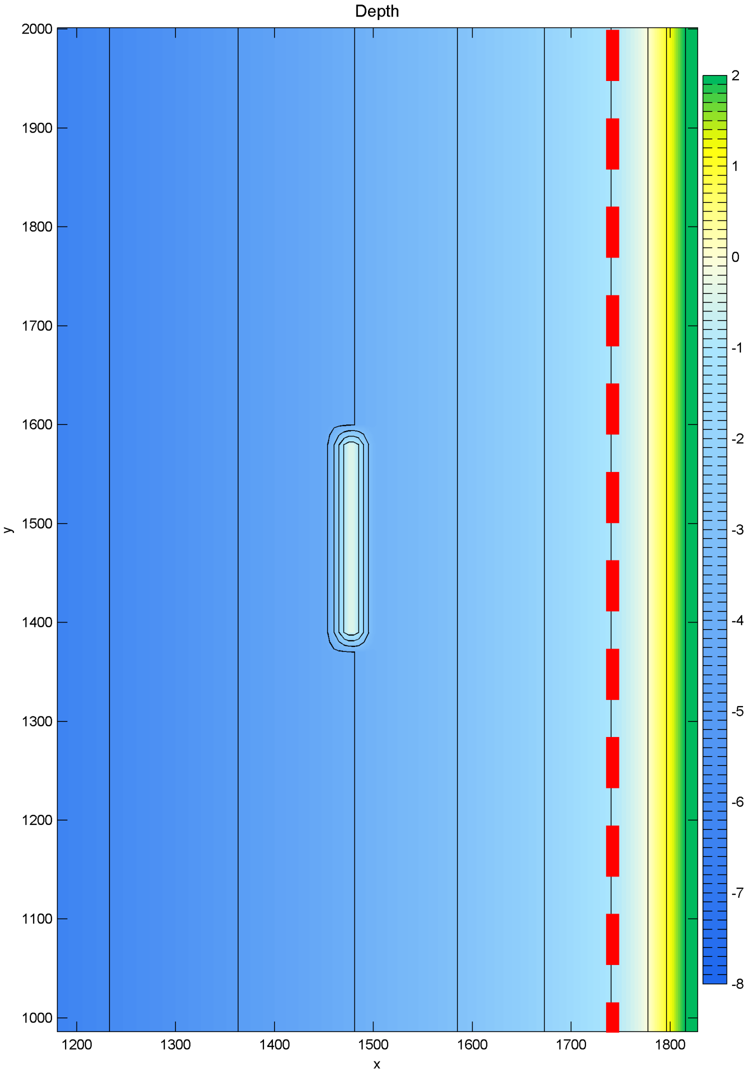

*Figure F.2 Alongshore water levels case 1*

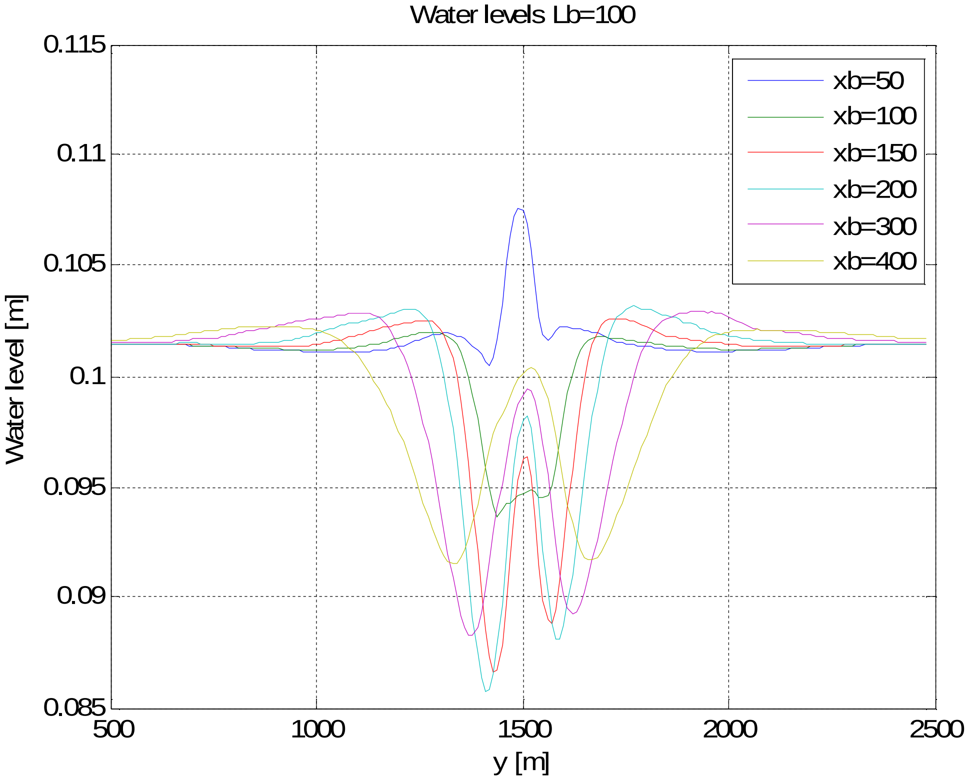


*Figure F.3 Alongshore depth averaged velocity case 1*

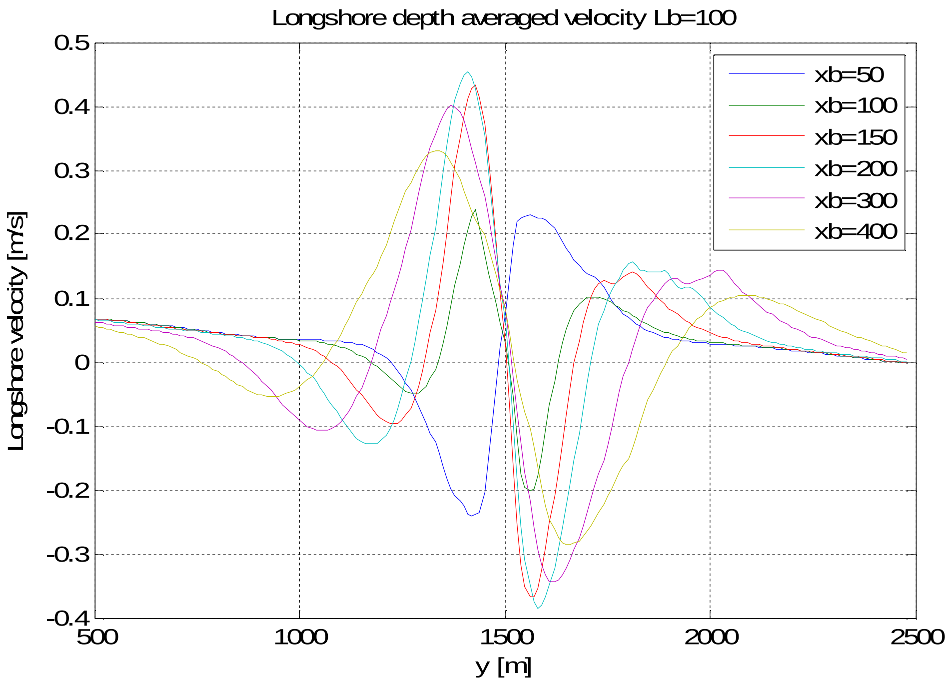

*Figure F.4 Alongshore water levels case 2*

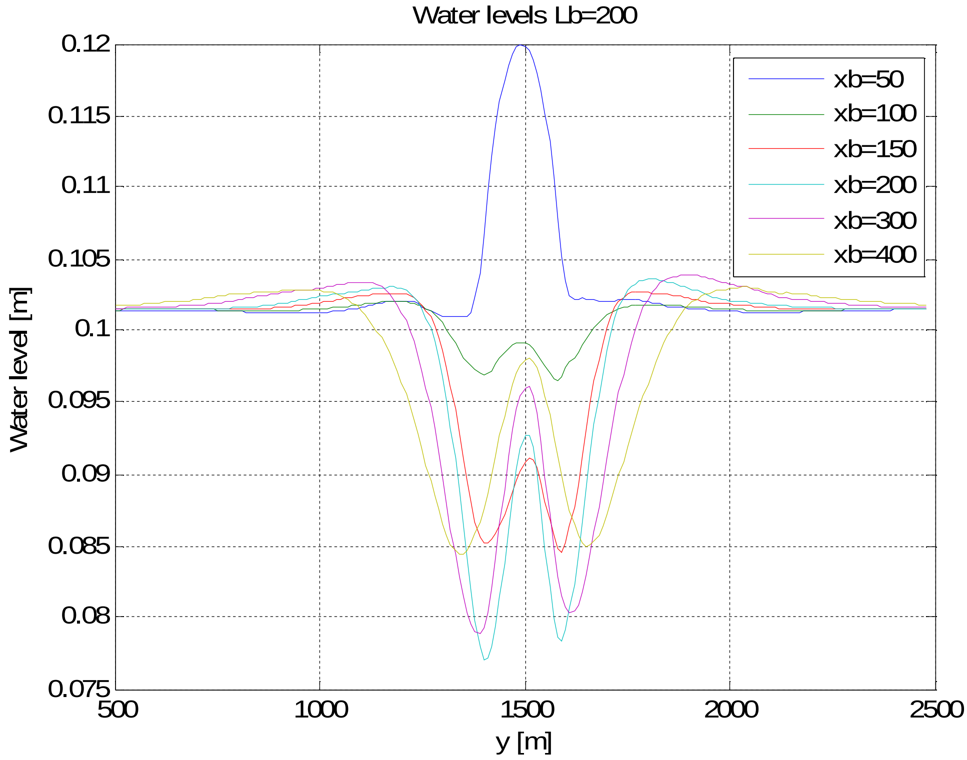


*Figure F.5 Alongshore depth averaged velocity case 2*

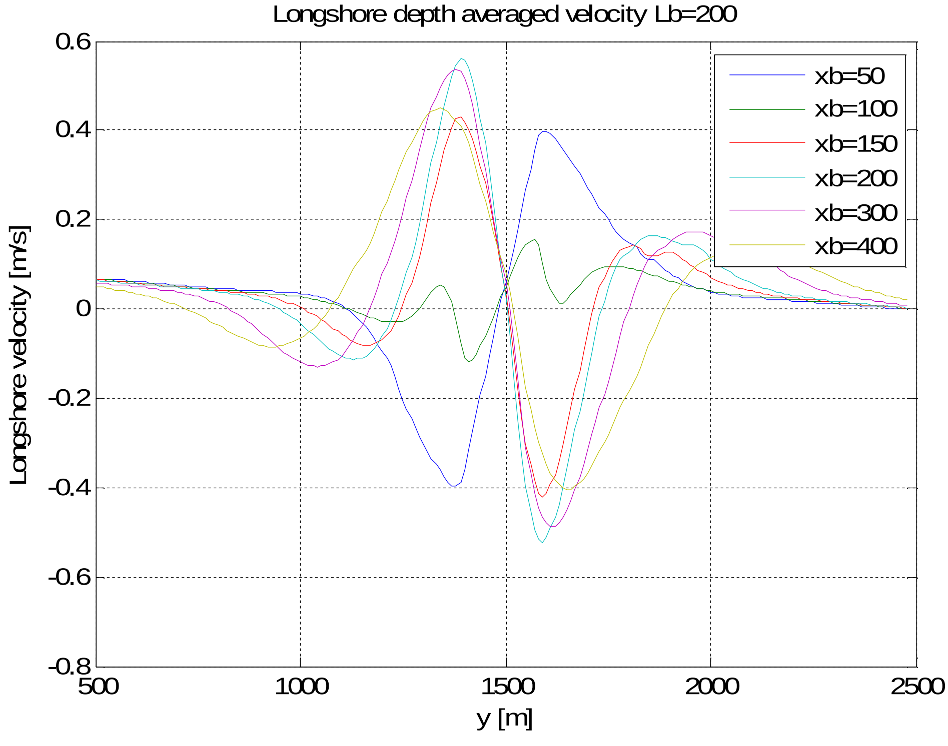

*Figure F.6 Alongshore water levels case 3*

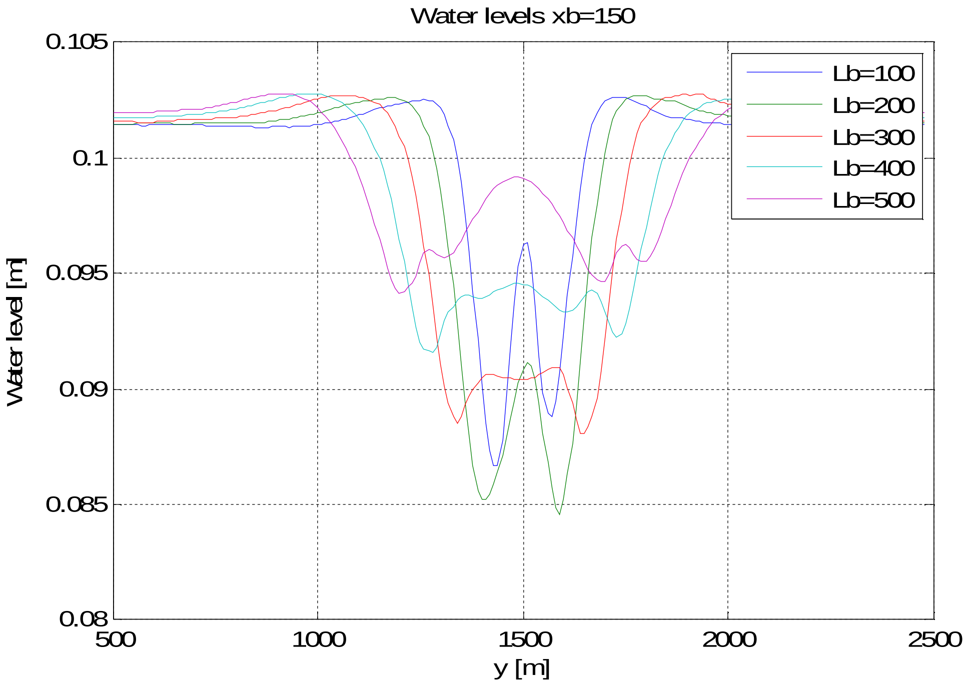


*Figure F.7 Alongshore depth averaged velocity case 3*

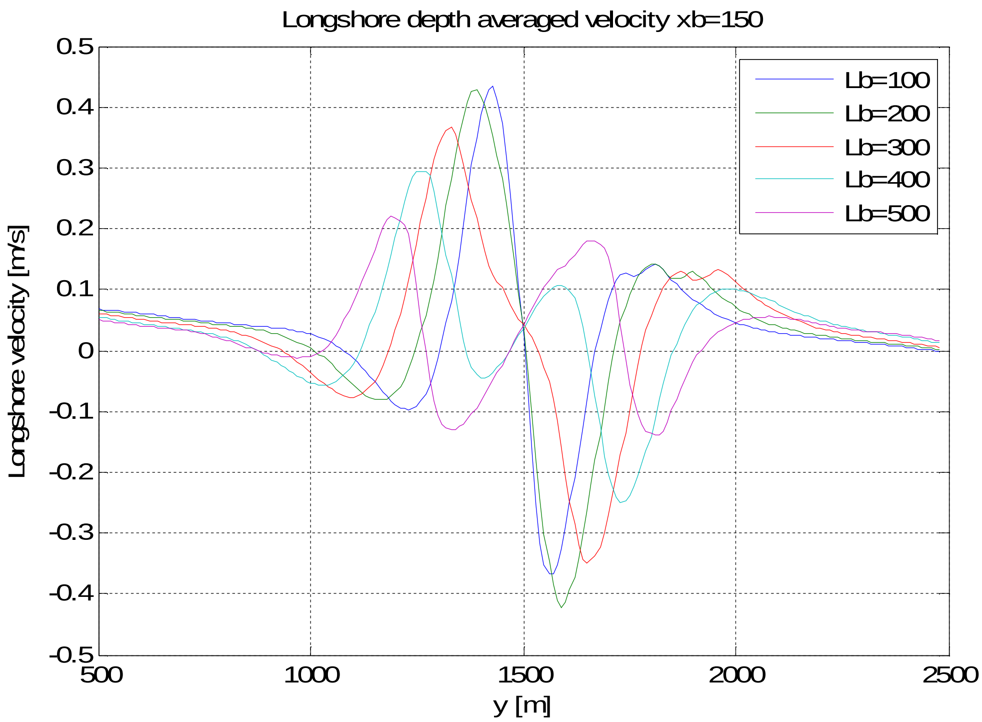

Figure F.8 Alongshore water levels case 4

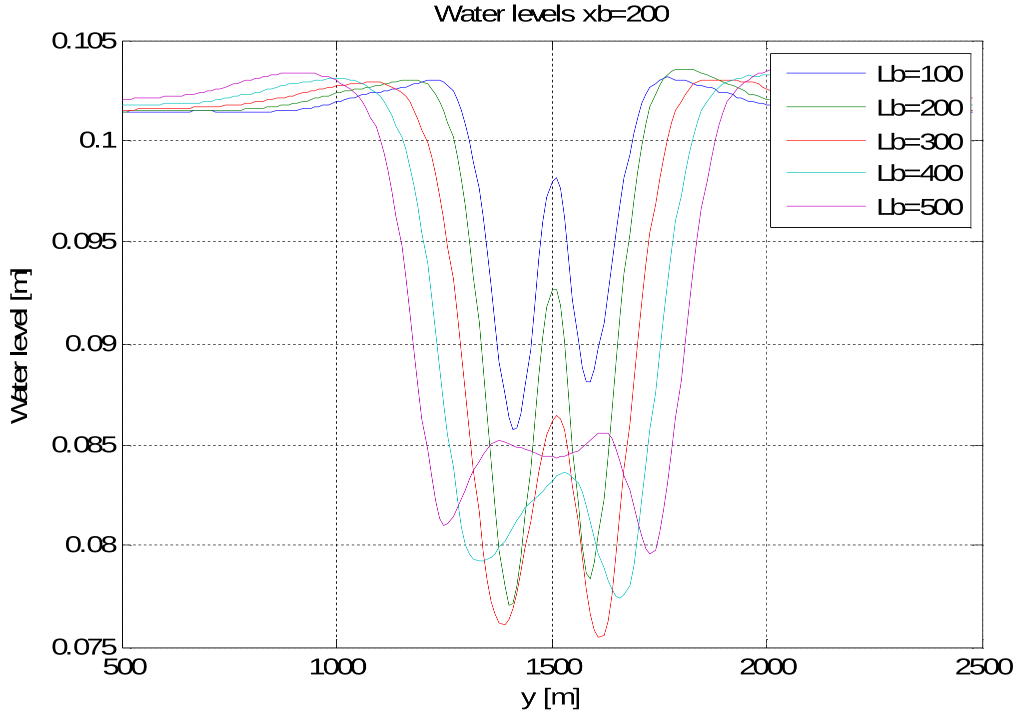


Figure F.9 Alongshore depth averaged velocity case 4

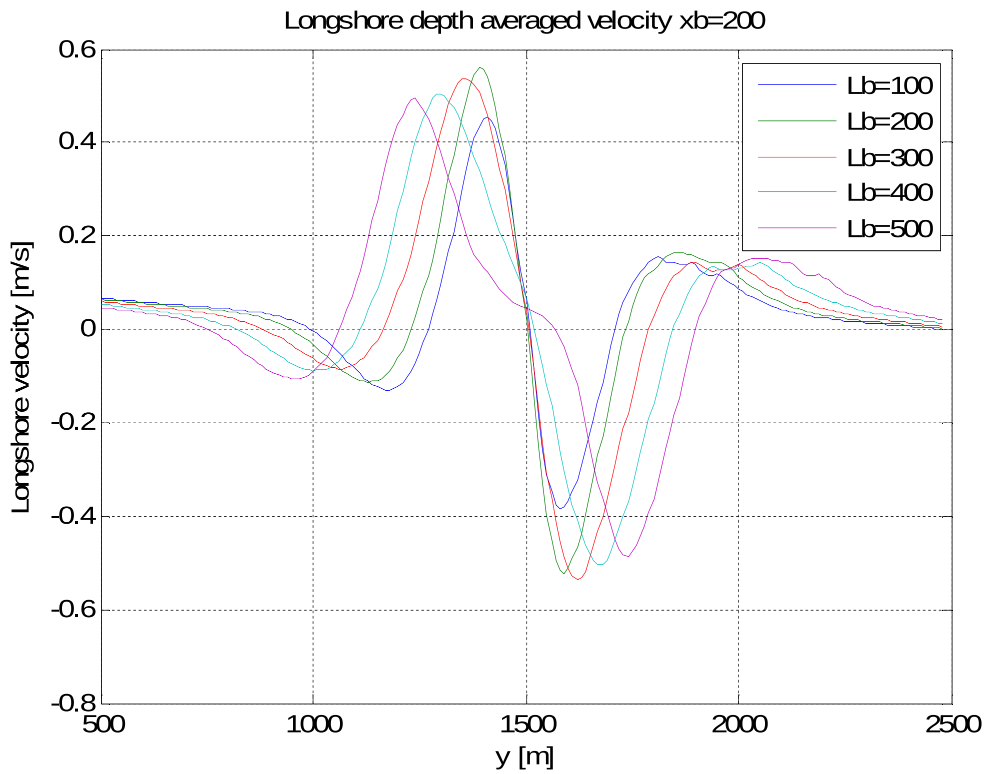

# G Influence of net flow over submerged breakwater

Another process is the three dimensional effect of the mass transport over the SBW. Interesting to see is what effect this flow has on the hydrodynamics of the zone behind the breakwater. To solely present the effect of the mass-transport, a new runs are made in Delft 3D. Using three cases of different offshore distance and replace the wave forcing by a forced flow, similar to the wave induced mass transports over the breakwater. Although this is not entirely correct, due to, amongst others, the influence of wave forcing in alongshore direction (see paragraph 4.5), however the resulting water level set-up to return the water offshore will be interesting. In Delft3D, modelling the mass-transport without wave forcing is done by defining intake and outlet discharges, separated by an obstacle. Results of the influence on the water level can be seen in Figure G.1 - Figure G.3.

*Figure G.1 Total wave-induced water level set-up including wave forcing. Left xb=50m, middle xb=100m, right xb=200m. Hs= 2m.*

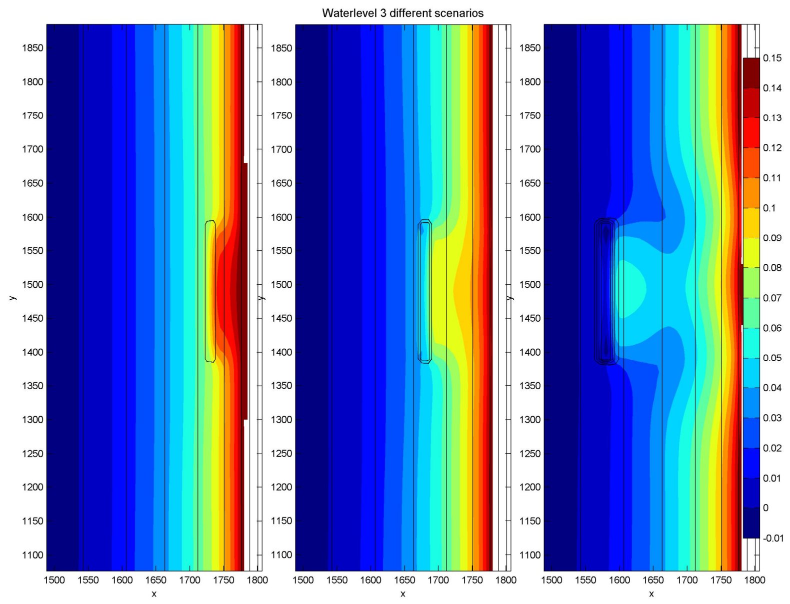

*Figure G.2 Mass-transport over the submerged breakwater with wave induced forcing. Blue xb=200m, red xb=100m, green xb=50m.*

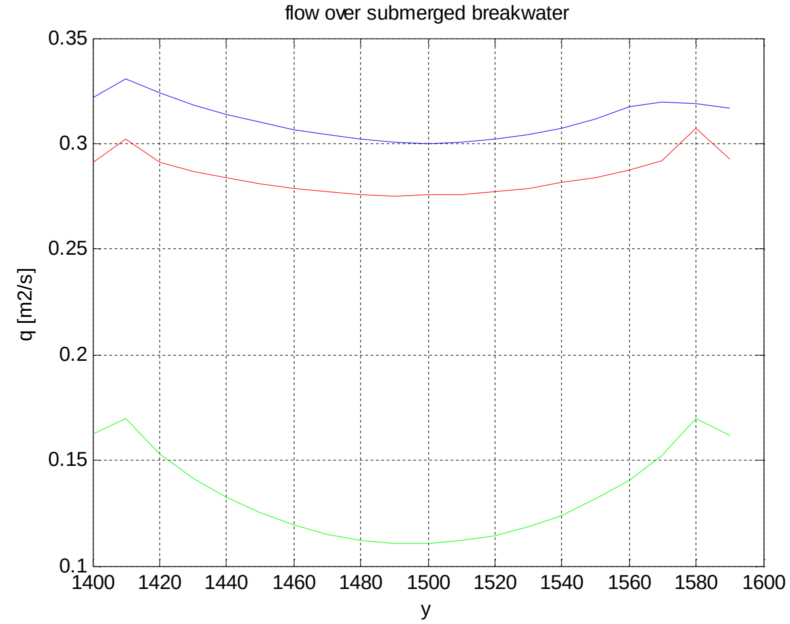


*Figure G.3 Water level set-up due to mass-transport over the submerged breakwater only. Left xb=50m, middle xb=100, right xb=200*

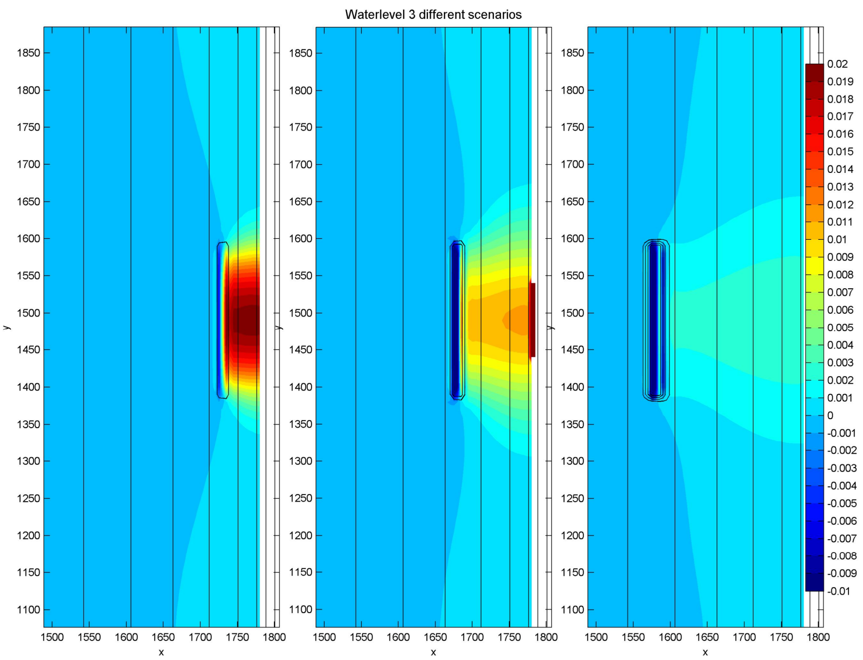


Clearly, the water level set-up due to the mass transport over the breakwater, the ponding mechanism, is of a different order than the total water level set-up including the wave forcing. Nevertheless, when set-up differences are small between the uniform coastline compared to the water level behind the breakwater, this influence cannot be neglected.

Another interesting phenomenon is the difference in set-up due to the mass-transport only between the different layouts. The difference in flux over the breakwater is in the order of 0.5 between the $x_b$=200m and $x_b$=50m case, but the difference in water level set-up is a factor of 20 difference. This can be explained by comparing the mass transport from the shadow zone as an open channel, for instance described by a chezy type formula. If the total flow remains the same and the width of the channel is decreasing, it compensates by an additional water level gradient. In addition, when xb decreases the averaged water depth of this ‘channel’ is also decreasing, having an inverse quadratic relation to the water level gradient. This explains the strong relation between the offshore distance of the SBW and the water level set-up. As mentioned in previous paragraphs when taking xb/Lb to zero, other processes like the return flow over and through (porous flow, if possible) the SBW become important.

Concluding, the mass-transport over the SBW is import for near shore SBW. By increasing the offshore distance, decreasing the breakwater length or otherwise reducing the mass transport over the SBW, the set-up due to this mass-transport rapidly decreases. As previous paragraphs introduced, by keeping the water level set-up behind the SBW lower compared to the uniform coastline, a accretive flow pattern occurs. Chapter 4 will explain this process more elaborate by studying the cross-shore and alongshore momentum balance.

# H Sensitivity analysis design parameters

## H.1 Lb >> xb (2 dimensional case)

*Figure H.1 Cross-shore flow (velocities)*

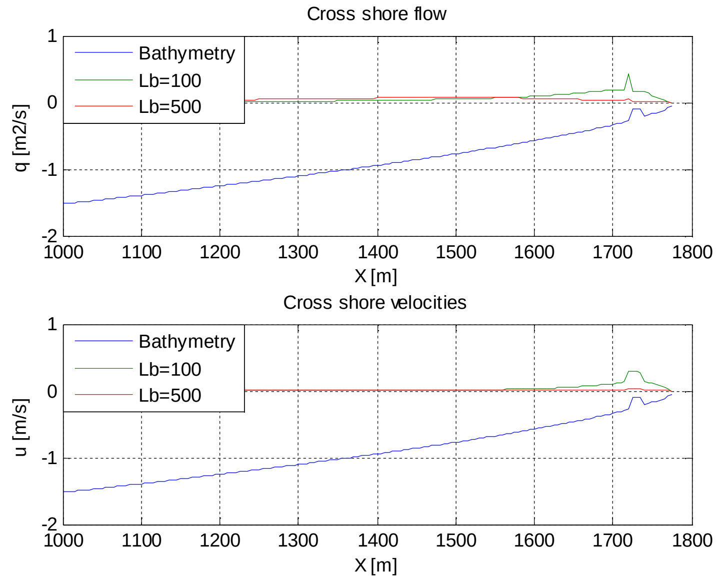


*Figure H.2 flow over the SBW*

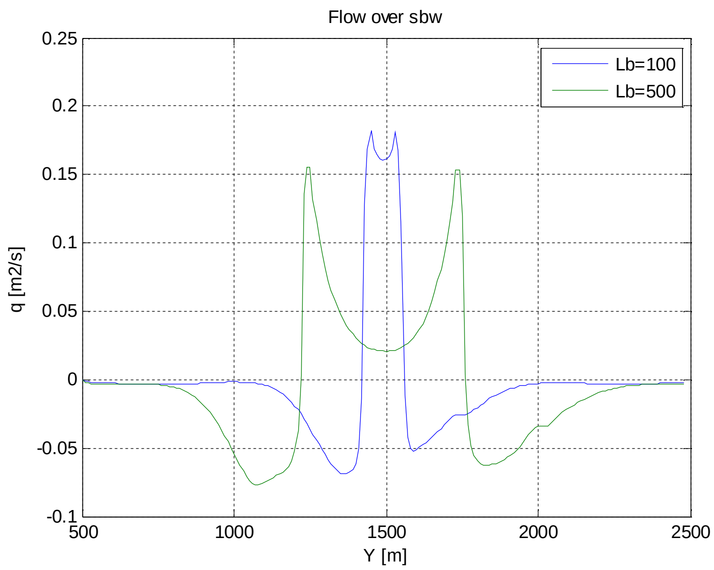

*Figure H.3 Depth averaged velocity over SBW*

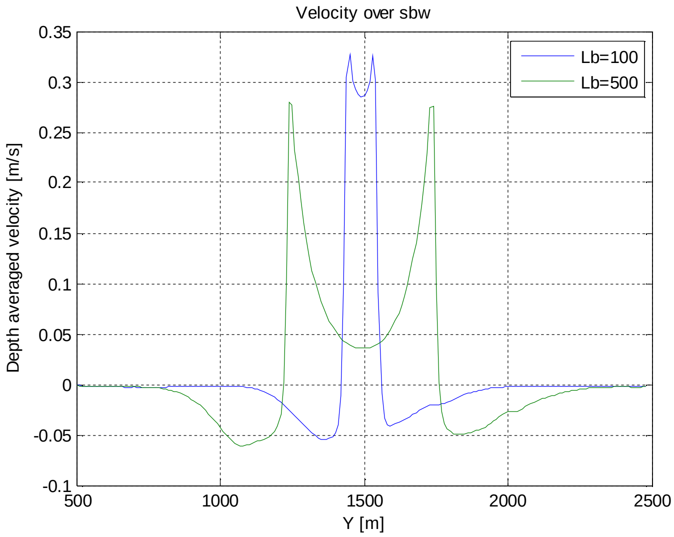


*Figure H.4 Cross-shore water levels over the SBW*

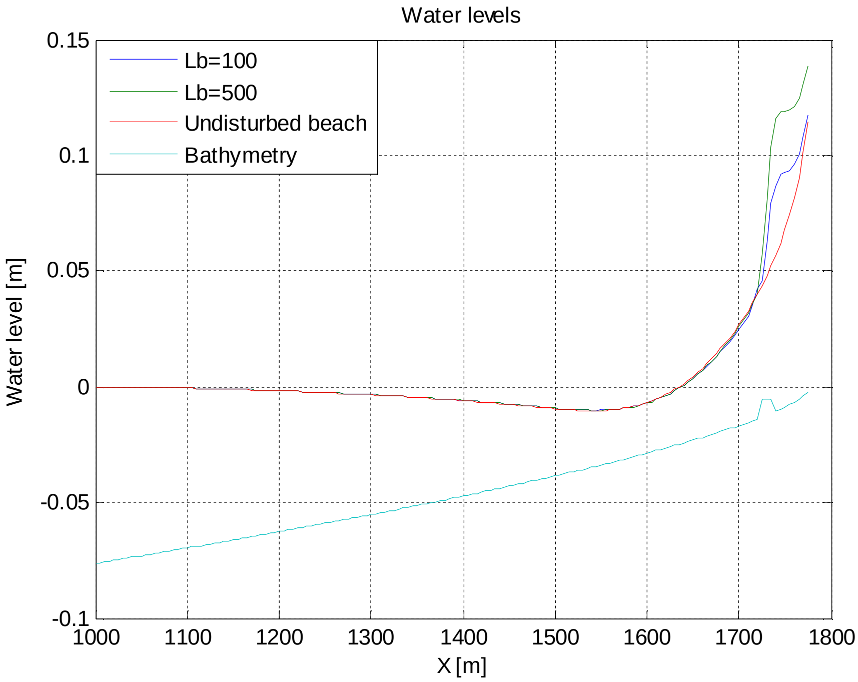

## H.2 Bottom roughness

*Figure H.5 Cross-shore flow (velocities) over SBW*

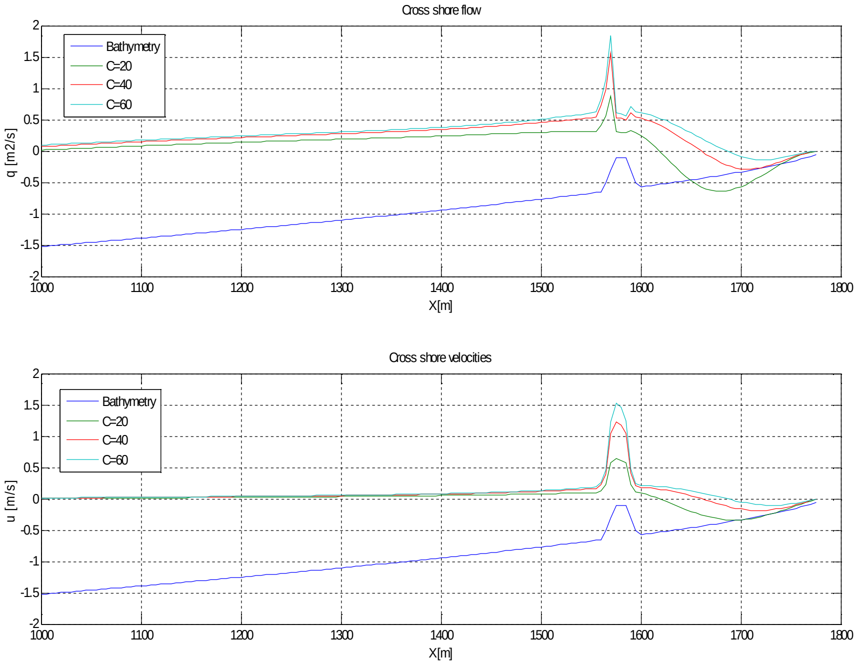


*Figure H.6 Depth averaged flow over the SBW*

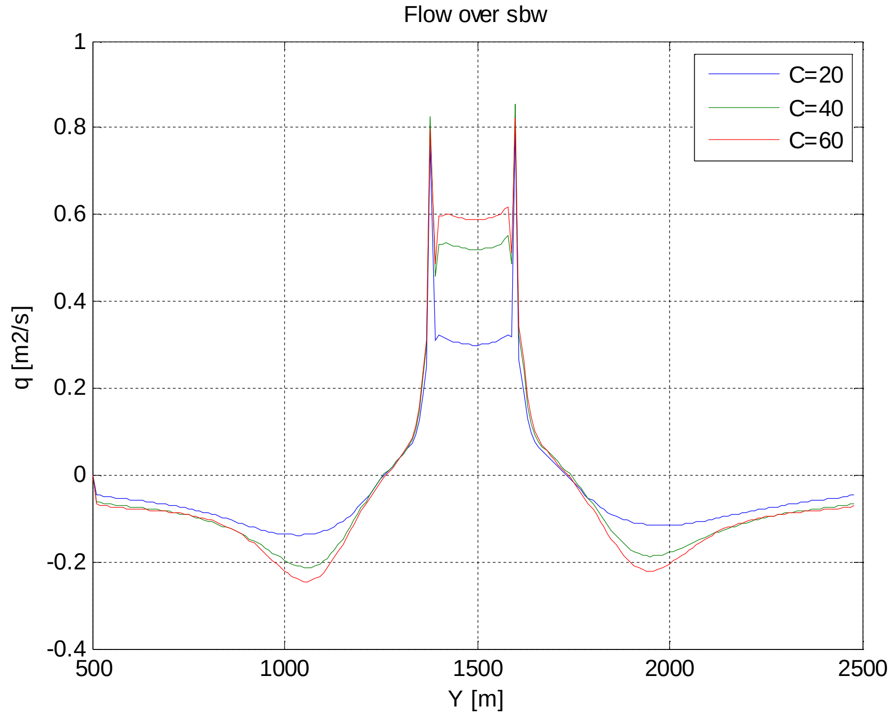

*Figure H.7 Depth averaged velocity over SBW*

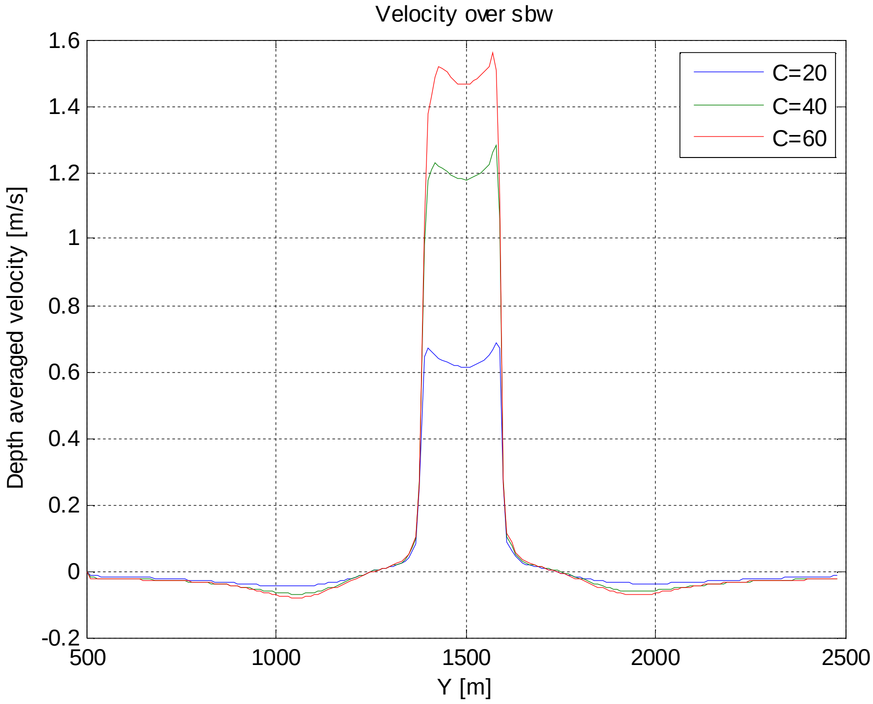


*Figure H.8 Cross-shore water level set-up over the SBW*

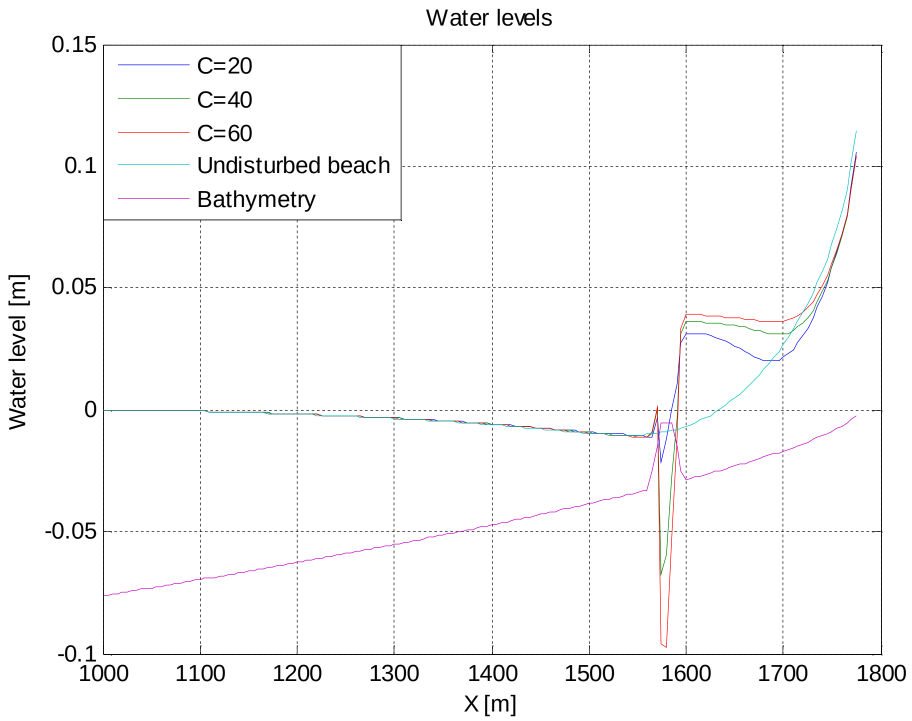

*Figure H.9 Wave heights over the SBW*

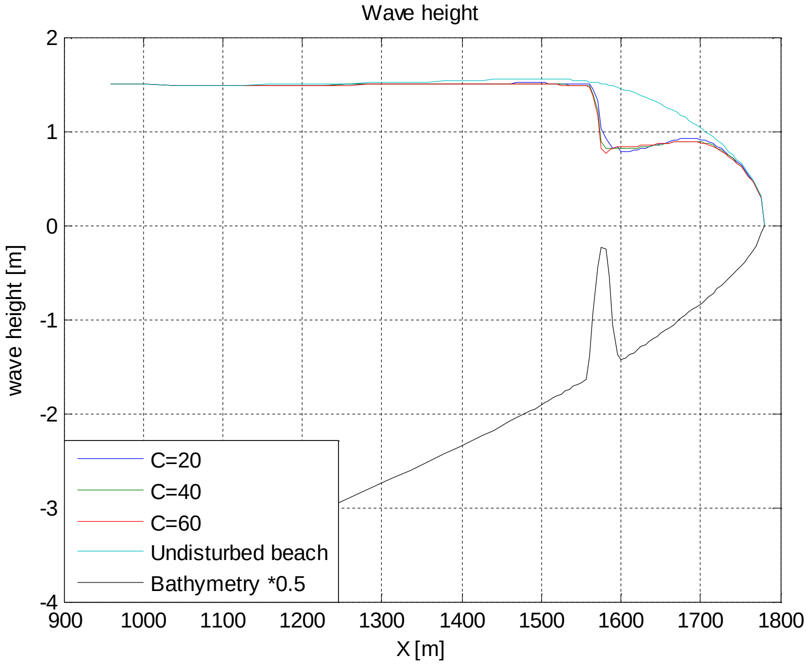

## H.3 Crest height

*Figure H.10 Cross-shore flow (velocities) over SBW*

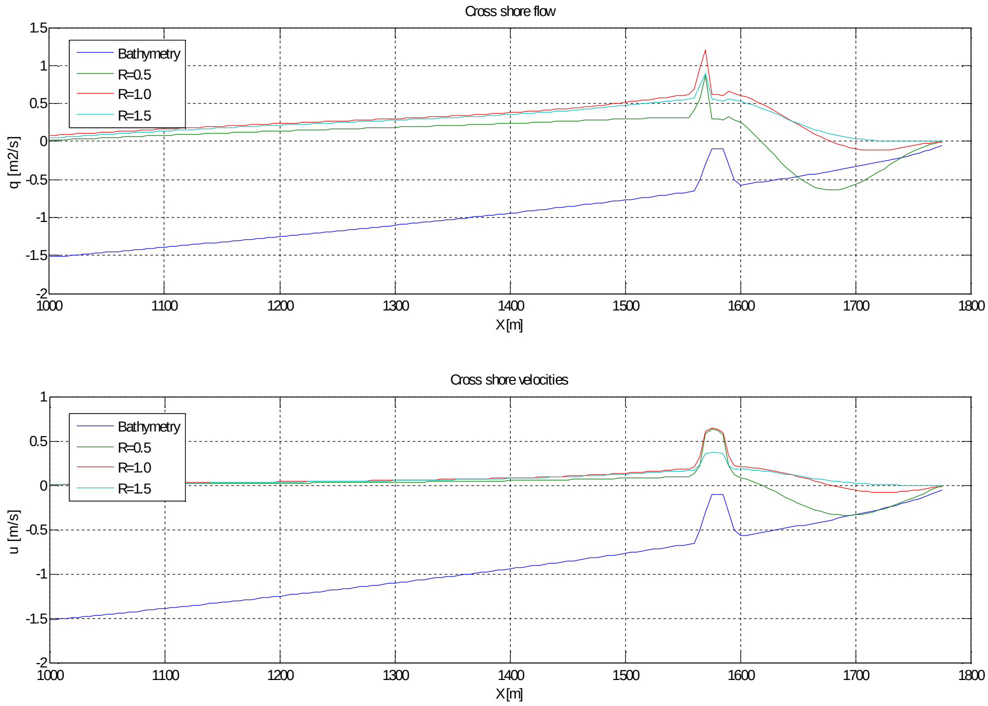


*Figure H.11 Depth averaged flow over the SBW*

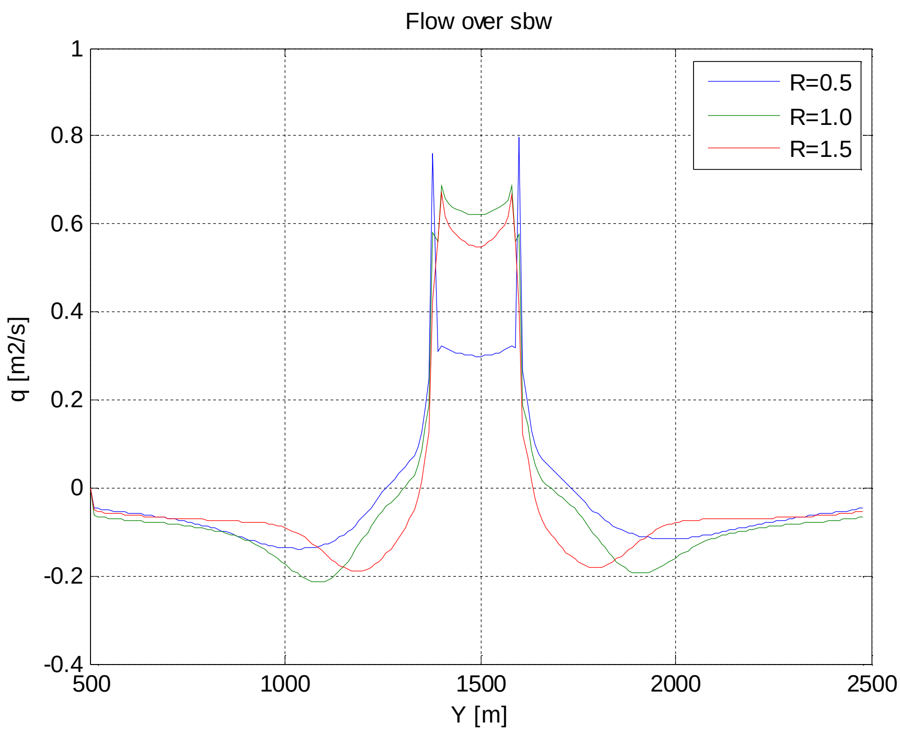

*Figure H.12 Depth averaged flow velocity over SBW*

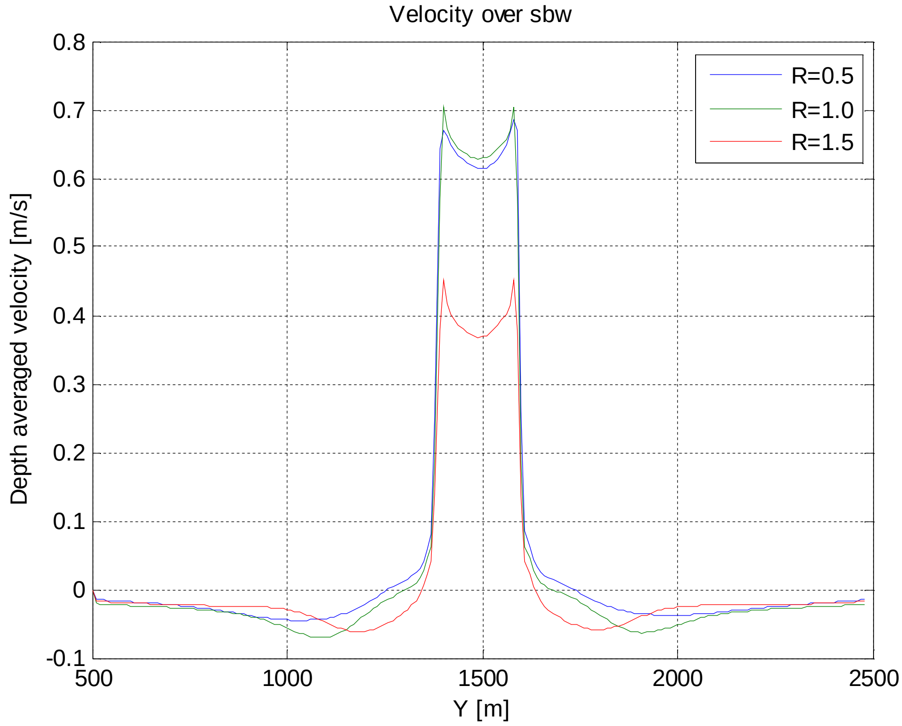


*Figure H.13 Water level set-up over SBW*

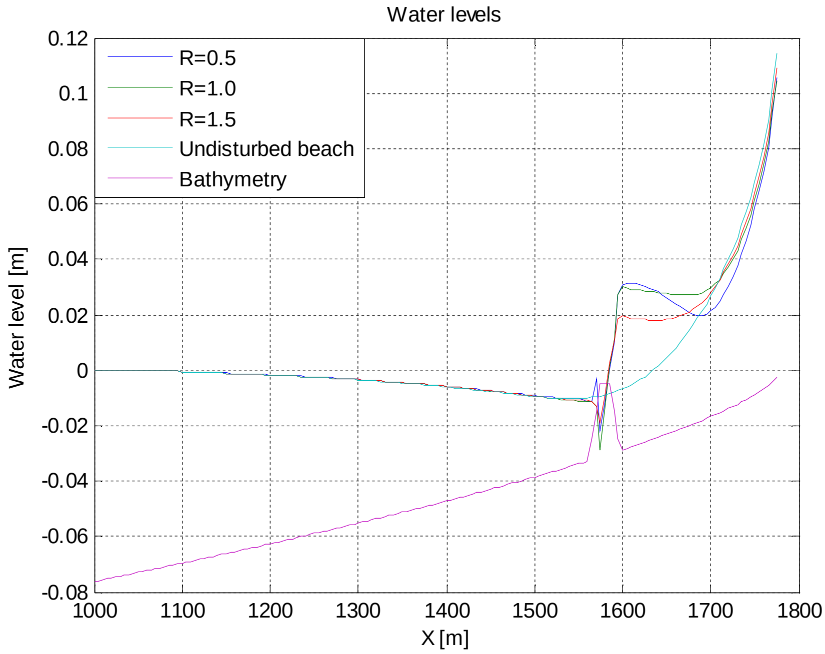

*Figure H.14 Wave height over the SBW*

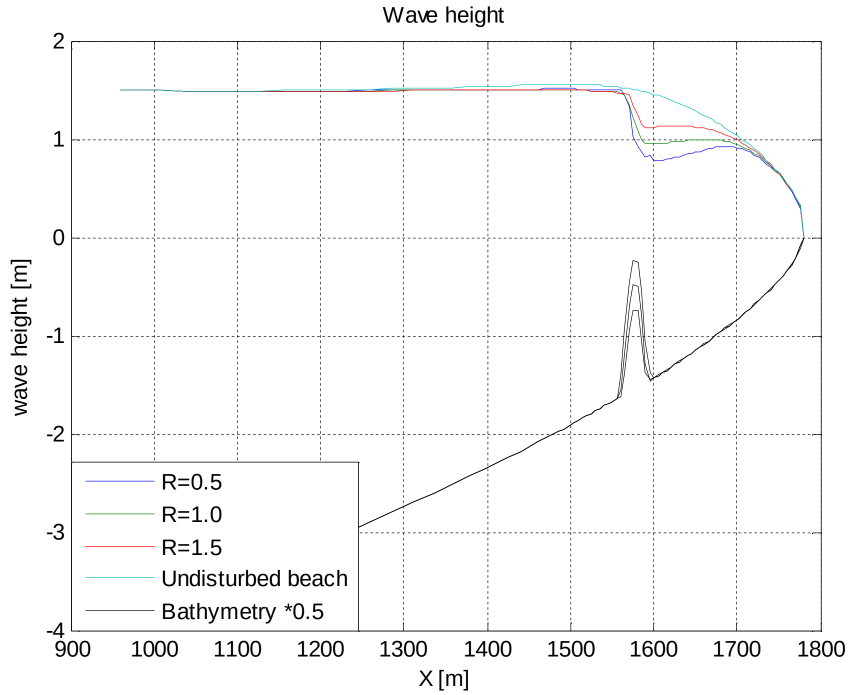

## H.4 Crest width

*Figure H.15 Cross-shore flow (velocities) over SBW*

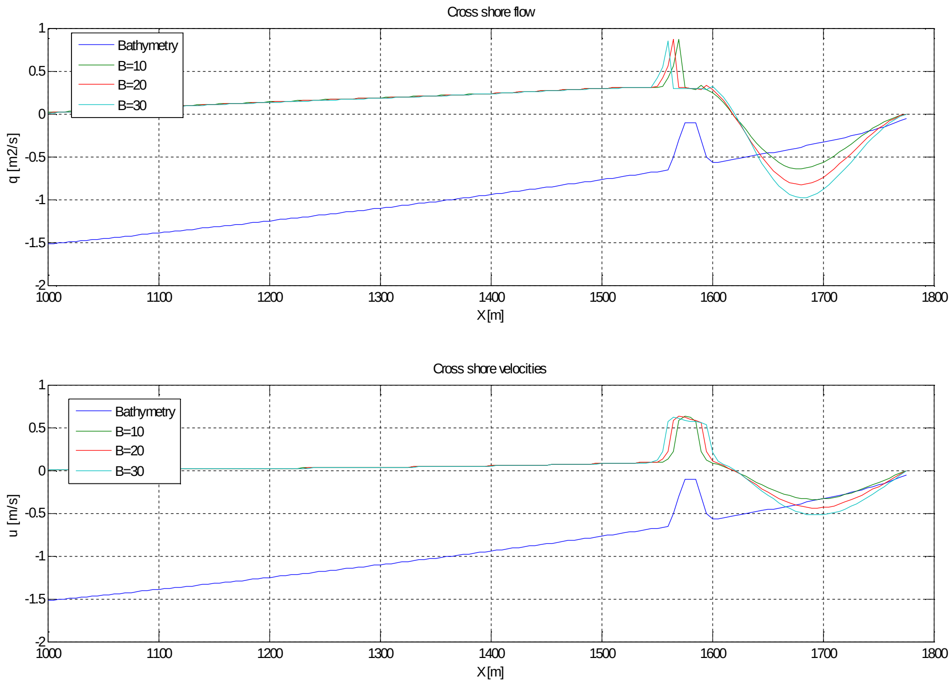


*Figure H.16 Depth averaged flow over SBW*

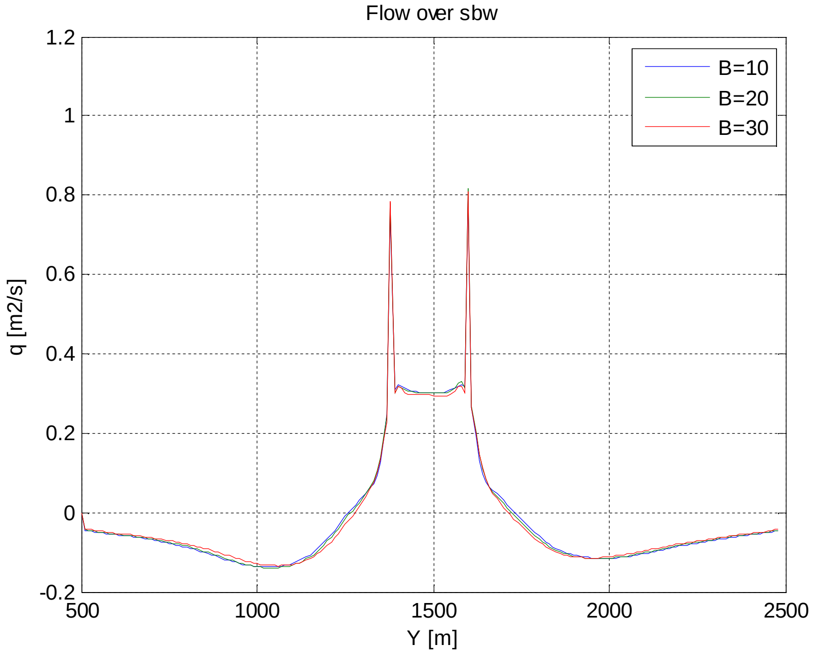

*Figure H.17 Depth averaged velocity over SBW*

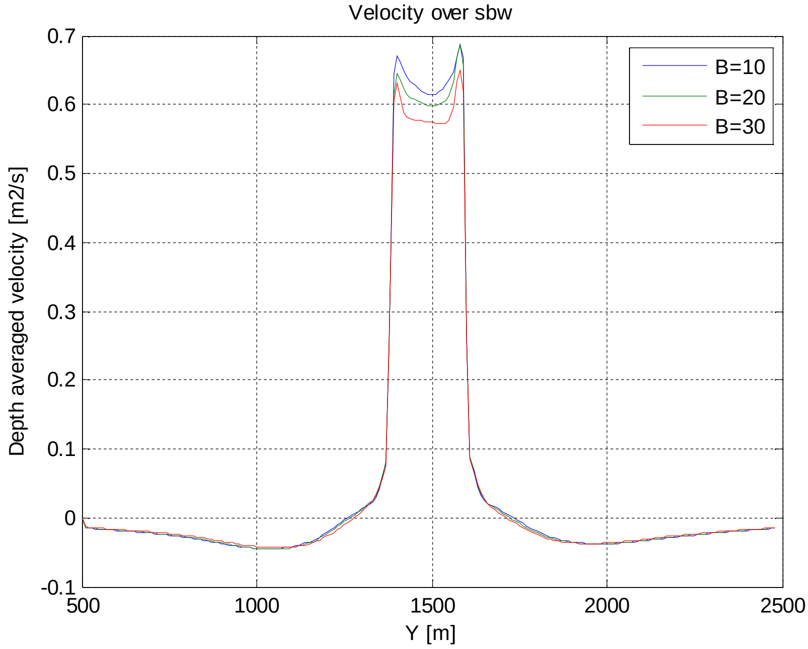


*Figure H.18 Water level set-up over the SBW*

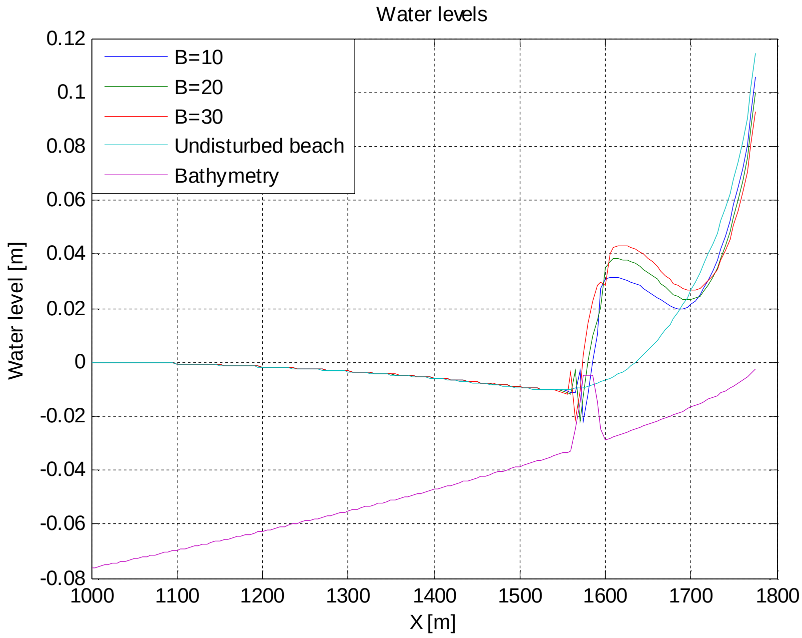

*Figure H.19  wave height over the SBW*

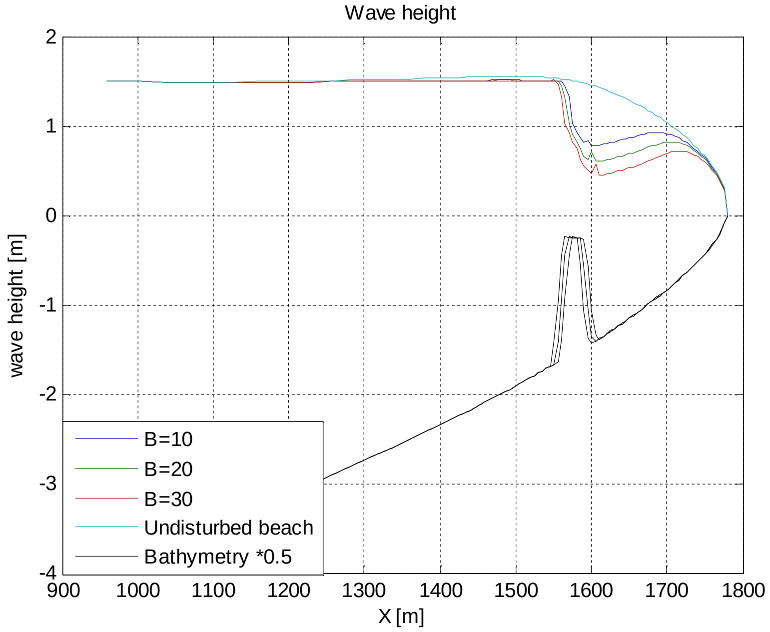

## H.5 Wave height

*Figure H.20 Cross-shore flow (velocities) over SBW*

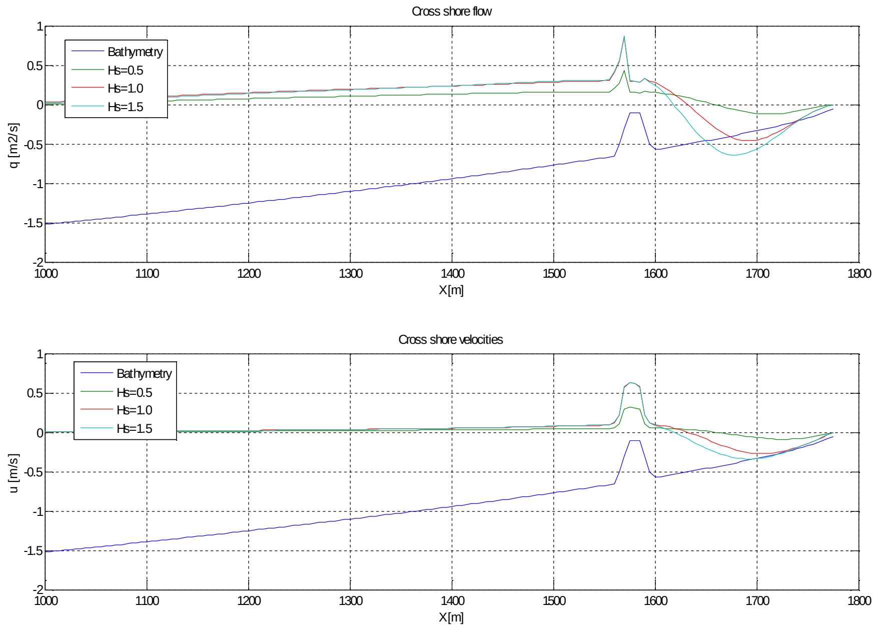


*Figure H.21 Depth averaged flow over SBW*

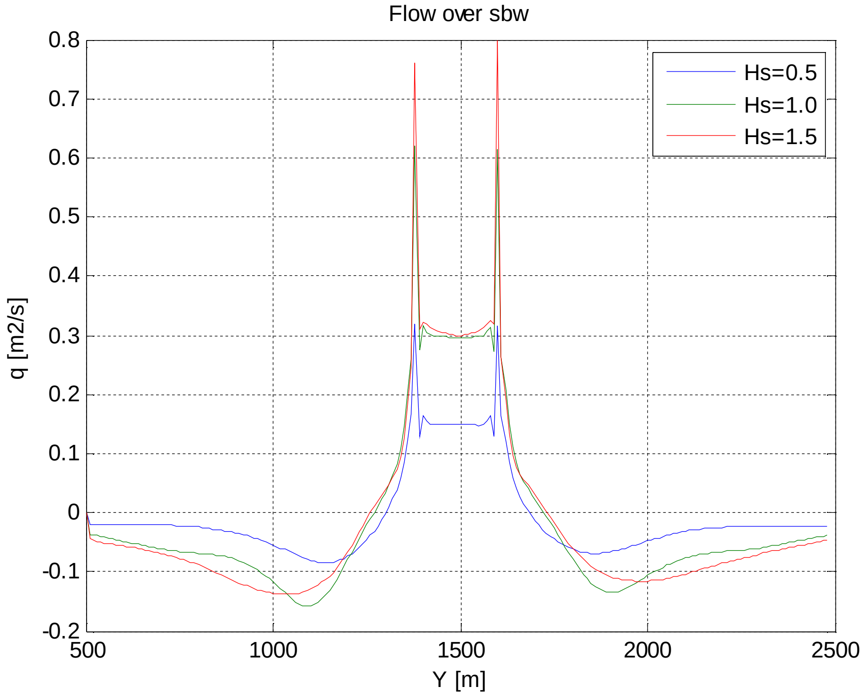

*Figure H.22 Depth averaged velocity over SBW*

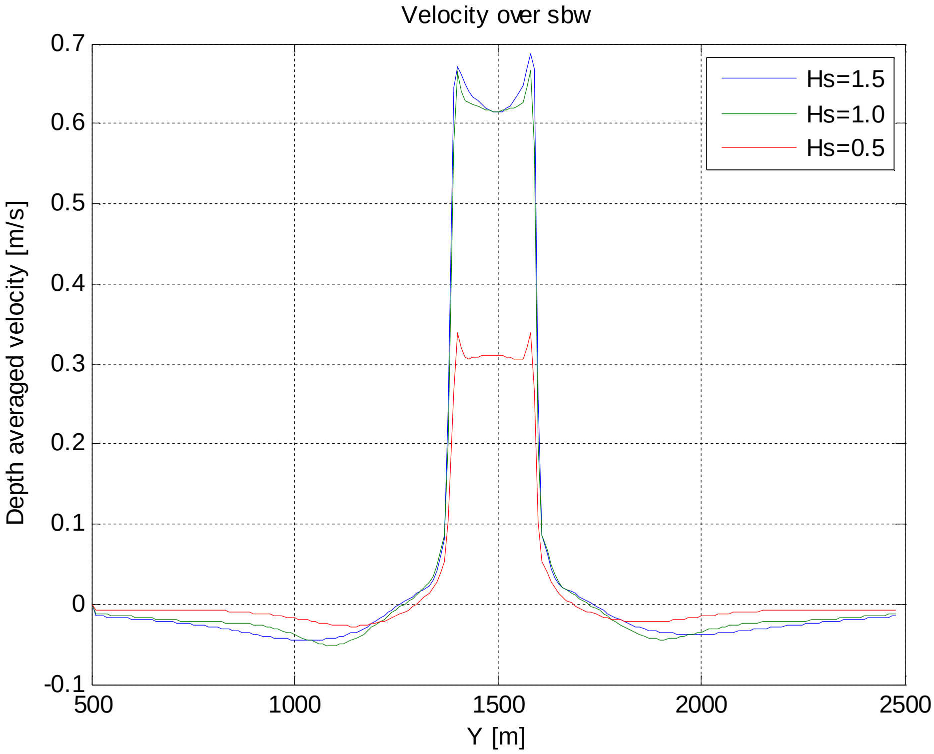


*Figure H.23 Wave height over SBW*

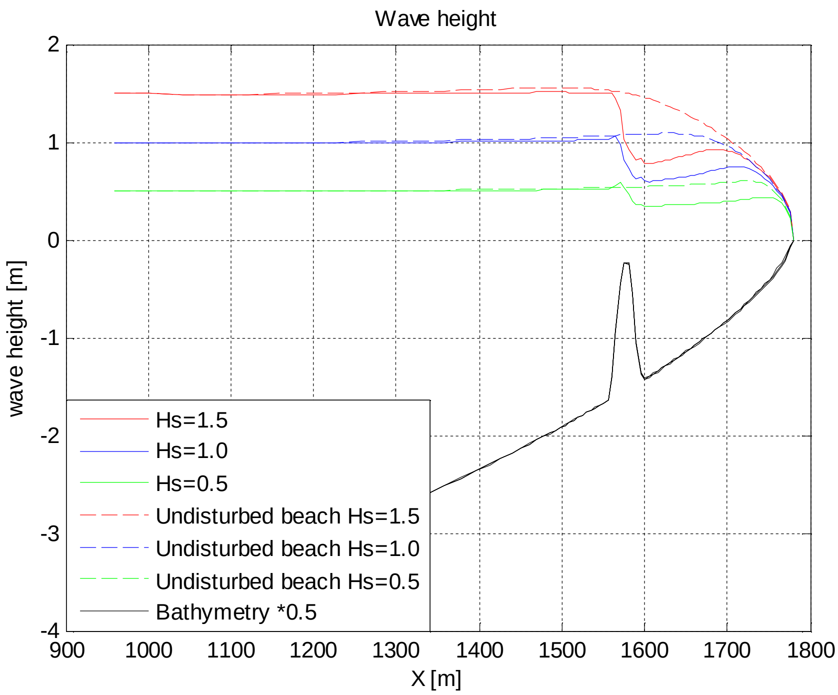

*Figure H.24 Water levels over SBW*

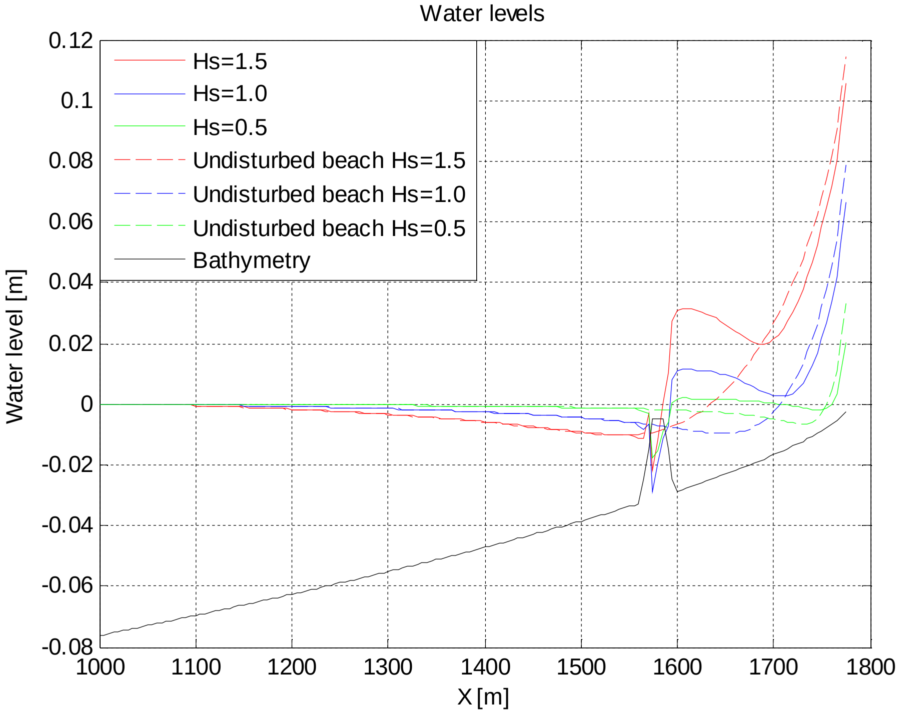

# I Hydrodynamic and morphological results

*Figure I.1 Hydrodynamic and morphological results xb=50m, Lb=100m*

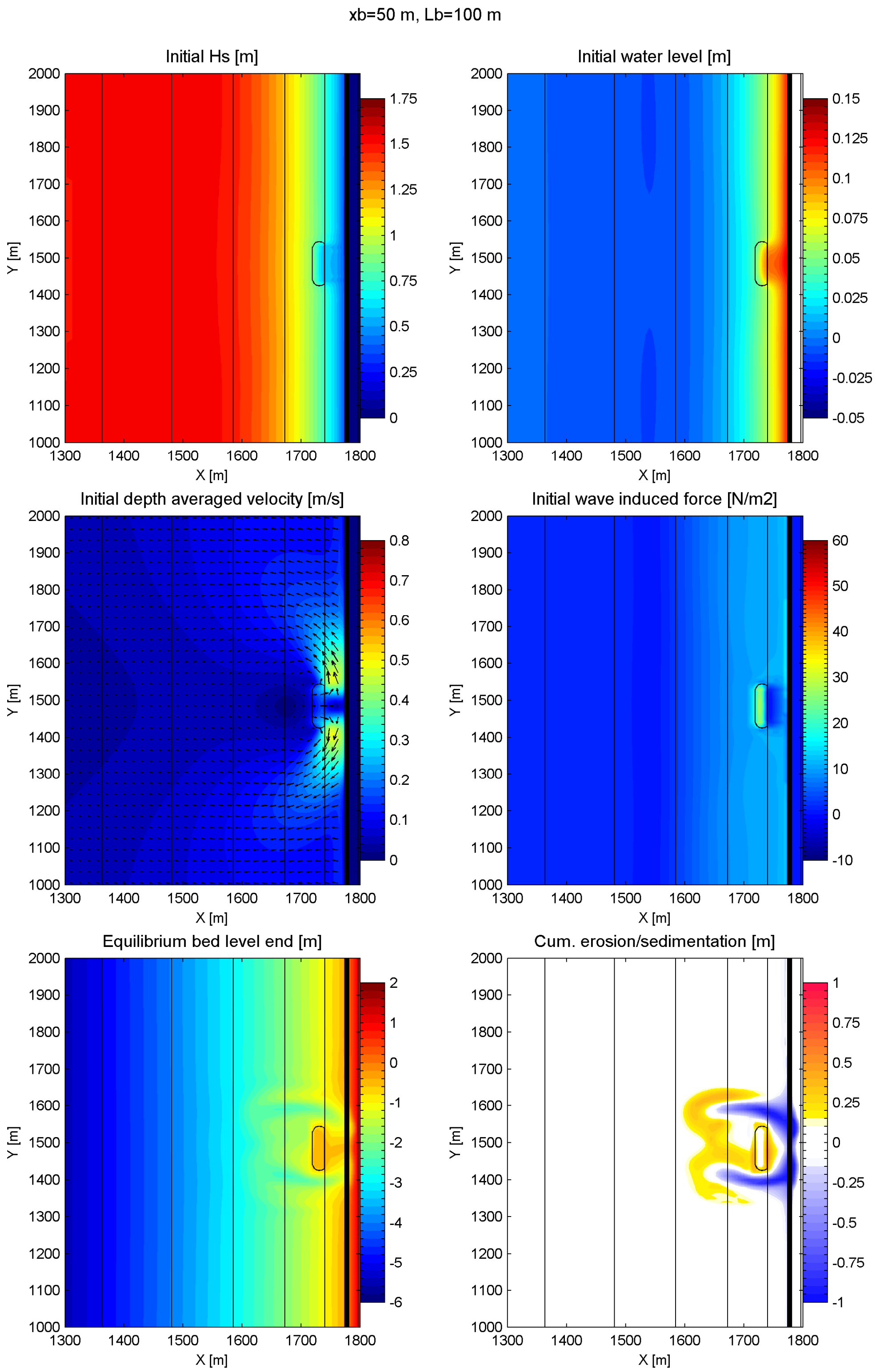

*Figure I.2 Hydrodynamic and morphological results xb=100m, Lb=100m*

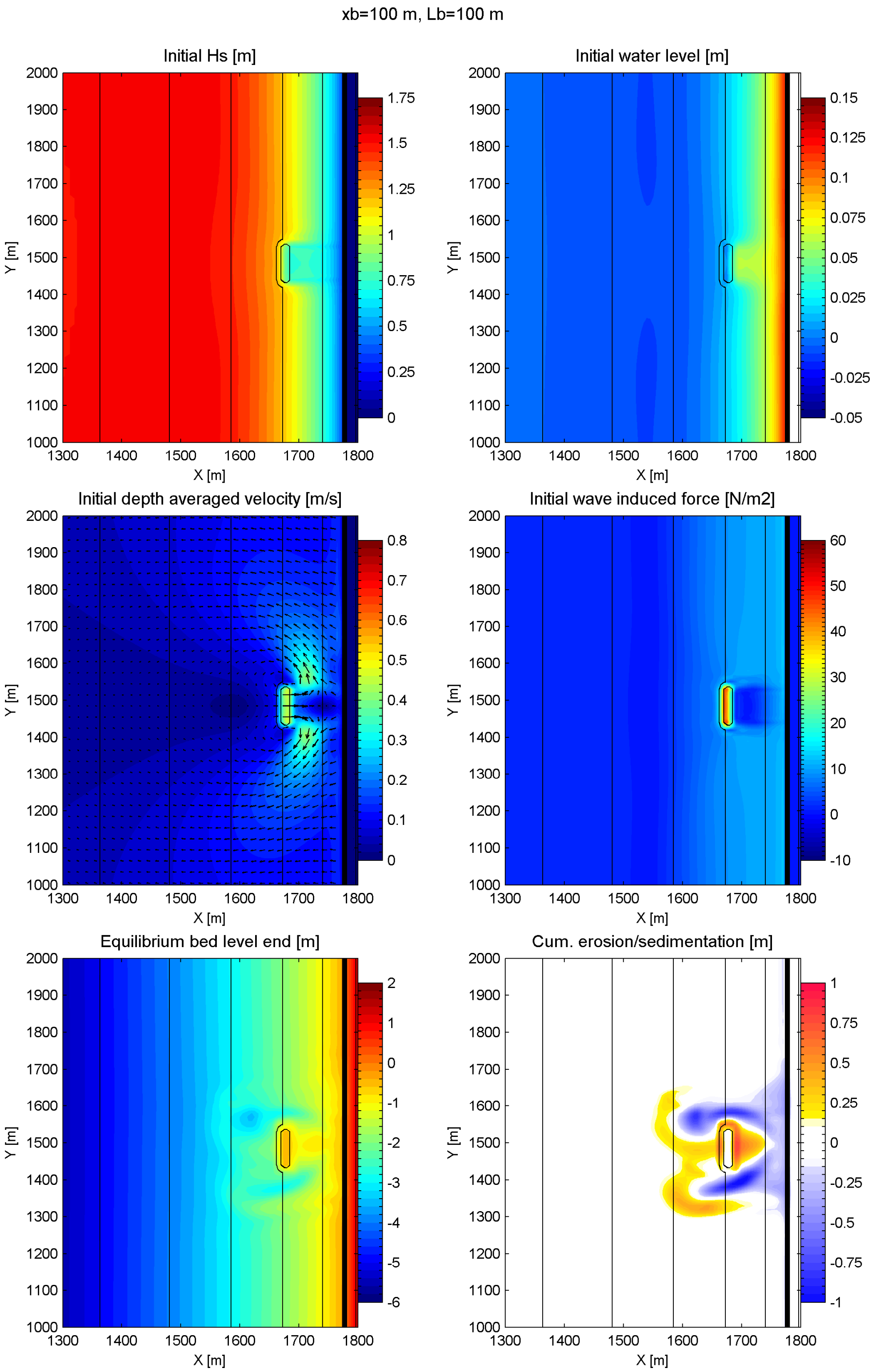

*Figure I.3 Hydrodynamic and morphological results xb=150m, Lb=100m*

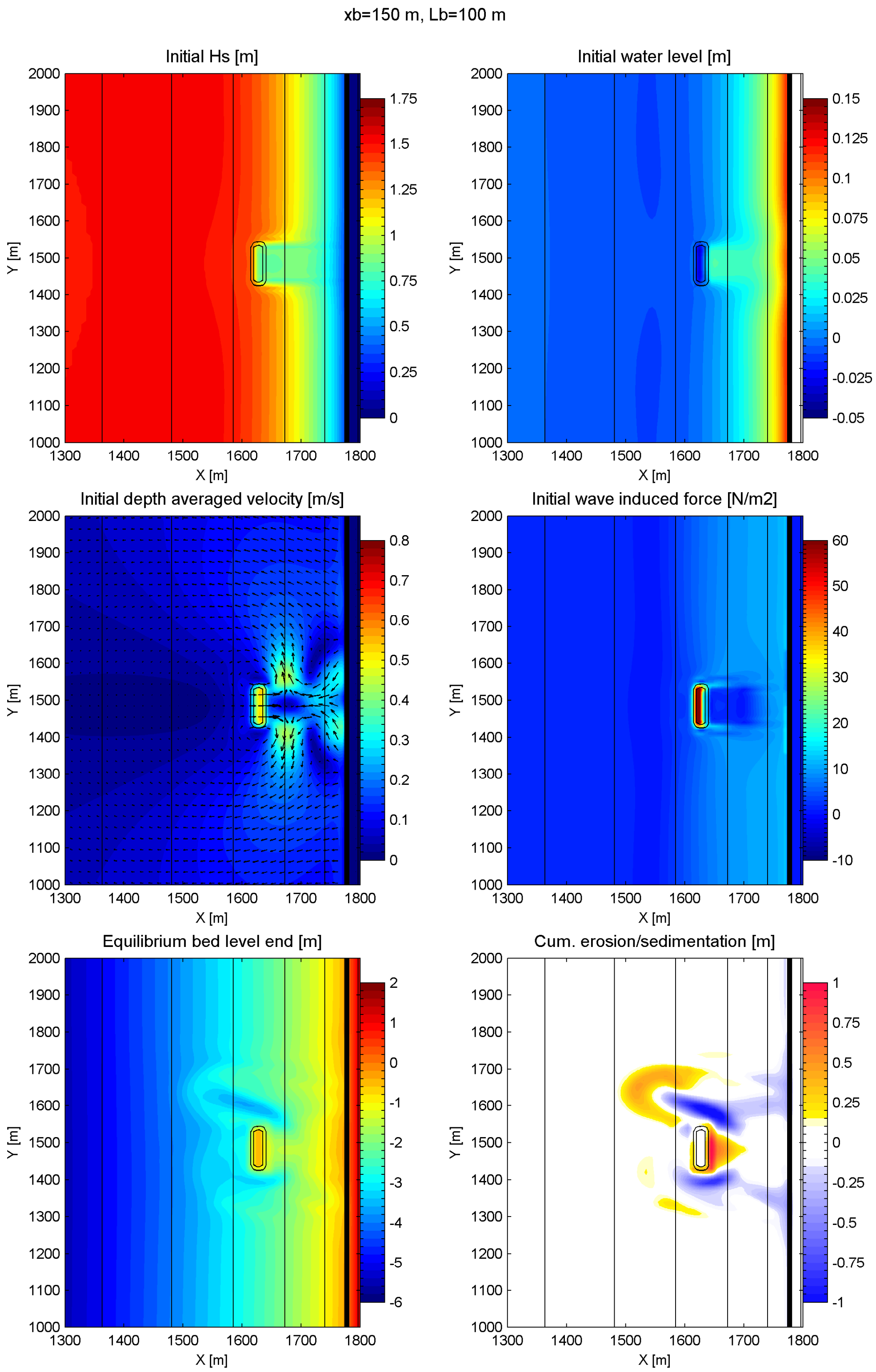

*Figure I.4 Hydrodynamic and morphological results xb=200m, Lb=100m*

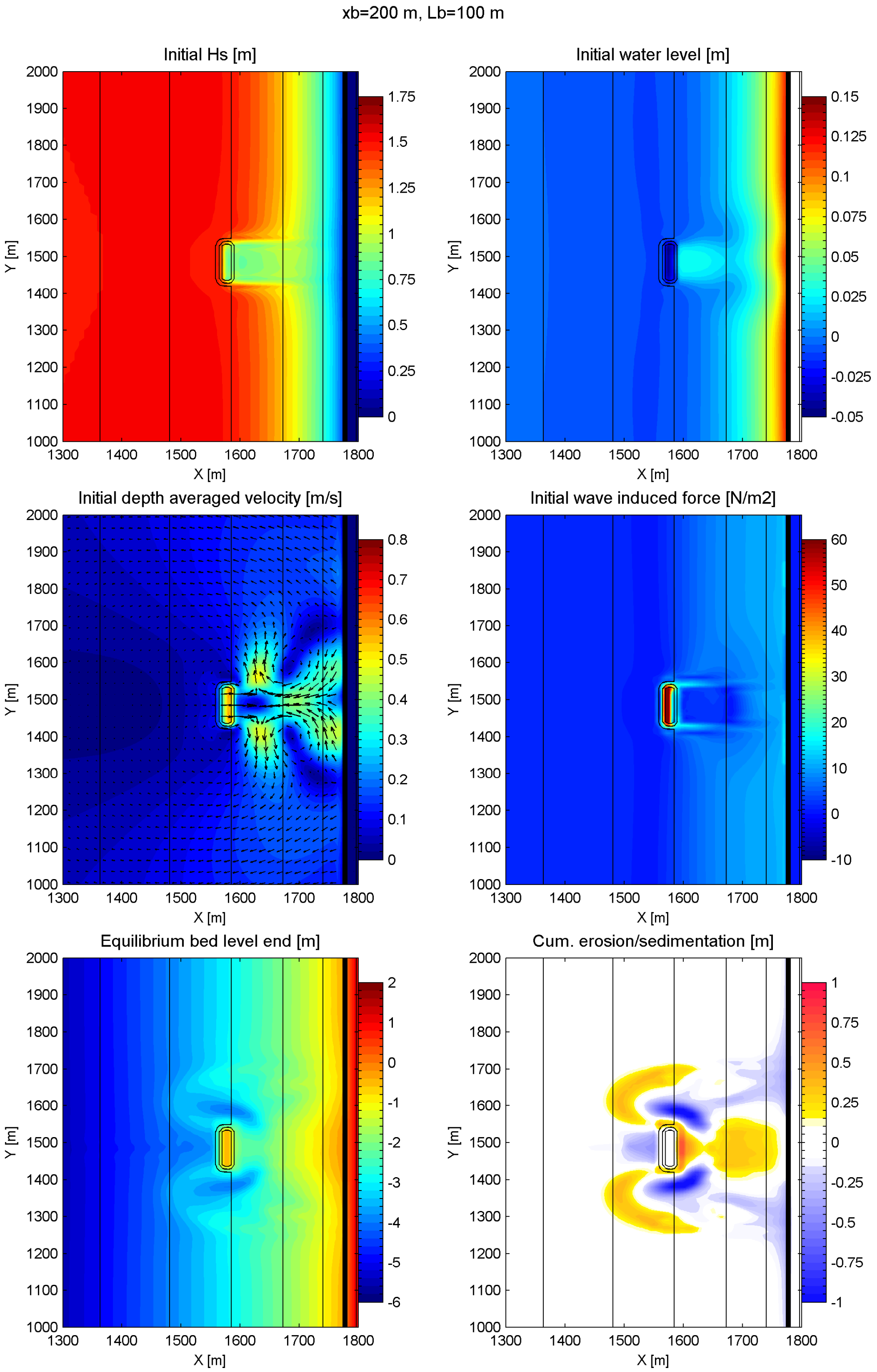

*Figure I.5 Hydrodynamic and morphological results xb=300m, Lb=100m*

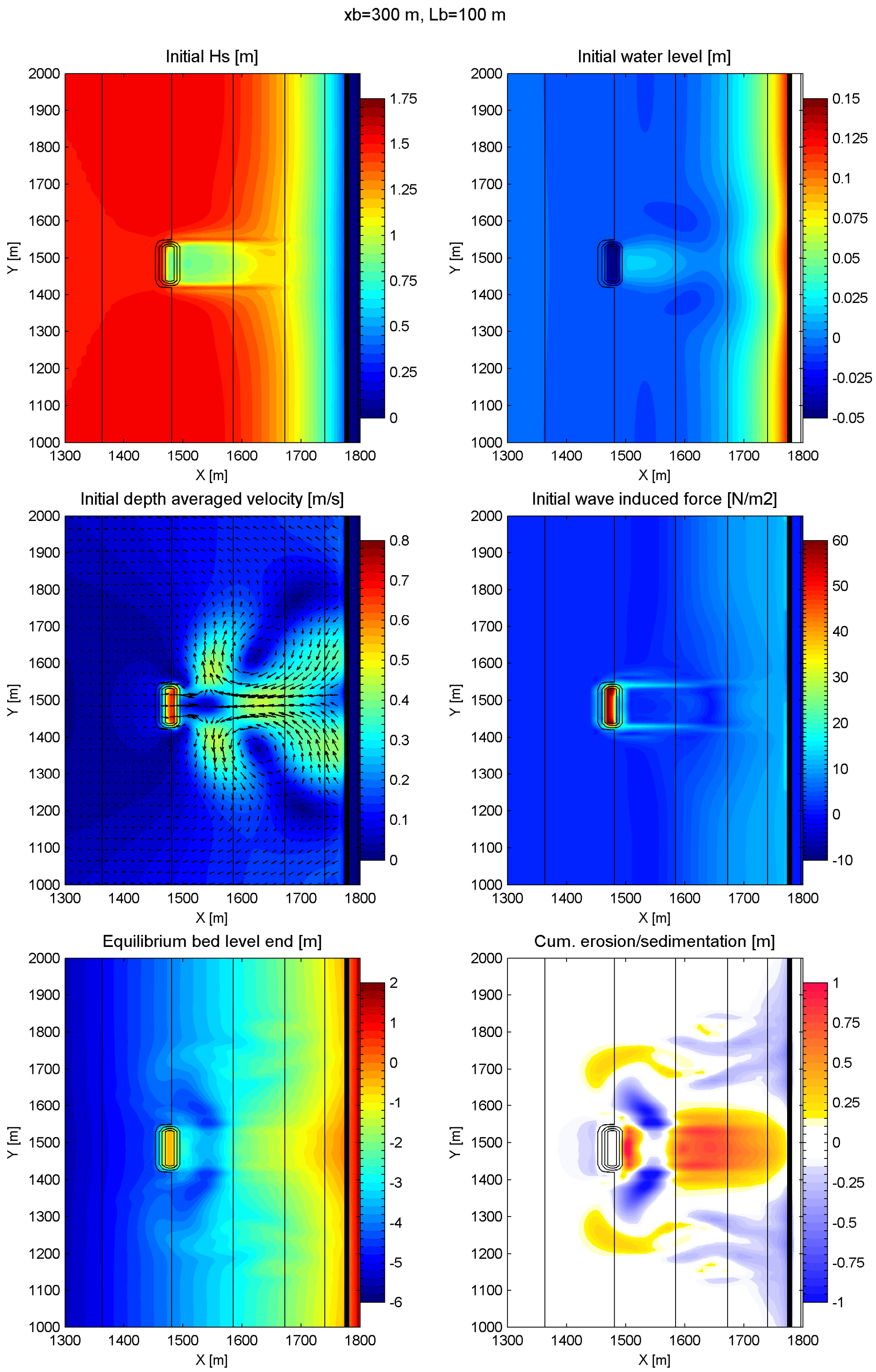

*Figure I.6 Hydrodynamic and morphological results xb=400m, Lb=100m*

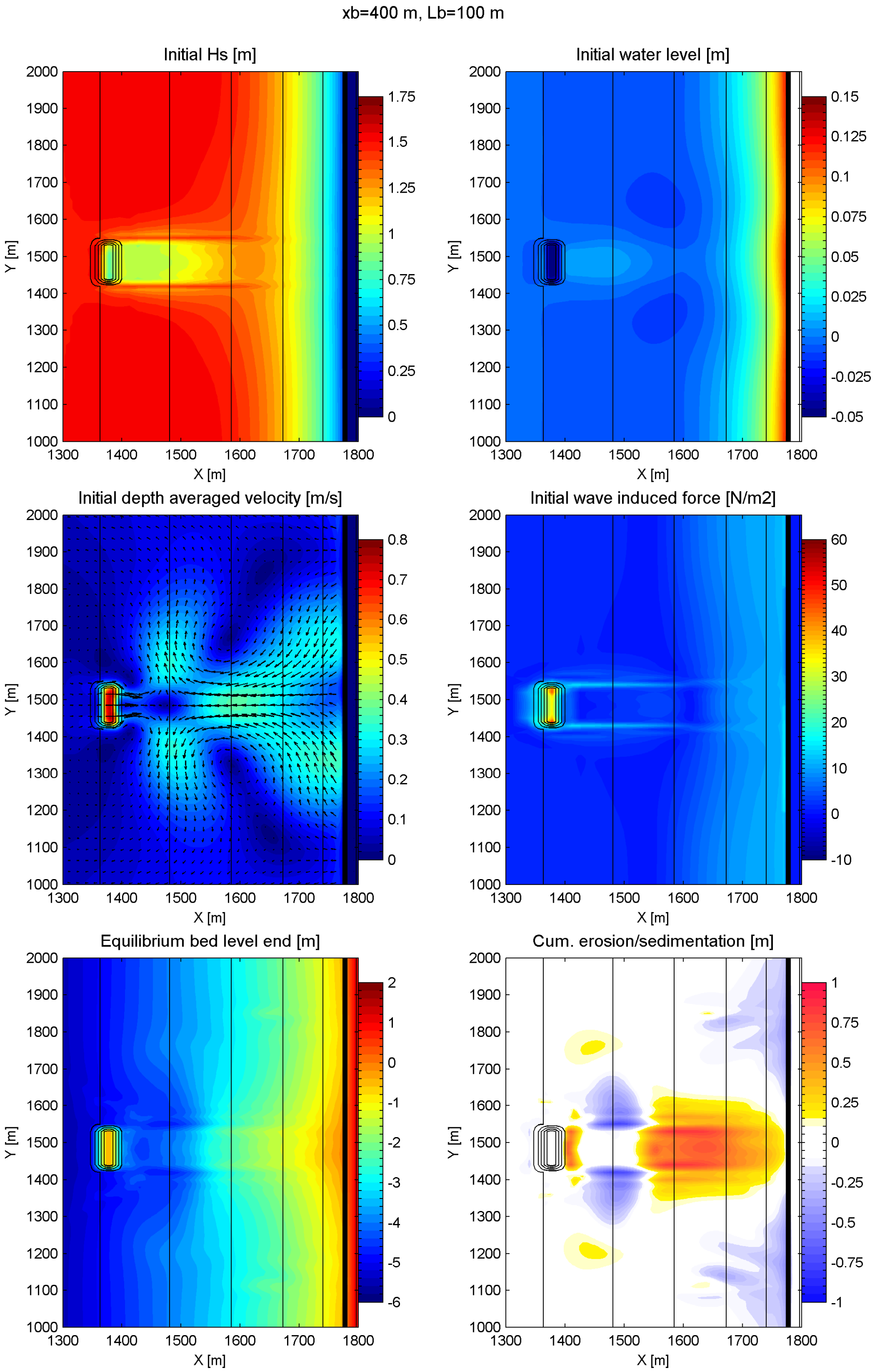

*Figure I.7 Hydrodynamic and morphological results xb=50m, Lb=200m*

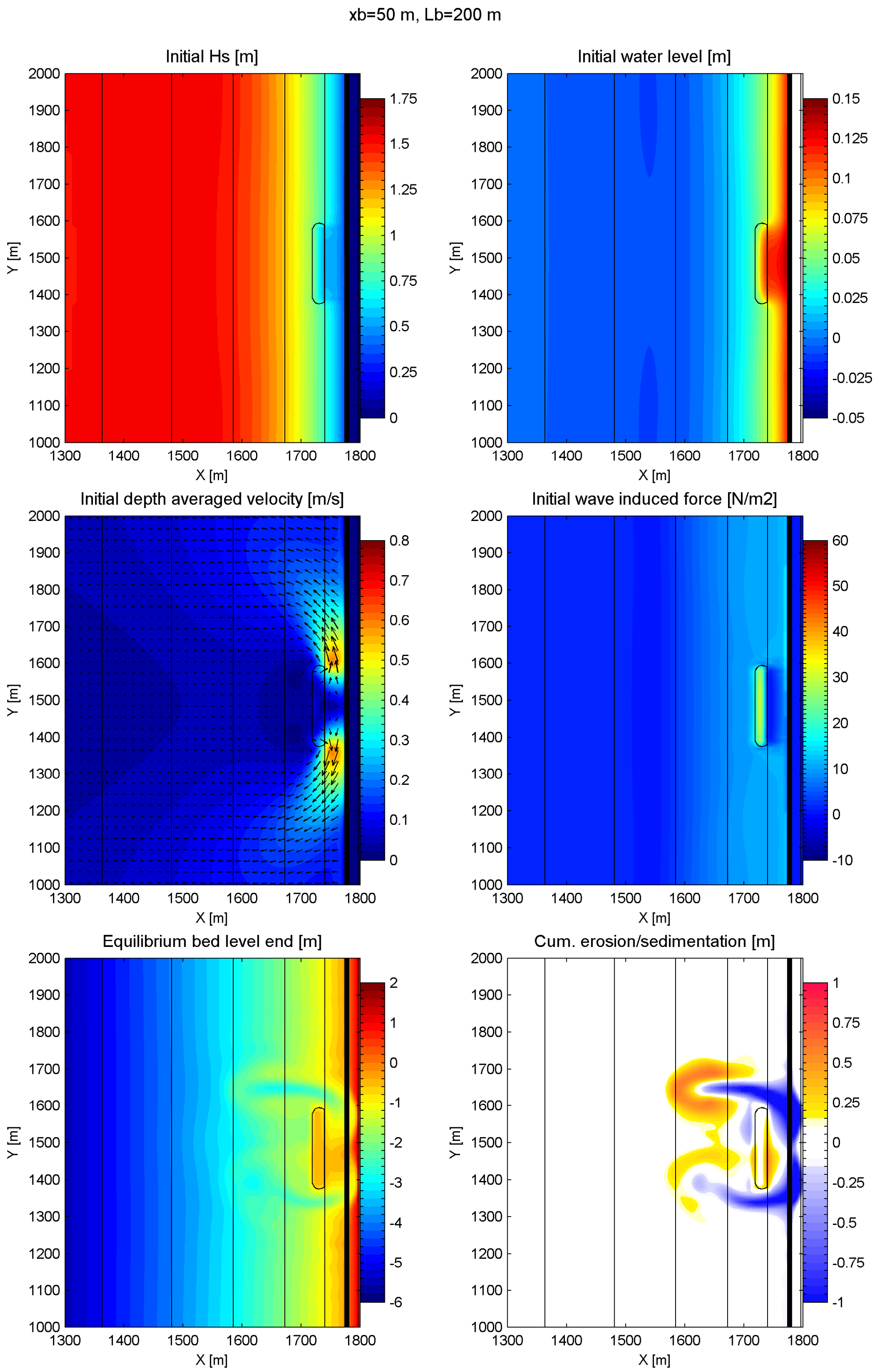

*Figure I.8 Hydrodynamic and morphological results xb=100m, Lb=200m*

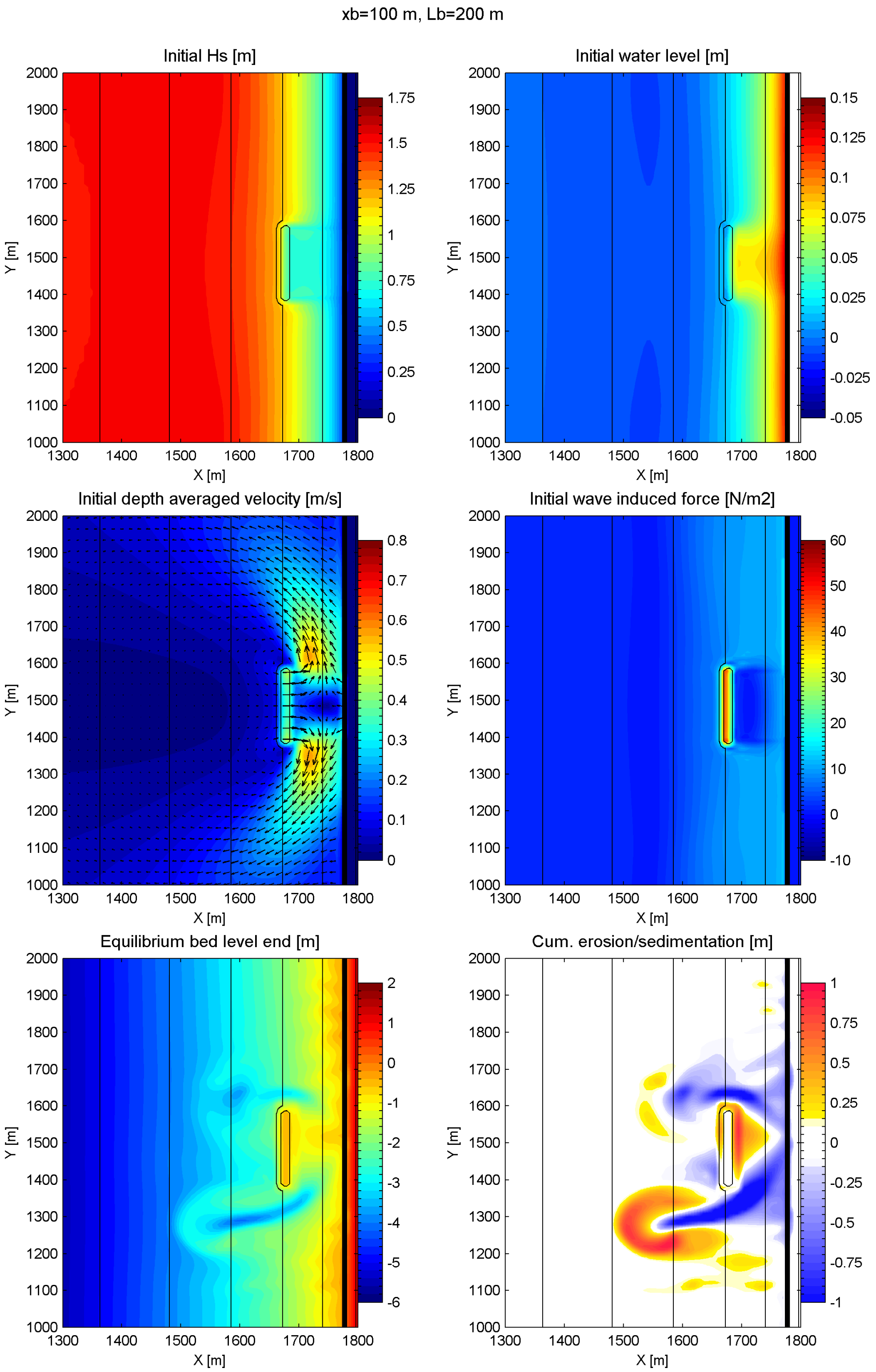

*Figure I.9 Hydrodynamic and morphological results xb=150m, Lb=200m*

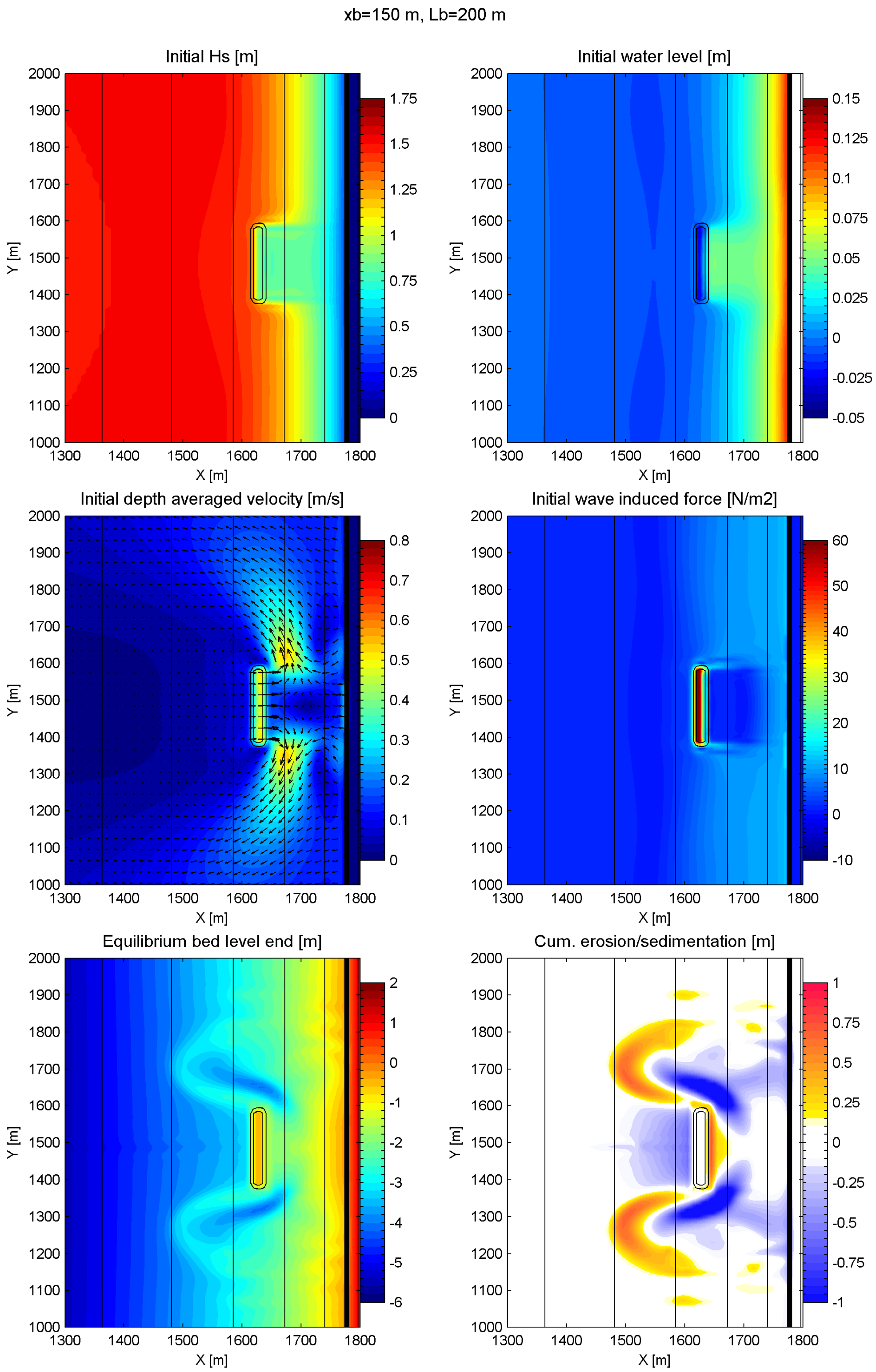

*Figure I.10 Hydrodynamic and morphological results xb=200m, Lb=200m*

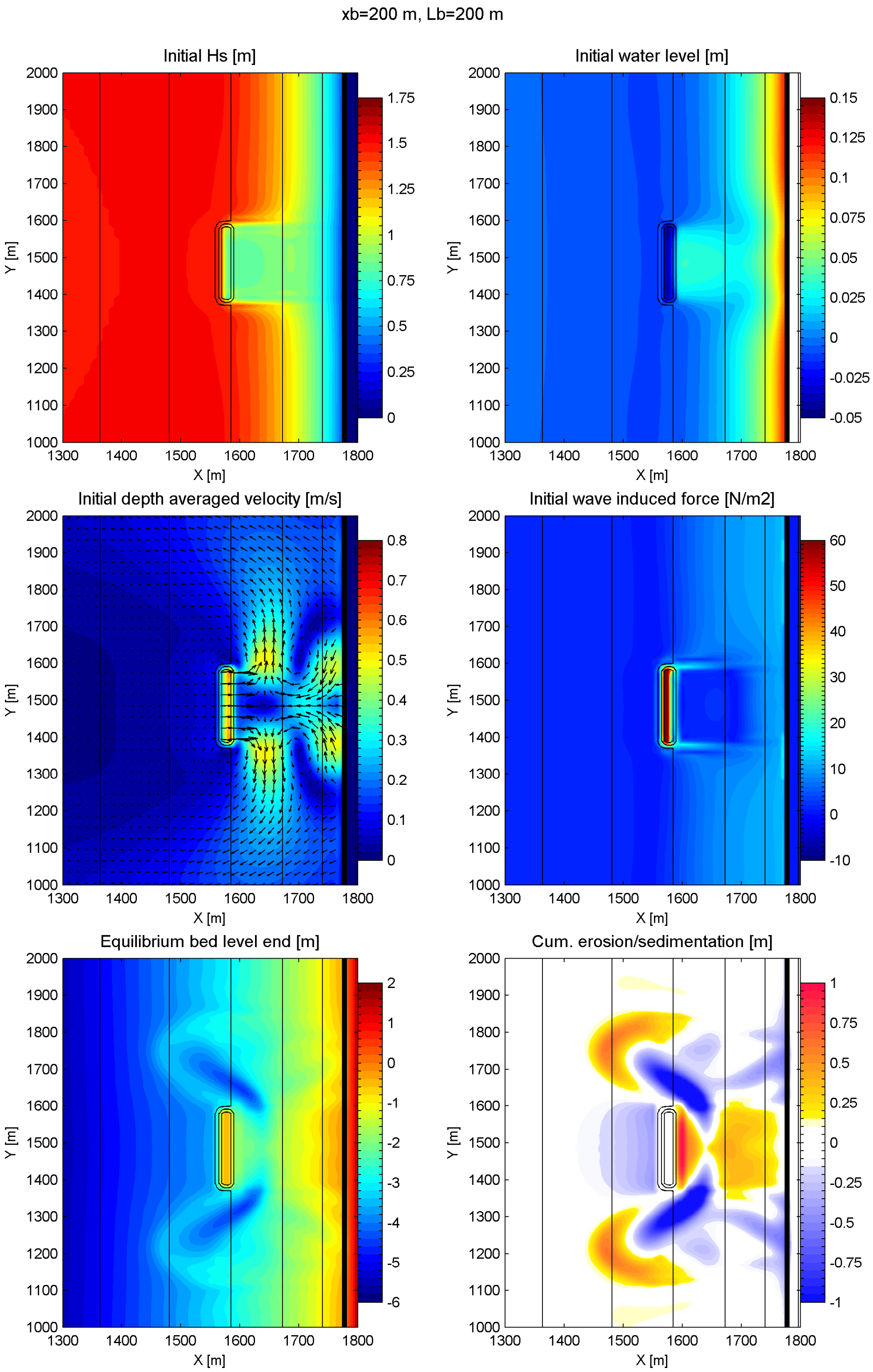

*Figure I.11  Hydrodynamic and morphological results xb=300m, Lb=200m*

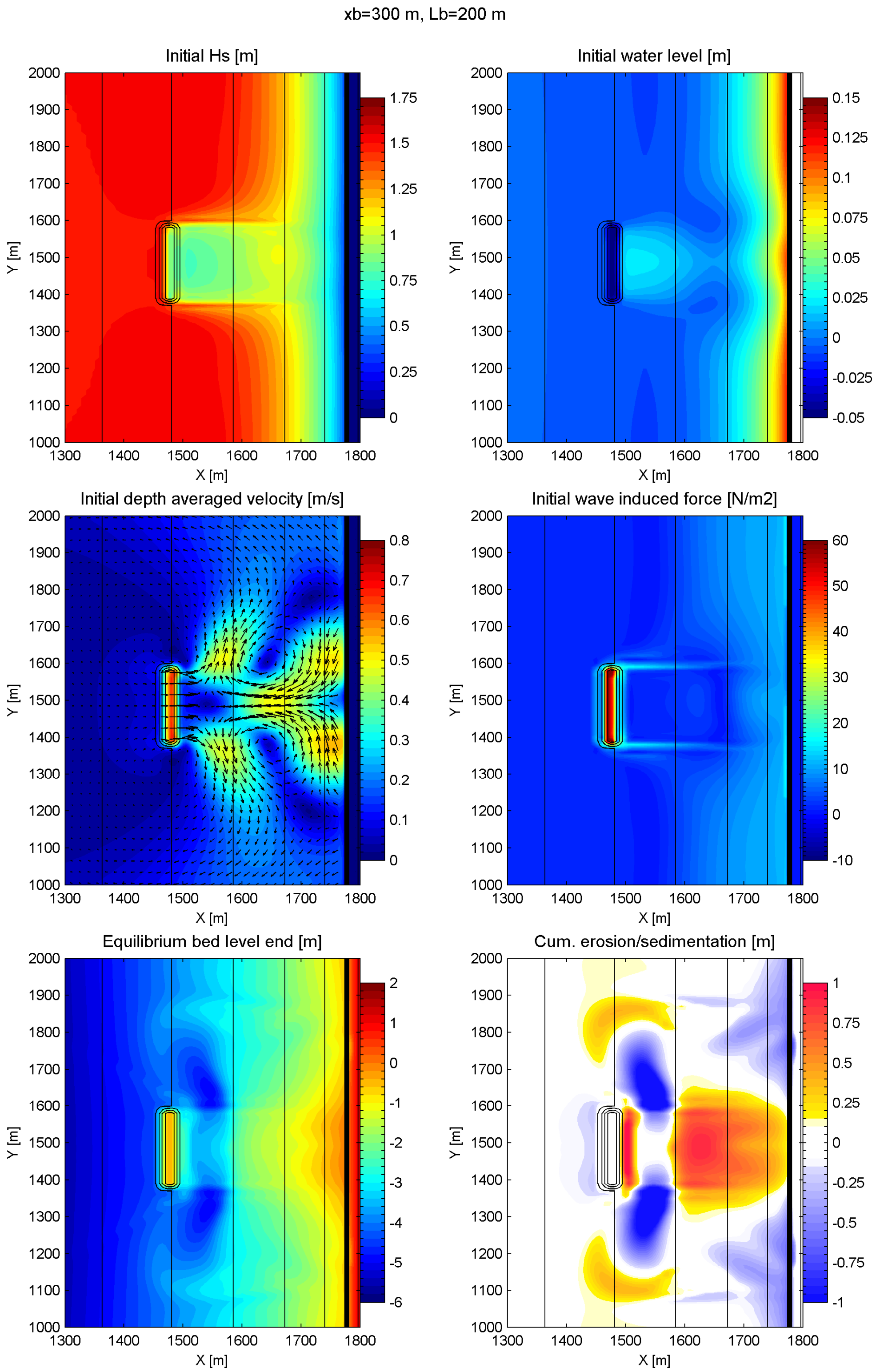

*Figure I.12 Hydrodynamic and morphological results xb=400m, Lb=200m*

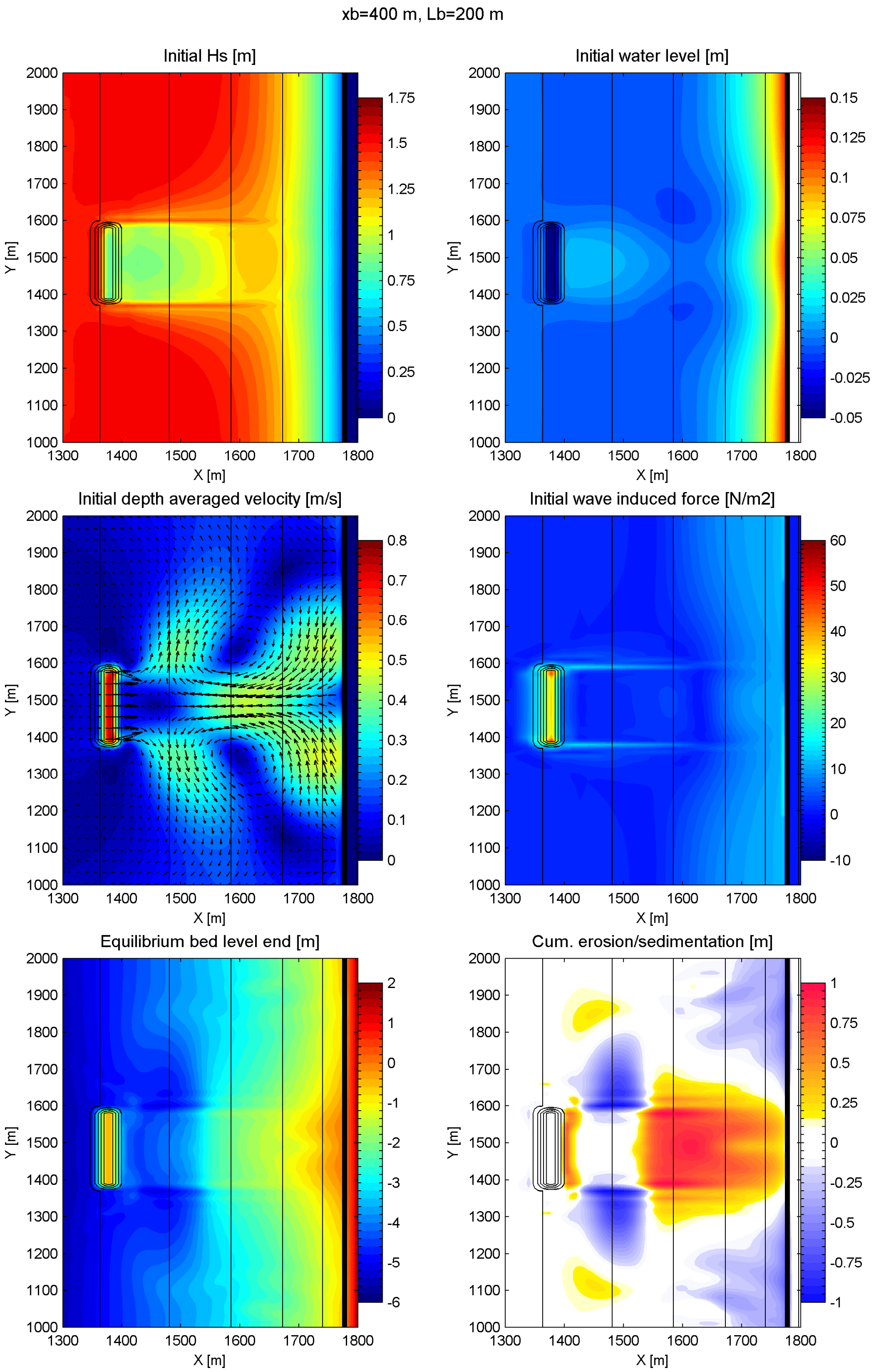

*Figure I.13 Hydrodynamic and morphological results xb=150m, Lb=100m*

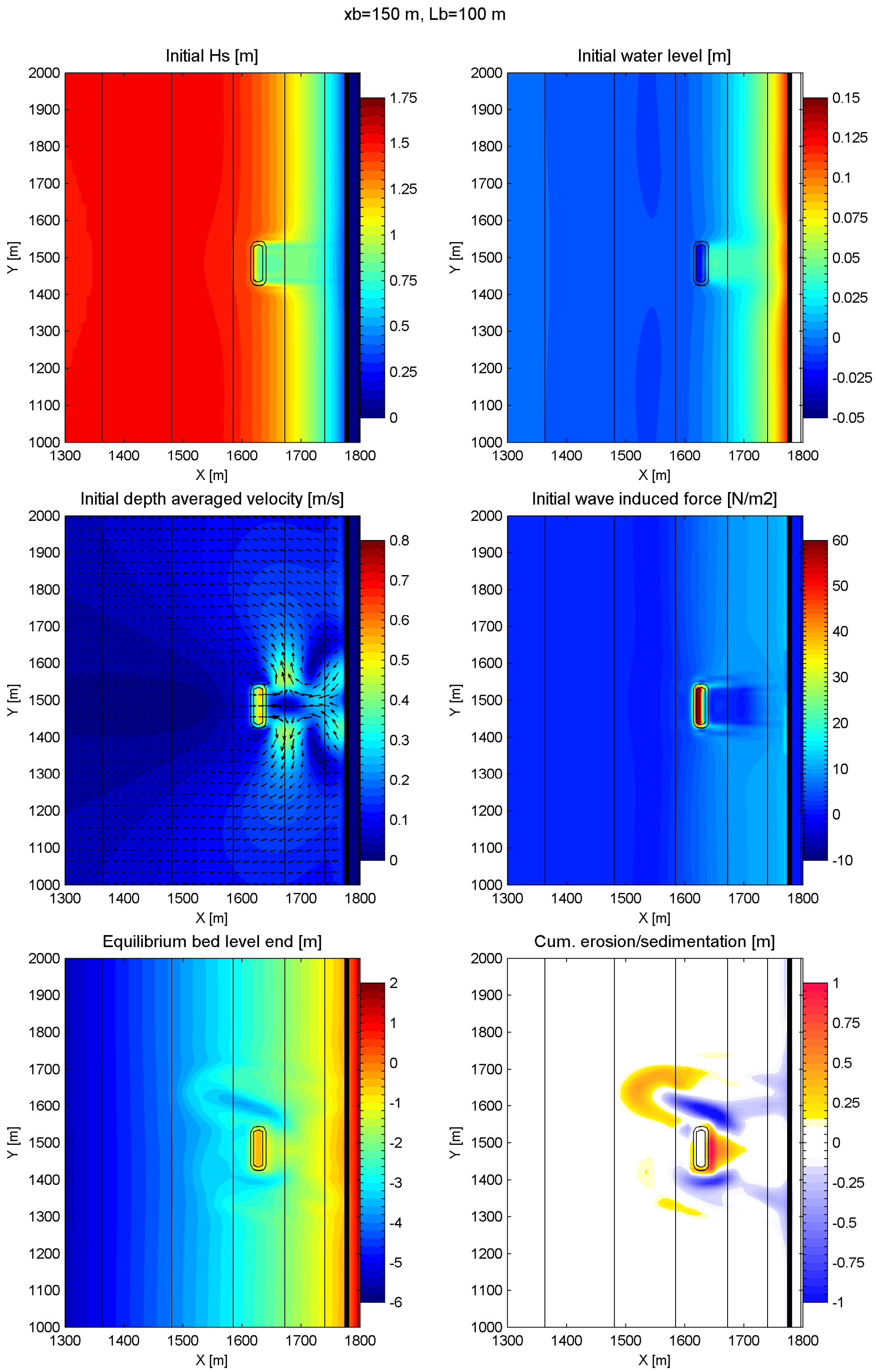

*Figure I.14 Hydrodynamic and morphological results xb=150m, Lb=200m*

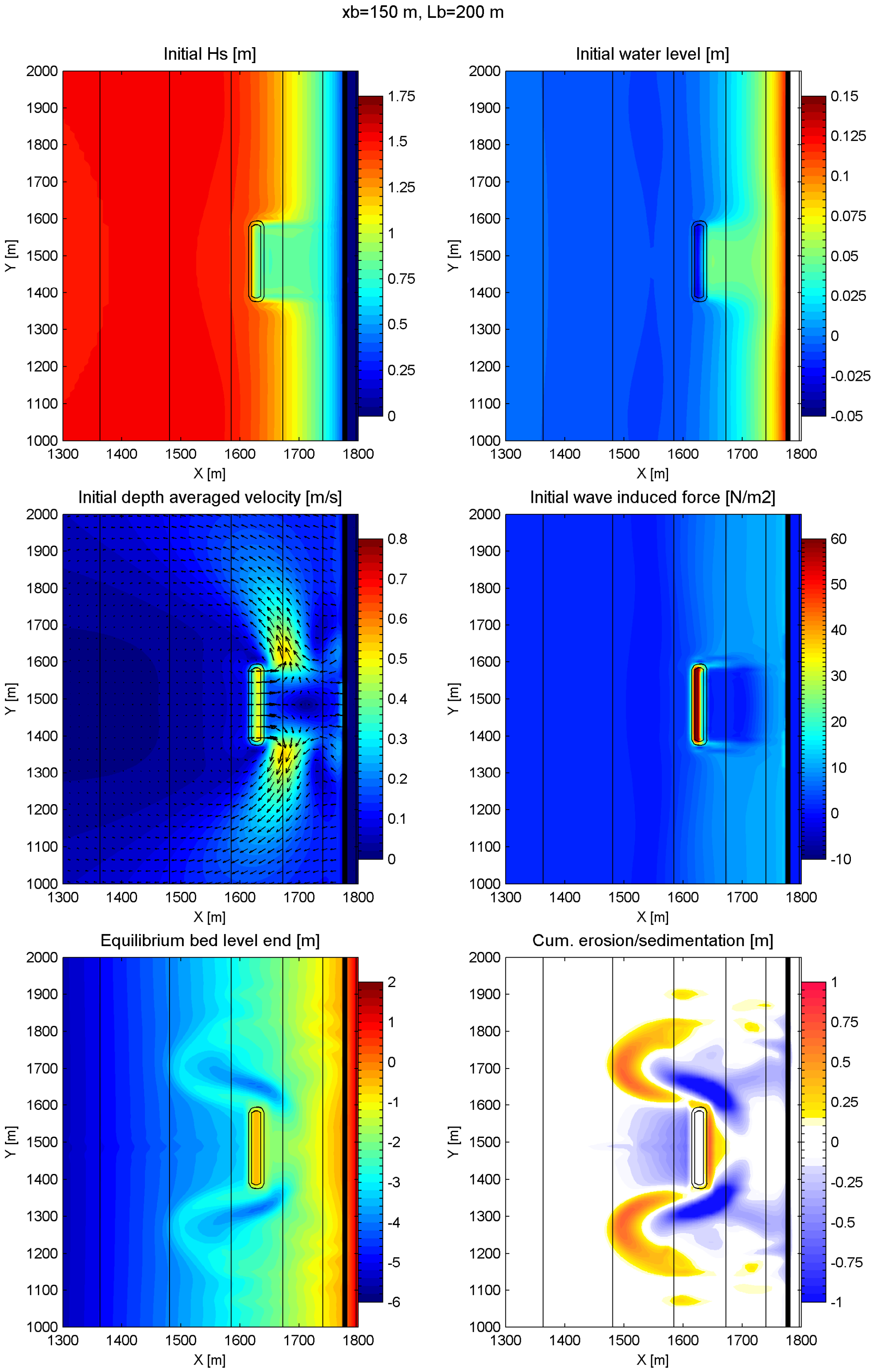

*Figure I.15  Hydrodynamic and morphological results xb=150m, Lb=300m*

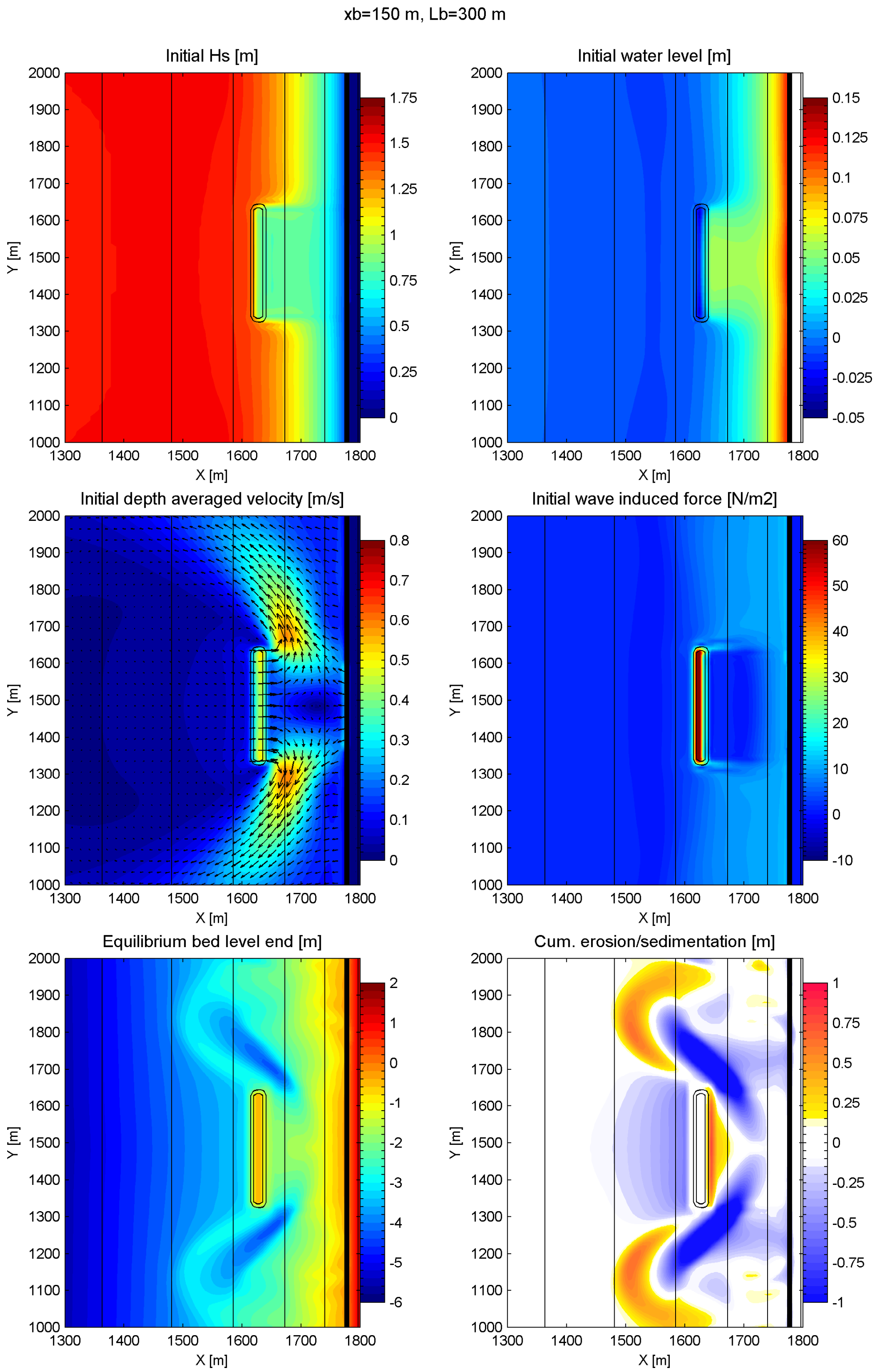

*Figure I.16 Hydrodynamic and morphological results xb=150m, Lb=400m*

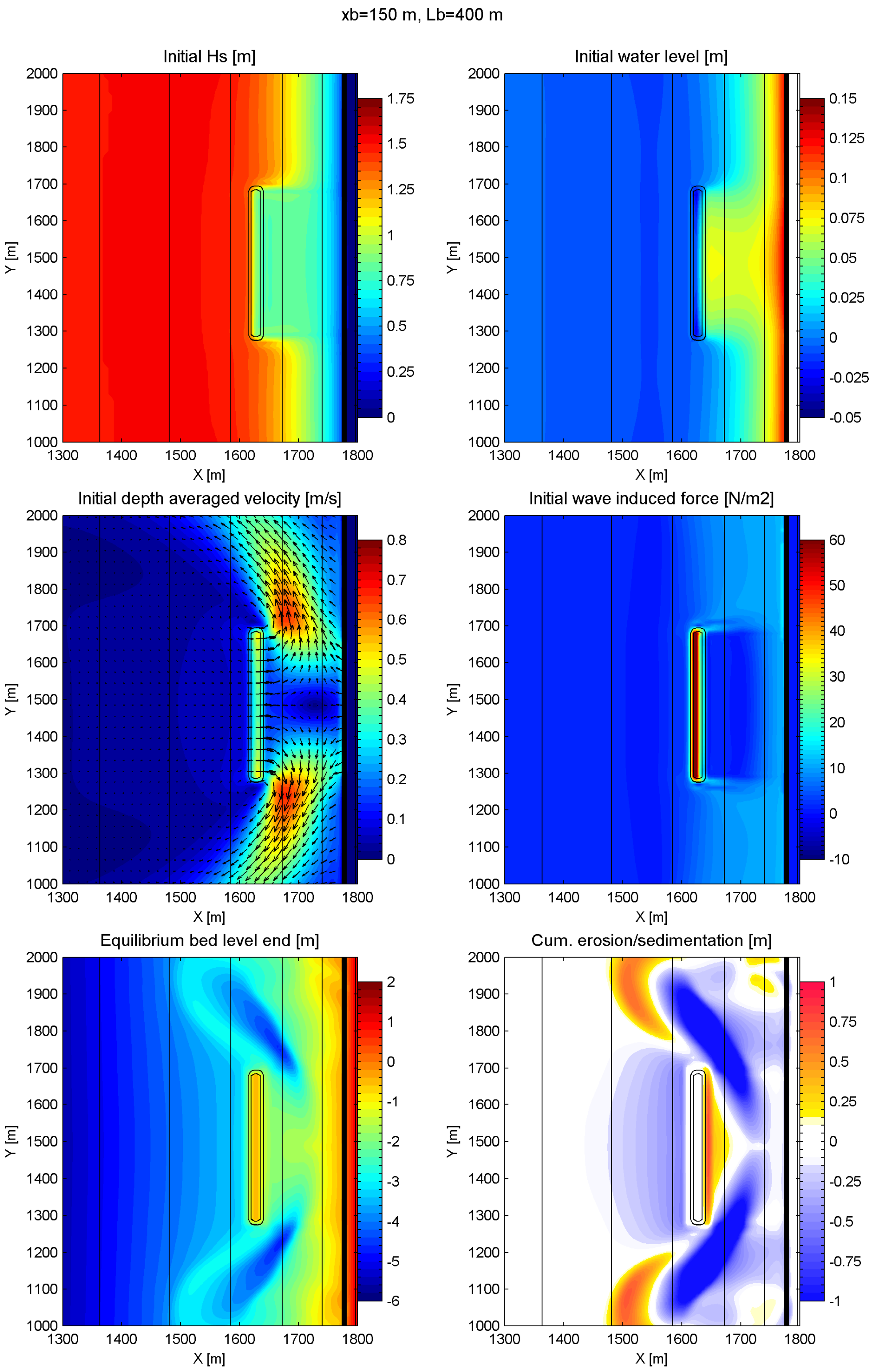

*Figure I.17 Hydrodynamic and morphological results xb=150m, Lb=500m*

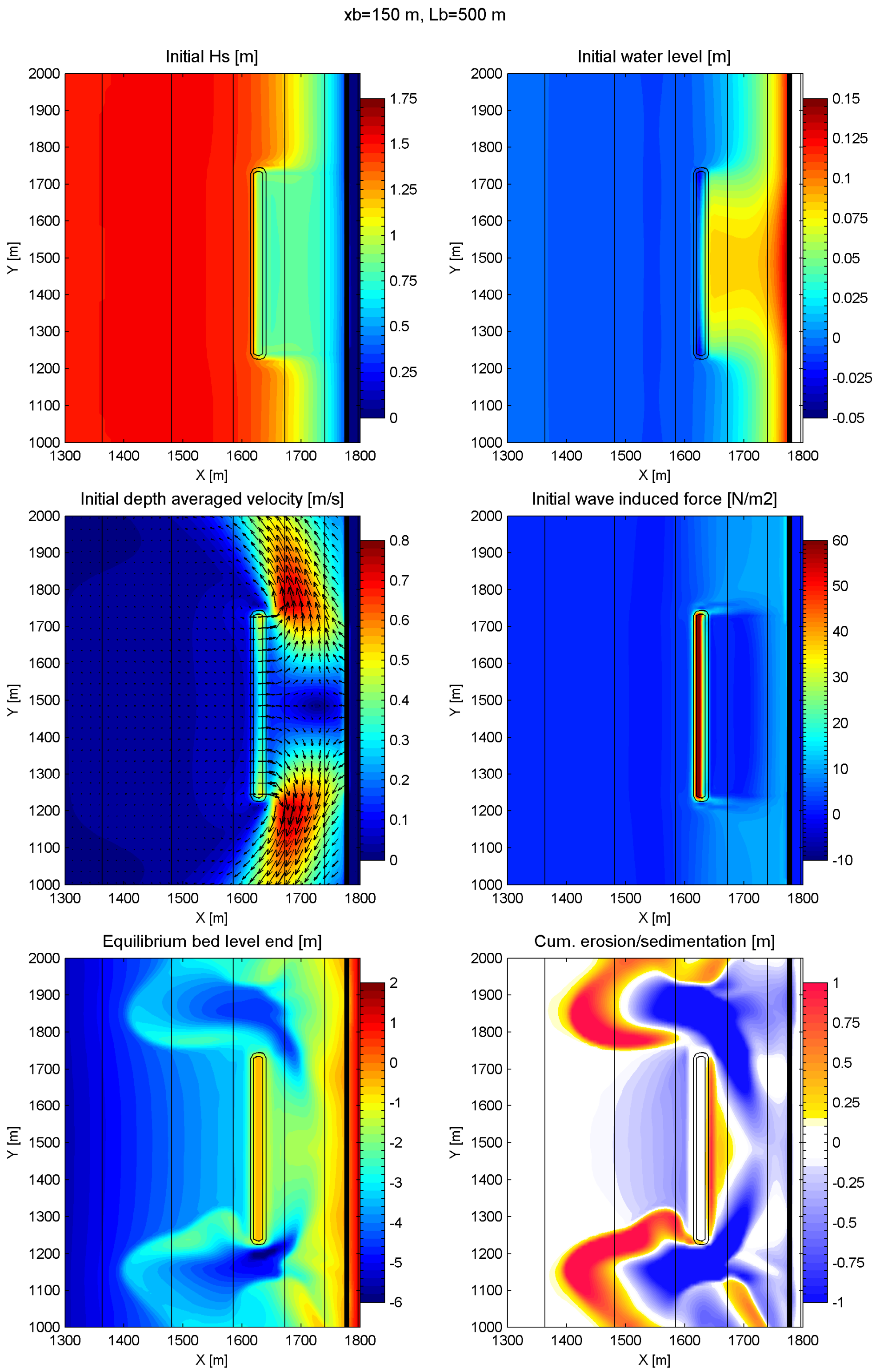

*Figure I.18 Hydrodynamic and morphological results xb=200m, Lb=100m*

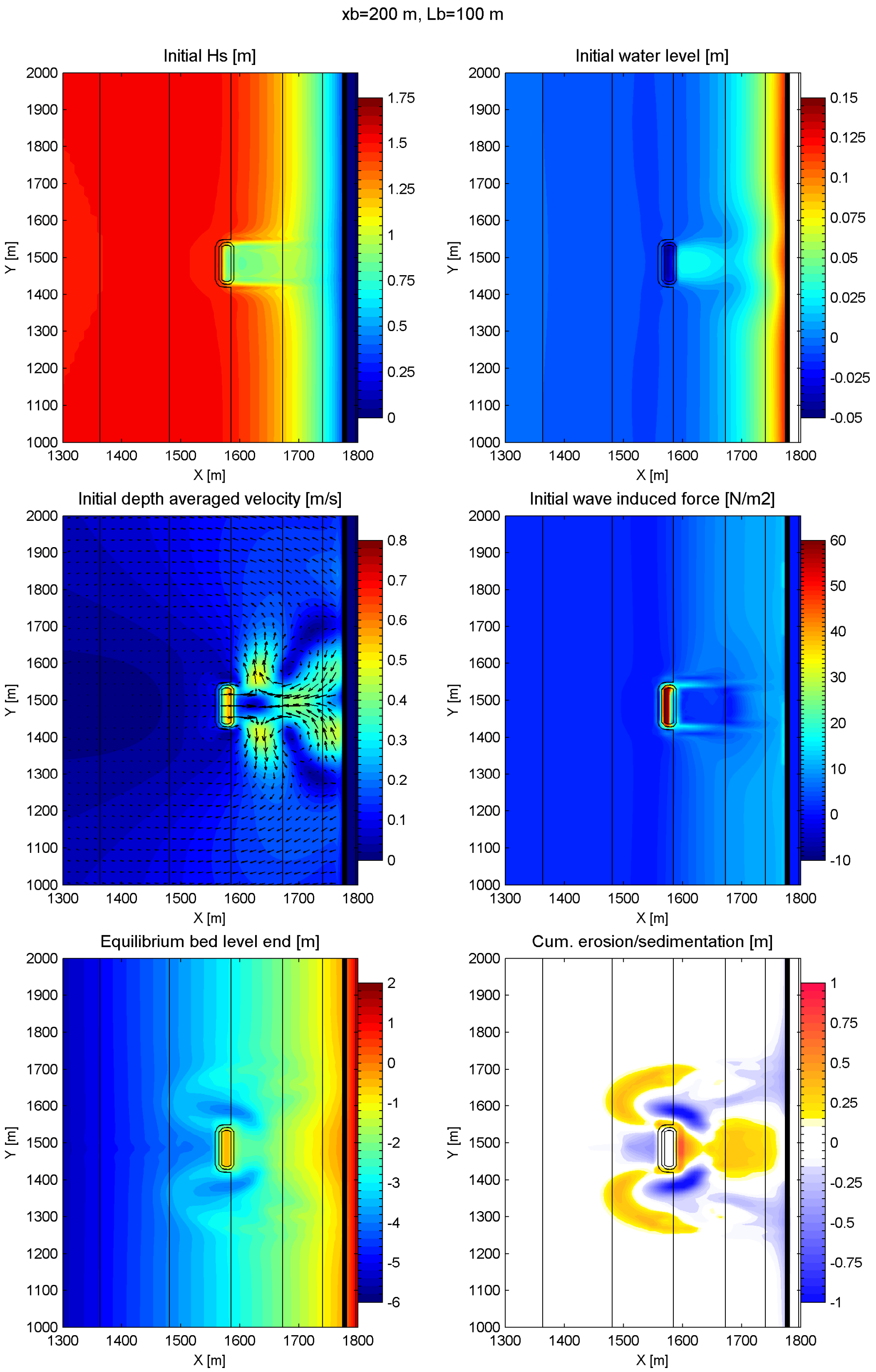

Figure I.19 Hydrodynamic and morphological results xb=200m, Lb=200m

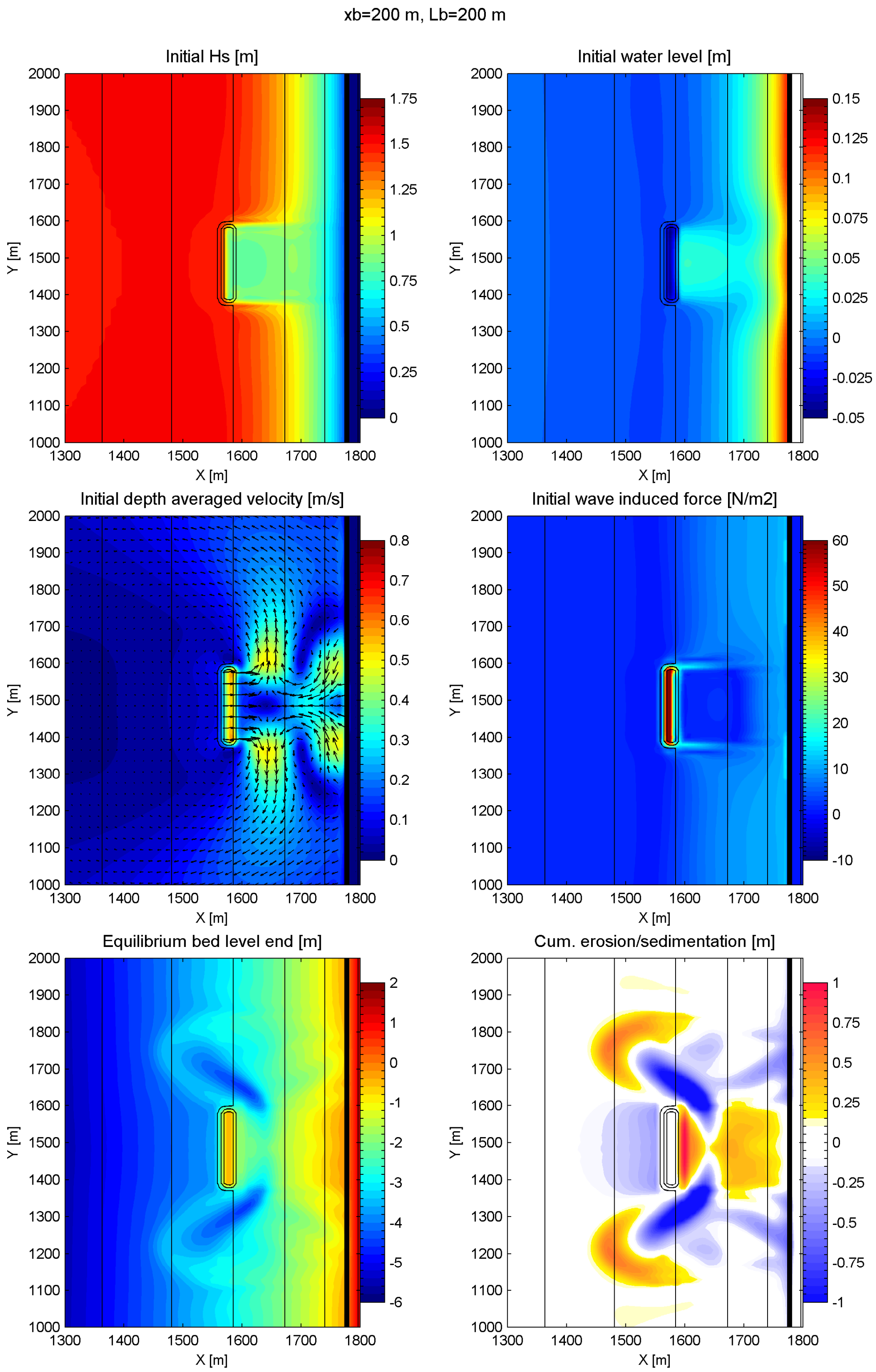

*Figure I.20 Hydrodynamic and morphological results xb=200m, Lb=300m*

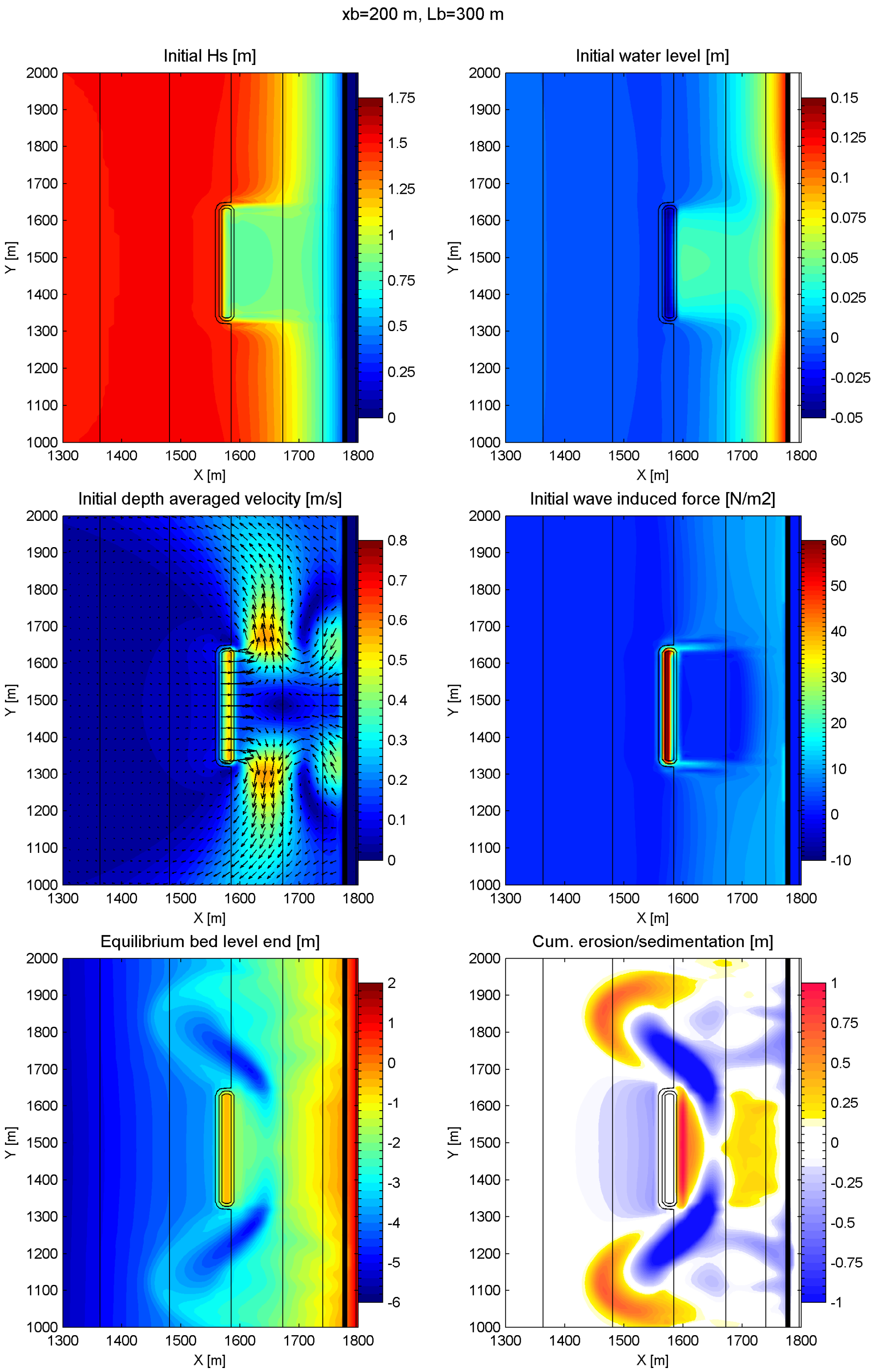

*Figure I.21 Hydrodynamic and morphological results xb=200m, Lb=400m*

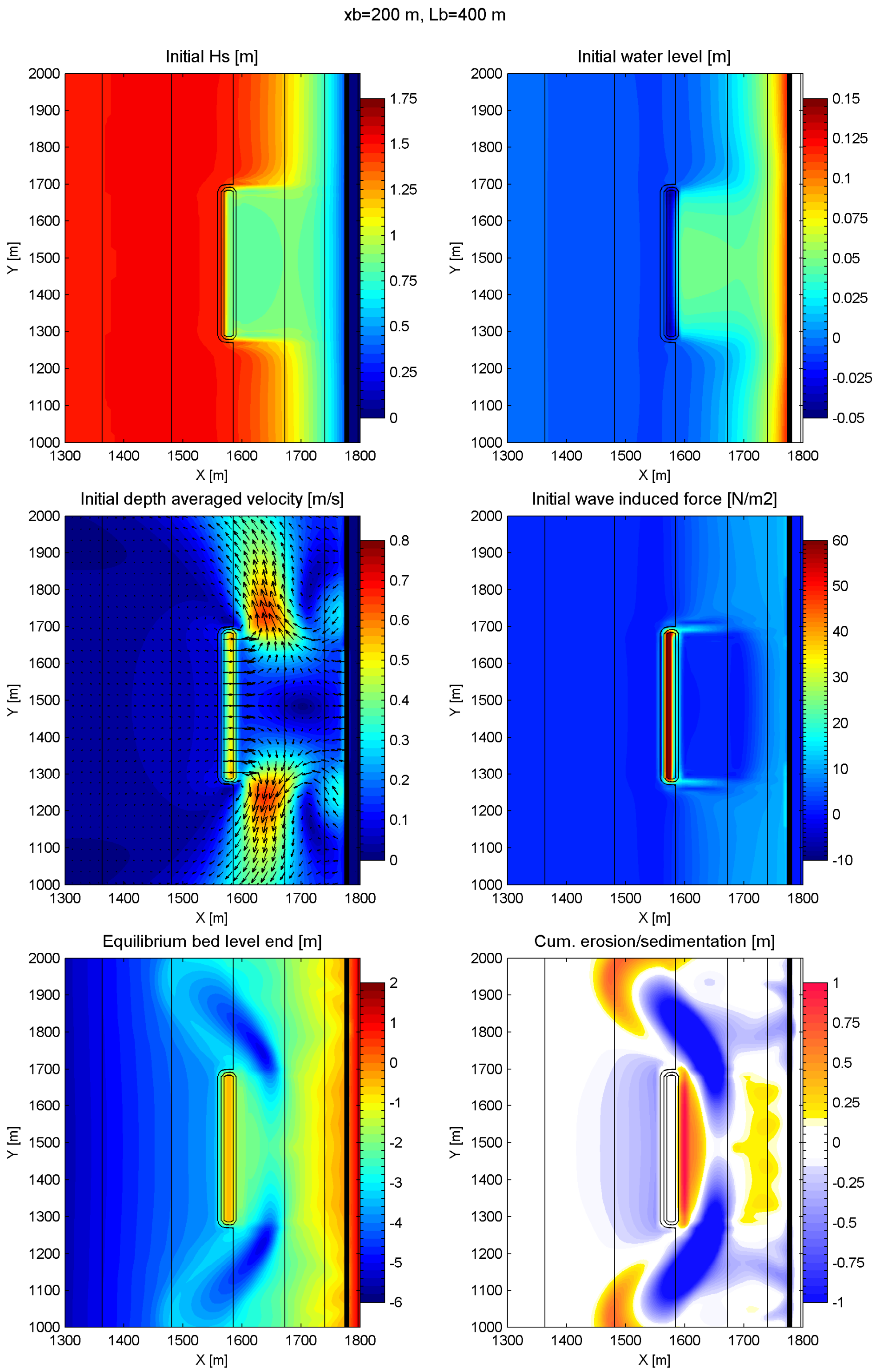

*Figure I.22 Hydrodynamic and morphological results xb=200m, Lb=500m*

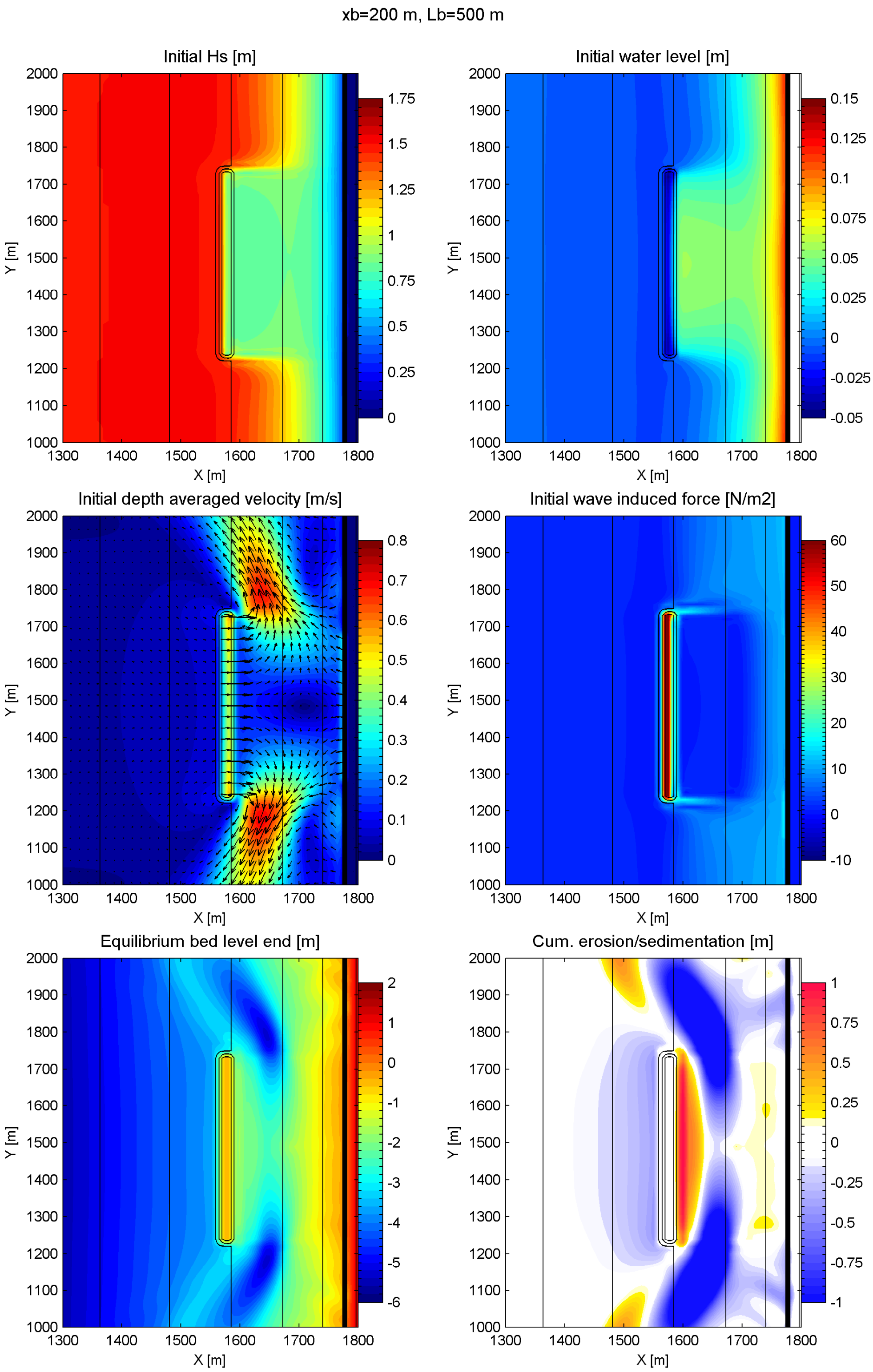

# J List of figures appendices

# K List of tables appendices